Modeling and Optimization of Sustainable Hydrogen Supply Chain Network Design.

Linfei Feng

THÈSE DE DOCTORAT DE L'ÉTABLISSEMENT UNIVERSITÉ BOURGOGNE FRANCHE-COMTÉ

PRÉPARÉE À L'UNIVERSITÉ DE TECHNOLOGIE DE BELFORT-MONTBÉLIARD

École doctorale n°37

Sciences Pour l'Ingénieur et Microtechniques

Doctorat d'Automatique

par

LINFEI FENG

Modeling and Optimization of Sustainable Hydrogen Supply Chain Network Design

Thèse présentée et soutenue à Belfort, le 12 Juillet 2024

Composition du Jury :

DESCHINKEL KARINE	Professeur, Université de Franche-Comté	Présidente
HAMANI NADIA	Maître de conférences HDR, Université Picardie Jules Verne	Rapportrice
HADJ-HAMOU KHALED	Professeur, INSA Lyon	Rapporteur
GRANGEON NATHALIE	Maître de conférences HDR, Université Clermont Auvergne	Examinatrice
MANIER MARIE-ANGE	Professeur, Université de Technologie de Belfort-Montbéliard	Directrice de thèse
MANIER HERVÉ	Maître de conférences, Université de Technologie de Belfort-Montbéliard	Co-directeur de thèse

N° | X | X | X |

ABSTRACT

In the global effort to reduce carbon emissions and transition to renewable energy sources, hydrogen is increasingly recognized as a pivotal element in sustainable energy strategies. This thesis explores the complexities of hydrogen supply chain network design (HSCND), integrates various energy sources, production technologies, storage solutions, and transportation modes within a hydrogen economy, in order to optimize a future deployment of the infrastructures of these chains. The main body of the thesis is composed of three parts.

Firstly, the thesis introduces a life cycle optimization modeling framework for HSCND, which incorporates life cycle cost (LCC) and life cycle emission assessment (LCA) into a bi-objective optimization model. This model is a mixed integer linear program (MILP). It aims to minimize the levelized cost of hydrogen (LCOH) and to reduce the global warming potential (GWP). A ϵ-constraint type method is then implemented to explore the trade-offs between economic efficiency and environmental impacts, through a detailed case study in the Franche-Comté region of France.

Secondly, building upon this foundational work, the model extends to accommodate multi-period scenarios with centralized storage strategies within the mixed integer linear programming (MILP) model. For each scenario, the model is solved using a commercial optimization solver (Cplex). This extension takes into account factors such as continuity in facility construction, fluctuations in hydrogen demand and supply, and mass balance considerations. A case study in the French metropole delves into system configurations under various forecasted demand scenarios, underscoring the economic benefits of the proposed model and strategy compared to two decentralized models.

Finally, the research further evolves to address computational challenges in optimizing large-scale hydrogen supply chains. A matheuristic method that combines a metaheuristic approach with mixed integer linear programming is proposed to improve computational efficiency. This solution method is implemented with Python language and the commercial solver Cplex. It is validated through tests on instances across France, which demonstrates its good performance in handling the complex and variable nature of large-scale HSC networks. Overall, this thesis contributes to the field of sustainable and economically viable HSCND by providing modeling and optimization tools.

Keywords: Hydrogen supply chain network, Optimization of the design, Multi-period, Bi-objective, Centralized vs decentralized storage, Mixed integer linear programming, Metaheuristic

RÉSUMÉ

Dans l'effort mondial visant à réduire les émissions de carbone et à passer aux sources d'énergie renouvelables, l'hydrogène est de plus en plus reconnu comme un élément central des stratégies énergétiques durables. Cette thèse explore certains des problèmes liés à la conception des réseaux d'approvisionnement en hydrogène (HSCND), en intégrant diverses sources d'énergie, technologies de production, solutions de stockage et modes de transport au sein d'une économie de l'hydrogène, afin d'optimiser un déploiement futur des infrastructures de ces chaînes logistiques. Le corps principal de la thèse est composé de trois parties.

Dans un premier temps, la thèse introduit un cadre de modélisation pour l'optimisation du cycle de vie pour le HSCND, qui intègre le coût du cycle de vie (LCC) et l'évaluation des émissions tout au long du cycle de vie (LCA), dans un modèle d'optimisation bi-objectif. Ce modèle, de type programmation linéaire en nombres entiers mixtes (PLNE), vise à minimiser le coût actualisé de l'hydrogène (LCOH) et à réduire les émissions de gaz à effet de serre (GES). Une méthode de type ϵ-contrainte est ensuite implémentée pour explorer les compromis entre l'efficacité économique et les impacts environnementaux, à travers une étude de cas détaillée dans la région française de la Franche-Comté.

Dans un deuxième temps, en s'appuyant sur ce travail fondamental, le modèle est étendu pour prendre en compte des scénarios multipériodes avec des stratégies de stockage centralisées introduites au sein du modèle de programmation linéaire en nombres entiers mixtes (PLNE). Pour chacun de ces scénarios, le modèle est résolu à l'aide d'un solveur d'optimisation commercial (Cplex). Cette extension intègre également des facteurs tels que la pérennité des infrastructures construites, les fluctuations de la demande et de l'offre en hydrogène, ainsi que des considérations liées à l'équilibrage des flux d'hydrogène. Une étude de cas réalisée sur la métropole française examine les configurations du système selon divers scénarios de demande prévus, soulignant les avantages économiques du modèle et de la stratégie proposés par rapport à deux modèles décentralisés.

Enfin, les travaux de recherche s'intéressent davantage à relever les défis informatiques liés à l'optimisation des chaînes d'approvisionnement en hydrogène à plus grande échelle. Une méthode de type matheuristique combinant une approche métaheuristique avec un programme linéaire mixte en nombres entiers est proposée pour améliorer l'efficacité des calculs. Cette méthode de résolution est implémentée en Python et utilise le solveur commercial Cplex. Elle est validée grâce à une mise en œuvre sur des instances à l'échelle de la France, ce qui démontre ses bonnes performances dans la gestion de la nature complexe et variable des réseaux HSC à grande échelle. Dans l'ensemble, cette thèse contribue au domaine des HSCND durables et économiquement viables, en fournissant des outils de modélisation et d'optimisation.

Mots clés : Chaîne logistique de l'hydrogène, Optimisation de la conception, Problème multi-périodes, Problème bi-objectif, Stockage centralisé vs décentralisé, Programmation linéaire en nombres entiers mixtes, Métaheuristique

ACKNOWLEDGEMENTS

Since arriving in Belfort in October 2020, these four years have flown by in the blink of an eye, quickly nearing the end. Here, I experienced the lockdowns during the pandemic, as well as the reopening afterwards. The city's peaceful, freedom and inclusivity have made me fall in love with it. I have also witnessed a broader world and met outstanding and interesting people, all of which I deeply cherish.

During this brief educational journey, i would like to express my deep gratitude to my supervisor, Marie-Ange Manier, for her invaluable guidance and the broad direction she provided throughout this journey. Her expertise and insights have been fundamental in shaping the trajectory of my research, offering a solid foundation upon which I built my work.

I am also very grateful to my co-supervisor, Herve Manier, whose attention to detail and systematic guidance have been crucial in refining my research. Patient explanations from Herve also have greatly enhanced my understanding and appreciation of the finer points of my research. His constructive feedback and rigorous review sessions have undoubtedly improved the quality of my work.

Finally, I am sincerely grateful to my colleagues for their support and collaboration that enriched my research experience. I am also deeply indebted to my friends whose company and unwavering support have given me a lot of strength, given me a lot of happiness, and helped me get rid of the negative emotions that occasionally arise. I must also extend a special thank you to my family and my husband, whose support and sacrifices have not only enabled but also motivated me to pursue my goals. Their love and understanding have been a source of strength for me.

Along the way, there has been happiness, disappointment, joy, and loneliness. I am grateful for my perseverance in the field of research. Although progress has been slow, I have continuously moved towards my goals. I am thankful for my curiosity and my enduring love for life. I hope to continue to strive and live passionately in the future.

CONTENTS

I

Context and Problems

1

INTRODUCTION

1.1/ CONTEXT

The 2030 Agenda for Sustainable Development, adopted by all United Nations Member States in 2015 introduce 17 Sustainable Development Goals (SDGs) such as Affordable and Clean Energy and Climate Action (United Nations, 2015). The COP28 conference in Dubai in 2023 marked a pivotal turn away from the fossil fuel era, with a landmark agreement aimed at capping the global temperature rise at 1.5°C. This agreement mandates a cut in greenhouse gas emissions by 43% by the year 2030, relative to the levels in 2019. It also emphasizes doubling the capacity of renewable energy sources and increasing energy efficiency by 100% within the same timeframe (United Nations Framework Convention on Climate Change, 2023). Over 100 countries, including China, the United States, and the European Union, have announced plans for reaching net-zero emissions sometime mid-century (Sönnichsen, 2021). Today, the energy sector is the most significant source of global CO_2 emissions, followed by the transportation sector, as many countries continue being heavily reliant on fossil fuels in these sectors. Emission reductions in the energy sector are essential for sustainable development. To make a change, the Glasgow Climate Pact is the first global agreement to explicitly include parties pledging to reduce the use of fossil fuels (United Nations Framework Convention on Climate Change, 2021).

Hydrogen has been considered as a possible transportation fuel since the 1970s (Bockris, 2013). It is now recognized as an important direction in the global energy transition. van Renssen (2020) pointed out that hydrogen has great potential to do three things: store surplus renewable power when the grid cannot absorb it; help decarbonize hard-to-electrify sectors such as long-distance transportation and heavy industry; replace fossil fuels as a zero-carbon feedstock in chemicals and fuel production. Besides, Hydrogen as an energy carrier bridges the gap between energy sources, electricity networks, the transportation sector, the industrial sector, and residential use, as shown in Fig. 1.1. With hydrogen and electricity as energy carriers, future energy systems will gain resilience and security, enable renewable energy sources to make a greater contribution and improve air quality. Moreover, hydrogen is an energy source with multiple energy properties and is suitable for various scenarios. It not just links various energy sectors, but it also possesses unique raw material and fuel properties, finding applications in the chemical and metallurgical sectors (International Energy Agency, 2021c). Additionally, it stands out for its high energy density when compared to alternative renewable sources like biofuel (Zore, Yedire, Pandi, Manickam, & Sonawane, 2021). Thus, hydrogen has the potential to enhance the mobility of low-carbon energy systems.

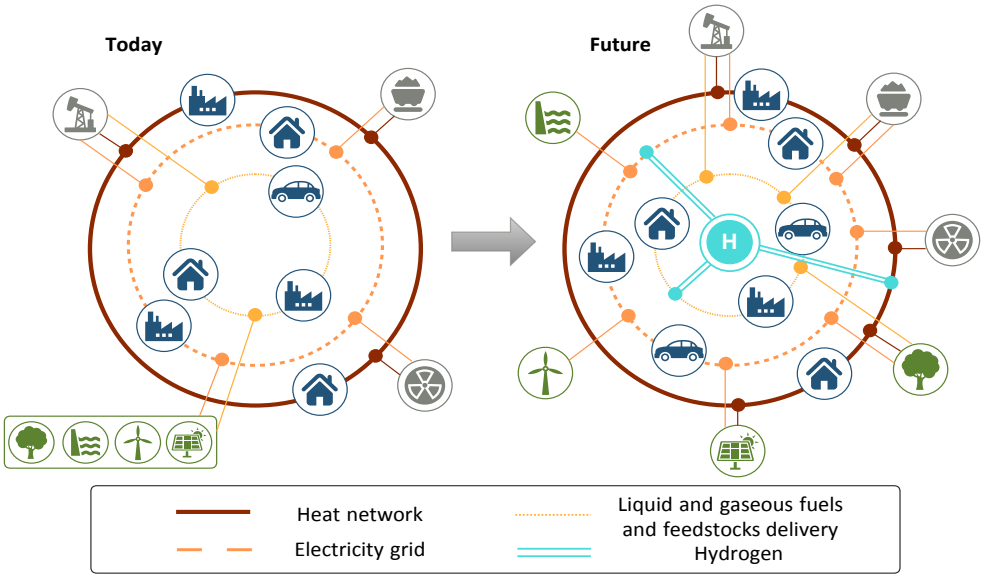

Figure 1.1: Hydrogen as a energy vector linking diverse energy networks (International Energy Agency, 2021c)

Though hydrogen's potential is clear, its current use remains limited, requiring significantly increased efforts for broader adoption. Hydrogen demand stood at 90 Mt in 2020, practically all for refining and industrial applications and produced almost exclusively from fossil fuels, resulting in close to 900 Mt of CO_2 emissions (International Energy Agency, 2021b). More hydrogen application scenarios and much faster adoption of low-carbon hydrogen are needed to put the world on track for a sustainable energy system by 2050. However, new hydrogen application is now limited in the transportation sector. The lack of hydrogen infrastructures partly explains the sluggish pace of hydrogen adoption by new users. Take the transportation sector as an example. Only about 35,000 hydrogen fuel cell electric vehicles (FCEV) were in operation worldwide as of the end of 2020, compared to 8.55 million battery electric vehicles (International Energy Agency, 2021a; Statista Search Department, 2021). Another fact is that there were only 540 hydrogen fueling stations in operation worldwide in 2020, compared to 1.25 million public charging stations available all over the world (International Energy Agency, 2021a; Statista Search Department, 2021).

The limited widespread use of hydrogen energy is primarily attributed to the high cost of its production, especially green hydrogen produced through the electrolysis of renewable energy sources. Currently, the cost of green hydrogen in various regions ranges from 3 to 8 euros per kilogram, depending on the price that can be achieved for renewable energy in that region (PricewaterhouseCoopers, 2022). Compared to traditional fossil fuels, it does not have an advantage due to this cost difference, which is a significant barrier to its adoption. Additionally, some technologies for producing, storing, and using hydrogen, particularly in areas such as transportation and industrial processes, are still in the development or early deployment stages. Further research and development are needed to improve efficiency and reduce costs. Moreover, safety management issues also play a crucial role in the adoption process. Furthermore, as Abdin et al. (2020) argued, hydrogen is an energy vector around which many infrastructures should be constructed. International Energy Agency (2019) noted that the development of hydrogen infrastruc-

ture is slow and holding back widespread adoption. Hydrogen prices for consumers are highly dependent on how many fueling stations there are, how often they are used and how much hydrogen is delivered per day.

Overall, the convergence of technological innovation, environmental sustainability, and economic viability form the key to the development of Hydrogen Supply Chain Network (HSCN). The complex integrated hydrogen supply chains needed systematic methodologies to design and plan. Besides, in configuring supply chain networks, decision-makers such as governments, energy companies, regulators, industry experts, and public societies frequently find it necessary to integrate the views and needs of all parties in order to strike a balance between the sustainability of energy supply, economic efficiency, and environmental impact. Making these decisions is typically complex and requires cooperation. Decision makers vary from country to country and region to region, due to the nature of their political systems and energy markets (Pflugmann & De Blasio, 2020). To keep the supply chain running at high performance by controlling the costs and other factors of the supply chain as much as possible and early realization of the hydrogen economy, the hydrogen supply chain network design (HSCND) model is one of the best tools to evaluate all possible alternatives. Built models based on an optimization framework can integrate a wide range of information and large amounts of data to provide relevant decision-makers with optimal strategies.

1.2/ OBJECTIVES OF THE THESIS

The objective of this thesis is to develop and optimize a Hydrogen Supply Chain Network (HSCN) to balance economic viability with environmental sustainability, address uncertainties, and achieve sustainable development of the supply chain. This entails crafting a multi-period, multi-objective optimization model that integrates a wide array of energy sources, production technologies, storage strategies, and transportation modes within a hydrogen economy.

Specifically, the target includes: (1) Conducting Economic and Environmental Performance Evaluations to align the supply chain with sustainability and financial viability; (2) Crafting Efficient Supply Chain Configurations by developing adaptable models responsive to policy changes, fluctuations in market prices for energy and feedstocks, and technological advancements, aimed at determining the best locations, sizes, and technologies for hydrogen production, storage, and distribution; (3) Integrated the Advanced Production and Storage Technologies to enhance the supply chain's adaptability and robustness; (4) Optimizing transportation networks by identifying the most cost-effective and environmentally friendly transportation options for hydrogen and its feedstocks; and (5) Creating algorithms to tackle the large-scale computational challenges associated with this model, ensuring effective supply chain optimization.

By addressing these areas, the overall objective seeks to pave the way for the scalable, sustainable, and economically viable deployment of hydrogen as a key component of the global energy transition, contributing to the reduction of carbon emissions and the advancement of clean energy technologies.

1.3/ OUTLINE OF THE THESIS

To fulfill these objectives, the dissertation is structured into six distinct sections. Chapter 1 serves as the introduction, outlining the critical research objectives to be met within this thesis. Chapter 2 delves into a comprehensive review of the latest advancements in hydrogen supply chain network design, encompassing the developments in production, storage, transportation, and refueling technologies, the methodologies and characteristics of supply chain modeling, as well as the solution approach and challenges. This chapter aids readers in understanding the current state of research on the topic and identifies existing gaps in the literature.

The next three chapters detail the contributions of the thesis. In Chapter 3, the methodology used to evaluate the cost and environmental impacts of HSCN is proposed, while a bi-objective optimization model is developed based on it. Then, a case study is proposed to describe the application of the model in the various scenarios in the region of Franche-Comte. Chapter 4 extends the problem mentioned in Chapter 3 by considering multiple periods, centralized storage strategies, and various hydrogen transportation forms. The mixed integer planning model is optimized with constraints characterized by multiple periods, e.g., continuous use and expansion of facilities, uncertainty demand, and balancing of storage. To validate the efficiency of the supply chain under this strategy, the model is applied to a French national scale case. The discussion extends to comparing centralized versus decentralized storage strategies and the effectiveness of different transportation networks in minimizing costs and environmental footprints. Chapter 5 focuses on addressing the computational challenges encountered in large-scale scenario analyses through algorithm design. It explores the development and application of hybrid metaheuristic algorithms to overcome the complexities of modeling and optimizing HSCN, demonstrating their efficacy in enhancing computational efficiency and model scalability.

Finally, chapter 6 concludes the thesis by summarizing the key findings, and contributions to the field of HSCND optimization, and also proposes future research directions.

ABBREVIATIONS

AEM	Anion Exchange Membrane
AWE	Alkaline Water Electrolysis
BG	Biomass gasification
CCS	Carbon capture and storage
CG	Coal gasification
CSHSCN	Centralized storage hydrogen supply chain network
DBSCAN	Density-Based Spatial Clustering of Applications with Noise
DCF	Discounted cash flow
FCEV	Fuel cell electric vehicle
FCR	Fixed charge rate
GA	Genetic algorithm
GH_2	Faseous hydrogen
GHG	Greenhouse gas emissions
GWP	Global warming potentials
HSC	Hydrogen supply chain
HSCN	Hydrogen supply chain network
HSCND	Hydrogen supply chain network design
HyBECCS	Hydrogen Bioenergy with Carbon Capture and Storage
IRR	Internal rate of return
LCA	Life cycle assessment
LCC	Life cycle costing
LCI	Life cycle inventory
LCIA	Life cycle impact assessment
LCO	Life cycle optimization
LCOE	Levelized cost of energy
LCOH	Levelized cost of hydrogen
LH_2	Liquid hydrogen
LHV	Lower heating value
LP	Linear Programming
MACRS	Modified accelerated cost recovery system
MILP	Mixed Integer Linear Programming
MINLP	Mixed Integer Nonlinear Programming
NLP	Nonlinear Programming
NSGA-II	Non-dominated sorting genetic algorithm
PCA	Principal component analysis
PEM	Proton Exchange Membrane
PV	Present Value
RES	Renewable energy sources
SCND	Supply chain network design
SOEC	Solid Oxide Electrolysis
SMR	Steam methane reforming
TAC	Total annual cost
TDC	Total daily cost
TtW	Tank-to-wheels
TSCC	Total supply chain cost
WtT	Well-to-tank
WtW	Well-to-wheels.

2

State of Art

2.1/ Introduction

The Hydrogen Supply Chain (HSC) constitutes a complex network of interconnected facilities, or nodes, depicted in the Fig.2.1 as its superstructure. This network starts with an energy node that supplies the feedstock essential for hydrogen production technologies and ends at individual refueling stations. Within this network, each node plays a unique role and interacts in a specific way to forge an efficient hydrogen supply framework. The critical nodes include:

- Feedstock Node: Marks the beginning of the HSC, tasked with supplying necessary raw materials for hydrogen production, including water, fossil fuels, biomass and so on;
- Production Node: Raw materials undergo transformation into hydrogen through various technologies such as electrolysis, steam methane reforming, and biomass gasification, with the selection based on factors like cost, efficiency, resource availability, and environmental considerations;
- Storage Facility Node: Post-production, hydrogen is stored in specialized facilities, ensuring the supply chain's reliability and security;
- Transportation Nodes: These nodes facilitate hydrogen's movement from production to storage or storage sites to its final use locations, utilizing pipelines, compressed or liquefied hydrogen transporters, or other means like rail or ship, based on factors like distance, cost, and safety;
- Refueling Station Nodes: Representing the supply chain's end, these nodes deliver hydrogen to end-users, with their development and operation being crucial for promoting hydrogen as a viable energy source for transportation.

The hydrogen supply chain is designed and coordinated through these nodes to ensure the efficient flow of hydrogen. A high degree of information and logistics integration among the nodes is required for the HSC to effectively respond to market changes and meet the growing demand for hydrogen energy.

This chapter thoroughly reviews articles on HSC from scientific journals, spanning supply chain advancements, model categorizations, performance evaluations, and solution

strategies. First, the components that are integral to the hydrogen supply chain are explored, including feedstock selection, production methods, carbon capture technologies, storage and transportation methods, and the application of hydrogen energy to various end-users. Next, the section categorizes the HSCND models and analyzes the methodology and geographic context of the applications of the different studies. In the section 2.4, the characteristics of the models in the reviewed papers are discussed in detail, including key decision points in the supply chain, model types, spatial scales, and sources of technology, performance indices, periodicity, uncertainty, and investment strategies. The performance indices section focuses on evaluating the financial, environmental, and safety performance of HSCNDs, as well as other important metrics. In section 2.5, various approaches to address the challenges of the HSC model are explored, and, finally, the key findings are summarized and future research directions for the thesis are proposed.

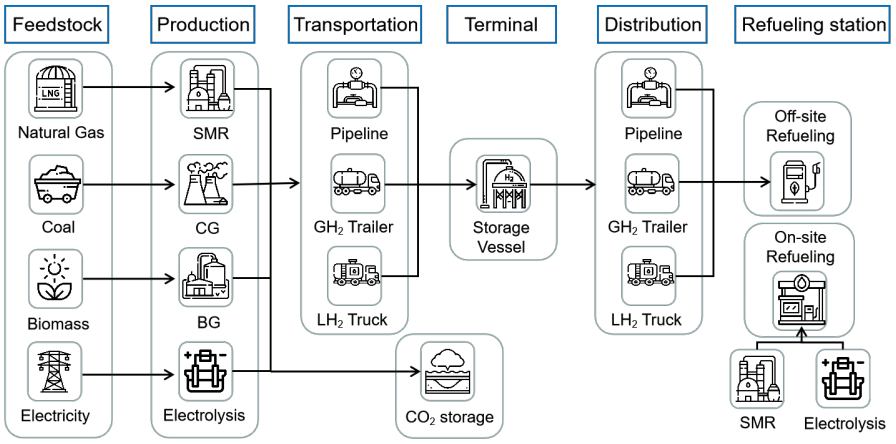

Figure 2.1: Superstructure of HSCN

2.2/ SUPPLY CHAIN COMPONENT

2.2.1/ FEEDSTOCK

A wide variety of raw materials can be used to produce hydrogen such as natural gas, coal, biomass, and electricity. Presently, the predominant source of hydrogen, constituting 96% of production, is non-renewable energy, with natural gas as its primary component (Erbach & Jensen, 2021). This source is reasonable in the short term to fulfill existing hydrogen demand, while water electrolysis will replace the current reliance on natural gas in the medium to long term to transition to fully sustainable production (Boretti & Banik, 2021).

Coal is the traditional source for hydrogen production, and current coal reserves last approximately 150 years at annual consumption levels. Nevertheless, the adverse effects associated with coal mining and utilization, including groundwater pollution and greenhouse gas emissions, have led to its exclusion as a viable raw material in certain countries, such as Spain (Navas-Anguita, García-Gusano, Dufour, & Iribarren, 2021).

Biomass relies on a range of primary resources such as wood, wood wastes, agricultural crops, agricultural waste, municipal solid wastes, animal wastes, food processing wastes, aquatic plants, algae, and more. Notably, wood and wood waste constitute the majority at 64%, with urban solid waste following at 24%, agricultural waste at 5%, and other sources making up the remainder(Demirbas, Mustafa, & Havva, 2009). The seasonal nature of biomass is distinctive.

For electrical energy, it can be obtained from the grid as well as from renewable energy sources. Solar and wind energy are the primary renewable sources under exploration and utilization. Geothermal energy, available in 26 countries(Ghazvini, Sadeghzadeh, Ahmadi, Moosavi, & Pourfayaz, 2019), is harnessed for water electrolysis to produce hydrogen in some regions(Yilmaz & Kanoglu, 2014)(Kanoglu, Bolatturk, & Yilmaz, 2010). Nuclear energy can also be used for hydrogen production, especially in France with a high proportion of nuclear power. The economics of hydrogen production through electrolysis heavily hinge on electricity prices, and a surplus of nuclear power significantly influences hydrogen operations(Cany, Mansilla, da Costa, & Mathonnière, 2017). For the water resources used in electrolysis, their cost has always been ignored in most studies, assuming an unlimited supply. In water-scarce regions, seawater desalination is considered for hydrogen production by some studies. They designed an integrated system involving a solar tower for hydrogen production through desalination(Siddiqui & Dincer, 2018). In addition, oxygen is also a necessary raw material, but it is not discussed in the previous paper.

Hydrogen is classified into three categories: grey, blue, and green. Grey hydrogen is generated by reforming fossil fuels. When carbon emissions are captured, stored, or utilized during the production process, the hydrogen is referred to as blue. Conversely, green hydrogen is produced using renewable feedstock and relies on a sustainable energy source for both raw material conversion and facility operation. (Atilhan et al., 2021).

2.2.2/ PRODUCTION

Hydrogen production from natural gas predominantly employs methane steam reforming, a concept initially introduced in 1932 (Boretti & Banik, 2021). In this process, natural gas undergoes catalytic conversion to yield H_2 and CO, with subsequent separation, followed by CO reacting with water vapor to generate CO_2 and H_2. Steam reforming of natural gas stands as a conventional method for hydrogen production, widely employed across industries, particularly in the chemical and petrochemical sectors, owing to its mature technology and high conversion efficiency. Notably, if carbon emissions from the production process are sequestered, hydrogen produced through this method exhibits a low carbon footprint, thereby potentially contributing to the production of CO_2-free hydrogen (Schneider, Bajohr, Graf, & Kolb, 2020). Additionally, hydrogen production from pyrolyzed natural gas represents another technological avenue, albeit not yet commercialized on a large scale.

Gasification stands as a crucial process for converting solid fuel into gas. In the context of coal gasification, the process involves reacting coal, either in the form of water slurry or pulverized, with a gasification agent such as steam or oxygen. This reaction occurs under elevated temperatures and pressures, resulting in the production of syngas comprising constituents like CO, CO_2, H_2, CH_4, H_2O, and others (Midilli, Kucuk, Topal, Akbulut, & Dincer, 2021)(Gnanapragasam & Rosen, 2017). Within the gasifier, CO is

segregated from H2, and a subsequent transformation of CO into H_2 and CO_2 transpires through reactions with water vapor. Following this, acid-washing procedures, involving the reaction of CO_2 with SO_2, and hydrogen purification processes are conducted to attain high-purity hydrogen (Midilli et al., 2021)(Gnanapragasam & Rosen, 2017). Although coal gasification stands out as the most commercially viable method for hydrogen production compared to alternatives, it is accompanied by significant environmental implications (Farhana, Mahamude, & Kadirgama, 2024).

Biomass gasification and bio-oil reforming from biomass pyrolysis represent two extensively researched pathways for hydrogen production utilizing biomass as the primary feedstock. In the gasification method, biomass is decomposed into hydrogen and other synthesis gases at high temperatures, utilizing variable pressure adsorption for other products. The biomass pyrolysis involves the rapid pyrolysis of biomass followed by the reforming of the hydrocarbon fraction of the resulting bio-oil. One significant drawback of these processes is the formation of tar during the decomposition of the biomass feedstock (Kırtay, 2011). Gasification typically operates at higher temperatures than pyrolysis and yields greater energy output compared to pyrolysis (Balat, 2008). In scenarios where biomethane serves as the primary raw material, research by Antonini et al. (Antonini et al., 2020) underscores its potential to yield negative greenhouse gas emissions throughout the supply chain. Specifically, when digestate is utilized as an agricultural fertilizer, with a substantial portion of the carbon retained in the soil, hydrogen production based on biowastes can result in system-level negative lifecycle greenhouse gas emissions, even in the absence of Carbon Capture and Storage (CCS) technologies. Furthermore, the integration of CCS into biomethane-based hydrogen production processes leads to overall negative emissions in all cases.

Hydrogen production via water electrolysis represents a sustainable method known as green hydrogen production. Over the long term, this technology is anticipated to supersede the current reliance on fossil fuel technologies due to its minimal carbon emissions (Gielen, Taibi, & Miranda, 2019). Various processes for water electrolysis exist, including Proton Exchange Membrane (PEM), Alkaline Water Electrolysis (AWE), Anion Exchange Membrane (AEM), and Solid Oxide Electrolysis (SOEC). PEM technology is widely favored for its efficient production of high-purity hydrogen with minimal maintenance challenges. AWE technology exhibits robust capabilities for large-scale production and finds extensive application in commercial hydrogen production. AEM technology offers a cost-effective solution, substituting precious metal catalysts with conventional, low-cost electrocatalysts (El-Shafie, 2023). SOEC technology has high conversion efficiencies (reaching more than 90), low energy consumption, and low associated emissions. However, solid oxide electrolysis cells operate at higher temperatures and therefore require longer start-up times. Moreover, additional treatment is required to obtain high-purity hydrogen from the mixture of hydrogen and water vapor produced by SOEC technology, rendering it still under development (Chi & Yu, 2018). Despite these advancements, the cost of hydrogen production via water electrolysis remains considerably higher compared to fossil fuel-based production methods.

Another method of hydrogen production involves by-products. Notably, hydrogen derived from chlor-alkali plants' by-products is regarded as a highly promising and cost-effective source of hydrogen presently available. During the production of chlorine gas, hydrochloric acid, and sodium chlorate in chlor-alkali plants, exhaust gases containing hydrogen are generated regardless of the electrolysis process employed (D.-Y. Lee, Elgowainy, & Dai, 2018)(Yáñez, Ortiz, Brunaud, Grossmann, & Ortiz, 2018). Similarly, in

petrochemical plants and refineries, substantial quantities of hydrogen are generated as by-products, with some portions utilized as internal fuel within these industrial complexes (Jeong & Han, 2011). Additionally, glycerol, a by-product of biodiesel synthesis, also can undergo conversion to biohydrogen through catalytic steam reforming or fermentation processes (Khademi, Alipour-Dehkordi, & Nalchifard, 2023)(Haron, Mat, Abdullah, & Rahman, 2018)(Slinn, Kendall, Mallon, & Andrews, 2008). Furthermore, Steel production and coke-making enterprises also produce hydrogen as a by-product, which can be cleaned and purified of its toxic components in the mixed gas to yield 36-62 vol% H_2 (Yáñez et al., 2018).

In summary, methane steam reforming technology stands as the most viable option presently for hydrogen production. While coal gasification offers economic advantages, its significant environmental impact poses considerable concerns. Biomass gasification faces limitations in mass production and has yet to see widespread commercial adoption. The high production costs associated with electrolysis, particularly when utilizing renewable energy sources, render it economically challenging without significant technological advancements. Although studies have demonstrated the economic benefits of industrial by-product hydrogen, its large-scale industrial utilization remains limited.

2.2.3/ CARBON CAPTURE

Carbon capture refers to capturing carbon dioxide as it is produced, compressing it into a supercritical fluid, and then sequestering it. The system consists of three main components, carbon dioxide capture, carbon dioxide transport, and carbon dioxide storage. The carbon dioxide is captured by absorption, adsorption, membrane separation, and cryogenic separation, and then transported by ship or pipeline (Pires, Martins, Alvim-Ferraz, & Simões, 2011).Storage location options include depleted oil and gas fields or deep seas (Newell & Ilgen, 2019). Carbon capture rates based on chemical cycling systems can reach over 99 percent (Cormos, Petrescu, & Cormos, 2014). SMR and CG technologies are typically used in conjunction with technologies that capture and store carbon dioxide emissions. By capturing emissions rather than discharging them, these processes reduce atmospheric greenhouse gas emissions and produce blue hydrogen (Thitakamol, Veawab, & Aroonwilas, 2007). J. Li, Wei, Liu, Li, and Yan's research found that after adopting CCS technology, the carbon footprint of coal-based hydrogen production can approach that of hydrogen produced via solar power generation. In addition, a recently introduced concept combines biotechnology with carbon dioxide (CO2) capture and storage, defined as HyBECCS (Hydrogen Bioenergy with Carbon Capture and Storage). This approach can achieve net-negative hydrogen emissions (Full, Merseburg, Miehe, & Sauer, 2021).

2.2.4/ STORAGE

Hydrogen can be stored in multiple forms and through various technologies. The main storage technologies are illustrated in Figure.2.2, which can be divided into three major categories: physical storage, chemical storage, and material-based storage. This includes compressed hydrogen, liquefied hydrogen, cryo-compressed hydrogen, physical adsorption hydrogen, metal hydrides, complex hydrides, Liquid Organic Hydrogen Carriers (LOHC), or liquid organic hydrides. Each method has its characteristics and is suitable

for different application scenarios (Usman, 2022).

The most widespread and practical method of storing compressed hydrogen is in high-pressure steel cylinders, typically stored at a pressure of 20 MPa. In new types of lightweight composite cylinders, pressures of up to 80 MPa can be withstood (Züttel, 2004). Since hydrogen is not corrosive, liquefied hydrogen can be stored in relatively thin and inexpensive tanks. However, the liquefaction temperature of hydrogen is $-253\,^{\circ}$C, so liquefying hydrogen requires a significant amount of energy, making it very costly. Cryo-compressed hydrogen combines aspects of both compressed hydrogen and cryogenic hydrogen, reducing evaporative losses in the storage process of liquefied hydrogen, but the construction of infrastructure poses a significant challenge. Metal hydrides and complex hydrides can offer higher hydrogen storage capacity compared to compression and liquefaction, and they are also safer than gas compression and liquefaction. However, their disadvantages include high hydrogen release temperatures and the production of undesirable gases during the process (J. Ren, Musyoka, Langmi, Mathe, & Liao, 2017). Composite hydrides also offer high hydrogen storage capacity, but additional research is needed to improve their release kinetics. Physical adsorption of hydrogen is characterized by high adsorption and desorption rates, but these materials typically have a high surface area. The use of Liquid Organic Hydrogen Carriers (LOHC) involves reacting with hydrogen-deficient organic molecules and releasing hydrogen in the presence of an appropriate dehydrogenation catalyst. This method offers enhanced safety, efficiency, high-density hydrogen storage, and good recyclability. However, it currently faces challenges related to cost, reversible thermodynamics and kinetics, volume, and toxicity. Further research is required before practical application

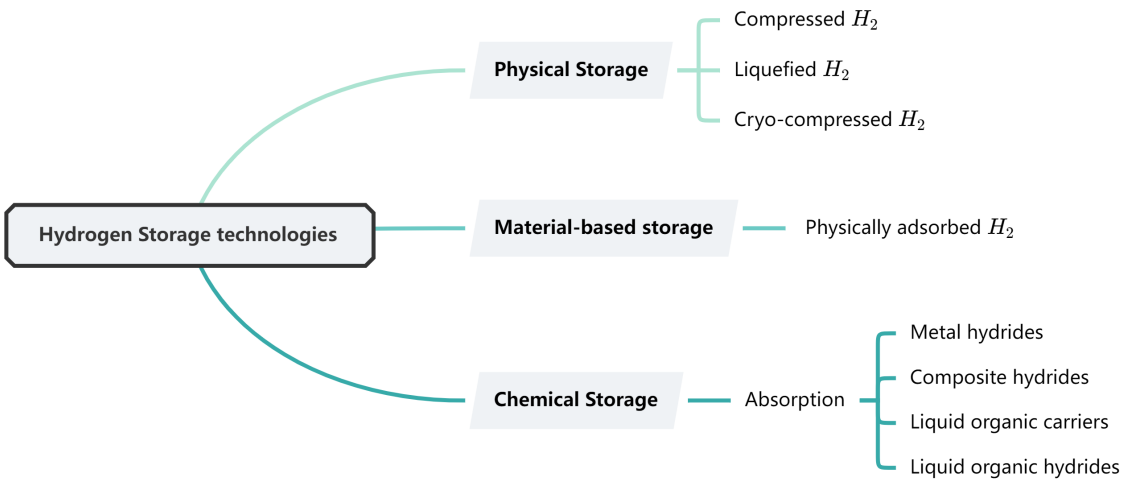

Figure 2.2: Hydrogen storage technologies

2.2.5/ TRANSPORTATION

Due to hydrogen existing in different forms at various temperatures and pressures, there are different transportation methods, with the most common being compressed gas cylinders, cryogenic liquid tankers, and pipelines. Gaseous hydrogen is transported using compressed gas cylinders, offering low operational costs, relatively low energy consumption, and quick hydrogen charging and discharging response times, making it suitable for

Table 2.1: Comparison of different hydrogen transportation methods (adapted from Singh et al.)

Transportation Mode	Pipeline	Liquid(tank)	Tube trailer
Capacity	- Up to 100 ton/h	- Up to 4000 kg per truck	-Up to 400 kg per trailer (standard)
Capital cost	- €200,000 - 1000,000 per km	- €5000,000 per truck	- €250,000 per trailer
Energy required	- Pipeline compressors	- Transport fuel	- Transport fuel
Efficiency	- 99.2% per 100km	- 99% per 100 km for transportation	- 94% per 100 km for transportation
Suitable for	- Large and very large quantities of gas	- Long distances	- Small distances

short distances and dispersed users, and is currently the most popular used storage and transportation method. However, this form of transport demands high-pressure tolerance for equipment, has a low hydrogen density per unit volume, and lower safety. Hydrogen is transported in liquid form via tank truck or other means. This hydrogen transportation method has a high energy density and efficiency, suitable for medium to long distances. However, due to the low liquefaction temperature of hydrogen, the liquefied hydrogen stored in tanks can be lost due to evaporation and gasification (Faye, Szpunar, & Eduok, 2022). Pipeline systems are considered the best method for the extensive transportation of hydrogen. They offer the advantages of low transportation costs, low energy consumption, and fewer emissions. Moreover, since pipelines are installed underground, they are safer and more reliable than other modes of transport. However, due to the difficulty of laying pipelines and the high one-time investment costs, large-scale hydrogen pipeline transportation is currently challenging to achieve. To mitigate the impact of pipeline laying costs, some researchers have proposed mixing hydrogen with the natural gas network, which can address the cost issues associated with new pipelines. The case in Germany shows that reconfiguring pipelines can reduce hydrogen transmission costs by more than 60% (Cerniauskas, Junco, Grube, Robinius, & Stolten, 2020). However, the technical feasibility of the pipelines must be considered during the integration process. Additionally, different mixing concentrations also pose numerous challenges in terms of safety and other aspects. Their application requires a careful balance, taking into account the actual conditions of the pipelines (Melaina, Antonia, & Penev, 2013).

The table 2.1 compares the three main modes of hydrogen transport.

2.2.6/ REFUELING

Hydrogen stations are similar to liquefied petroleum gas stations or natural gas filling stations. Hydrogen is stored within the station's storage facilities and then dispensed into the required equipment via a distributor. Based on the storage form of hydrogen, stations can be categorized into liquid hydrogen stations and gaseous hydrogen stations. Depending on the hydrogen supply chain, they can be classified as off-site refueling stations and on-site refueling stations. In an off-site refueling station, hydrogen is produced by production plants located in various places and then stored and transported to the station by appropriate means. An on-site refueling station means that hydrogen is produced, stored, and distributed directly at the station, without transport. Steam methane reforming and water electrolysis are the two most common methods of hydrogen production at on-site refuel-

Table 2.2: Comparison of hydrogen properties with other fuel (Ishaq et al., 2022)

Fuel	HHV (MJ/kg)	LHV (MJ/kg)	Minimum Ignition Energy(MJ)	Auto Ignition Temperature(℃)	Flame temperature(℃)
Hydrogen	141.6	119.9	0.017	585	2207
Methane	55.5	50.0	0.30	540-630	1914
Diesel	44.8	42.5	-	180-320	2327
Gasoline	47.3	44.5	0.29	260-460	2307
Methanol	22.7	18.0	0.14	460	1870

ing stations (Genovese & Fragiacomo, 2023). Currently, most hydrogen stations can store between 100 to 500 kilograms of gaseous hydrogen per day, and over 1000 kilograms of liquid hydrogen due to its high density. On-site stations, limited by technology and environmental factors, produce hydrogen in the range of 100kg to 1000kg per day (Apostolou & Xydis, 2019). In some areas, refueling stations combines the two approaches to compensate for the supply problems caused by insufficient on-site production rates (Alazemi & Andrews, 2015).

2.2.7/ END-USERS

Hydrogen is an efficient and clean energy option compared to other gas or liquid fuels. The table 2.2 compares the performance of hydrogen with other common fuels, including propane, methane, gasoline, diesel, and methanol. It has a higher Lower Heating Value (LHV) and Higher Heating Value (HHV), meaning that the same mass of hydrogen can provide more energy. So, it can be widely applied in transportation, industry, commerce, and residential sectors. In the transportation sector, hydrogen can serve as a clean fuel for vehicles, including cars, buses, trucks, and even trains. In the iron and steel metallurgy industry, hydrogen is utilized as a reducing agent, aiding in decarbonization efforts and enhancing process efficiency. In energy production, hydrogen serves as a clean fuel for power generation through fuel cells or combustion processes. It can also function as a storage tool, addressing the seasonal imbalances of renewable energy sources (Jiang et al., 2021). Additionally, hydrogen plays a crucial role in the petrochemical processes, serving as a raw material for the production of ammonia, methanol, and other valuable chemicals. In the commercial and residential sectors, hydrogen fuel can provide reliable thermal energy and electricity for commercial buildings, residential homes, and off-grid applications. Currently, the industrial sector accounts for 90% of hydrogen applications, with only 10% used in other sectors (WHA International, 2023).

2.3/ CLASSIFICATION OF HSCND MODEL

This review included scientific papers published from 2003 to 2023, focusing on keywords such as hydrogen supply chain, network design, hydrogen infrastructure strategic, and hydrogen energy system. A total of 124 relevant studies were identified through this search. The common journals in which these articles were published include the International Journal of Hydrogen Energy, Energy, Applied Energy, and Chemical Engineering Research and Design. The Fig.2.3 depicts the frequency of research paper publications within the field of hydrogen supply chain every two years. It illustrates a notable upward

trajectory in research outputs over the years, commencing with a mere three publications during the 2004-2005 interval and increasing to 29 publications during 2022-2023. This surge signifies a mounting scholarly and potential industrial intrigue in the design of hydrogen supply chain networks, underscoring the expanding acknowledgment of hydrogen's prospective contribution to energy transition and sustainability endeavors. Such growth is likely fueled by advancements in hydrogen technologies and an increased emphasis on efforts to decarbonize.

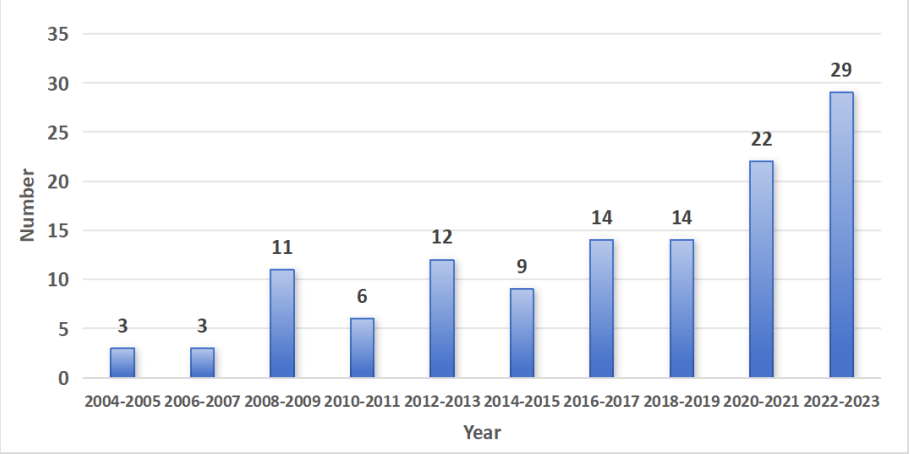

Figure 2.3: The number of published papers in the field of hydrogen supply chain network design (2003-2023)

Map (Fig.2.4) showing the number of case studies on the world's hydrogen energy supply chain by country, with darker colors indicating a higher number of academic and possibly industrial research in the region. The map reveals a wide geographical spread of research interest in hydrogen energy, spanning North America, Europe, Asia, and parts of Africa and the Middle East. The countries with the highest number of studies include South Korea (18), France (16), the USA (12), and the UK (12), indicating a strong national focus on hydrogen energy as part of their energy transition and sustainability strategies. China with 11 articles, Germany with 9 articles, and Italy and Spain each with 5 articles also show emerging interest and investment in hydrogen energy. Other countries are still in their infancy or have not been fully explored, with less than 5 articles available.

Next, we further categorized the reviewed papers based on the characteristics of the supply chains and models, with the information displayed in Tables 2.3. These distinctions involve the types of models, time periods, objective functions, the scope of the supply chain covered, uncertainties, regions of case studies, etc. The following sections provide detailed descriptions of each characteristic.

Table 2.3: Related studies of hydrogen supply chain design

Articles	Year	Model type			Period		Objective		Structure		Uncert
		LP/MILP	NLP/MINLP	OTH	SP	MP	SO	MO	PC	EC	
Joffe et al.	2004			✓	✓		✓		✓		
Hugo et al.	2005	✓			✓			✓	✓		
Tseng et al.	2005			✓	✓		✓			✓	
Almansoori and Shah	2006	✓			✓		✓		✓		
Brey et al.	2006	✓			✓			✓	✓		
Ball et al.	2007			✓	✓		✓			✓	

Articles	Year	Model type			Period		Objective		Structure		Uncert
		LP/MILP	NLP/MINLP	OTH	SP	MP	SO	MO	PC	EC	
Contaldi et al.	2008	✓			✓		✓			✓	
Ingason et al.	2008	✓			✓		✓		✓		
Kim et al.	2008	✓				✓	✓			✓	✓
Kim and Moon	2008	✓			✓			✓		✓	
Li et al.	2008	✓				✓		✓		✓	
Lin et al.	2008			✓		✓		✓	✓		
Qadrdan et al.	2008			✓		✓		✓		✓	
Strachan et al.	2009	✓			✓		✓			✓	
Almansoori and Shah	2009	✓				✓	✓			✓	
Hajimiragha et al.	2009	✓				✓	✓		✓		
Kamarudin et al.	2009	✓			✓		✓		✓		
Sabio et al.	2010	✓				✓		✓		✓	✓
Guillen-Gos albez et al.	2010	✓			✓			✓	✓		
Parker et al.	2010	✓			✓		✓		✓		
Elia et al.	2011	✓			✓						
Konda et al.	2011	✓			✓		✓			✓	
Murthy Konda et al.	2011	✓			✓		✓			✓	
Gim et al.	2012	✓			✓		✓		✓		
Almansoori and Shah	2012	✓				✓	✓			✓	✓
Brey et al.	2012	✓			✓		✓		✓		
Han et al.	2012	✓			✓		✓		✓		
Sabio et al.	2012	✓				✓		✓		✓	
Dagdougui et al.	2012	✓				✓	✓			✓	
Andre et al.	2013		✓		✓		✓		✓		
Almaraz et al.	2013	✓			✓			✓		✓	
Han et al.	2013	✓			✓			✓		✓	
Balta-Ozkan and Baldwin	2013	✓			✓			✓	✓		
Yang and Ogden	2013	✓				✓	✓		✓		
Gondal and Sahir	2013		✓			✓	✓		✓		
Andre et al.	2014		✓		✓		✓		✓		
Dayhim et al.	2014	✓				✓	✓			✓	✓
Almaraz et al.	2014	✓			✓			✓		✓	
Almaraz et al.	2014	✓				✓	✓			✓	
Amoo and Fagbenle	2014			✓		✓	✓		✓		
Krishnan et al.	2014	✓			✓		✓		✓		
Jagannath and Almansoori	2014		✓		✓		✓		✓		✓
Almaraz et al.	2015	✓				✓		✓		✓	
Nunes et al.	2015	✓				✓	✓			✓	✓
Hwangbo et al.	2016	✓				✓	✓			✓	✓
Almansoori and Betancourt-Torcat	2016	✓			✓		✓			✓	
Cho et al.	2016			✓	✓		✓		✓		
Robles et al.	2016	✓			✓			✓		✓	
Kim and Kim	2016	✓				✓	✓			✓	
Sgobbi et al.	2016	✓			✓		✓			✓	
Woo et al.	2016	✓			✓		✓			✓	
Sun et al.	2017	✓			✓		✓		✓		
Hwangbo et al.	2017	✓			✓		✓			✓	✓
Reuß et al.	2017			✓	✓		✓		✓		
Kim and Kim	2017	✓			✓		✓			✓	
Moreno-Benito et al.	2017	✓				✓	✓			✓	
Ogumerem et al.	2017	✓				✓		✓		✓	
Won et al.	2017	✓				✓	✓		✓		✓

Articles	Year	Model type			Period		Objective		Structure		Uncert
		LP/MILP	NLP/MINLP	OTH	SP	MP	SO	MO	PC	EC	
Bique and Zondervan	2018	✓				✓	✓			✓	
El-Taweel et al.	2018	✓				✓	✓		✓		
Hwangbo et al.	2018	✓			✓			✓	✓		✓
Rodl et al.	2018			✓	✓		✓			✓	
Wulf and Kaltschmitt	2018			✓	✓			✓	✓		
Yanez et al.	2018	✓			✓		✓		✓		
Reuß et al.	2019	✓			✓		✓		✓		
Han and Kim	2019	✓				✓	✓			✓	
Cho and Kim	2019	✓				✓	✓		✓		
Timmerberg and Kaltschmitt	2019	✓			✓		✓		✓		
Bique et al.	2019	✓			✓			✓	✓		
Ochoa Robles et al.	2019	✓				✓		✓	✓		
Camara et al.	2019	✓				✓		✓		✓	✓
Reuß et al.	2019			✓	✓					✓	
Seo et al.	2020	✓			✓		✓			✓	
Robles et al.	2020	✓			✓			✓		✓	
Fazli-Khalaf et al.	2020	✓				✓	✓		✓		✓
Gabrielli et al.	2020	✓			✓			✓	✓		
Ehrenstein et al.	2020	✓			✓			✓	✓		
Yang et al.	2020	✓				✓	✓			✓	✓
Ochoa Bique et al.	2020	✓			✓		✓			✓	✓
Cantu et al.	2020	✓			✓			✓		✓	
Li et al.	2020	✓			✓		✓			✓	
Ren et al.	2020			✓	✓			✓	✓		
Robles et al.	2020	✓				✓		✓		✓	
Jiang et al.	2021	✓			✓		✓		✓		
Stockl et al.	2021	✓			✓		✓			✓	
Guler et al.	2021	✓			✓		✓			✓	
He et al.	2021	✓				✓	✓		✓		
Cantu et al.	2021	✓				✓		✓		✓	
Shamsi et al.	2021	✓			✓		✓			✓	
Hong et al.	2021			✓	✓				✓		
Luise et al.	2021	✓			✓		✓			✓	
Carrera and Azzaro-Pantel	2021	✓				✓		✓		✓	
Talebian et al.	2021	✓				✓		✓		✓	
Kazi et al.	2021	✓			✓		✓		✓		
Li et al.	2022	✓			✓			✓		✓	
Yoon et al.	2022	✓				✓	✓			✓	
Mai et al.	2022	✓				✓	✓			✓	
Tao et al.	2022	✓			✓		✓		✓		
Reyes-Barquet et al.	2022	✓			✓			✓	✓		✓
Almaraz et al.	2022	✓				✓		✓		✓	
Guo et al.	2022			✓	✓		✓		✓		
Ge et al.	2022	✓			✓		✓		✓		
Mah et al.	2022	✓			✓		✓		✓		
Maggio and Mazzetta	2022	✓			✓		✓			✓	
Parolin et al.	2022	✓			✓		✓		✓		
Jin et al.	2022	✓			✓		✓		✓		
Erdogan and Gule	2023	✓			✓			✓	✓		
Li et al.	2023	✓				✓		✓		✓	
Forghani et al.	2023	✓				✓	✓		✓		
Hermesmann et al.	2023			✓	✓		✓		✓		

Articles	Year	Model type			Period		Objective		Structure		Uncert
		LP/MILP	NLP/MINLP	OTH	SP	MP	SO	MO	PC	EC	
Oh et al.	2023	✓			✓		✓		✓		
Ibrahim and Al-Mohannadi	2023	✓			✓			✓	✓		
Peng et al.	2023			✓	✓			✓	✓		
Erdogan et al.	2023	✓			✓			✓		✓	
Dong et al.	2023	✓			✓		✓			✓	
Ryu et al.	2023	✓			✓		✓			✓	
Vijayakumar et al.	2023	✓			✓		✓			✓	
Rathi et al.	2023	✓			✓		✓		✓		
Perez-Uresti et al.	2023		✓			✓	✓			✓	✓
Maestre et al.	2023	✓			✓		✓		✓		
Ransikarbum et al.	2023			✓			✓		✓		
Cantu et al.	2023		✓			✓		✓	✓		
Meng et al.	2023	✓			✓			✓	✓		

LP: Linear programming; MILP: Mixed integer linear programming; NLP: Nonlinear programming; MINLP: Mixed integer nonlinear programming; OTH: Dynamic programming, Techno-economic model, differential game, multi-criteria decision analysis; SP: Single period; MP: Multiple period; SO: Single objective; MO: Multiple objective; PC: Partial supply chain; EC: Entire supply chain; Uncert: Uncertainty.

2.4/ MODELING FEATURES

2.4.1/ DECISIONS

In the decision-making process within the hydrogen supply chain network, decisions can broadly be categorized into two main types: technical and operational decisions, and market and policy decisions. The first category focuses on how to produce and distribute hydrogen energy efficiently, safely, and sustainably. It involves decisions directly related to the technology selection and operational management of hydrogen production, storage, transportation, and distribution. Specific aspects include the methods of hydrogen production, siting and sizing of production facilities, storage methods, transportation tools, route chosen, and the layout of hydrogen supply stations. The second category of decisions is concerned with long-term strategic planning, market analysis, policy response, and investment risk management. It primarily focuses on forecasting the demand for hydrogen, including demand predictions across various markets such as transportation and industrial production, the strategies to cope with demand fluctuations, financial assessment, risk management of capital investments, the environmental impact evaluation of the hydrogen supply chain, such as greenhouse gas emissions, local environmental effects, and the assessment of social and economic contributions and potentially social issues. This also includes considerations of government policies and regulations, such as subsidy policies and environmental standards, and their impact on industry development along with corresponding operational strategies. These decisions are interdependent and collectively affect the efficiency, cost, reliability, and sustainability of the hydrogen energy supply chain.

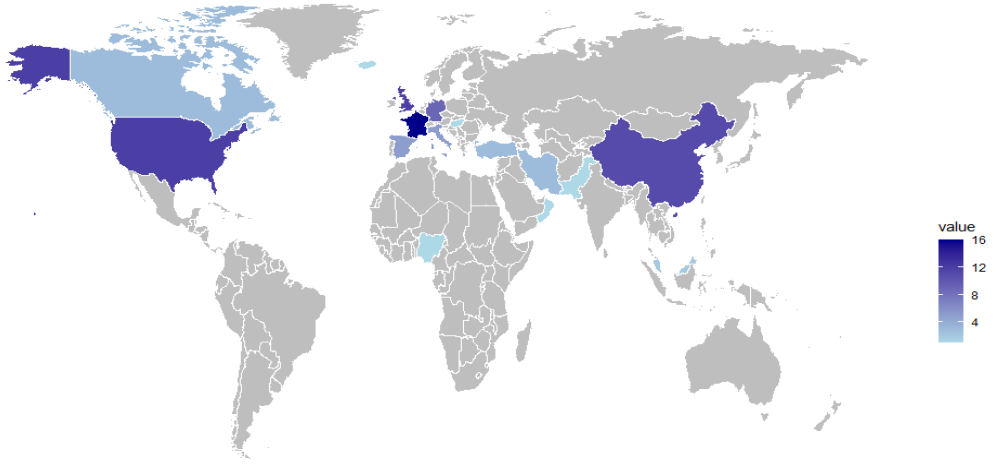

Figure 2.4: Number of HSC case studies around the world

2.4.2/ MODEL TYPE

The analysis of the distribution of modeling techniques used in HSC studies reveals a diverse array of approaches, with Mixed Integer Linear Programming (MILP) emerging as the predominant method, featured in 87 articles. This dominance underscores MILP's critical role in addressing the multifaceted decision- making processes in HSC, capable of integrating both continuous and discrete variables. Linear Programming (LP) follows, utilized in 16 articles. Less frequent are Nonlinear Programming (NLP) and Mixed Integer Nonlinear Programming (MINLP), represented in 2 and 4 articles respectively. These methods are usually targeted at hydrogen-specific scenario problems, such as biomass-based renewable energy (Gondal & Sahir, 2013), refinery application (Jagannath & Almansoori, 2014), and hydrogen transmission (André et al., 2013; André, Auray, De Wolf, Memmah, & Simonnet, 2014). Beyond these, the literature also explores Dynamic Programming in 4 articles and techno-economic analysis models in 10, with singular mentions of differential game theory and multi-criteria decision analysis.

2.4.3/ SPATIAL SCALE

In terms of spatial scale, the articles we analyzed were categorized into international, national, regional, and urban/industrial park dimensions. Detailed spatial scale distribution of reviewed papers are shown in Fig.2.5. The data reveal a predominant focus on models within national boundaries, accounting for 60% of the total. This emphasis likely mirrors the significant role that national energy policies, infrastructure, and market dynamics play in influencing the evolution of hydrogen supply chains. Regarding the regional scale, which includes 39 instances, there is a notable focus on the specific production of raw materials and technologies. This suggests that regional attributes, such as the availability of renewable energy sources, the industrial demand for hydrogen, and the pre-existing energy infrastructure, are crucial in determining the feasibility and optimization of hydrogen supply chains. Consequently, regional models prove indispensable for customizing hydrogen supply chain strategies, allowing for the effective utilization of local resources and fulfilling local demands.

In contrast, the International and Urban/Industrial park scales are less represented, accounting for only 3% and 4% of all studies respectively. Models at the urban/industrial park scale are notably pertinent for addressing the distinct hydrogen needs of urban environments and industrial sectors. These may encompass uses in transportation, various industrial operations, and hydrogen refueling infrastructures. The majority of focus at the international level is predominantly confined to the aspect of energy transportation. The investigation by Timmerberg and Kaltschmitt (2019) delves into the feasibility and economics of harnessing North Africa's abundant renewable resources, namely wind and solar energy, for the production of renewable hydrogen, subsequently transported to Central Europe via existing gas pipelines. Through linear optimization techniques, it identifies the variability in production costs across different locales, thereby laying the groundwork for sustainable energy exchange between North Africa and Europe, and highlighting the strategic importance of location in optimizing hydrogen production costs. Another study evaluates the importation of hydrogen into Singapore, focusing on techno-economic and environmental factors like cost, energy penalty, and carbon reduction. It highlights pipeline transmission from Malaysia and Indonesia as optimal for the power and industry sectors due to its cost-effectiveness and low environmental impact. This method is particularly efficient for distances up to 4500 km, showcasing the minimal energy penalty involved (Hong et al., 2021). Hermesmann, Tsiklios, and Müller (2023) evaluate the environmental impacts of cross-border vs local hydrogen production, utilizing renewable sources for electrolysis. The study reveals that the significance of transport distance diminishes as the energy transition progresses, suggesting a future where long-distance hydrogen transport becomes more viable environmentally. Sgobbi et al. (2016) investigate hydrogen's role in the decarbonization of Europe's energy sector, utilizing the JRC-EU-TIMES model to analyze different scenarios. Their research emphasizes hydrogen's critical role in deeply reducing carbon emissions, especially in sectors difficult to decarbonize. They highlight the essential need for supportive policy frameworks and technological progress to fully unlock hydrogen's decarbonization potential. Overall, the potential for international cooperation in hydrogen production, distribution and utilization remains an area worthy of further exploration, especially in the context of global efforts to decarbonize energy systems.

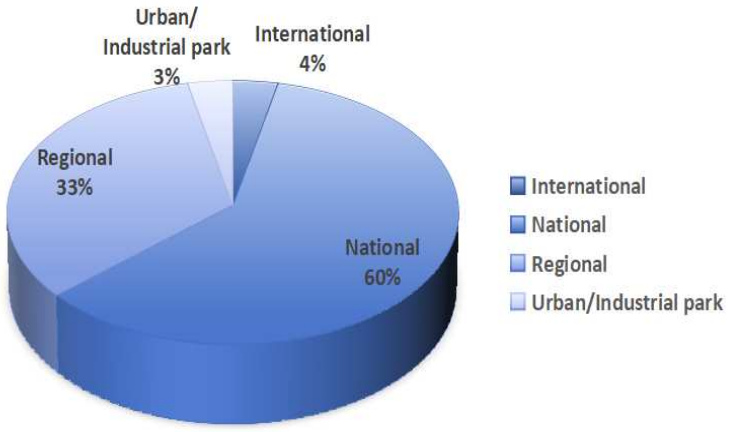

Figure 2.5: Spatial scale distribution of reviewed papers

2.4.4/ Supply Chain Structure

In the reviewed papers, 60 articles focused on specific sectors of the supply chain, including individual production, transportation, and refueling, as well as combinations such as production and transportation, production and storage, production and refueling, and storage and refueling. Meanwhile, 64 articles integrated all units of the supply chain, including every step from sourcing raw materials to the point of refueling.

In the process of studying the complete supply chain, we discovered that it also has different level structures. Most research focuses on the three-echelon supply chain. This structure includes the initial stage of hydrogen production, the middle stage of transporting and distributing hydrogen from the production site to storage facilities or directly to the point of use, and the final stage of delivering hydrogen to the end-users. In this structure, hydrogen storage usually occurs at the production node or the point of use. Two studies explored the four-echelon supply chain, which adds a storage and conditioning layer to expand the three-tier structure and is usually available to have two-stage transportation. In the research by Seo, Yun, and Lee (2020), after hydrogen is produced, it is transported to a storage center for storage and possible conditioning, such as compression or liquefaction, before being transported from the storage facilities to various distribution points to provide hydrogen to the end-users. Similarly, (Forghani, Kia, & Nejatbakhsh, 2023) established a two-stage supply chain framework, where the first stage includes the production and storage of hydrogen, and the second stage corresponds to the distribution from storage to demand points. In both stages, hydrogen can be transported through a tube trailer or pipeline.

2.4.5/ Technology Source

”Technology Source” refers to the study of a combination of multiple technologies or a single technology within a model. Each hydrogen production technology possesses its unique cost structure, influenced by factors such as technological maturity, energy sources, and operational efficiency. Evaluating multiple technologies within the same model allows for the identification of the most cost-effective solutions under various economic and environmental conditions. Additionally, the use of diverse resources enhances system flexibility and adaptability to local energy sources. Besides, relying on a single production technology within the supply chain could expose it to higher risks associated with technological failures, resource scarcity, or fluctuations in energy prices. Incorporating multiple technologies can spread these risks and ensure more stable hydrogen production. On the other hand, models focused on a single production technology offer the advantage of a deeper investigation into the specific operational, economic, and environmental aspects of that technology, making it closer to real-case scenarios. The literature includes 85 articles that explore models with a combination of technologies, for example, Gabrielli, Charbonnier, Guidolin, and Mazzotti (2020) investigated the design of a low-carbon HSCN based on a variety of raw materials such as natural gas, electricity, and biomass energy, and considered carbon capture and storage facilities in the network; Contaldi, Gracceva, and Mattucci examining approximately 40 distinct hydrogen technologies throughout the stages of production, transportation, and consumption in the Italien energy system.

The results particularly emphasize the importance of a variety of production technologies,

such as steam methane reforming and electrolysis, in forging a viable and environmentally friendly HSC. Meanwhile, 38 articles explore a single technology, mostly focusing on renewable energy, including solar energy (Bique & Zondervan, 2018), biomass (Cho & Kim, 2019; Reyes-Barquet et al., 2022; Cho, Woo, Kim, & Kim, 2016), wind energy (Yang, Jiang, & You, 2020; M. Kim & Kim, 2017a) and so on.

2.4.6/ PERFORMANCE INDICES

2.4.6.1/ FINANCIAL

In the design of Hydrogen Supply Chain Networks (HSCND), cost is a primary metric used for performance evaluation in the majority of models. These models typically account for costs associated with the construction of facilities for hydrogen production, storage, and refueling stations, operational expenses, and raw material costs. In 2005, Hugo et al. proposed an assessment for parts of the supply chain, including production and refueling operations (Hugo, Rutter, Pistikopoulos, Amorelli, & Zoia, 2005). Subsequently, Almansoori and Shah developed a comprehensive calculation model for evaluating demand within the supply chain, production plants, storage facilities, and transportation modes. The model determines the best infrastructure and operations to minimize costs. (Almansoori & Shah, 2006).

Following their work, many models have been based on this framework to estimate costs associated with the supply chain (Güler, Geçici, & Erdoğan, 2021)(Almaraz, Azzaro-Pantel, Montastruc, & Boix, 2015)(Robles, Azzaro-Pantel, & Aguilar-Lasserre, 2020)(Almansoori & Shah, 2009)(Almansoori & Shah, 2012).

Beyond the conventional facility costs, some studies also consider the cost of carbon dioxide emissions, typically manifested as a carbon tax, charging a fee for each unit of carbon dioxide emitted (Peng, Xin, & Xie, 2023)(Ibrahim & Al-Mohannadi, 2023). The construction and operational costs of CCS systems are also considered in some models (L. Li, Manier, & Manier, 2020)(Almansoori & Betancourt-Torcat, 2016). Its costs include expenses for capturing CO2 emissions, transportation, and infrastructure construction, and operational costs for CO2 storage. The research conducted by Jesus Ochoa Robles(Robles, Azzaro-Pantel, Garcia, & Lasserre, 2020) includes additional external costs, encompassing carbon dioxide, noise, local pollution, and the mitigation costs associated with platinum consumption. The social values of these factors are assessed and assigned different prices over each period.

Furthermore, the concept of Levelized Cost of Hydrogen (LCOH) has been introduced in some studies (Almaraz, Rácz, Azzaro-Pantel, & Szántó, 2022)(L. Li et al., 2020)(Seo et al., 2020)(Maestre, Ortiz, & Ortiz, 2023)(Yang et al., 2020). The calculation of LCOH aids in understanding the average cost per unit of hydrogen throughout its lifecycle in the hydrogen energy supply chain, from production and storage to transportation and final use. It is a critical indicator for evaluating the economic viability of different hydrogen production technologies, supply chain configurations, or project investments, as well as for comparing hydrogen energy costs with other energy sources.

In addition to the above calculation methods, some studies aim to maximize profits as their objective. The model proposed by Nader et al. calculates the objective function as the selling price of hydrogen energy, subtracting the purchase price of raw materials and certain slack variables (El-Taweel, Khani, & Farag, 2018). In the framework outlined by

Ogumerem et al. (Ogumerem, Kim, Kesisoglou, Diangelakis, & Pistikopoulos, 2018), the primary aim is to optimize system revenue, computed as the disparity between income generated from products and by-products and the associated operating cost. Reyes-Barquet er al. also focus on maximizing the total system profit. This is accomplished by calculating the difference between the revenue earned by the storage site and the total annual costs. The total annual cost includes the operating costs of hydrogen production, transportation and storage, from generation in the electrolysis system to storage at the Storage and Dispatch Station.The hydrogen sales price is based on the gasoline sales price at each station, taking into account the power offered by each type of vehicle (gasoline-powered and hydrogen fuel cell electric vehicles) to derive a cost-per-kilometer, which is then used to set a competitive sales price for hydrogen (Reyes-Barquet et al., 2022).

2.4.6.2/ ENVIRONMENTAL

Environmental assessment plays a crucial role in the design and optimization of hydrogen supply chain networks, ensuring sustainability and minimizing ecological impacts. Assessing the environmental impacts of hydrogen supply chain (HSC) operations necessitates a comprehensive approach encompassing various ecological factors. Fundamental to this assessment is the quantification of greenhouse gas emissions, including CO2 , CH4 and N2O, along the supply chain, often measured in total emissions or emissions per unit. In the reviewed paper, most of them quantify the environmental impact on the hydrogen supply chain by summarizing the greenhouse gas (GHG) emissions (measured in carbon dioxide equivalent) during the production, storage and transportation stages of the supply chain. The assessment involves calculating the GHG emissions from hydrogen production by considering the amount produced and the specific emissions factors for each production technology, determining the emissions from storage based on hydrogen quantities and the corresponding storage-related emissions factors, and evaluating transportation emissions by taking into account the distances traveled by different modes of transportation and their associated emissions factors per kilometer. In addition, researchers usually employ the Global Warming Potential (GWP) indicator to understand the overall atmospheric heat radiation absorption due to these emissions.

2.4.6.3/ SAFETY

Transitioning to a hydrogen economy at scale necessitates a rigorous examination of safety risk across production, storage, transportation, and usage due to hydrogen's comparable flammability to traditional fuels and distinct hazardous behaviors under specific scenarios. The Figure 2.6 shows a hydrogen tank explosion in an Austrian industrial park. The safety risk evaluation within the hydrogen supply chain involves analyzing potential hazards throughout the supply chain stages. Primary concerns encompass hydrogen's flammability, leakage possibilities, integration with existing infrastructures, and the reliability of hydrogen-based technologies.

Kim et al.(El-Taweel et al., 2018) formulated mathematical expressions to quantify the overall safety risk, incorporating the relative risks associated with production sites, storage sites, and transportation routes. These calculations account for the relative risk based on activity type and the population density of the activity's location. Transportation risk

assessment includes external risk factors (the potential risk transportation routes impose on surrounding areas) and internal risk factors (pertaining to the mode of transport and distance covered). The application of Failure Modes and Effects Analysis aids in identifying possible failures and their outcomes. Subsequent risk assessments leverage data from safety reports to estimate the likelihood of unforeseen incidents and their consequences. A risk rating matrix then categorizes each hazard's risk level according to its consequence and frequency. Further advancing this domain, Woo et al. (J. Kim, Lee, & Moon, 2011) introduced an index-based risk assessment framework for hydrogen infrastructure, evaluating the relative risk levels of critical supply chain activities—production, storage, and transport—while also incorporating regional characteristics like population density to ascertain a region's relative impact level. This model employs quantitative risk analysis for hydrogen-related activities and regional impact assessment based on specific area attributes, including population density. Adaptations of this framework have been applied across the entire supply chain and other research models, facilitating a comprehensive safety evaluation (Almaraz, Azzaro-Pantel, Montastruc, Pibouleau, & Senties, 2013)(Almaraz et al., 2015).

Beyond that, security is not only a technical issue, but also a social and psychological one. As with any other device, consumers are concerned about the reliability and safety of new technologies as well as new systems, especially applications that require direct technical interaction. The hydrogen economy will only get better if consumers believe that hydrogen energy is sufficiently safe. An important way to increase consumer confidence is to develop internationally recognised standards and norms, so policy makers should develop and focus on this approach to promote the successful integration of hydrogen energy into the energy system (Edwards, Kuznetsov, & David, 2007).

Figure 2.6: Hydrogen explosion (2023-Austria) Collins (2023)

2.4.6.4/ ADDITIONAL PERFORMANCE MEASURES

Carrera and Azzaro-Pantel present a bi-objective optimization framework for the strategic design of Hydrogen and Methane Supply Chains. This research simultaneously addresses the need for hydrogen, specifically for fuel cell vehicles, and as a necessary feedstock in the methanation process for synthetic methane production. In addition to traditional metrics such as total annual cost and global warming potential associated with the hydrogen supply chain, their analysis also includes the cost of renewable methane

production (Carrera & Azzaro-Pantel, 2021).

The model introduced by Fazli-Khalaf, Naderi, Mohammadi, and Pishvaee (2020) not only addresses economic, environmental, and social responsibility considerations but also introduces a novel reliability aspect. The objective function for delivery reliability prioritizes enhancing the operational reliability of the hydrogen supply chain by minimizing the projected quantity of defective delivered product. This is achieved by employing an exponential probability function to assess the reliability of production facilities over the planning horizon, accounting for the likelihood of uninterrupted operation. Such an objective guarantees the utilization of more dependable facilities with reduced failure rates for production, thus mitigating the risk of delivery interruptions and deficiencies.

Policy is also an important performance measure in the supply chain design process. Ransikarbum, Chanthakhot, Glimm, and Janmontree (2023) utilized Thailand as a case study, and employed group decision analysis to evaluate procurement decision standards within the hydrogen supply chain. The research found political acceptability as the foremost criterion in Thailand, with a global weight of 0.514. Besides, in recent years, to advance the hydrogen energy sector's commercial viability, various nations have already adopted distinct developmental pathways and strategies. These strategies primarily encompass the provision of suitable economic backing, tax benefits, and standardization efforts. For instance, the United States unveiled its "Roadmap to a US Hydrogen Economy" in 2020, aiming to broaden hydrogen utilization across the country by 2030 and achieve sales exceeding 750 billion dollars by 2050 (Cell et al., 2020). Meanwhile, Canada has tailored its policies and incentives to reflect the unique attributes of its provinces; Quebec, for example, vigorously supports green hydrogen production leveraging its plentiful water resources, whereas Alberta focuses on integrating natural gas production with carbon capture technologies. In the European Union, a commitment of €10 billion has been made under the Clean Hydrogen for Europe initiative to support the energy transition, planning to allocate 100 billion euros towards funding hydrogen electrolyzer production, storage, and distribution projects between 2020 and 2030 (Lebrouhi, Djoupo, Lamrani, Benabdelaziz, & Kousksou, 2022). Similarly, South Korea has launched its "Green Growth" initiative, offering policy support for hydrogen energy development (Ki-Jong, 2012).

2.4.6.5/ MULTI-OBJECTIVE

In the design process of hydrogen supply chain networks, there exist multiple conflicting objectives such as minimizing costs, maximizing supply chain reliability, minimizing environmental impacts (e.g., greenhouse gas emissions), and maximizing socio-economic benefits. Achieving optimality in one objective may lead to suboptimal outcomes in others. For instance, opting for coal gasification technology to produce hydrogen to minimize costs will undoubtedly result in higher emissions compared to the more expensive water electrolysis technology. Multi-objective optimization allows decision-makers to consider various facets of the hydrogen supply chain, thereby finding an optimal balance among diverse objectives.

In the publications we reviewed, the majority of models employ mono-objective optimization, with the vast majority focusing on cost optimization and a smaller portion on emissions optimization. A total of 40 articles developed multi-objective models. Among these, most chose to analyze both cost and environmental factors, such as Almansoori and Betancourt-Torcat (2016) and Cantú, Azzaro-Pantel, and Ponsich (2021) devised a model

to plan the hydrogen supply chain network under economic and environmental conditions constraints, Reyes-Barquet et al. (2022) designed the supply chain that uses electricity generated from agro-industrial residues of the sugarcane industry in Mexico as an energy source, with the goal of maximizing annual profit while minimizing greenhouse gas emissions to the greatest extent possible. One-third of the studies opted to optimize cost, environment, and safety simultaneously. Almaraz et al. (2013) inspired by Almansoori and Shah to develop a multi-objective model. The model optimized three objectives, including supply chain total cost, global warming potential, and safety risk. Only Sabio, Gadalla, Guillén-Gosálbez, and Jiménez proposed a model that considers total cost after discounting and the related financial risk. Table 2.4 provides a detailed listing of the indicators considered in each study.

2.4.7/ PERIODICITY OF INVESTMENT

The examined papers were organized according to their periodicity into two groups: single-period and multi-period models. A total of 79 studies were dedicated to single-period optimization, while 42 studies delved into multi-period modeling. Models of single-period optimization focus on a particular time frame, highlighting the importance of cost efficiency and operational effectiveness during this interval. This method streamlines the decision-making process, allowing for quick adaptations in strategy to accommodate changes in the market and technology. On the other hand, multi-period optimization covers several time intervals, accounting for variations in supply and demand, technological innovations, and the implications of policy changes over an extended period. Although it facilitates a more detailed decision-making framework in the face of complex scenarios, it also introduces greater complexity into the decision-making process.

2.4.7.1/ SINGLE-PERIOD

Joffe, Hart, and Bauen (2004) provides a comprehensive examination of the burgeoning hydrogen refueling infrastructure in London, assessing two primary scenarios: Incremental on-site electrolysis and the use of imported industrial liquid hydrogen for refueling stations. It underscores the complexities involved in transitioning public transport to hydrogen fuel and the critical need for strategic planning to establish a feasible hydrogen refueling infrastructure. The previous study focused on two elements, production and distribution. The study of Almansoori and Shah (2006) integrates these components into a cohesive framework that identifies optimal infrastructure and operating costs for the hydrogen supply chain. The study emphasizes the importance of considering technical constraints and economic factors in infrastructure planning. In these studies, single-period models have been capable of providing comprehensive evaluations and designs for supply chains. Additionally, to address complex supply chain scenarios, numerous studies have adopted an approach of altering certain parameters and running the model multiple times to derive diverse strategies. Through this approach, it is possible to identify optimal strategies that are robust under various conditions, thus enhancing the decision-making process in the field of supply chain management.

Contaldi et al. (2008) carries out an in-depth evaluation of various hydrogen implementation scenarios in Italy, including a Baseline scenario and an Alternative one, with the latter forecasting a significant uptick in hydrogen's market share. Almaraz et al. (2015)

Table 2.4: Classification of HSC models with multiple objectives

Reference papers	Financial		Environmental		Social Risk	Other
	Cost	Profit	Emissions	GWP	Safety	
Hugo et al. (2005)	✓			✓		
Brey et al. (2006)	✓		✓			
Li et al. (2008)	✓			✓		
Lin et al. (2008)	✓		✓			
J. Kim and Moon (2008)	✓		✓		✓	
Guillen-Gosalbez et al. (2010)	✓		✓			
Hwangbo et al. (2018)	✓			✓		
Qadrdan et al. (2008)	✓			✓		
Sabio et al.(2010)	✓				✓	
Sabio et al. (2012)	✓		✓			
Almaraz et al. (2013)	✓			✓	✓	
Han et al. (2013)	✓		✓		✓	
Balta-Ozkan and Baldwin (2013)	✓		✓			
Almaraz et al. (2015)	✓			✓	✓	
Robles et al. (2016)	✓			✓	✓	
Wulf and Kaltschmitt (2018)	✓		✓			
Ogumerem et al. (2018)		✓				
Bique et al. (2019)	✓		✓		✓	
Ochoa Robles et al. (2019)	✓		✓			
Camara et al. (2019)	✓			✓		
Fazli-Khalaf et al. (2020)	✓		✓		✓	✓
Robles et al. (2020)	✓			✓	✓	
Cantu et al. (2021)	✓		✓			
Gabrielli et al. (2020)	✓		✓			
Ehrenstein et al. (2020)	✓		✓			
Cantu et al. (2020)	✓			✓		
L. Ren, Zhou, and Ou (2020)	✓			✓		
Robles et al. (2020)	✓	✓		✓		
Carrera and Azzaro-Pantel (2021)	✓			✓		✓
Talebian et al. (2021)	✓		✓			
L. Li, Feng, Manier, and Manier (2022)	✓			✓		
Reyes-Barquet et al. (2022)		✓		✓		
Almaraz et al. (2022)	✓			✓	✓	✓
Ibrahim and Al-Mohannadi (2023)	✓		✓			
Peng et al. (2023)	✓		✓			
Erdogan et al.(2023)	✓		✓		✓	
Cantu et al. (2023)	✓			✓		
Meng et al. (2023)	✓		✓		✓	
M. Li, Ming, Huo, Mu, and Zhang (2023)	✓		✓			
Erdoğan and Güler (2023)	✓		✓		✓	

GWP: Global warming potential.

introduced a detailed framework for HSC design, showcasing how hydrogen infrastructure can be feasibly implemented at both regional and national levels. In the French case study, projections for future hydrogen demand take into account various scenarios of market penetration from 2020 to 2050, with an anticipated steady rise in the market share of FCEVs. These scenarios are instrumental in assessing the design and operational tactics of Hydrogen Supply Chains (HSC) across different time intervals. Similarity, A study delves into Turkey's HSC network by 2050, methodically analyzing a spectrum of demand scenarios, from a modest 5% to an ambitious 50% HFCV penetration rate. This investigation employs a multi-objective optimization model that balances weighs cost, CO2 emissions, and safety considerations (Erdoğan, Geçici, & Güler, 2023).

2.4.7.2/ MULTI-PERIOD

Almansoori and Shah (2009) expanded upon their earlier work by formulating a multi-period mathematical model. This model segments the planning horizon into several time frames, allowing for consideration of the gradual escalation in hydrogen demand and the consequent requirement for infrastructure expansion. Through this staged methodology, the model can adjust to evolving circumstances, facilitating step-by-step decisions regarding the establishment of production facilities, storage units, and transportation infrastructures. Yoon, Seo, and Lee (2022) similarly divide the planning timeline into various intervals to accommodate the slow rise in hydrogen demand and the associated requirements for infrastructure development. The multi-period model built enables incremental decisions to be made in establishing production sites, storage capacity, and transportation systems in response to changing scenarios. In addition, these studies also designed the hydrogen entire network over multiple periods based on different hydrogen demand scenarios in the future. (Almansoori & Shah, 2012)(Nunes, Oliveira, Hamacher, & Almansoori, 2015)(Dayhim, Jafari, & Mazurek, 2014). Moreover, Güler et al. (2021) proposed a multi-period model aimed at addressing Turkey's transportation sector's demand in the HSC network for the forthcoming three decades. S. Han and Kim (2019) and Cho and Kim (2019) propose a comprehensive approach to complex strategic decision-making over a long time period based on renewable energy systems and biomass systems, respectively. Overall, the multi-period approach enables decision-makers to account for the dynamic nature of hydrogen demand and infrastructure development costs, leading to efficient and cost-effective HSC management, thereby facilitating a scalable and sustainable hydrogen economy.

2.4.8/ UNCERTAINTY

Managing uncertainty within the Hydrogen Supply Chain (HSC) is essential, given the dynamic advancements in hydrogen production technologies, shifts in market demand, modifications in regulations, and changes in the prices of raw materials and energy. Such uncertainties can profoundly affect the planning, design, and execution of HSCs. In contrast, deterministic models might not offer the required flexibility and adaptability, rendering them less practical for real-world operations and future strategizing.

2.4.8.1/ SOURCES

The analysis of the literature segmented the papers by their identified sources of uncertainty, broadly covering three key areas: market uncertainty, concerning hydrogen energy's demand and supply; economic uncertainty, including the capital cost related to hydrogen energy's production, storage, transport, and refueling, along with operational expenses, fluctuation in raw material prices, and variability in hydrogen product prices; and technological uncertainty, involving the practicality and productivity of technologies throughout the supply chain. We found that among the 19 papers reviewed, demand is the most frequently studied source of uncertainty, followed by the operational costs of the system and the supply rate of raw materials. Other uncertainties, including the prices of raw materials, capital costs, the price of hydrogen energy, and the availability of energy received significantly less attention. Table 2.5 displays the specific information.

Moreover, many studies have also conducted scenario planning, where developing and analyzing multiple scenarios based on different assumptions about the future (for example, high and low hydrogen demand, and changes in the regulatory environment). This approach aids strategic planning by assessing the effects of multiple uncertainties, although these analyses are not depicted in the table presented (Ingason, Ingolfsson, & Jensson, 2008; Qadrdan, Saboohi, & Shayegan, 2008; Konda, Shah, & Brandon, 2011; J.-H. Han, Ryu, & Lee, 2012; Murthy Konda, Shah, & Brandon, 2012; M. Kim & Kim, 2016; Ogumerem et al., 2018; Almaraz et al., 2022).

Demand uncertainty represents a significant challenge in the management of the hydrogen energy supply chain. It can lead to either overinvestment or insufficiency in production capacity, storage facilities, and the design of logistics networks, thereby impacting the system's overall efficiency and cost-effectiveness. In addressing demand uncertainty, most studies typically consider the penetration rate of hydrogen energy in the transportation sector over different periods (J. Kim, Lee, & Moon, 2008; Almansoori & Shah, 2012; Dayhim et al., 2014; Nunes et al., 2015; Hwangbo, Nam, Han, Lee, & Yoo, 2018; Yang et al., 2020; Ochoa Bique, Maia, Grossmann, & Zondervan, 2023; Vijayakumar, Jenn, & Ogden, 2023). Only one article took into account the uncertainty in hydrogen demand due to the variability of crude oil raw materials or the specifications of the final products in a refinery. This model facilitated the optimal allocation, routing, and flow distribution of hydrogen between production and consumption units within the refinery (Jagannath & Almansoori, 2014).

Hydrogen energy projects often necessitate substantial capital investment and long-term operations. As technological advancements are made and economies of scale are achieved, the costs associated with equipment and technology are on a downward trend. However, the pace and extent of this trend carry uncertainty, which can significantly affect the prediction of long-term investment decisions and the period for cost recovery. Fazli-Khalaf et al. (2020) addressed mixed uncertainty problem, primarily focusing on the costs of establishing and operating a hydrogen supply chain network, including production, storage, transportation, and distribution. Additionally, two other studies discussed the uncertainty surrounding operational costs (Sabio et al., 2010; Hwangbo, Lee, & Han, 2017). The production costs of hydrogen energy are also influenced by the fluctuation in energy prices, such as electricity and natural gas prices, particularly for electrolysis-based hydrogen production. The uncertainty in energy prices adds to the unpredictability of operational costs, thereby affecting the competitive pricing of hydrogen energy. Hwangbo, Lee, and Han (2016) specifically considered the uncertainty in the prices of raw materials such as fuel, water, electricity, and natural gas. The study modeled these uncertainties using stochastic methods, capturing the potential variations in raw material costs by defining scenarios with associated probabilities.

The consideration of uncertainty in the supply rate of raw materials mainly exists in renewable energy systems because their supply has obvious intermittent and variable characteristics. Reyes-Barquet et al. (2022) focused on the sugarcane industry, estimated hydrogen production potential based on the availability of electricity generated from burning sugarcane bagasse. The study distinguished between the harvesting and non-harvesting seasons, accounting for the fluctuating electricity rates and energy availability for hydrogen production, with each period's length treated as an uncertain parameter modeled through probability distributions. Similarly, Guo, Tan, Zhu, and Gu (2022) explored the supply uncertainty of available straw resources to design and optimize various types of biomass-based renewable hydrogen production systems, facilitating logistics opera-

tions under demand fluctuation conditions and providing strategic decisions for planning biomass-to-hydrogen systems. Yang et al. (2020) considered the uncertainties in wind power supply and hydrogen demand. Meanwhile, Won, Kwon, Han, and Kim (2017) developed a model to determine the optimal configuration and operation of a hydrogen supply system powered by renewable energy sources (RES), including wind turbines, photovoltaic panels, dish-Stirling power systems for electricity generation, and technologies for hydrogen production and supply. Collectively, these models more accurately simulate actual hydrogen supply chain networks (HSCNs), enabling rational infrastructure deployment and operation, thus bringing economic and environmental benefits to the entire supply chain. Moreover, Câmara, Pinto-Varela, and Barbósa-Povoa (2019) discuss about the availability of primary energy sources (PES).

2.4.8.2/ MODELING APPROACHES

In most models, stochastic programming approaches are employed, incorporating random elements into the HSC model. This is achieved by considering a variety of possible future scenarios and their corresponding probabilities. For instance, Reyes-Barquet et al. (2022) utilizes probability distributions for key parameters to capture the inherent uncertainty in agro-industrial waste supply and hydrogen demand. Hwangbo et al. (2016) uses the inverse normal cumulative distribution function (NORMINV) to generate scenarios for raw material price fluctuations. Additionally, some models employ a two-stage stochastic programming approach to account for uncertainty in operational conditions. In this model, Almansoori and Shah (2012) uses the sample average approximation technique to address the demand uncertainty problem. Another study makes preliminary decisions in the first stage and adjusts these decisions after the uncertainties are revealed (in the second stage) Jagannath and Almansoori (2014).

Alternative approaches encompass Fuzzy Programming, where uncertain parameters and decision variables are depicted through fuzzy numbers or sets; Chance Constraint Programming, which assigns a probability level to each constraint, establishing the bounds of the constraint with a specified confidence level; and Density-Based Spatial Clustering of Applications with Noise (DBSCAN), a method that clusters points that are closely situated according to a predefined distance metric, while identifying points in areas of low density as outliers. Fazli-Khalaf et al. (2020) introduces a hybrid fuzzy possibility flexible planning approach, designed to address both the uncertainty in cost parameters and the adaptability of model capacity constraints and demands simultaneously. A study optimizes two types of uncertainties concurrently: wind power uncertainty is managed through chance-constrained programming, while hydrogen demand uncertainty is tackled using a density-based clustering approach. The DBSCAN technique creates numerous potential demand scenarios via Monte Carlo simulation, clustering these scenarios around a central, core scenario if they have a significant number of neighbors. By averaging out the scenarios within each cluster, a ”representative” demand scenario is produced for use in the network’s optimal design model. This method offers improved resilience to the variability inherent in real-world hydrogen fuel demand (Yang et al., 2020).

Table 2.5: Classification of uncertainty throughout the reviewed article

Classification of Uncertainty	Parameter	Articles
Market	Transportation Demand	(J. Kim et al., 2008) (Almansoori & Shah, 2012) (Dayhim et al., 2014) (Nunes et al., 2015) (Hwangbo et al., 2017) (Hwangbo et al., 2018) (Yang et al., 2020) (Ochoa Bique et al., 2023) (Vijayakumar et al., 2023)
	Industry demand	(Jagannath & Almansoori, 2014)
Financial	Raw material price	(Hwangbo et al., 2016)
	Hydrogen price	(Rathi, Pinto, & Zhang, 2023)
	Capital cost	(Fazli-Khalaf et al., 2020)
	Operating cost	(Sabio et al., 2010) (Hwangbo et al., 2017) (Fazli-Khalaf et al., 2020)
Technology	Availability of energy sources	(Câmara et al., 2019)
	Feedstock Supply rate	(Won et al., 2017) (Yang et al., 2020) (Reyes-Barquet et al., 2022) (Guo et al., 2022)

2.4.9/ INVESTMENT STRATEGY

An effective investment strategy can enhance the competitiveness of hydrogen by optimizing costs, risks, and environmental impacts across the entire supply chain. Several researchers have optimized the structure and operational strategies of the HSC. Timmerberg and Kaltschmitt (2019) considered to produce hydrogen in North Africa from renewable energy sources and transported to Europe by existing pipelines of natural gas. This system could ignore the need to build and adapt infrastructure and make hydrogen become the cheapest form of fuel supply for electricity. Seo et al. (2020) design a hydrogen network structure with a centralized hydrogen storage area and found that a centralized storage system can reduce the total annual cost of the entire hydrogen supply chain. G. He, Mallapragada, Bose, Heuberger, and Gençer (2021) developed a supply chain network model with flexible transmission and storage scheduling, which enables hydrogen trucks and pipelines to be used for two functions, transport tools and storage resources. The application results in the eastern US show that flexible scheduling of hydrogen transmission and storage resources is essential for cost minimization and the choice of production technology. J.-S. Lee et al. (2022) compared five different storage technologies during intercontinental hydrogen transportation in terms of economic and environmental performance. They found the toluene-methylcyclohexane supply chain is the most cost-effective and environmentally friendly technology for long-distance seaborne hydrogen transportation. Forghani et al. (2023) introduced a model employing pipelines and tube trailers for hydrogen transport, leading to a satisfied supply chain design compliant with

CO_2 emission regulations. (Yoon et al., 2022) Integrate by-product hydrogen sources and existing infrastructure natural gas (NG) pipelines into supply chain design models. The study found that utilizing NG pipelines and by-product hydrogen significantly reduces the levelized cost of hydrogen. The cost savings are more pronounced when both resources are used together, demonstrating their synergistic effects on minimizing total HSC costs.

2.5/ SOLUTION METHODS

2.5.1/ MATHEMATICAL PROGRAMMING

The issues discussed are predominantly resolved through the development of a linear programming model (16 cases) or a mixed-integer linear programming model (86 cases), utilizing optimization solvers for resolution. Almansoori and Shah (2009) crafted a deterministic model for the hydrogen supply chain network, aiming to minimize the average total daily cost, and solved it with the GAMS commercial software tool, a choice also made by (Shamsi, Tran, Akbarpour, Maroufmashat, & Fowler, 2021) and (Carrera & Azzaro-Pantel, 2021). The rest of the deterministic models that focus on a single objective are often processed using the CPLEX solver. Linear programming challenges are tackled using the simplex method or its derivatives within these commercial solvers. To solve mixed integer linear programming problems, the branch and bound method is typically employed, breaking down the main issue into manageable sub-problems for resolution. This method aims to find the optimal solution but its efficiency is influenced by the problem's specific characteristics, such as constraint tightness and the diversity and types of variables involved. In more intricate scenarios that involve expansive networks over numerous periods, a variety of raw materials, and multiple objectives, the computational demand escalates, often making it impractical to obtain a global optimal solution within a reasonable timeframe using commercial solvers. To reduce the computational complexity of the model, the Two-Step Sequential Strategy has been introduced in several studies. Sabio et al. (2010) initially tackles a simplified version of the problem by treating integer variables as continuous, which establishes the lower bound for the optimal solution. Following this, the slave problem is addressed by applying the master problem's solution to outline a narrower problem scope, reintegrating integer constraints to refine the solution further. This method edges closer to the optimal solution with the benefit of reduced computational load. Cantú et al. (2021) convert the issue into a two-level optimization challenge. The upper-level concerns revolve around strategic decisions in HSC planning, including the ideal location, scale, and variety of production and storage units. Linear programming methods are applied at the lower level for the continuous optimization of production efficiency and transportation flow.

2.5.2/ METAHEURISTIC ALGORITHM

2.5.2.1/ GENERIC SUPPLY CHAIN PROBLEM WITH METAHEURISTICS

The studies we reviewed in this section are all applied to general supply chains. Metaheuristic algorithms are adept at tackling intricate optimization challenges. These methods, unlike exact solutions, may not always deliver the optimal solution but are capable of identifying high-quality solutions efficiently and with reduced computational demands.

Their use in addressing complex supply chain issues has been extensively investigated. Goodarzian, Kumar, and Abraham (2021) developed a hybrid genetic algorithm for resolving the complex multi-supplier, multi-period inventory routing problem, demonstrating superior performance and effectiveness for large-scale problems compared to the Cplex solver. Saracoglu, Topaloglu, and Keskinturk (2014) presented a novel integer linear programming model for the multi-product, multi-period inventory dilemma, enhancing it with a genetic algorithm that includes a local search feature for efficiently managing large-scale problems. Goodarzian et al. (2021) introduced two metaheuristic algorithms, a hybrid of genetic algorithm with simulated annealing and another combining genetic algorithm with particle swarm optimization, specifically designed to address the intricacies of large-scale supply chains that incorporate extensive datasets. Salahi, Daneshvar, Homayounfar, and Shokouhifar (2021) offered a hybrid genetic-simulated annealing algorithm, noted for its high efficiency despite demanding more CPU time. Sánchez, Martín, and Zhang (2021) studied a heuristic decomposition approach for supply chains with large-scale seasonal energy storage. These contributions underscore the effectiveness of metaheuristic methods in refining supply chain optimization, providing adaptable and potent solutions for complex and data-heavy issues.

2.5.2.2/ HYDROGEN SUPPLY CHAIN PROBLEM WITH METAHEURISTICS

We only found a few studies focused on hydrogen energy supply chains. Ehrenstein, Wang, and Guillén-Gosálbez (2019) propose a heuristic method for the selection of scenarios based on the sample-average approximation method to deal with the risk from rare events in the management of the hydrogen supply chain while reducing CPU running time. Robles, Azzaro-Pantel, and Aguilar-Lasserre (2020) explores the use of a non-dominated sorting genetic algorithm (NSGA-II) to solve multi-objective optimization problems in the hydrogen supply chain and applies it to the Midi-Pyrénées region of France. It found that the solutions produced have the same order of magnitude as obtained by mixed integer linear programming methods, while the approach proposed is more robust. Y.-B. Woo and Kim (2019) developed a matheuristic method to address the hydrogen supply chain problem with replenishment cycles based on the genetic algorithm and combined with mixed integer linear programming for the mono-period cases.

2.5.3/ MULTI-OBJECTIVE APPROACHES

In the studies examined, multi-objective problems are commonly addressed through the ϵ-constraint method (21 articles), which results in a collection of Pareto optimal solutions. This approach converts a multi-objective problem into multiple single-objective problems by optimizing one objective primarily and setting the others as constraints within defined limits. The Pareto frontier that emerges encompasses all potential optimal solutions. Decision-makers then select the most suitable solution based on their preferences. Other solution methods can be divided into Weighted sum, Genetic Algorithm, Multi-objective Evolutionary Algorithms, Fuzzy approach, progressive hedging algorithm, and ϵ-constraint with lexicography. The table 2.6 shows corresponding reference papers.

The research of Yoon et al. (2022) employs objective functions such as total daily cost (TDC), total daily global warming potential, and total relative risk index. Multi-objective optimization is conducted using the ϵ-constraint method, while the final solution is se-

lected from Pareto optimal solutions using the M-TOPSIS (Multi-criteria Optimal Solution and Worst Solution Ranking) method. By assigning varied weights to different objectives, this method facilitates determining the dominance of each solution and aids decision-makers in selecting from multiple optimal solutions. Sabio, Kostin, Guillén-Gosálbez, and Jiménez (2012) combines multi-objective optimization with principal component analysis (PCA). After generating a set of Pareto-optimal solutions using the MILP model, PCA is applied to these solutions. The Lexicography method refers to the ranking of objectives according to their importance. The optimization is then performed in stages, starting with the highest priority objective. ϵ-constraint combined with Lexicography ensures that the solution found before the next objective is considered is optimal for the highest priority objective. This was verified in the study of Câmara et al. (2019)

The weighted constraint technique merges all objectives into a single composite function by summing up the objectives, each multiplied by its respective weight, with the total of these weights equal to 1. This approach simplifies the problem into a solitary objective. Erdoğan et al. (2023) applied this strategy to simultaneously address the objectives of minimizing costs, CO2 emissions, and risks.

Genetic algorithms draw their inspiration from natural selection and genetic processes. This algorithm works with groups of potential solutions, employing mechanisms of selection, crossover, and mutation to progress toward improved solutions. Three studies applied it and Robles, Azzaro-Pantel, and Aguilar-Lasserre (2020) particular emphasis on a variant termed the NSGA-II. This approach guarantees a diversity of solutions and enables the automatic generation of balanced solutions that take into account various objectives. Cantú et al. (2021) introduced a multi-objective evolutionary algorithm to balance financial expenses against environmental impact, yielding a range of Pareto-optimal outcomes. It is based on the genetic algorithms. Meanwhile, Two other articles written by Cantu et al. also introduce this method (Cantú, Ponsich, Azzaro-Pantel, & Carrera, 2023; Cantú, Azzaro-Pantel, & Ponsich, 2020).

J.-H. Han, Ryu, and Lee (2013) employs a fuzzy methodology to determine balanced solutions among various goals. This method initially pinpoints the optimal and least desirable outcomes in terms of economics, safety, and environmental impact. Subsequently, linear association functions are established for these fuzzy goals, scaling all objective values to a range between 0 and 1, depending on their proximity to the best and worst scenarios. The aim of the optimization is to enhance the collective fulfillment of all objectives. Fazli-Khalaf et al. (2020) also employs a mixed fuzzy possibilistic flexible programming method to solve the multi-objective optimization problem of designing a hydrogen supply chain network. This approach integrates various objectives, including cost minimization, environmental impact reduction, and social responsibility enhancement. The Progressive Hedging algorithm works to address this challenge by decomposing the complex stochastic problem into simpler, scenario-based subproblems. It then iteratively refines the solutions to these subproblems, ensuring that they converge to feasible and optimal solutions (Meng, He, Hu, & Han, 2023).

2.6/ CONCLUSION

This chapter offers an extensive overview of contemporary research themes and developments in optimizing and modeling issues related to Hydrogen Supply Chain Network

Table 2.6: Classification of solution method for multi-objective problems

Classification of solution methods	Articles
Weighted sum	(Erdoğan et al., 2023)
Genetic Algorithm	(Robles, Almaraz, & Azzaro-Pantel, 2016)
	(Robles, Azzaro-Pantel, & Aguilar-Lasserre, 2020)
	(Reyes-Barquet et al., 2022)
Multi-objective Evolutionary Algorithms	(Cantú et al., 2020)
	(Cantú et al., 2021)
	(Cantú et al., 2023)
Fuzzy	(Fazli-Khalaf et al., 2020)
	(J.-H. Han et al., 2013)
progressive hedging algorithm	(Meng et al., 2023)
ϵ-constraint with lexicography	(Câmara et al., 2019)
ϵ-constraint	21 multi-objective articles

Design (HSCND). The literature is classified according to supply chain configurations including feedstock, production, transportation, and end-users, as well as modeling attributes such as decision variables, spatial and temporal resolution, technology source, performance measures, cyclicality, stochasticity, and the portfolio of investment strategies, alongside solution methodologies.

The literature review clearly demonstrates that despite the extensive body of research dedicated to optimizing supply chain systems, gaps persist that warrant further exploration. Notably, while evaluations concerning economic viability and environmental impact have been conducted, there is still a lack of detailed research defining these performance indicators. Furthermore, each critical sector of the supply chain, including production, storage and conditioning, transportation and distribution, and refueling, plays a pivotal role. The Four-echelon supply chain models, particularly those addressing multi-period scenarios and environmental impact assessments, received scant attention in existing studies. Additionally, among the solution methodologies explored, there lacks a universally acknowledged and effective strategy capable of managing the complexities inherent in large-scale Hydrogen Supply Chain (HSC) design endeavors efficiently.

Based on the above research gaps, the thesis focuses on the entire hydrogen energy supply chain system. It begins by conducting a Techno-economic analysis of the supply chain, improving economic and environmental performance indicators, and assessing the application prospects of hydrogen energy under various scenarios from both cost and emission perspectives. Then, this research designs a four-echelon centralized storage supply chain model to address the multi-period, multi-objective environmental investment strategy problem in the HSC. Finally, it integrates metaheuristics to solve computational challenges within the model. The main content is arranged as shown in the figure 2.7.

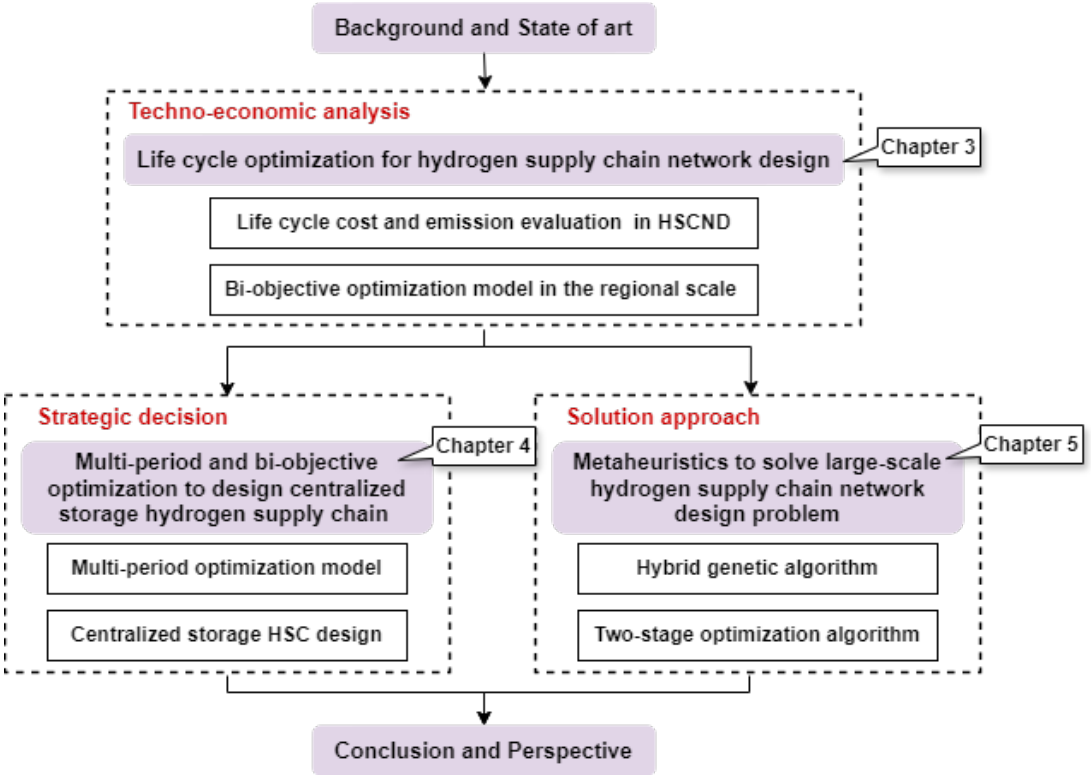

Figure 2.7: Organization of thesis

II

CONTRIBUTION

3

LIFE CYCLE OPTIMIZATION FOR HSCND

This chapter focuses on the development of a life cycle optimization (LCO) modeling framework for the design of hydrogen supply chain networks. The framework integrates the methodologies of life cycle cost (LCC) evaluation and life cycle emission assessment (LCA) within a bi-objective optimization model, targeting both the levelized cost of hydrogen (LCOH) and the global warming potential (GWP) intensity as its core objectives. To resolve this optimization problem, the ϵ-constraint method is employed, facilitating an exploration of the trade-offs between economic efficiency and environmental impact. The utility of the proposed LCO framework is demonstrated through its application to a case study in Franche-Comté, France, serving as a comparative analysis. The approach presented in this chapter enhances the economic and environmental performance indicators previously used in HSCND papers, providing solutions for sustainable HSCND.

3.1/ INTRODUCTION

Governments worldwide are providing support through financial incentives and regulatory measures to realize the vision of decarbonization. International Energy Agency (2021b) claimed that 17 governments had released hydrogen strategies, and more than 20 governments have publicly announced they are working to develop strategies. Numerous companies are seeking to tap into hydrogen business opportunities. Hydrogen Council (2021) reported that 200 hydrogen projects and ambitious investment plans had been announced. Fig. 3.1 shows the distribution of these projects.

As mentioned in the previous chapter, there are substantial hurdles that must be tackled to facilitate a successful shift towards hydrogen-based energy systems and the establishment of a hydrogen economy. One of the main obstacles is the high cost of the hydrogen supply chain, as it is consistently more costly to utilize hydrogen compared to fossil fuels. Although governments have imposed various policies (such as lower tax rates) to bridge the gap between fossil fuels, these measure falls short of offsetting the higher cost (International Energy Agency, 2021b). Meanwhile, emissions from processes other than the end-use application, including manufacturing, storage, and transportation cannot be ignored. Adopting a hydrogen energy program aims to reduce overall greenhouse gas emissions to achieve the stringent climate policy goal(Gül, Kypreos, Turton, & Barreto, 2009). Hydrogen consumption at the end user can produce zero emissions, but the other

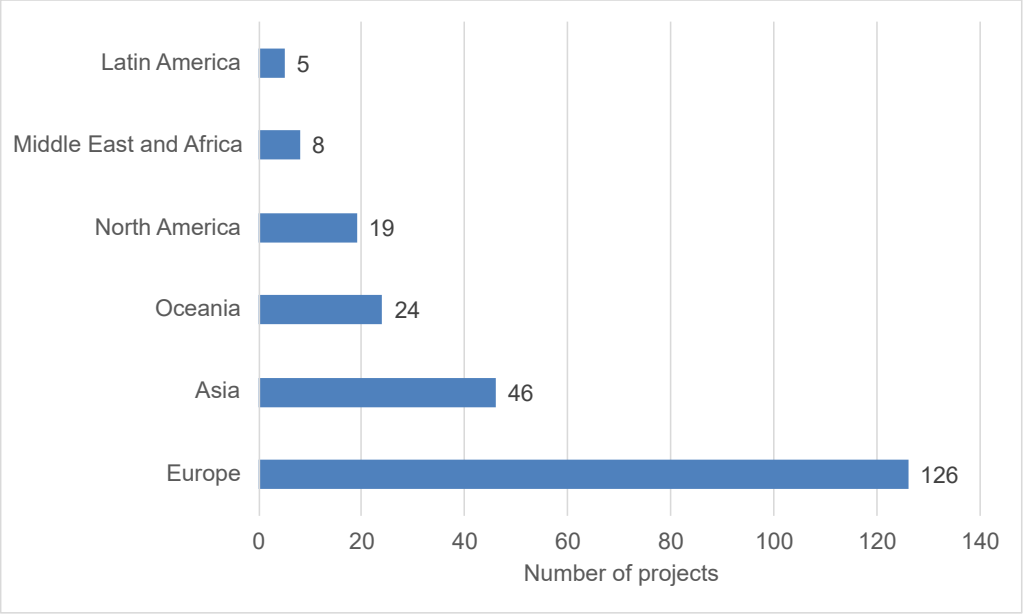

Figure 3.1: Global hydrogen projects announced by region 2021 (Sönnichsen, 2021).

processes in the supply chain, such as the production of blue hydrogen (use of methane as a feedstock and reduction of greenhouse gas emissions through carbon capture and storage technologies) and grey hydrogen (without any technologies to reduce or capture CO2 emissions), have a very high environmental impact(Ocko & Hamburg, 2022). It is impossible to have the most economical and environmentally friendly supply chain of hydrogen at the same time (Wulf & Kaltschmitt, 2018). Therefore, in the modeling process, how to scientifically evaluate and define both aspects has a significant impact on supply chain network design.

HSCND is a subset of supply chain network design (SCND). Due to growing concerns about global climate change and carbon emissions, more and more SCNDs are labeled with “green” or “sustainability”. Life cycle optimization (LCO), a multi-objective optimization involving life cycle costing (LCC) and life cycle assessment (LCA), has been widely used in SCND for its ability to evaluate the environmental and economic performance of alternative systems simultaneously. The design of the HSCN in the transportation sector begins with raw materials and ends with the sale of hydrogen at refueling stations. There are multiple choices available in each section, and optimization approaches help decision-makers select the optimal planning and operation strategies.

The purpose of this chapter is to conduct an LCO methodology for HSCND and to develop a mathematical model that encompasses the entire hydrogen supply network. The modeling framework is completed by the author and colleagues. The remainder of this chapter is divided into five main sections. Section 3.2 analyzes the economic evaluation and emissions assessment relevant scientific literature. Section 3.3 describes in detail the LCC and LCA in HSCND. Section 3.4 presents the proposed bi-objective modeling framework. Section 3.5 describes the selection of instances, input data, as well as results and discussions. In the end, Section 3.6 provides the conclusions for this research.

3.2/ LITERATURE REVIEW

3.2.1/ SUPPLY CHAIN NETWORK DESIGN

Due to growing concerns about global climate change and carbon emissions, more and more SCND publications are labeled with ”green” or ”sustainability”. Waltho, Elhedhli, and Gzara (2019) reviewed the literature on green SCND. They investigated environmental policies adopted in SCND. The prevalent sources of emissions within the supply chain were also listed. The authors indicated that the life cycle assessment had been selected by many researchers as a technique to account for a product's environmental impact comprehensively. Moreno-Camacho, Montoya-Torres, Jaegler, and Gondran (2019) provided a systematic literature review of the sustainability metrics used in the SCND problem. Three dimensions of sustainability, economic, environmental, and social, were characterized and classified. The authors found a highlighted emphasis on environmental considerations. Lotfi et al. (2021) offered a way to enhance the sustainability of an SCND by considering renewable energy. A two-stage robust stochastic optimization model was proposed. Closed-loop supply chain network design has also received considerable attention as it ensures many diverse industries toward sustainability (MahmoumGonbadi, Genovese, & Sgalambro, 2021). Salehi-Amiri, Zahedi, Akbapour, and Hajiaghaei-Keshteli (2021) developed a closed-loop SCND for the walnut industry in the agricultural sector. Mixed-integer linear programming (MILP) was used to optimize the overall costs of the agricultural supply chain with the consideration of forward and reverse logistics. A new closed-loop SCND proposed by Chouhan, Khan, and Hajiaghaei-Keshteli (2022) is inspired by the disorganized disposal of by-products from sugarcane mills. The proposed sustainable sugarcane supply chain network considers carbon taxes on the emission from industries and during transportation of goods.

3.2.2/ LIFE CYCLE OPTIMIZATION IN SCND

Life cycle optimization (LCO) has been widely used in supply chain network design for its ability to simultaneously evaluate the environmental and economic performance of alternative systems (Qu et al., 2018). LCO enables static life cycle assessment (LCA) and techno-economic analysis, such as life cycle costing (LCC), to be performed dynamically to generate and optimize alternative strategies. Gao and You (2017) addressed the life cycle economic and environmental optimization of a supply chain network considering both design and operational decisions under uncertainty. The model is tested with Illinois, USA's county-level hydrocarbon biofuel supply chain. Gao and You (2018a) proposed a modeling framework integrating LCO methodology with the dynamic material flow analysis approach for sustainable design of shale gas supply chain. The LCO framework developed by Gao and You (2018a) was applied to case studies on emissions throughout the bioethanol life cycle. The framework considers emissions from feedstock production, transportation, and end-use. Gao and You (2018b) applied an LCO approach to a well-to-wire shale gas supply chain in the UK. Three environmental categories are considered: life cycle greenhouse gas emissions, water consumption, and energy consumption.

Tian, Meyer, Lee, and You (2020) developed a sustainable design of geothermal power systems under economic and environmental criteria through the LCO approach. N. Zhao, Lehmann, and You (2020) discussed the LCO within the poultry litter supply chain, focus-

ing on pyrolysis technologies designed to transform poultry waste into biofuel and biochar sustainably. The multi-objective LCO optimization framework maximizes annualized profit per functional unit and minimizes the annual CO_2-equivalent greenhouse gas emissions per functional unit. X. Zhao and You (2021) proposed an LCO framework to determine the economically and environmentally optimal high-density polyethylene chemical waste recycling technology pathway. The LCO problem is formulated as a multi-objective mixed-integer nonlinear fractional programming problem and solved by an optimization algorithm that integrates the inexact parametric algorithm and branch-and-refine algorithm. Solis et al. (2021) developed a multi-objective LCO model that simultaneously optimizes cost and environmental impact. They adopted the principle of resource recovery and recirculation to design a sustainable circular bioeconomy. Negri et al. (2021) developed an LCO model for the design and optimization of the supply chain of BECCS (bioenergy with carbon capture and storage). The model explored the complexity of the infrastructures involved in realizing a large-scale system and the sequestration potential of bioenergy in Europe.

3.2.3/ Economic performance measures used in previous HSCND studies

Nearly half of the HSCND optimization models choose to minimize the total daily cost (TDC). In contrast, others prefer to minimize the total annual cost (TAC) or total supply chain cost (TSCC), as shown in Table 3.1 [1].

We classified the cost calculation methods into three types and used the TSCC as an example to show their differences.

- *Type A:* More than half of the models simply combine the capital and operating cost of various supply chain components (such as supply facilities and transportation vehicles):

$$TSCC = \sum_t (FCC_t + TCC_t + FOC_t + TOC_t) \tag{3.1}$$

  where FCC_t and FOC_t are the facility capital and operating cost in period t, respectively. TCC_t and TOC_t are the transportation capital and operating cost in period t, respectively.

- *Type B:* Discounting all the costs to the start year:

$$TSCC = \sum_t [(FCC_t + TCC_t) * DR_t + FOC_t + TOC_t] \tag{3.2}$$

  where DR_t is the discount rate of time period t, it can be used to convert future cash flows into current values, which is defined as:

$$DR_t = \frac{1}{(1+d)^{t-1}} \quad \forall \quad t \tag{3.3}$$

  where d is the discount rate.

[1] Although the objective in Refs. (Ogumerem et al., 2018; Parker, Fan, & Ogden, 2010) is maximizing the profit; it is obtained with given demands, supplies, and hydrogen market price.

Table 3.1: Economic performance measures used in previous studies (Part One)

	Performance measures			Calculation methods		
	TDC	TAC	TSCC	Type A	Type B	Type C
Agnolucci, Akgul, McDowall, and Papageorgiou (2013)			•		•	
Almansoori and Betancourt-Torcat (2016)	•					•
Almansoori and Shah (2012)	•			•		
Bique, Maia, La Mantia, Manca, and Zondervan (2019)		•		•		
Bique, Maia, Grossmann, and Zondervan (2021)	•			•		
Cantú et al. (2021)	•					•
Cho et al. (2016)		•				•
Dayhim et al. (2014)	•			•		
Almaraz et al. (2013)	•			•		
Almaraz, Azzaro-Pantel, Montastruc, and Domenech (2014)	•			•		
Almaraz et al. (2015)	•			•		
Ehrenstein, Galán-Martín, Tulus, and Guillén-Gosálbez (2020)			•	•		
Fazli-Khalaf et al. (2020)			•	•		
Gabrielli et al. (2020)		•				•
Güler et al. (2021)	•			•		
Gunawan, Williamson, Raine, and Monaghan (2021)	•					•
J.-H. Han et al. (2012)	•			•		
J.-H. Han et al. (2013)	•			•		
C. He, Sun, Xu, and Lv (2017)		•		•		
Hwangbo et al. (2017)	•			•		
Johnson and Ogden (2012)		•				•
Kazi, Eljack, El-Halwagi, and Haouari (2021)		•		•		
M. Kim and Kim (2017b)	•			•		
M. Kim and Kim (2016)	•			•		
A. Kim, Kim, Lee, Lee, and Lim (2021)		•				•
Lahnaoui, Wulf, Heinrichs, and Dalmazzone (2018)			•		•	
L. Li et al. (2020)	•			•		
Mah et al. (2022)		•				•
Moreno-Benito, Agnolucci, and Papageorgiou (2017)			•		•	
Konda et al. (2011)		•			•	
Nunes et al. (2015)	•			•		
Ochoa Robles, Giraud Billoud, Azzaro-Pantel, and Aguilar-Lasserre (2019)	•					•
Ogumerem et al. (2018)			•		•	
Parker et al. (2010)		•				•
Reuß, Grube, Robinius, and Stolten (2019)			•	•		
Sabio et al. (2012)			•		•	
Seo et al. (2020)			•	•		
Shamsi et al. (2021)	•			•		
Sun et al. (2017)			•	•		
Vom Scheidt, Qu, Staudt, Mallapragada, and Weinhardt (2022)		•				•
Wickham, Hawkes, and Jalil-Vega (2022)			•	•		
Won et al. (2017)		•				•
Y.-b. Woo, Seolhee, Jiyong, and Kim (2016)		•				•
Yang et al. (2020)		•		•		
Yoon et al. (2022)		•		•		
H. Zhao, Kamp, and Lukszo (2021)		•		•		

TDC: total daily cost; TAC: total annual cost; TSCC: total supply chain cost.
Type A: simple combination of capital and operating cost;
Type B: discounting all the costs to the start year;
Type C: taking into account the capital charge.

- *Type C:* Taking into account the capital charge:

$$TSCC = CCF * \sum_{t}(FCC_t + TCC_t) + \sum_{t}(FOC_t + TOC_t) \tag{3.4}$$

where CCF is the capital charge factor, which is defined as:

$$CCF = \frac{d(1+d)^N}{(1+d)^N - 1} \tag{3.5}$$

where N is the length of the analysis period.

HSCND decisions involve large monetary sums, and investments are usually evaluated based on their return rate (Melo, Nickel, & Saldanha-da Gama, 2009). However, the

return on investment has been severely neglected, with only a few models considering the capital charge. Melo et al. (2009) noted that substantial investments lead to a period without profit; therefore, investors wish to invest under the constraint that a minimum return will be gradually achieved. The optimal solution may imply a lack of investor interest if the return on investment is not considered within the model.

It is well acknowledged that the primary purpose of optimization modeling is to provide support for the decision-making process, and economic performance measures should be the critical reference for stakeholders. However, to a large extent, the measures used in previous models serve only to find the optimal configuration of HSCNDs. In other words, the total daily cost is meaningless to policymakers, investors, and markets (customers), mainly because those decisions are made after various comparisons that are taken place not only *inside* the supply chain network but also *outside* the system. Unfortunately, these measures (like total daily cost) cannot be used to compare HSCNDs with other alternatives such as biomass, gasoline, and electricity.

Moreover, except for very recent work by Mah et al. (2022), in all other HSCND models, the authors assume that the lifetime of all supply chain components is greater than or equal to the analysis period. This assumption may lead to inaccurate estimations of capital costs because the replacement cost has been neglected. As shown in Fig. 3.2, the tractor of a GH_2 (gaseous hydrogen) truck has a lifetime of only five years (Department of Energy, 2006). Often a multi-period model sets the analysis period to 20-30 years, and therefore at least three replacements are needed for each tractor employed in the HSCN. In addition, no model takes into account tax and depreciation (except the work of Almansoori and Betancourt-Torcat (2016)). Components of HSCN have different depreciation periods, as illustrated in Fig. 3.2. Therefore, reasonable estimations of capital costs should take this consideration into account.

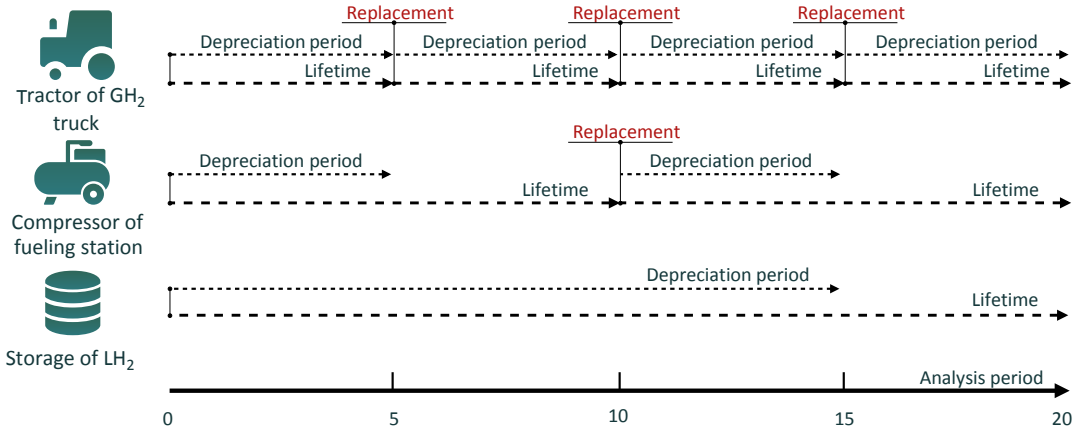

Figure 3.2: Difference between three time-related concepts: analysis period, component lifetime, and depreciation period

3.2.4/ ENVIRONMENTAL PERFORMANCE MEASURES USED IN PREVIOUS HSCND STUDIES

One reason why it is essential to focus on hydrogen alternatives is the risks entailed by climate change (Guillén-Gosálbez, Mele, & Grossmann, 2010). Therefore the environmen-

tal impact is a critical performance measure of HSCN. A consumer survey carried out by the California Air Resources Board (ARB) in 2020 provided fundamental insight into the benefits that FCEV adopters feel primarily motivated their purchase decision (California Air Resources Board, 2020). The most often cited as important was reducing environmental impacts; nearly twice as many respondents chose this over the next-highest factor, savings on the total cost of ownership. This means that the degree of impact on the environment reduced by changing transportation fuel serves as an essential reference for potential FECV buyers. The potential environmental impact plays a vital role in all hydrogen energy-related decision-making processes. For policymakers, comparisons between the environmental impacts of various alternative energy projects are a critical reference to formulate appropriate stimulus policies. Therefore, it is suggested that all studies on HSCND include an environmental impact assessment.

Over the years, there has been an ongoing shift from the traditional end-of-pipe evaluations of waste emissions to life cycle assessment (LCA), where the boundaries are expanded to include every stage in the life cycle. The term *life cycle* refers to the notion that a fair, holistic assessment requires the assessment of feedstock acquirement, production, transportation, and use (Wikipedia contributors, 2020). In an alternative fuel vehicle, most emissions would occur before the fuel reaches the vehicle. Therefore it should carefully consider the life-cycle performance of the fuel supply system. The LCA approach has been widely adopted in comparative analyses of various fuel pathways for road transportation (Orsi, Muratori, Rocco, Colombo, & Rizzoni, 2016; X. Yan & Crookes, 2009; Hwang, 2013; Faria et al., 2013), while it also plays an important role in the design and optimization of energy supply chains. For instance, LCAs have been used to define the environmental performance of supply chains of chemical products (Guillén-Gosálbez & Grossmann, 2009), biomass (You & Wang, 2011), biofuel (Gebreslassie, Slivinsky, Wang, & You, 2013; Gebreslassie, Waymire, & You, 2013; Gong & You, 2014; Wu, Wang, Lee, & Chang, 2017), bioelectricity (Yue, Slivinsky, Sumpter, & You, 2014), and shale gas (Gao & You, 2015). The two major advantages of LCAs are: it is a quantitative method, and it allows researchers to cover the entire life cycle of the product, process, or activity being assessed; it includes a damage model that links the emissions released and waste generated to the corresponding environmental damage (i.e., its contribution to climate change) (Guillén-Gosálbez et al., 2010).

We found fourteen papers on HSCND that include environmental performance measures. J.-H. Han et al. (2013) conducted a multi-objective optimization design of hydrogen infrastructures. Here, the environmental performance measure is represented by the total mitigation cost of CO_2 for HSCN, which comprises emission trading costs and costs related to the carbon capture and storage (CCS) system. The former is obtained by multiplying the price of carbon emission credit and the volume of emissions trading in hydrogen production plants. In contrast, the latter consists of the facility capital cost and operating cost of the CCS system. The major weakness of this approach is that the performance measure serves only to find the optimal solution, and it cannot be used to compare the environmental performance of an HSCND studied with different results or other energy supply chains.

The environmental performance measure in the models of Refs. (Almaraz et al., 2013, 2014, 2015; L. Li et al., 2020; Bique et al., 2019; Ochoa Robles et al., 2019; Gabrielli et al., 2020; Bique et al., 2021; Cantú et al., 2021; Shamsi et al., 2021) is expressed by the total emissions of the HSCN. The emissions related to each echelon of the supply chain are calculated separately, and then they are added together to form the objective. This

approach can be seen as a simplified LCA because only CO_2 emissions are evaluated relative to production, storage, and transportation. The emissions generated by production and storage are mainly dependent on the hydrogen production rate. In contrast, the emissions brought by transportation are determined by the flow rate of hydrogen, the transportation mode, and the delivery distance. Only two studies (Refs. (Ogumerem et al., 2018; Sabio et al., 2012)) stated that the LCA approach had been employed. A common weakness of these two papers regarding the LCA is the lack of the life cycle inventory (LCI) analysis.

3.2.5/ RESEARCH GAP

We did a systematic literature review in the above, including recent SNCD publications, LCO, HSCND, and performance measures adopted in these HSCND models. A trend towards sustainability can be identified in the domain of SCND. Two key aspects distinguish a sustainable SCND from other conventional designs. One aspect is related to performance measures and how these measures are defined; The other is the modeling strategy. Undoubtedly, a sustainable SCND should involve at least two of three dimensions, i.e., economic, environmental, and social. Additionally, how these performance measures are defined also matters. Life cycle costing and life cycle assessment are more and more adopted in recent SCND publications. On the other hand, life cycle optimization receives considerable attention as a suitable modeling strategy for a sustainable SCND.

HSCND is a sub-domain of SCND; however, sustainable HSCND papers are still hard to find. The review above indicates that economic and environmental performance measures used in previous HSCND papers need to be improved. Moreover, the LCO modeling framework should be established for the HSCND. Therefore, this chapter aims to provide our solution for a sustainable HSCND. In the following, life cycle costing and life cycle assessment are introduced to improve economic and environmental performance measures. The modeling framework of life cycle optimization is established with bi-objective optimization.

3.3/ LIFE CYCLE OPTIMIZATION OF HYDROGEN SUPPLY CHAIN NETWORK DESIGN

In this section, firstly, we illustrate how to perform life cycle costing in HSCND. Specifically, we introduce the levelized cost of hydrogen (LCOH) as an economic performance measure obtained through a fixed charge rate (FCR) methodology with a pre-defined internal rate of return (IRR). After that, we conduct a life cycle inventory (LCI) analysis for HSCND to be used in the LCA. Through bi-objective optimization, LCC and LCA are integrated into the modeling framework of life cycle optimization.

3.3.1/ LIFE CYCLE COSTING (LCC) IN HSCND

To perform LCC in HSCND, the LCOH is employed as the economic performance measure. The related methodology (FCR) and concept (IRR) are introduced, followed by a

numerical example.

3.3.1.1/ THE INTERNAL RATE OF RETURN (IRR)

The IRR on an investment or project is the ”annualized effective compounded return rate” or rate of return that sets the net present value of all cash flows (both positive and negative) from the investment equal to zero (Wikipedia contributors, 2021). It is one of the most popular measures used in project selection and capital budgeting (Huang, 2007). In the energy sector, the IRR is often used as one of the economic performance measures in optimization models or technical-economic analyses of single facilities. For example, an IRR serves as one of the economic indices for sizing and optimizing the structure of solar collection systems (Badescu, 2006), while it has also been employed to assess the economic performance of various co-generation plants (Biezma & Cristóbal, 2006; Ruan, Liu, Li, & Wu, 2016; Uris, Linares, & Arenas, 2015). In the domain of supply chain network design, the IRR is often given as a financial parameter used in the calculation of other economic measures. For instance, in an optimization model of biomass-ethanol supply chain (Lin, Rodríguez, Shastri, Hansen, & Ting, 2013), the annual biorefinery capital-related costs include depreciation, amortized loan payments, and the internal return requirement for investors. The facility investors owned 40% equity and required 10% of an IRR for their investment. Another example concerns a multi-objective optimization model of natural gas transmission networks. One of the objectives is minimizing the transportation fare, considering an attractive return on investment for the entrepreneurs. Such an IRR is coherent with the risks associated with this economic activity.

3.3.1.2/ THE LEVELIZED COST OF HYDROGEN (LCOH)

The LCOH is one of the many expressions of the levelized cost of energy (LCOE). Its calculation process is shown in Eq.3.6. THD_t is the total hydrogen demand in the time period t. CC_t and OC_t represent the capital and operating costs. The calculation process is also schematized in Fig. 3.3. In simple terms, the LCOE is the total cost of the entire system, divided by the energy supplied by the system. The LCOE has been widely used in the energy field, such as to evaluate the economic performance of wind turbines (Ashuri, Zaaijer, Martins, van Bussel, & van Kuik, 2014), solar photovoltaic systems (Branker, Pathak, & Pearce, 2011), and hybrid renewable energy systems (Bernal-Agustín & Dufo-López, 2009; Iverson, Achuthan, Marzocca, & Aidun, 2013). At the same time, it has also been used as the objective in the design and optimization of renewable energy and shale gas supply chains (Cucchiella & D'Adamo, 2013; Gao & You, 2015). The concept of LCOH plays a key role in the Hydrogen Analysis (H2A) project conducted by the U.S. Department of Energy (Department of Energy, 2006, 2015, 2012). The H2A model determines the LCOH from a facility with a specific hydrogen production capacity. The advantages of taking the LCOH as the economic performance measure can be concluded as: (i) it allows comparisons of different production and delivery technologies with different lifetimes, project sizes, different capital costs, and capacities; (ii) it could serve as a reference for policymakers to formulate incentives based on a comparison of various alternative energy projects; (iii) investors and FCEV manufacturers could use this value to estimate the feasibility of their plans of investment or manufacturing; and (iv) LCOH can be seen as the minimum hydrogen selling price at fueling stations, which serve as a critical reference for potential FCEV buyers.

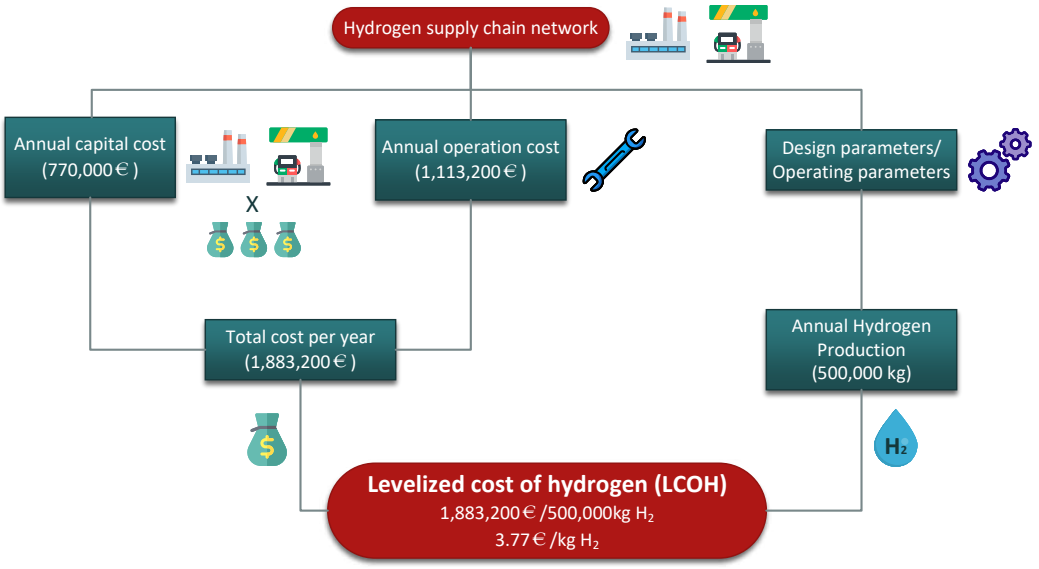

Figure 3.3: The concept of LCOH

$$LCOH = \frac{\text{Sum of costs over lifetime}}{\text{Sum of hydrogen demand over lifetime}} = \frac{\sum_{t=1}^{n} CC_t + OC_t}{\sum_{t=1}^{n} THD_t} \tag{3.6}$$

3.3.1.3/ THE FIXED CHARGE RATE (FCR) METHODOLOGY

The two main methods for determining the LCOH are the discounted cash flow (DCF) model and fixed charge rate (FCR) analysis (Previsic, 2011). Discounted cash flow calculates the value of an investment today based on the expected future cash flows. FCR methodology determines the amount of annual revenue needed to cover investments. While, both of them need to be fed with various datasets, including capital cost, production cost, operating cost, and various financial parameters, as illustrated in Fig. 3.4. Compared to the FCR, the DCF model runs a comprehensive and detailed analysis of all projections of future cash inflows and outflows, thereby providing a reasonable estimation of the LCOH. However, it needs more future forecast data, as shown in the dotted box in the figure. So, FCR analysis is simpler and easier to use and especially suitable for large-scale optimization models. With the FCR method, LCOH can be calculated as follows:

$$LCOH = \frac{FCR * \sum_{t}(FCC_t + TCC_t + FRC_t + TRC_t) + \sum_{t}(FOC_t + TOC_t)}{THD} \tag{3.7}$$

where FRC and TRC are the facility and transportation replacement costs, respectively. The replacement cost is distributed over the lifetime of the project, and can be obtained by (taking FRC as an example):

$$FRC_t = \frac{(1+ir)^{t-1} * FCC}{(1+d)^{t-1}} \tag{3.8}$$

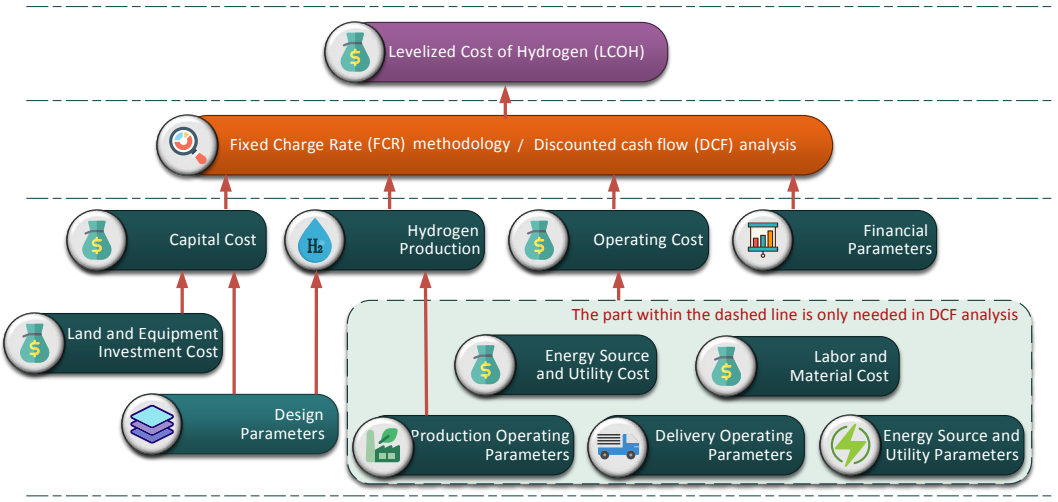

Figure 3.4: Two main methods of determining the LCOH and the required datasets

where ir is the inflation rate. The FRC and TRC are equal to 0 if the replacement does not take place in the time period t. The replacement cost can also be estimated based on industry experience. For some central hydrogen production plants, the replacement cost can be divided into unplanned and planned costs. The former is often set to 0.5% of the total capital cost, while the latter depends on the specific equipment and technologies (Department of Energy, 2012).

In mathematical terms, the FCR is defined as the amount of revenue per dollar of investment that must be earned each year to cover the carrying charges on that particular investment. The equation for the FCR is shown below (Short, Packey, & Holt, 1995):

$$FCR = \frac{CCF * [1 - b * Tax * \sum_{n=1}^{M} \frac{V_n}{(1+d)^n} - tax_c]}{1 - Tax} \tag{3.9}$$

where M is the depreciation period. b is the fraction of the depreciable base (the depreciable fraction of capital costs). Tax gives the total tax rate. V_n is the fraction of the depreciable base that must be depreciated in year n. N represents the length of the analysis period. tax_c is the tax credit, and CCF is the capital charge factor, which is defined by Eq. 3.5.

If the entire capital investment is assumed to be depreciable and no tax credits are assumed, the FCR equation reduces to the following:

$$FCR = \frac{CCF * [1 - Tax * \sum_{n=1}^{M} \frac{V_n}{(1+d)^n}]}{1 - Tax} \tag{3.10}$$

A depreciation method needs to be selected. For instance, in the H2A analysis project, the modified accelerated cost recovery system (MACRS) is used to depreciate each delivery component's investment. The depreciation table is shown in Table 3.2. When the depreciation period is determined, the following portion of the FCR equation:

$$\sum_{n=1}^{M} \frac{V_n}{(1+d)^n} \tag{3.11}$$

is equivalent to taking the present value of each of the MACRS depreciation amounts corresponding to the selected depreciation period (represented by the term $PV(depreciation)$ in Eq. (3.12)). For example, when the depreciation period is set to seven years, then Formula (3.11) is equal to 0.721. Thus, the FCR equation becomes:

$$FCR = \frac{CCF * [1 - Tax * (PV(\textit{depreciation}))]}{1 - Tax} \tag{3.12}$$

Table 3.2: MACRS depreciation table

MACRS Depreciation Period						
Depreciation Period	3	5	7	10	15	20
1	33.33%	20.00%	14.29%	10.00%	5.00%	3.75%
2	44.45%	32.00%	24.49%	18.00%	9.50%	7.22%
3	14.81%	19.20%	17.49%	14.40%	8.55%	6.68%
4	7.41%	11.52%	12.49%	11.52%	7.70%	6.18%
5		11.52%	8.93%	9.22%	6.93%	5.71%
6		5.76%	8.92%	7.37%	6.23%	5.29%
7			8.93%	6.55%	5.90%	4.89%
8			4.46%	6.55%	5.90%	4.52%
9				6.56%	5.91%	4.46%
10				6.55%	5.90%	4.46%
11				3.28%	5.91%	4.46%
12					5.90%	4.46%
13					5.91%	4.46%
14					5.90%	4.46%
15					5.91%	4.46%
16					2.95%	4.46%
17						4.46%
18						4.46%
19						4.46%
20						4.46%
21						2.23%
Total	100.00%	100.00%	100.00%	100.00%	100.00%	100.00%
Present value	0.832	0.773	0.721	0.654	0.517	0.434

The discount rate in the calculation of the present value is set to 10%.

3.3.2/ A NUMERICAL EXAMPLE

We use an example to demonstrate how to introduce the LCC into HSCND models. As depicted in Fig. 3.5, various technologies are available at each echelon of an HSCN, and the main target of the optimization model is to find the pathway or pathway mix that maximizes or minimizes the predefined objective. One possible pathway has been chosen as an example, as shown in Fig. 3.5.

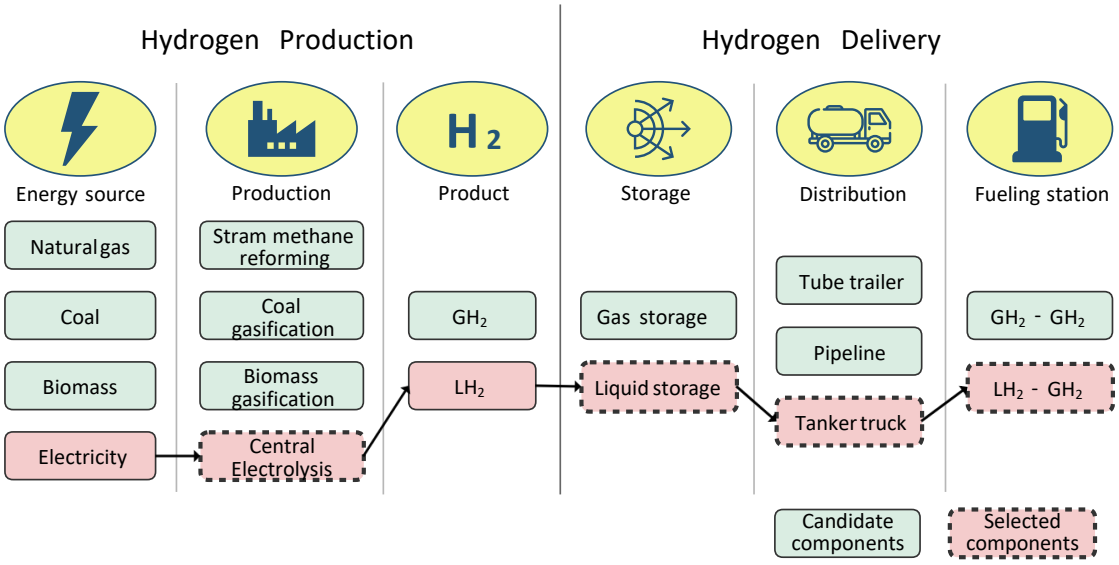

Figure 3.5: A pathway of the HSCN is selected to show how to perform LCC in HSCND models

Hydrogen is produced in the central electrolysis plant. The LH_2 storage site co-located with the production plant includes liquefier and liquid storage. Liquid hydrogen is loaded onto LH_2 trucks and then transported to the LH_2 fueling station. We assume the yearly hydrogen delivered is 1,095,000 kg, an analysis period of 20 years, an IRR of 10%, while the capital charge factor (CCF) can be obtained by Eq. (3.5) as 0.12. The total tax rate is assumed as 39%. The depreciation period of each component (or their primary equipment) is listed in Table 3.3.

Table 3.3: A numerical example of how to perform LCC in HSCND models: Part One

	Depreciation length (years)	Lifetime (years)	Present value of depreciation	FCR
Central production	7	20	0.721	0.138
LH_2 storage				
Liquefier	15	20	0.517	0.154
LH_2 pump	15	20	0.517	0.154
Liquid storage	15	20	0.517	0.154
Remainder	15	20	0.517	0.154
LH_2 truck				
Tractor	5	5	0.773	0.134
Tank trailer	5	20	0.773	0.134
LH_2 fueling station				
Storage	7	20	0.721	0.138
Dispenser	7	10	0.721	0.138
Remainder	7	20	0.721	0.138

Data source: The Hydrogen Analysis (H2A) project of the U.S. Department of Energy (Department of Energy, 2006, 2015, 2012).

The present value of depreciation of each component (equipment) can be obtained by querying Table 3.2. We then obtain the FCR through Eq. (3.12). Note that the LH_2 truck

and fueling station includes the types of equipment with a lifetime less than the analysis period. The replacement cost of these types of equipment can be calculated by Eq. (3.8). It should also be noted that although the life of the central production is longer than the analysis period, there are still replacement costs, as the electrolysis plant involves equipment with different life spans. The replacement cost is estimated based on industry experience (Department of Energy, 2012). Table 3.4 shows that the unit yearly capital cost is obtained by multiplying the unit total capital cost and the FCR.

Table 3.4: A numerical example of how to perform LCC in HSCND models: Part Two

	Initial capital cost (€)	Replacement cost (€)	Unit total capital cost (€)	Unit yearly capital cost (€/year)	Unit yearly operating cost (€/year)
Central production	2,864,491	909,267	3,773,758	522,000	1,477,261
LH_2 storage				4,326,386	1,185,105
Liquefier	23,641,367	0	23,641,367	3,630,825	1,063,351
LH_2 pump	378,694	0	378,694	58,159	5,386
Liquid storage	3,702,006	0	3,702,006	568,551	99,515
Remainder	448,300	0	448,300	68,849	16,854
LH_2 truck				95,811	334,446
Tractor	66,000	96.694	162,694	21,872	328,228
Tank trailer	550,000	0	550,000	73,939	6,218
LH_2 fueling station				155,657	98,929
Storage	588,724	0	588,724	81,434	43,288
Dispenser	29,095	11,009	40,103	5,547	2,675
Remainder	496,481	0	496,481	68,675	53,025

Data source: The Hydrogen Analysis (H2A) project of the U.S. Department of Energy (Department of Energy, 2006, 2015, 2012). Note: US dollar to Euro (USD to EUR) exchange rate is 0.88.

In Table 3.5, the numbers of units are decision variables defined by the optimization process. The total yearly capital and operating costs correspond to each set of the number of units. Dividing the total yearly cost by the yearly hydrogen delivered, we obtain the total LCOH and the contributions of each component. To summarize, the work in Tables 3.3 and 3.4 is done before the optimization process, and its main purpose is to identify the unit yearly capital costs, which serves as inputs of the optimization model. Then these inputs contribute to defining the LCOH.

Table 3.5: A numerical example of how to perform LCC in HSCND models: Part Three

	Number of units	Yearly capital cost (€/year)	Yearly operating cost (€/year)	Total yearly cost (€/year)	LCOH (€/kg H_2)
Central production	2	1,044,001	2,954,523	3,998,524	3,65
LH_2 storage	2	8,652,772	2,370,210	11,022,981	10,07
LH_2 truck	1	95,811	334,446	430,257	0.40
LH_2 fueling station	6	933,941	593,572	1,527,514	1.40
Total		10,726,526	6,252,750	16,979,276	15,51

Data source: The Hydrogen Analysis (H2A) project of the U.S. Department of Energy (Department of Energy, 2006, 2015, 2012). Note: The conversion rate between USD and EUR is 0.88.

3.3.3/ LIFE CYCLE ASSESSMENT (LCA) IN HSCND

The procedures of LCAs form a part of the ISO 14000 environmental management standards (ISO, 2006). According to the standards, an LCA involves four main phases: (i) a goal and scope definition; (ii) an LCI analysis; (iii) a life cycle impact assessment (LCIA); and (iv) life cycle interpretation, as depicted in Fig. 3.6.

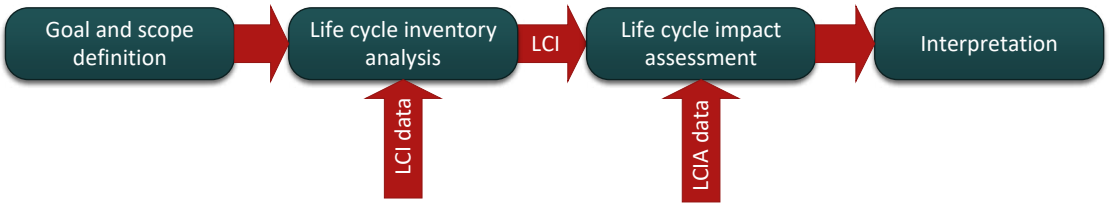

Figure 3.6: The procedures involved in LCAs, as defined by the ISO 14000 environmental management standards (ISO, 2006)

3.3.3.1/ PHASE ONE: GOAL AND SCOPE DEFINITION

The goal of an LCA in an HSCND is to evaluate the life cycle environmental impact for the proposed system. The scope of LCA in Fig. 3.7 is based on three boundary definitions by well-to-tank (WtT), tank-to-wheels (TtW), and well-to-wheels (WtW). The WtT incorporates primary fuel (feedstock) production, transportation, and (hydrogen) production and distribution. The TtW focuses on vehicle operations. All three HSCND models that include an LCA (Refs. (Ogumerem et al., 2018; Guillén-Gosálbez et al., 2010; Sabio et al., 2012)) take the scope of WtT. The functional unit that quantifies the service delivered by the supply system also needs to be defined in this step. According to the ISO, classical LCAs must report environmental impacts in terms of a "functional unit" for a better comparison of the impacts associated with alternative products (Gao & You, 2015). For instance, in the work of Gao and You (2015), the natural gas delivered through a shale gas supply chain is considered to be a fuel for electricity generation. Therefore a functional unit of one MWh of electric power generated at the power plant is employed. In the context of the hydrogen supply system, the functional unit is often set as one kilogram of hydrogen distributed at a hydrogen fueling station. Another technical detail that should be defined in the first step is the impact categories, such as human toxicity, smog, global warming, and eutrophication (Wikipedia contributors, 2020). For the design of hydrogen and other energy supply chains, the most selected impact category is global warming, usually represented by greenhouse gas emissions (GHG). Damage to human health is also used in two HSCND models (Sabio et al., 2012; Guillén-Gosálbez et al., 2010).

3.3.3.2/ PHASE TWO: THE LIFE CYCLE INVENTORY (LCI)

The LCI is a compilation of the inputs (resource) and outputs (emissions) from the product over its life-cycle (Wu et al., 2017). The LCI analysis is crucial in an LCA because it quantitatively defines the relationship between the system and the environment. The LCI analysis involves creating an inventory of flows from and to nature for a product system.

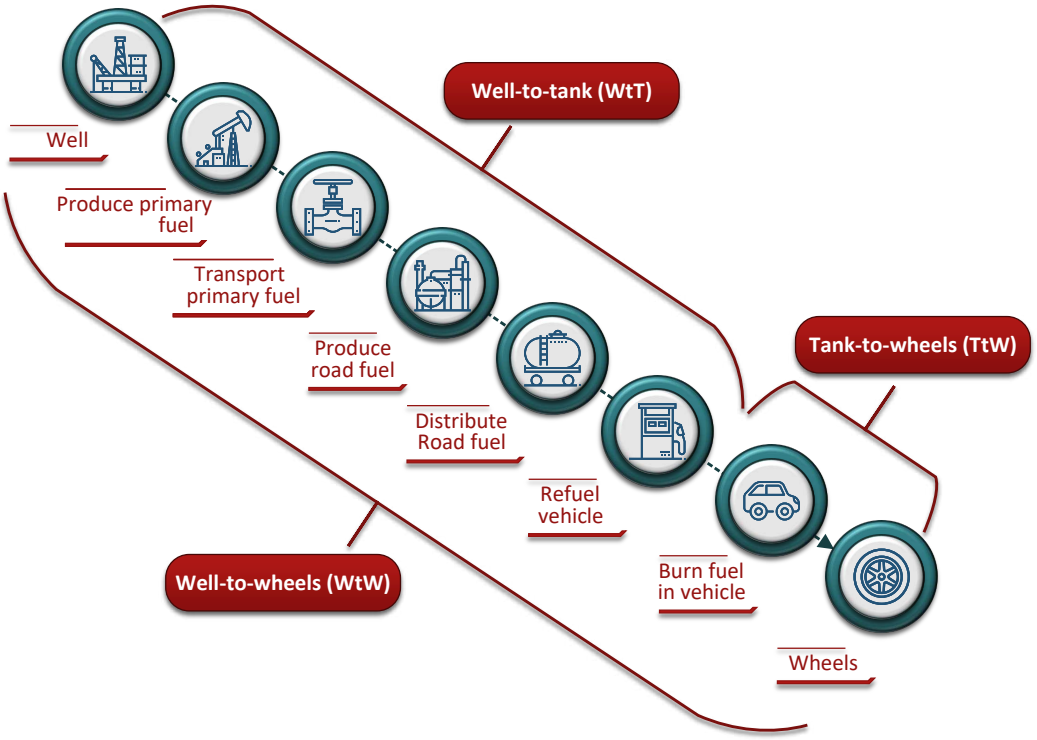

Figure 3.7: The scope of LCA in the transportation sector: WtT, TtW, and WtW

We found that most optimization models of energy supply chains do not include an LCI analysis. Therefore we propose an LCI analysis in the LCA of an HSCND.

As illustrated in Fig. 3.8, we divided the hydrogen supply chain into four primary *processes*: hydrogen production, storage (where hydrogen is stored and loaded onto trucks for delivery to stations), transportation, and fueling stations. Each process has two or more types of *technology*, each technology requires the input of a *utility* and (or) an *feedstock*. For this example, the feedstock includes natural gas, coal, biomass, and water. The utility consists of electricity (from solar, wind, geothermal energy, nuclear, etc.), natural gas, and diesel. The process of hydrogen production includes steam methane reforming, coal gasification, biomass gasification, electrolysis, and on-site electrolysis. Hydrogen can be stored in gaseous and liquid storage sites. Tanker trucks and tube trailers are two kinds of transportation technology. Gaseous station and liquid station are operated. The connections between the process, utility, and feedstock indicate the demand for each technology.

The value of these demands is provided in Table 3.6. For example, producing one kilogram of hydrogen through biomass gasification requires 19.39 kilograms of biomass, 0.29 kWh of electricity, and 0.55 Nm^3 of natural gas. In comparison, the delivery of one kilogram of gaseous hydrogen for each kilometer requires 5.25 mL of diesel. It can be seen that all the data are related to the functional unit defined in the goal and scope definition,

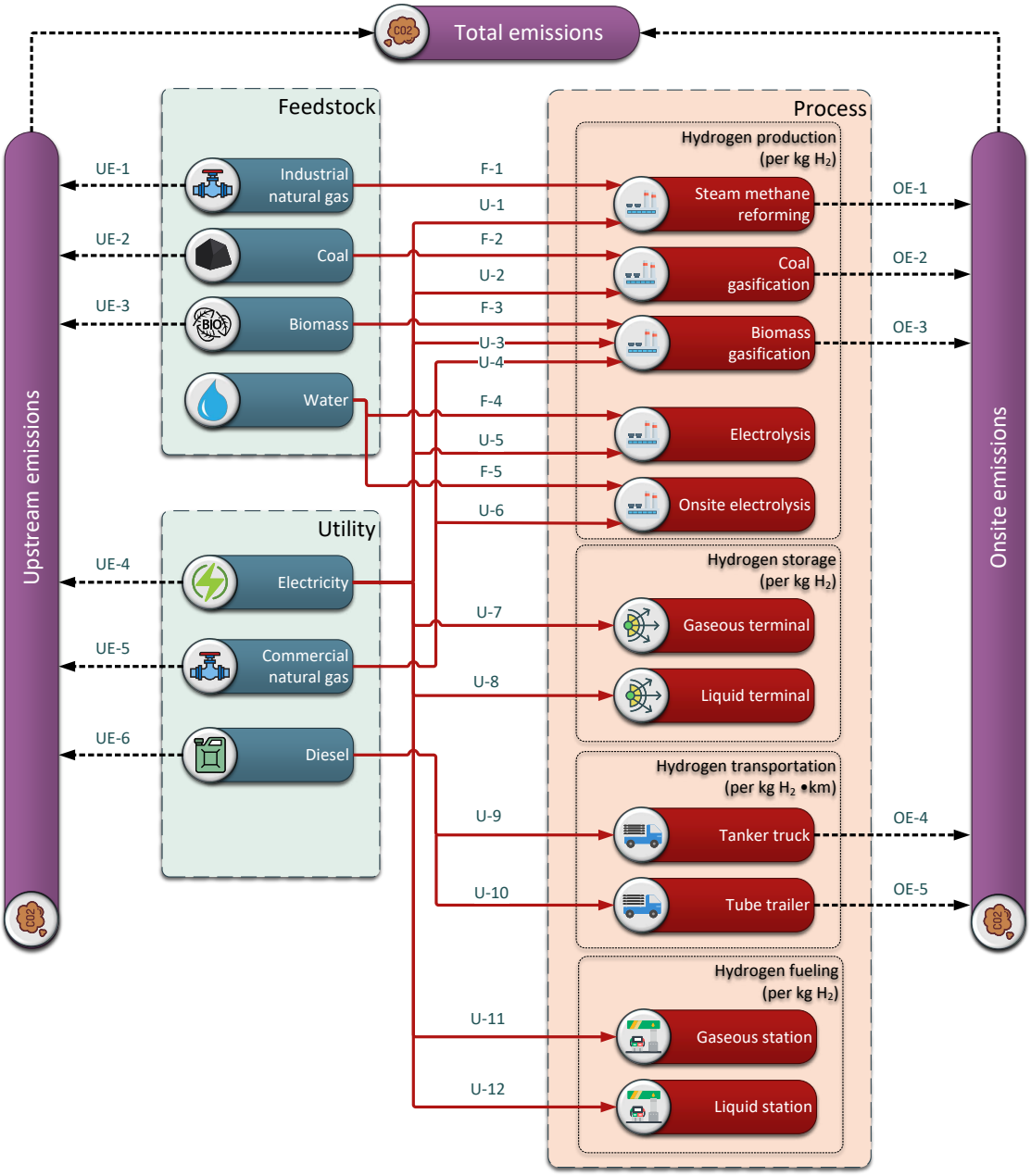

Figure 3.8: The LCI analysis intended for use in the LCA of an HSCND

as shown in the second column of Table 3.6. The generation and transportation of each feedstock and utility produce emissions that are defined as *upstream*. In contrast, the emissions produced within the process are labeled *on-site* (e.g., the emissions related to the hydrogen production based on fossil fuel and the emissions related to hydrogen transportation, which consumes diesel). There are no on-site emissions for the process requiring only electricity input, like the hydrogen storage and fueling station. Detailed information of the emissions can be seen in Table 3.7, which includes the unit emission of the three primary types of greenhouse gas: CO_2, CH_4, and N_2O.

The proposed LCI analysis defines the system inputs (feedstock and utility) and outputs (upstream and on-site emissions). The flowchart and tables adopted in this example suit

Table 3.6: Detailed information related to the inputs of each technology

	Value	Unit	Note	Ref.
F-1	4.07	$Nm^3/kg\ H_2$	-The LHV of hydrogen is 120 MJ/kg;	[1]
U-1	1.11	$kWh/kg\ H_2$	-The LHV of natural gas is 38.3 MJ/Nm^3.	[2]
F-2	11.75	$kg/kg\ H_2$	-The LHV of coal is 29.3MJ/kg;	[3]
U-2	3.18	$kWh/kg\ H_2$	-The production capacity is 5,000 kg H_2/day.	[2]
F-3	19.39	$kg/kg\ H_2$	-The biomass includes 50.4% carbon and 22.6% moisture;	[4]
U-3	0.29	$kWh/kg\ H_2$	-The LHV of hydrogen is 120 MJ/kg;	
U-4	0.55	$Nm^3/kg\ H_2$	-The LHV of natural gas is 120 MJ/kg;	
U-5	41.66	$kWh/kg\ H_2$	-Hydrogen is produced by grid electrolysis of water;	[5]
U-6	41.66	$kWh/kg\ H_2$	-The LHV of hydrogen is 33.33 kWh/kg.	[5]
U-7	2.70	$kWh/kg\ H_2$	-The storage site is co-located with a production facility; -The hydrogen is compressed and loaded onto tube trailers; -The vessel's operating pressure is 35MP;	[6]
U-8	10.50	$kWh/kg\ H_2$	-The storage site is co-located with a production facility; -Hydrogen is liquefied and loaded onto tanker trucks.	[7]
U-9	0.09	$mL/kg\ H_2 \cdot km$	-Hydrogen delivered per tank is 4,000 kg;	[8]
U-10	0.95	$mL/kg\ H_2 \cdot km$	-Hydrogen delivered per tube is 380 kg; -The tube trailer's operating pressure is 35MP.	[8]
U-11	2.43	$kWh/kg\ H_2$	-The fueling station takes gaseous hydrogen from tube trailers;	[9]
U-12	0.37	$kWh/kg\ H_2$	-The fueling station takes liquid hydrogen from tanker trucks.	[9]

[1] (Azzaro-Pantel, 2018); [2] (Department of Energy, 2012); [3] (Pareek et al., 2020); [4] (Kalinci, Hepbasli, & Dincer, 2012); [5] (S. S. Kumar & Himabindu, 2019); [6] (Sdanghi, Maranzana, Celzard, & Fierro, 2019); [7] (Peschel, 2020); [8] (Schoettle, Sivak, & Tunnell, 2016); [9] (Bauer, Mayer, Semmel, Morales, & Wind, 2019).

future studies concerning LCAs in HSCNDs.

3.3.3.3/ PHASE THREE: THE LIFE CYCLE IMPACT ASSESSMENT (LCIA)

This phase of the LCA is performed to evaluate the significance of potential environmental impacts, based on the LCI flow results (Wikipedia contributors, 2020). For example, suppose global warming has been selected as the impact category in the first step. In that case, the purpose of the LCIA is to quantify the GHG emissions in units of CO_2-equivalent, which is a metric that compares the radiative forcing associated with a GHG relative to that of CO_2. The characterization values for GHG emissions are based on global warming potentials (GWP) using the Intergovernmental Panel on the Fifth Assessment Report of Climate Change (IPCC) in 2013. Notably, the GWPs of a GHG is usually denoted by GWP-CO_2=1, GWP-CH_4=28, and GWP-N_2O=265 for a 100-year time horizon (Myhre, Shindell, & Pongratz, 2014).

Table 3.7: Detailed information related to the emissions

	Unit	Greenhouse gas emissions			Note	Ref.
		CO_2	CH_4	N_2O		
Upstream emissions						
UE-1	g/Nm^3	206.82	31.50	0.004	The LHV of natural gas is 38.3 MJ/Nm^3.	[1][2]
UE-2	g/kg	24.61	1.17	0.00	The LHV of coal is 29.3 MJ/kg.	[1]
UE-3	g/kg	-1,605	0.11	0.09	Woody biomass at plant gate.	[3]
UE-4	g/kWh	57.3	0.00	0.00	France average.	[4]
UE-5	g/Nm^3	206.82	4.98	0.004	The LHV of natural gas is 38.3 MJ/Nm^3.	[1]
UE-6	g/L	318.44	13.68	0.006	The LHV of diesel is 38 MJ/L.	[5]
On-site emissions						
OE-1	g/kg H_2	9,210.00	56.00	0.00	Without carbon capture and storage	[6]
OE-2	g/kg H_2	23,363.00	0.4	0.00	Without carbon capture and storage	[7]
OE-3	g/kg H_2	33,527.00	0.01	0.00	Without carbon capture and storage	[3]
OE-4	g/kg $H_2 \cdot$ km	0.18	0.00	0.00	Heavy-duty truck Average data of low, medium, high speed.	[8]
OE-5	g/kg $H_2 \cdot$ km	1.88	0.00	0.00	Heavy-duty truck Average data of low, medium, high speed.	[8]

[1] (Liu & Liu, 2021); [2] (Balcombe, Anderson, Speirs, Brandon, & Hawkes, 2017); [3] (Argonne National Laboratory, 2012); [4] (Statista, 2021); [5] (Liu & Liu, 2021); [6] (Budsberg, Crawford, Gustafson, Bura, & Puettmann, 2015); [7] (G. Li et al., 2020); [8] (Grigoratos, Fontaras, Giechaskiel, & Zacharof, 2019).

3.3.3.4/ PHASE FOUR: LIFE CYCLE INTERPRETATION

According to ISO 14040:2006 (ISO, 2006), this final step evaluates the sensitivity and assesses the completeness and consistency of the study. However, in most optimization models, this step has been replaced by the process of generating different design alternatives and identifying the best ones in terms of environmental performance (Gao & You, 2015; You & Wang, 2011; Gebreslassie, Slivinsky, et al., 2013; Yue, Kim, & You, 2013; Gebreslassie, Waymire, & You, 2013).

3.3.4/ BI-OBJECTIVE OPTIMIZATION

As illustrated in Fig. 3.9, the optimization tool and environmental impact assessment are coupled together to formulate the life cycle optimization modeling framework. The trade-

off between economic and environmental objectives is revealed in a set of Pareto-optimal solutions by solving the resulting bi-objective optimization problem. Finally, decision-makers' preferences can be articulated in the post-optimal analysis by selecting one of the solutions.

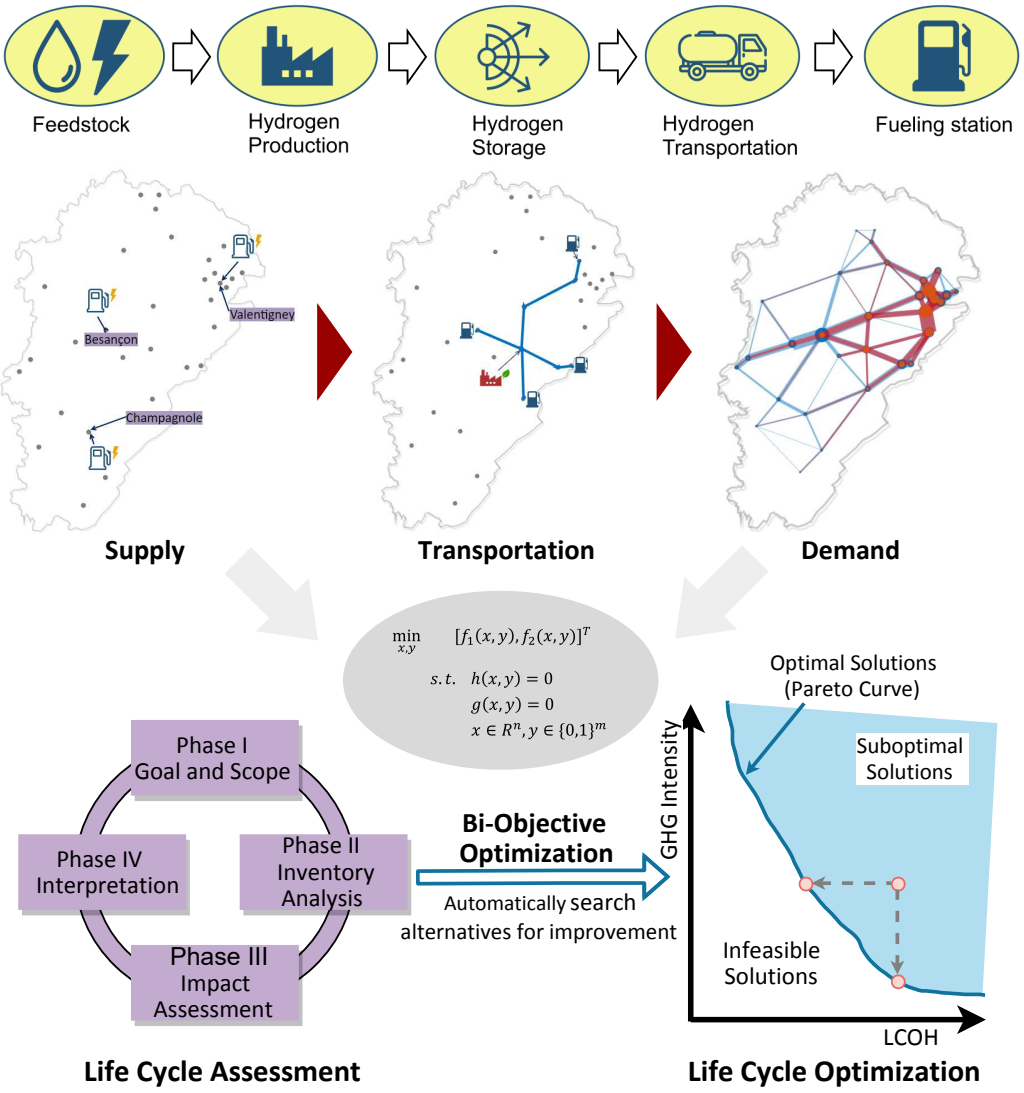

Figure 3.9: Life cycle optimization modeling framework

3.4/ MATHEMATICAL MODEL

3.4.1/ OBJECTIVE FUNCTION

3.4.1.1/ LIFE CYCLE COSTING

The first objective function is the minimization of the levelized cost of hydrogen. It can be described as the Eq. (3.14).

$$Minimize \qquad LCOH \tag{3.13}$$

$$\begin{aligned} LCOH = \frac{1}{THD}[FCR * \sum_{t}(FCC_t + TCC_t + FRC_t + TRC_t) \\ + \sum_{t}(FOC_t + TOC_t) + EC] \end{aligned} \tag{3.14}$$

where FCR can be given by Eq. (3.12). The FRC and TRC can be calculated based on Eq. (3.8). FCC is the facility capital cost which is defined as:

$$\begin{aligned} FCC = \sum_{p,i,k} NP_{pik} * pcc_{pik} + \sum_{i} NT_i * scc_i + \sum_{s,i,j} NF_{sij} * fcc_{sij} \\ + \sum_{o,j} NF_{oj} * fcc_{oj} + NR * ccc \end{aligned} \tag{3.15}$$

where NP_{pik}, NT_i, NF_{sij}, NF_{oj} represent the number of production plant (production technology p, hydrogen form i, plant size k), storage site (hydrogen form i), standard fueling station (technology s, hydrogen form i, size j) and on-site fueling station (technology o, size j) respectively. pcc_{pik}, scc_i, fcc_{sij}, and fcc_{oj} are the capital cost of each facility. NR represents the number of CO_2 storage sites and ccc is the capital cost of one site.

TCC is the transportation capital cost which is defined as:

$$TCC = \sum_{f} NV_f * tcc_f + \sum_{h} NV_h * tcc_h + cpcc * \sum_{n,m} X_{nm} * l_{nm} \tag{3.16}$$

where NV_f and NV_h denote the number of transportation equipment for feedstock transportation mode f and hydrogen transportation mode h, respectively. tcc_h represents the cost of each transportation equipment. $cpcc$ is the unit capital cost of CO_2 pipeline. X_{nm} equals one if CO_2 is transported from node n to m, and l_{nm} is the shortest distance between the two nodes.

FOC is the facility operating cost which is defined as:

$$\begin{aligned} FOC = \sum_{e} NE_e * eoc_e + \sum_{p,i,k} PR_{pik} * poc_{pik} + \sum_{i} SR_i * soc_i \\ + \sum_{s,i,j} FR_{sij} * foc_{sij} + \sum_{o,j} FR_{oj} * foc_{oj} + CR * coc \end{aligned} \tag{3.17}$$

where NE_e represents the number of feedstock supply sites that supply feedstock of type e to hydrogen production plants. eoc_e is the operating cost of one site of this type. PR_{pik} represents the production rate of hydrogen form i using technology p in size k plant. SR_i is the storage rate of hydrogen form i in the storage site. FR_{sij} and FR_{oj} give the fueling rates of standard and on-site fueling stations. poc_{pik}, soc_i, foc_{sij} and foc_{oj} denote the operation cost of per kilogram hydrogen in the process of production, storage, standard

fueling and on-site fueling. CR (defined in Eq. B.50) gives the total processing rate of CO_2. coc is the unit operating cost (per kg CO_2).

The transportation operating cost TOC includes the cost of hydrogen transportation (HTOC) and feedstock transportation (FTOC).

$$TOC = HTOC + FTOC \tag{3.18}$$

$HTOC$ is defined as:

$$HTOC = HFC + HLC + HMC + HGC \tag{3.19}$$

The four items on the right, fuel, labor, maintenance, and general costs, are calculated based on the model of L. Li et al. (2020). They are defined in the following Eqs. (3.20) - (3.23):

$$HFC = \sum_{h,n,m} fp_h * \frac{2 * l_{nm} * Q_{hnm}}{fe_h * tcap_h} \tag{3.20}$$

$$HLC = \sum_{h,n,m} dw_h * \frac{Q_{hnm}}{tcap_h} * (\frac{2 * l_{nm}}{sp_h} + lut_h) \tag{3.21}$$

$$HMC = \sum_{h,n,m} me_h * \frac{2 * l_{nm} * Q_{hnm}}{tcap_h} \tag{3.22}$$

$$HGC = \sum_{h,n,m} ge_h * \frac{Q_{hnm}}{tma_h * tcap_h} * (\frac{2 * l_{nm}}{sp_h} + lut_h) \tag{3.23}$$

In these equations, fp_h, dw_h, me_h, ge_h, and tcr_h represent the fuel price (per liter fuel), driver wage (per hour), maintenance expense (per km), general expense (per day), and vehicle rental cost (per vehicle) of hydrogen transportation mode h, respectively. fe_h, sp_h, $tcap_h$, tma_h, and lut_h denote the fuel economy, speed, capacity, availability (hours per day), and load/unload time of hydrogen transportation mode h, respectively. Q_{hnm} represents the hydrogen transportation flux (in mode h) from node n to m, and l_{nm} is the shortest distance between the two nodes.

$FTOC$ is defined as:

$$FTOC = FFC + FLC + FMC + FGC \tag{3.24}$$

The four items on the right-hand side are fuel, labor, maintenance, and general costs, respectively. Their definitions and calculation of the number of feedstock vehicles have the same forms as those of the hydrogen transportation operating cost.

EC represents the feedstock purchasing cost which is defined as:

$$EC = \sum_{e} ESR_e * euc_e \tag{3.25}$$

where euc_e is the price per unit of feedstock. ESR_e denotes the feedstock supply rate of type e. It is described as:

$$ESR_e = \sum_n (PESR_{ne} + OESR_{ne}) \tag{3.26}$$

where $PESR_{ne}$ is the supply rate of feedstock type of e at the node n. The $OESR_{ne}$ is the feedstock e supply rate supplied by node n to the on-site fueling station.

3.4.1.2/ LIFE CYCLE ASSESSMENT (LCA)

The second objective is the total global warming potentials factor, which can be calculated by converting all of the emission gas into CO_2. In this study, the emissions including CO_2, CH_4 and N_2O. Based on LCI research, GWP is described as follows.

$$Minimize \qquad GWP \tag{3.27}$$

$$GWP = EM_{CO_2} + 28EM_{CH_4} + 265EM_{N_2O} \tag{3.28}$$

EM_{CO_2}, EM_{CH_4}, and EM_{N_2O} denote the quantity of CO_2,CH_4 and N_2O emissions.

EM_g is the total emission of the type of greenhouse gas g. It is defined as:

$$EM_g = PER_g + SER_g + TER_g + FER_g \tag{3.29}$$

PER_g, SER_g, TER_g, and FER_g represent the greenhouse gas emission in the site of Hydrogen production, storage site, transportation and fueling, respectively. PER_g is defined as:

$$\begin{aligned} PER_g = &\sum_{p,i,k,e} PR_{pik} * F_{pe} * UE_{eg} + \sum_{p,i,k,u} PR_{pik} * U_{pu} * UE_{ug} \\ &+ \sum_{n,p,i,k} \left(PR_{npik} - (PR^c_{npik} * \gamma^c_{pik})\right) * OE_{pg} \\ &+ \sum_{o,j,e} FR_{oj} * F_{oe} * UE_{eg} + \sum_{o,j,e} FR_{oj} * U_{ou} * UE_{ug} \end{aligned} \tag{3.30}$$

PR_{pik} is the total production rate of production plants using the production technology p in hydrogen form i at the production center of size k. FR_{oj} represents the fueling rate of on-site fueling station. F_{pe} and F_{oe} denote the quantity of feedstock e requirement. UE_{eg} denotes upstream emissions for feedstock e and emission type g. U_{pu} denotes the amounts of utility u requirement for the production technology p. UE_{ug} denotes upstream emissions for utility u and emission type g. PR^c_{npik} represents the production rate of a production plant whose onsite emissions are processed. γ^c_{pik} is the production emission capture efficiency. OE_{pg} denotes on-site emissions for production technology p and emission type g.

SER_g is defined as:

$$SER_g = \sum_{n,i,u} SR_{ni} * U_{iu} * UE_{ug} \tag{3.31}$$

SR_{ni} is the storage rate at storage site n. U_{iu} represents the amounts of utility u requirement for the hydrogen in form i.

TER_g is defined as:

$$TER_g = \sum_{h,n,m,u} TR_{hnm} * 2 * l_{nm} * U_{iu} * UE_{ug} + \sum_{h,n,m} 2 * TR_{hnm} * 2 * l_{nm} * OE_{hg} \tag{3.32}$$

where TR_{hnm} is transportation flux between node n and m using transportation mode h. l_{nm} denotes the shortest distance from node n to m.

FER_g is defined as:

$$FER_g = \sum_{n,s,i,j,u} FR_{nsij} * U_{iu} * UE_{ug} \tag{3.33}$$

FR_{nsij} represents the fueling rate of a size j fueling station in the node n that uses technology s and hydrogen form i. The subscript g includes CO_2, CH_4, N_2O.

3.4.2/ CONSTRAINTS

Previous researchers have already proposed the HSCND model, which encompasses the entire hydrogen supply chain. This work aims to propose life cycle optimization on the HSCND model. Therefore, based on the mathematical model developed in Reference L. Li et al. (2020), we maintain all relevant constraints as outlined in the original work. Detailed constraints can be found in the appendix B.

3.4.3/ SOLUTION APPROACH

The model is formulated as a mixed-integer linear programming problem. To solve this bi-objective optimization problem, we use ϵ-constraint approaches. This method can achieve the purpose of transforming the bi-objective optimization problem into a mono-objective optimization problem (Mavrotas, 2009). The problem can be shown as $Minimize\ \ GWP$, which subject to: $LCOH \leq \epsilon_n (n = 0, 1, 2, ...N)$.

3.5/ CASE STUDY: FRANCHE-COMTÉ FRANCE

As mentioned before, this study is based on the previous HSCND model (L. Li et al., 2020), in which an HSCND model covers the entire hydrogen supply network. A total of 66 instances were generated and solved. By analyzing and comparing the results of these instances, the necessity of considering various components, such as feedstock

transportation, carbon capture, and storage, and fueling technology (standard and on-site), within a single framework is demonstrated. This HSCND model applied the mixed-integer linear programming approach to minimize the total cost of hydrogen. Franche-Comté was selected to test the model's ability.

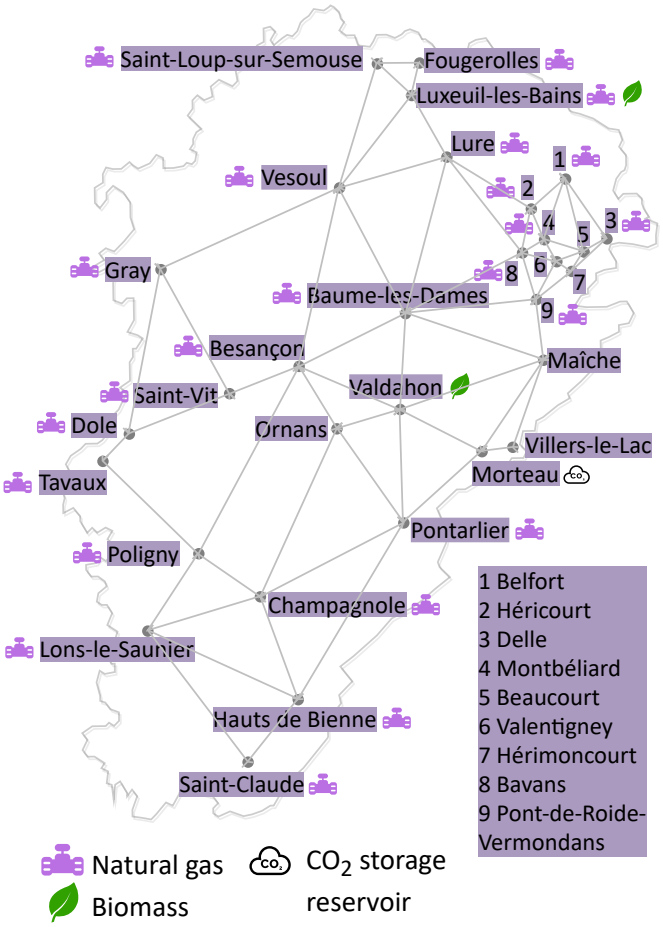

Figure 3.10: Franche-Comté network: Basic network, Natural gas distribution, biomass distribution, and location of a potential CO_2 storage site

The methodology proposed in this chapter, an LCO model, can be seen as an extension of the HSCND model towards life cycle optimization. The aim is to provide decision-makers with more comprehensive, more reasonable HSCND related references. Specifically, through the case study, we would like to demonstrate the following:

- The application of LCC would make a more comprehensive reflection of HSCN costs.
- Introducing LCA, especially LCI, can achieve a detailed description of HSCN related emissions.
- The trade-off between costs and emissions within an HSCND can be quantified and visualized through bi-objective optimization.

The case study in this chapter is also applied to Franche-Comté, France. The 31 most populous cities are selected as network nodes, as shown in Fig. 3.10. Fig. 3.10 also

presents the distribution of natural gas and biomass, which are feedstock to produce hydrogen. Detailed descriptions about Franche-Comté's road network, hydrogen fueling demand, and hydrogen supply network can be found in Ref. (L. Li et al., 2020).

This section chooses three representative instances from L. Li et al. (2020). Information and properties about these instances are shown in Table 3.8. We compare results obtained from solving the Instance-1 through the HSCND and the LCO models separately. The aim is to show the differences in the performance measure of HSCN costs. Similarly, Instance-2 is used to compare the emission performance measure of the two models. Instance-3 is employed to show the quantification of the trade-off involved in HSCND. Various hydrogen supply network configurations corresponding to specific Pareto optimal solutions are shown to strengthen the understanding of the trade-off between two performance measures, costs, and emissions.

Table 3.8: Instance information

Name in this study	Name in L. Li et al. (2020)	Feedstock	Hydrogen form	Carbon price (€/kg CO_2)	Fueling demand captured (%)
Instance-1	Set-B1-LC-HD	Natural gas	Gaseous	0.05	90
Instance-2	Set-D-LC-HD	Biomass	Gaseous	0.05	90
Instance-3	Set-E2-HC-HD	Biomass	Gaseous	0.27	90

It is noted that, compared to the HSCND model, apart from the introduction of LCO, there are two other modifications. Firstly, we introduce hydrogen storage into the HSCND. Storage sites are always co-located with production plants. Secondly, vehicles responsible for hydrogen and feedstock transportation are purchased instead of rented. So the cost of transportation is more detailed, and we can optimize the hydrogen transportation service more practically.

3.5.1/ THE EFFECT OF LCC ON HSCND

HSCN configurations obtained from solving Instance-1 with the HSCND model and LCO model are shown in Fig. 3.11. The two configurations have the same number and locations for fueling stations. However, the configuration of the LCO model involves one less production plant than the one of the HSCND model. The hydrogen transportation system is also adjusted correspondingly. This change is because the introduction of hydrogen storage increases facility-related capital costs. Therefore the model chooses to create two medium-sized production plants instead of two small-sized plus one medium-sized. The aim is to reduce capital costs and maintain the same total production rate.

To show the differences in the performance measure of HSCN costs, the minimized total cost from solving the HSCND model, the minimized LCOH from solving the LCO model (mono-objective), and their composition are illustrated in Fig. 3.12 and Fig. 3.13, respectively. It should be noted that emission costs are taken out from the total cost after running the HSCND model. The total cost and the LCOH consist of capital costs, feedstock costs, and operating costs. Compared to the total cost, the composition of LCOH shows four differences. First, replacement costs of facilities and vehicles are added. Second, the fixed charge rate methodology is applied. Third, capital costs of purchasing vehicles are added. Forth, hydrogen storage-related costs are listed.

We focus on the values of costs. Feedstock costs (Contri_EC) are the same for the to-

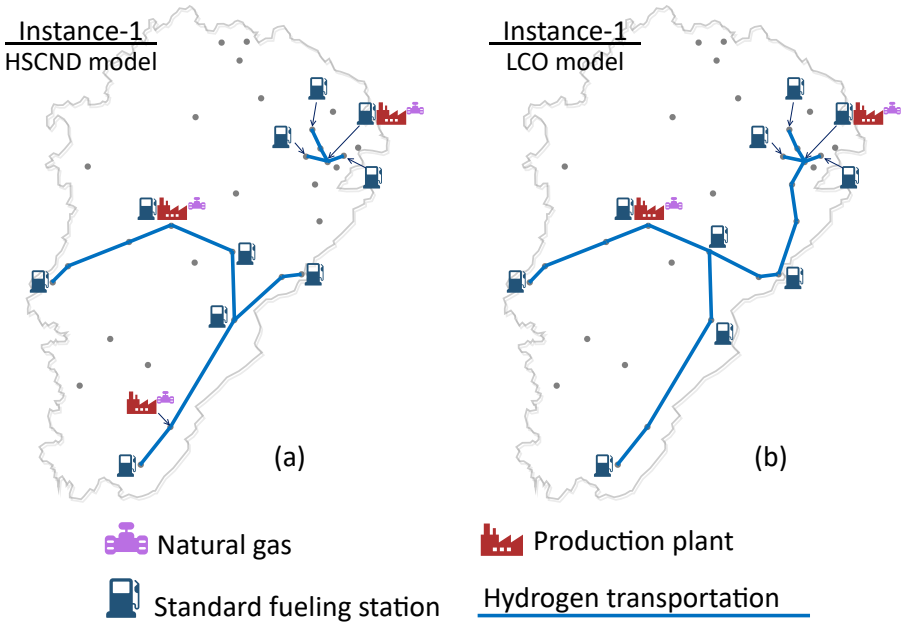

Figure 3.11: Configurations of Instance-1: (a) HSCND model; (b) LCO model

tal cost and LCOH. For operating costs (Contri_OC), the facility operating cost (FOC) of LCOH is larger than the total cost just because of the involvement of hydrogen storage. The removal of vehicle rental costs (HRC) should decrease operating costs related to hydrogen transportation (HTOC). Therefore, the operating costs of hydrogen transportation are larger in total cost than the ones in LCOH. The contribution of operating costs is 3.10 €/kg H_2 in LCOH, and 2.72 €/kg H_2 in total cost. The introduction of LCC has a major impact on capital costs. As can be seen in Fig. 3.13, replacement costs (FRC and TRC) significantly increase the LCOH. Transportation capital costs (TCC) are incurred in LCOH because vehicles are purchased instead of rented. The fixed charge rate method reduced the contribution of facility capital costs. Overall, the contribution of capital costs increased from 7.26 €/kg H_2 in total cost to 9.35 €/kg H_2 in LCOH. To sum, by introducing the LCC into HSCND, the LCO model considers costs more comprehensively, i.e., the addition of replacement costs. Moreover, the LCO model employs a more reasonable calculation approach, i.e., the fixed charge rate to obtain the levelized cost of hydrogen.

3.5.2/ THE EFFECT OF LCA ON HSCND

For Instance-2, configurations obtained from solving the HSCND model and LCO model are nearly the same (Only one location of fueling stations is different). Our focus is on the impact of LCA, especially LCI, on the performance measure related to emissions. Fig. 3.14 and Fig. 3.15 illustrate the composition of emission objective of HSCND model and LCO model, respectively. Since Instance-2 is based on biomass as feedstock for hydrogen, we see negative values for upstream production emissions. That is because the plants that are the source of biomass capture a certain amount of CO_2 through photosynthesis while they are growing. For onsite emission, the biogenic CO_2 is treated like fossil CO_2. It should also be noted that, although greenhouse gas emissions, including CO_2, CH_4, and N_2O, are considered in the LCO model, only the composition of CO_2 is shown in Fig. 3.15.

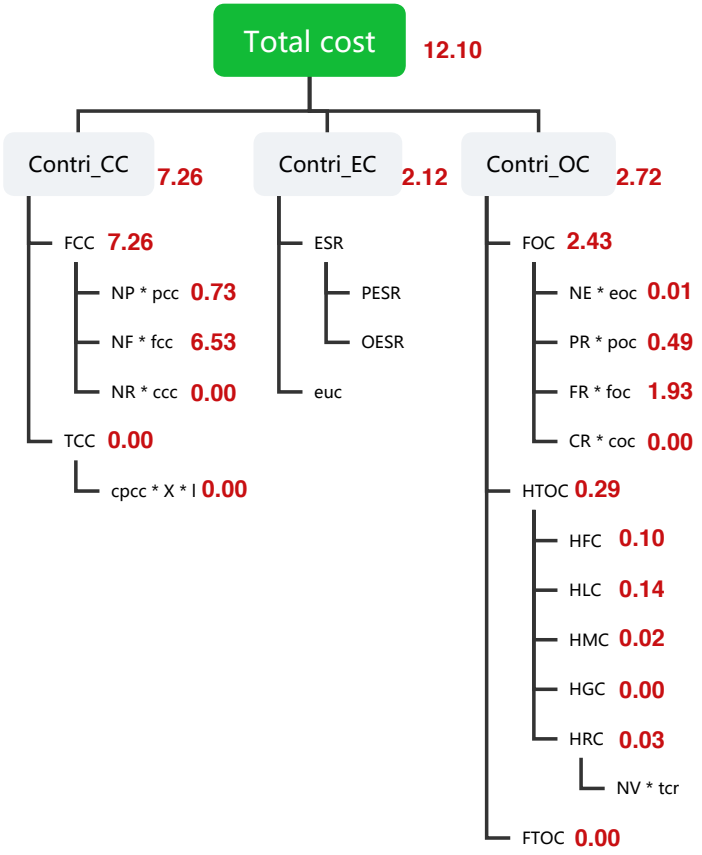

Figure 3.12: Composition of total cost by minimizing the cost objective in HSCND model (€/kg H_2)

The HSCND model's emission objective contains production, fueling, and transportation emissions. Production emissions are further divided into upstream and on-site emissions, while fueling and transportation emissions are not. In the LCO model, its emission objective involves storage-related emissions. Both fueling and transportation emissions include upstream and on-site emissions. Compared to the HSCND model, one remarkable change in the LCO model is that upstream emissions are split into feedstock and utility emissions. This detailed description is the benefit of introducing LCI analysis. The LCO model's production emissions include both feedstock and utility emissions. This is because there are both inputs of feedstock and utility in the production process. However, there is no feedstock input in the fueling and transportation process. Therefore, their upstream emissions contain only utility emissions.

A closer look at Fig. 3.14 and Fig. 3.15 can obtain more details. LCO model considers the utility emission, which the HSCND model does not. This explains why the LCO model has larger production emissions than the HSCND model. The LCO model's fueling emissions are about ten percent of the HSCND model's. It is probably due to the inappropriate proposition of emission factor in the HSCND model. LCO model's fueling emissions are obtained from LCI analysis, defining utility requirements and utility-related upstream emission factors. Therefore more reasonable emission values are achieved. It is also

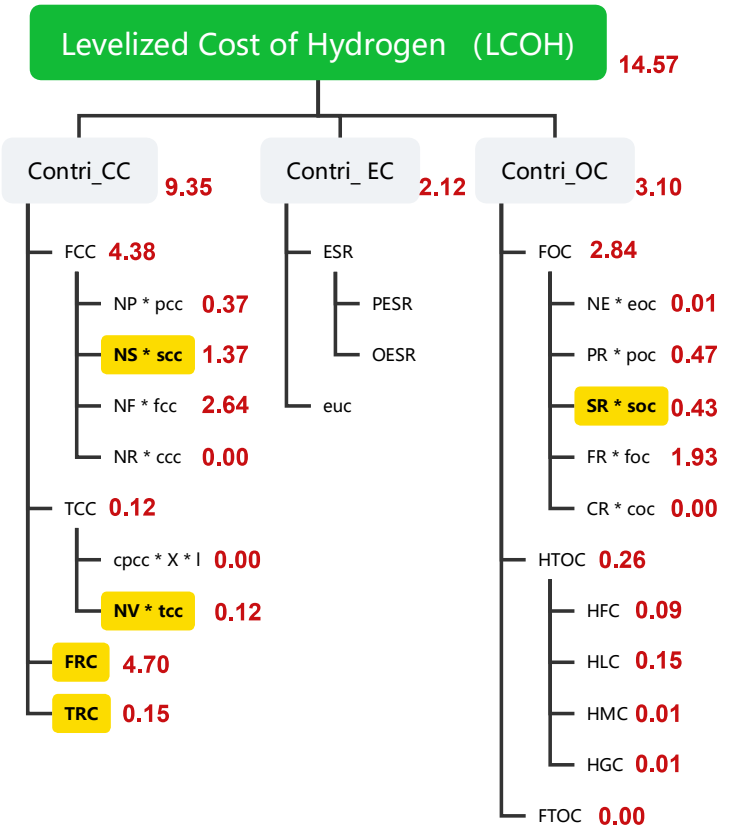

Figure 3.13: Composition of LCOH by minimizing the cost objective in LCO model (€/kg H_2)

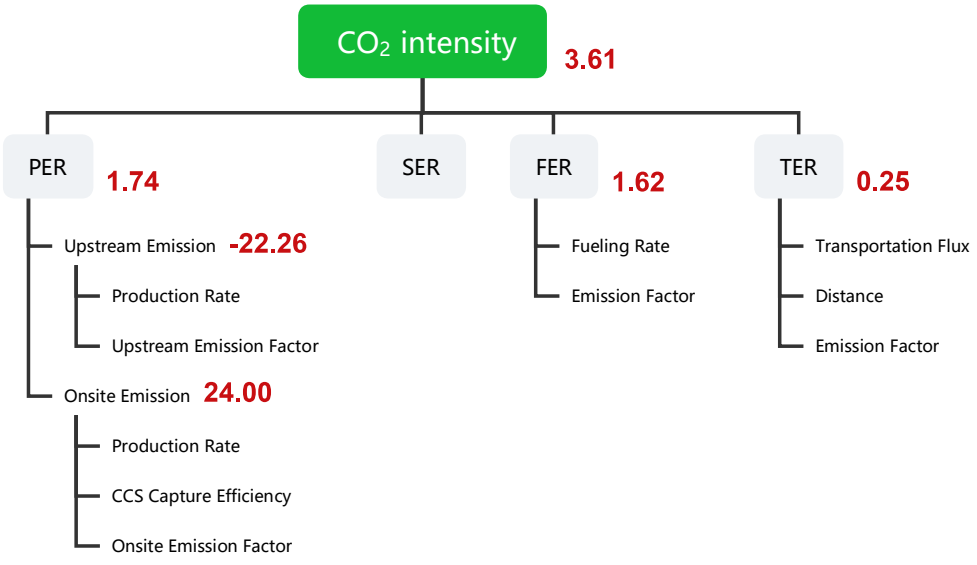

Figure 3.14: Composition of CO_2 intensity in HSCND model (kg CO_2/kg H_2)

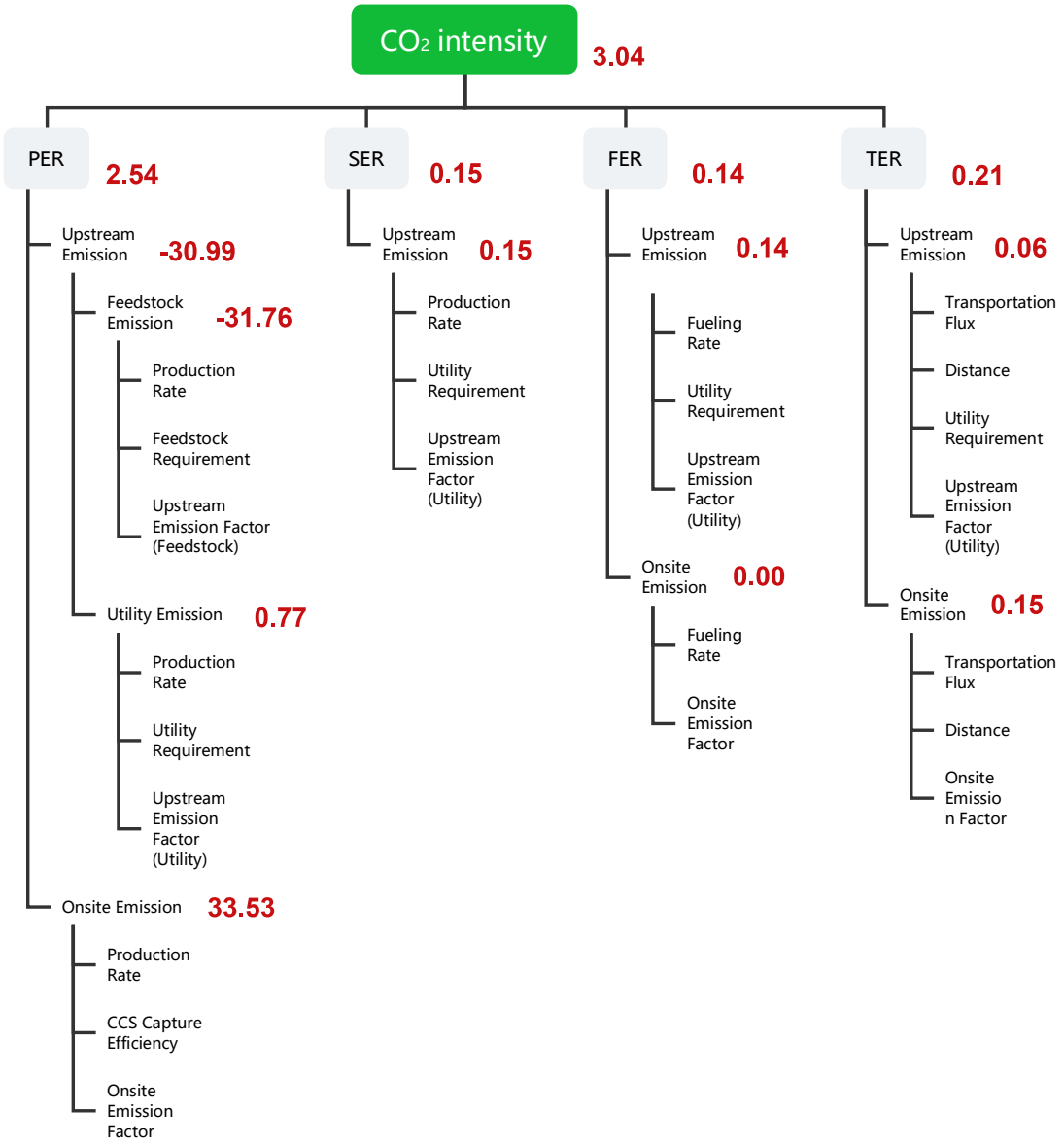

Figure 3.15: Composition of CO_2 intensity in LCO model (kg CO_2/kg H_2)

noticed that the LCO model's transportation emissions are further divided into upstream and onsite emissions. To sum, by introducing the LCA, especially LCI, into HSCND, the LCO model estimate emission more reasonably. Detailed emission classification offers a more accurate quantification of emissions from various sources. In addition, LCI analysis provides a good guide and reference for emission estimation.

3.5.3/ Results of LCO on HSCND

The life cycle optimization approach proposed in this chapter includes three main parts: life cycle costing to obtain more extensive involvement of HSCN costs; life cycle assessment to achieve more reasonable consideration of HSCN emissions; bi-objective optimization to combine LCC and LCA to provide decision-makers with Pareto optimal so-

lutions. Instance-3 is used to illustrate how LCC and LCA are integrated by bi-objective optimization to generate Pareto optimal solutions. Instance-3 allows the model to choose to apply the CCS system. Moreover, biomass is the single available feedstock to produce hydrogen. Therefore, the model can generate overall negative emissions (J. Yan, 2018; L. Li et al., 2020; del Pozo, Cloete, & Álvaro, 2021). The Pareto front obtained by solving the bi-objective model provides a holistic view of turning points, i.e., in what situation does the model choose to apply the CCS system; in what situation does the model produce negative emissions.

Fig. 3.16 shows a Pareto front which consists of five Pareto optimal solutions. Solution-A is the result of minimizing the single LCOH objective. It obtains the lowest value of LCOH, 18.6 €/kg H_2, and the highest GWP intensity, 3.68 kg CO_2 equivalent/kg H_2. The model does not apply the CCS system. Solution-B and the following solutions have large LCOH and small GWP intensity. It is because the model chooses to employ the CCS system. By capturing more CO_2 emissions, solutions get lower GWP intensity. It is noted that from Solution-B, we see values of GWP intensity are below zero, i.e., negative emissions. The reason for negative emission can be explained by the characteristic of biomass, whose upstream emission factor is negative. If a hydrogen production plant using biomass as feedstock adopts a CCS system, 90 % of its on-site emission will be captured so that the plant's CO_2 emissions are negative for every 1 kg of hydrogen produced using biomass (L. Li et al., 2020). Solution-C is very close to Solution-B, and we, therefore, expect little difference existing between their HSCN configurations. Solution-D and E reach a much lower GWP intensity due to more CO_2 emissions being captured by the CCS system. Moreover, the flat trend in the last two solutions indicates that the CCS system has run up all its processing capacity. It is tough for the model to decrease the GWP intensity further.

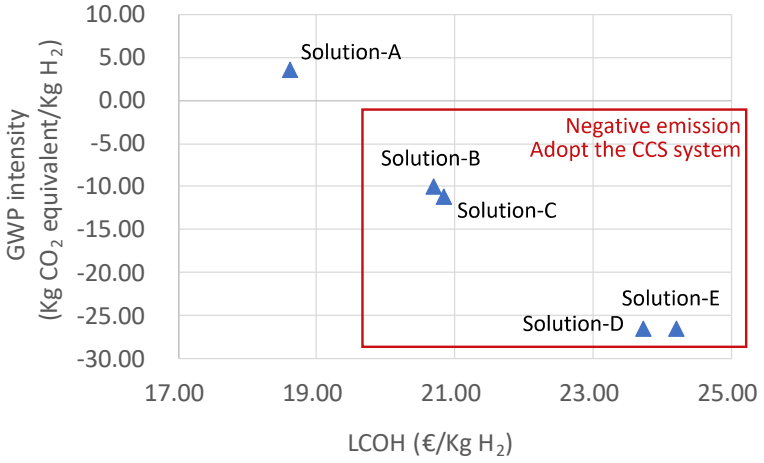

Figure 3.16: Pareto optimal solutions of Instance-3

We now focus on the configuration changes along the Pareto front. As shown in Fig. 3.17, though each solution has the same number and locations for production plants the same number for fueling stations, HSCN configuration keeps changing. In Solution-A, production plants located in Valdahon and Luxeuil-les-Bains supply hydrogen to their adjacent fueling stations. From Solution-B, the CCS system is adopted. As the single CO_2 storage site is located at Morteau, close to Valdahon, emissions from the Valdahon production plant are captured, transported, and stored. We know from Fig. 3.16 that Solution-B and C have closely objective values. Indeed, they have similar HSCN configurations and pro-

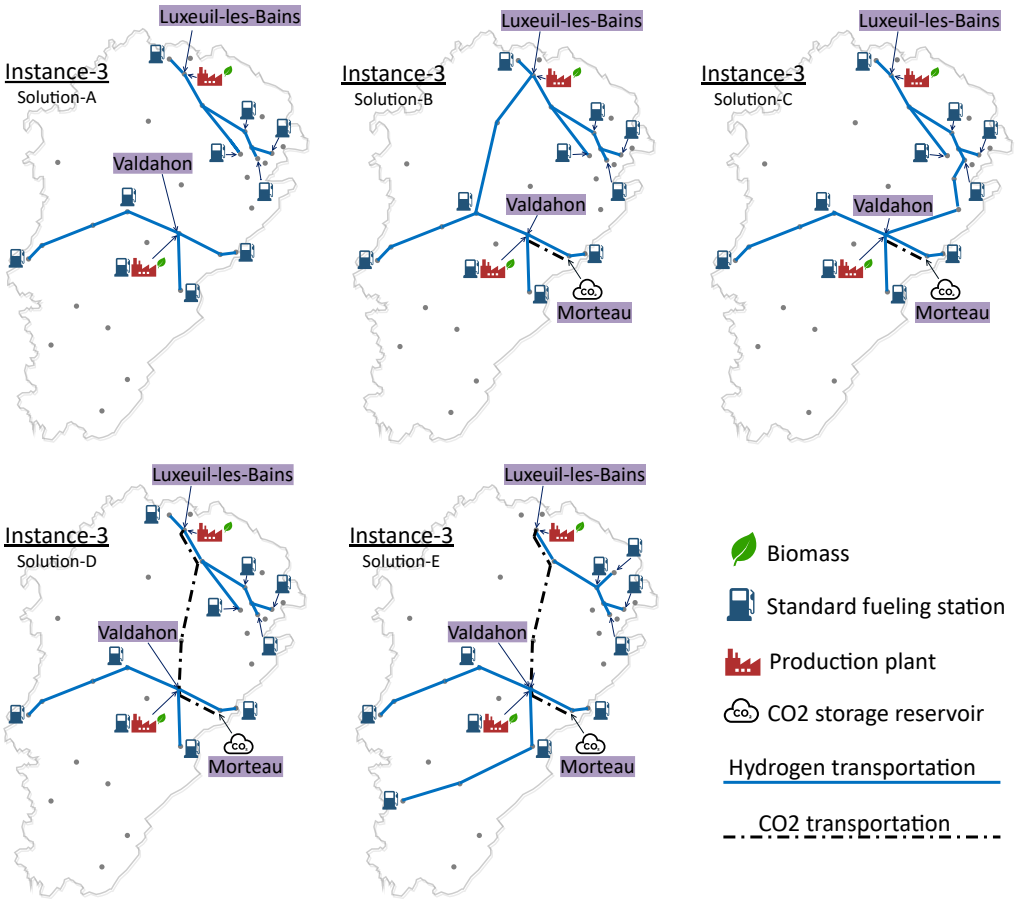

Figure 3.17: Configurations of Pareto optimal solutions of Instance-3

duction loads for two production plants. Configurations of Solution-D and E explain why they can reach a lower GWP intensity. The model chooses to build CO_2 transportation pipelines between two production plants. Luxeuil-les-Bains can benefit from the CCS system and reduce its onsite emissions. Therefore, the overall GWP intensity is decreased substantially. Correspondingly, the CO_2 processing rate is nearly doubled in Solution-D, compared to the previous value (from 84,032 kg CO_2/d to 172,290 kg CO_2/d). In addition, little difference between Solution D and F configurations proves that the HSCND has used up its emission reduction potential.

3.5.4/ SUMMARY

This section shows the effects of LCO on HSCND from three perspectives. It is demonstrated by Instance-1 that the employment of LCC can make a more comprehensive reflection of HSCN costs. Instance-2 proves that the introduction of LCA, especially LCI, can provide a detailed description of HSCN related emissions. Instance-3 shows the LCO model's ability to quantify and visualize the trade-off between costs and emissions within an HSCND.

3.6/ CONCLUSION

In this chapter, a systematic review of recent publications is conducted to identify the research gap. The review topics include SCND, LCO in SCND, HSCND, and performance measures adopted in previous HSCND publications. It is found that there are few sustainable HSCND papers. Previous economic and environmental performance measures of HSCND need to be improved. Therefore, this chapter contributes to the HSCND research domain by proposing an approach or solution for a sustainable HSCND.

The levelized cost of hydrogen (LCOH) is introduced as an economic performance measure, derived using a fixed charge rate (FCR) methodology that incorporates a predefined internal rate of return (IRR). Subsequently, a life cycle inventory (LCI) analysis is conducted for the HSCND to be utilized in the Life Cycle Assessment (LCA). By employing bi-objective optimization, Life Cycle Costing (LCC) and LCA are integrated into the life cycle optimization (LCO) modeling framework.

The mathematical model is tested by a case study that consists of three instances. The benefits of the LCO model are demonstrated from three perspectives. (i) Results obtained suggest that the introduction of LCC has a significant impact on capital costs. Replacement costs (FRC and TRC) significantly increase the LCOH. It is also found that the fixed charge rate method reduced the contribution of facility capital costs. (ii) By introducing the LCA, especially LCI, into HSCND, the LCO model estimate emission more reasonably. Detailed emission classification offers a more accurate quantification of emissions from various sources. (iii) The Pareto front obtained by solving the bi-objective model provides a holistic view of turning points, i.e., in what situation does the model choose to apply the CCS system; in what situation does the model produce negative emissions. It can be concluded that the LCO model could provide decision-makers with more comprehensive, more reasonable HSCN related references.

4

DESIGNING A CSHSCN WITH MULTI-PERIOD OPTIMIZATION

In this chapter, we move from a broad overview of optimizing the life cycle hydrogen supply chain to a focused exploration of centralized storage strategies within this system. Chapter 3 lays a foundation, examining the holistic impacts of hydrogen supply chain decisions on both economic and environmental fronts. It highlights the importance of life cycle costing and life cycle assessment for sustainable network design. Building upon this groundwork, this chapter focuses on the complexity of designing a centralized storage hydrogen supply chain network (CSHSCN). A new model is developed that not only adapts to the four-echelon centralized storage supply chain but also explores multiple periods while balancing the dual goals of economic feasibility and environmental sustainability. This approach reflects the dynamic nature of real hydrogen demand and supply, leveraging the flexibility of centralized storage to mitigate fluctuations and increase system resiliency.

4.1/ INTRODUCTION

Centralized supply chains, in contrast to decentralized ones, typically achieve economies of scale, which help in reducing the overall costs of the supply chain (Sahay & Ierapetritou, 2014). Centralized inventory management also facilitates more accurate inventory control and optimizes turnover. Moreover, centralized management can more effectively monitor and control safety stock levels, reducing the risks associated with improper storage conditions or poor inventory management across multiple regions. Previous research has considered various aspects of basic hydrogen supply chain design, including the multi-period, multi-objective, different region scales, various infrastructures, the uncertainty of the data, and so on. The summary of the relevant reviewed literature are shown in table 2.3.

However, these studies have seldom considered multiple periods and objectives within a particular strategy model. Research shows the economic advantages of a centralized storage hydrogen supply chain over a decentralized supply chain, while there is a lack of consideration of some important factors in the supply chain, including the assessment of the environmental impacts, uncertainty consideration, and the effect of the total cost optimization in the multi-period on the configuration of the supply chains. Therefore, the objective of this work is to propose a decision model for a hydrogen supply chain net-

work with centralized storage centers that takes into account the optimization of multiple objectives, the characteristics of multi-period (e.g. instability of resource availability), and the assessment of the environmental performance of the system. It aims to optimize the network configuration of the centralized storage hydrogen supply chain. The system's goals need to be achieved by adjusting the configuration facilities and transportation in different time periods. It can give decision-makers long-term investment planning advice.

As outlined in Chapter Two, the entire hydrogen energy supply chain is composed of numerous facilities and activities, including raw material suppliers, production plants, storage facilities, transportation, and hydrogen refueling stations. In the four-echelon network, the raw materials are transported from the supplier to the production plant, where the demanded form and quantity of hydrogen are produced and transported to the storage center, then conditioned and distributed by the storage center to the refueling station, and finally provided to the end customer. Specialized equipment can capture carbon dioxide in various production processes and be transported to the CO2 storage site. Hydrogen also can be produced and distributed locally on a small-scale plant. In the centralized network, the production plants and refueling stations are connected by fewer possible links using large-scale storage centers. Multiple forms of hydrogen with the same or different production locations are consolidated in one storage area and then distributed to the same or different final end-user location (Seo et al., 2020). So, there are three pathways of hydrogen transportation shown in figure 4.1, including the first hub transportation (from the different production cities to the same storage city), the second regional transportation (from the storage site to the demanding city) and direct transportation, where small quantities of hydrogen are transported directly to the town of demand without going through storage.

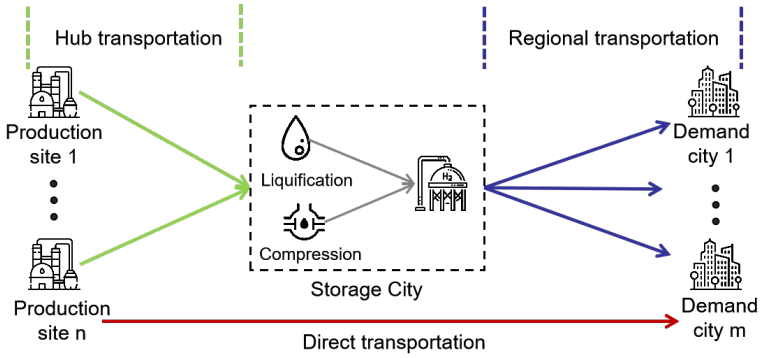

Figure 4.1: Hydrogen transportation pathway

In the supply chain system, the uncertainty includes the raw material prices, the raw material supply rate, the facilities price, and the customer demand. These data change between different periods and remain stable within the same period. For the flow of raw material between each node, the natural gas is transported only by pipeline, as gas transmission pipelines are covered in most cities. The electricity grid is also available at each node, so only the electricity transmission from the grid is considered. Biomass and coal are transported as solids by truck. Carbon dioxide is transported under pressure by truck. In our model, we have five types of storage facilities, gaseous, liquid, gaseous with liquefier, liquid with vaporizer, and liquid with liquefier and vaporizer. Hydrogen can be transported as gas or liquid by truck or pipeline, and the form also can be transformed between different sites. For example, hydrogen is produced in gaseous form at the production plants. Then it can be liquefied and stored at the storage center and transported

Table 4.1: The combinations of hydrogen form

No	Production form	Storage form	Regional transportation form	Refueling form
I1	Gaseous	Gaseous	Gaseous	Gaseous
I2	Gaseous	Liquid	Liquid	Liquid
I3	Gaseous	Liquid	Gaseous	Gaseous
I4	Liquid	Liquid	Liquid	Liquid
I5	Liquid	Liquid	Gaseous	Gaseous

in gaseous form to the refueling station. The complex hydrogen form transition combination is shown in table 4.1.

There is no limit to the number of production plants, storage centers, and refueling stations each node can build. Besides, the hydrogen system can choose to increase or reduce the capacity of the facilities or close the plant in each period. The decision plan is subject to the constraints of the supply rate of raw materials, the capacity of each facility, and consumer demand. Our task is to minimize the levelized costs and greenhouse gas emissions at the end of the planning horizon. The cost includes each stage's raw material, fixed investment, and operating costs. The final decision that can be obtained in the system includes:

- Location, quantity, and type of raw material supply in each periods;
- The number, location, scale, type, and output quantity of production plants and storage centers in each periods;
- The number, location, capacity, and type of refueling stations and Onsite refueling stations in each periods;
- Selection of the number of CO2 capture plants and storage location.
- Decision on the optimum quantity, route, and type of hydrogen transport in the hub, regional, and direct transportation in each periods.
- Emissions data generated at each node and time period during production, storage, transport, and distribution.

This chapter is organized as follows. The first section has given a brief overview of the issues addressed in the thesis. In Section 2, the bi-objective and multi-period centralized storage optimization model established through mathematical programming is introduced. Then, a national-scale case is applied to the model in section 3. In Section 4, the optimization model results are discussed, analyzed, and compared with other models. Finally, the section concludes with a summary of the contributions.

4.2/ MATHEMATICAL MODEL

The HSC optimization problem is formulated as a mixed integer programming model, which builds upon the model proposed in the previous chapter. It consists of the following sets and indices:

Table 4.2: Sets and indices

Sets	
$e \in E$	feedstock types (Natural gas, coal, biomass, electricity)
$f \in F$	transportation mood of feedstock(Pipeline, truck, power grid)
$g \in G$	greenhouse gas emission type(CO_2, CH_4, N_2O)
$h \in H$	transportation mode corresponding to hydrogen forms combination
$i \in I$	hydrogen physical forms combination in table 4.1
$j \in J$	off-site and on-site fueling station size(Small, medium, large, extra-large)
$k \in K$	production facility size(Small, medium, large)
$n, m \in N$	nodes
$o \in O$	on-site fueling technologies(Onsite-electrolysis)
$p \in P$	production technology(SMR, CG, BG, Electrolysis)
$r \in R$	storage facility size(Small, medium, large)
$t \in T$	time period
$u \in U$	utility type (Natural gas, electricity, diesel)
Parameters	
ccc	capital cost of a CO_2 storage site, €
coc	operating cost of CO_2 processing, €/kg CO_2
cpc_t	unit capital cost of CO_2 transportation pipeline, €/km
cph_t	unit capital cost of H_2 transportation pipeline, €/km
d	discount rate
dw_f	driver wage of feedstock transportation mode f, €/h
dw_{ht}	driver wage of hydrogen transportation mode h, €/h
DEM_{nt}	hydrogen demand for node n in time period t , kg H_2/d
$ecap_{net}^{max}$	upper limit of feedstock supply capacity , unit feedstock/d
$ecap_{net}^{min}$	lower limit of feedstock supply capacity, unit feedstock/d
euc_{et}	unit price of feedstock, €/unit
fcc_{ijt}	unit capital cost of standard fueling station, €
fcc_{ojt}	unit capital cost of on-site fueling station, €
fe_h	fuel economy of hydrogen transportation mode h, km/L fuel
foc_{ijt}	operation cost of standard fueling station, €/kg H_2
foc_{ojt}	operation cost of on-site fueling station, €/kg H_2
fp_{ht}	fuel price of hydrogen transportation mode h, €/L fuel
ge_{ht}	general expense of hydrogen transportation mode h, €/d
ir	inflation rate
l_{nm}	shortest distance between two different nodes, km
lut_h	load/unload time of hydrogen transportation mode h, h
me_{ht}	maintenance expense of hydrogen transportation mode h, €/km
pcc_{pikt}	unit capital cost of production plant, €
poc_{pikt}	operation cost of production plant, €/kg H_2
$pcap_{pikt}^{max}$	upper limit of production capacity, kg H_2/d
$pcap_{pikt}^{min}$	lower limit of production capacity, kg H_2/d
POR_t	pipeline transportation daily operating cost ratio
PVF_{ijt}	replacement factor of the stander fueling station
$PVOF_{ojt}$	replacement factor of the onsite fueling station
PVP_{pikt}	replacement factor of the production plant
$PVPC_t$	replacement factor of the CO_2 pipeline transportation equipment
$PVPH_t$	replacement factor of the H_2 pipeline transportation equipment
PVR_t	replacement factor of the CO_2 storage site
PVS_{irt}	replacement factor of the storage center
$PVTV_{ht}$	replacement factor of the vehicle direct transportation equipment
$PVTV1_{ht}$	replacement factor of the vehicle hub transportation equipment
$PVTV2_{ht}$	replacement factor of the vehicle regional transportation equipment
rc_{ft}	feedstock transportation equipment rental cost, €/d

scc_{irt}	unit capital cost of storage center, €
soc_{irt}	operation cost of storage center, €/kg H_2
sp_h	speed of hydrogen transportation mode h, km/h
$tcap1_h$	hydrogen hub transportation vehicle capacity, kg
$tcap_h^{max}$	upper limit of hydrogen direct transportation capacity, kg
$tcap_h^{min}$	lower limit of hydrogen direct transportation capacity, kg
$tcap1_h^{max}$	upper limit of hydrogen hub transportation capacity, kg
$tcap1_h^{min}$	lower limit of hydrogen hub transportation capacity, kg
$tcap2_h^{max}$	upper limit of hydrogen regional transportation capacity, kg
$tcap2_h^{min}$	lower limit of hydrogen regional transportation capacity, kg
$tcapp1_h^{max}$	upper limit of hydrogen hub pipeline transportation capacity, kg
$tcapp1_h^{min}$	lower limit of hydrogen hub pipeline transportation capacity, kg
$tcapp2_h^{max}$	upper limit of hydrogen regional pipeline transportation capacity, kg
$tcapp2_h^{min}$	lower limit of hydrogen regional pipeline transportation capacity, kg
tcc_{ht}	unit capital cost of direct transportation equipment, €
$tcc1_{ht}$	unit capital cost of hub transportation equipment, €
$tcc2_{ht}$	unit capital cost of regional transportation equipment, €
$tercap_{irt}^{max}$	upper limit of storage capacity, kg H_2
$tercap_{irt}^{min}$	lower limit of storage capacity, kg H_2
tma_h	availability of hydrogen transportation mode h, h/d
TE	decline rate of emissions from facility
THD	total hydrogen demand, kg
X	operating days in a period
$\delta_{t,(e,p)}$	conversion rate of feedstock at production plant
$\delta_{t,(e,f)}$	conversion rate of feedstock at on-site fueling station
Continuous variables	
CR_t	total processing rate of CO_2, kg CO_2/d
FOR_{nojt}	fueling rate of on-site fueling station, kg H_2/d
FR_{nijt}	fueling rate of standard fueling stations, kg H_2/d
FSR_{net}	feedstock supply rate, unit feedstock/d
NDV_{ht}	number of new transport equipment for direct transportation
NF_{nijt}	number of the newly built standard fueling station
NOF_{nojt}	number of the newly built on-site fueling station
NP_{npikt}	number of the newly built production plant
NPV_{ht}	number of new transport equipment for hub transportation
NR_{nt}	number of the newly built CO_2 storage reservoirs
NS_{nirt}	number of the newly built storage center
NSV_{ht}	number of new transport equipment for regional transportation
NV_{ft}	number of feedstock transportation vehicles
PR_{npikt}	production rate of production plants, kg H_2/d
SR_{nirt}	storage rate of storage center, kg H_2/d
TRD_{hnmt}	daily hydrogen direct transportation flux, kg/d
TRF_{fnmt}	feedstock transportation flux, unit feedstock/d
TRP_{hnmt}	daily hydrogen hub transportation flux, kg/d
$TRPP_{hnmt}$	daily hydrogen hub pipeline transportation flux, kg/d
TRS_{hnmt}	daily hydrogen regional transportation flux, kg/d
$TRSP_{hnmt}$	daily hydrogen regional pipeline transportation flux, kg/d
$XNPP_{nmt}$	number of new transport equipment for hub transportation
Intermediate Variables	
EC	total feedstock purchasing cost, €
EM_g	emissions of each type of gas g , kg
EM_{CH_4}	total emission rate of CH_4, kg/d
EM_{CO_2}	total emission rate of CO_2, kg/d
EM_{N_2O}	total emission rate of N_2O, kg/d
EMF_g	emissions during the process of hydrogen refueling, kg

EMP_g	emissions during the process of hydrogen production, kg
EMS_g	emissions during the process of hydrogen storage, kg
EMT_g	emissions during the process of hydrogen transportation, kg
EP	emission parameters in each period
ESR_{et}	total supply rate of feedstock sites, unit feedstock/d
FCC	total facility capital cost, €
FOC	total facility operating cost, €
FRC	total facility replacement cost, €
FTC	feedstock transportation operating cost, €
$FTRC$	feedstock transportation vehicles rental cost, €
HFC	hydrogen transportation fuel cost, €
HGC	hydrogen transportation general cost, €
HLC	hydrogen transportation labor cost, €
HMC	hydrogen transportation maintenance cost, €
HTD	hydrogen direct vehicle transportation operating cost, €
HTP	hydrogen hub vehicle transportation operating cost, €
HTS	hydrogen regional vehicle transportation operating cost, €
$OESR_{net}$	feedstock supply rate for on-site fueling station, unit/d
$PESR_{net}$	feedstock supply rate for off-site production plants, unit/d
PTP	hydrogen hub pipeline transportation operating cost, €
PTS	hydrogen regional pipeline transportation operating cost, €
PV	present value
TCC	total transportation capital cost, €
$TCCP$	total pipeline investment cost, €
$TCCV$	total road vehicle transportation capital cost, €
TOC	total transportation operating cost, €
TRC	total transportation replacement cost, €
$NTDV_{ht}$	number of direct transportation vehicle
NTF_{nijt}	total number of fueling station
$NTOF_{nojt}$	total number of on-site fueling station
NTP_{npikt}	number of production plant
$NTPV_{ht}$	number of pub transportation vehicle
NTS_{nirt}	number of the storage center
$NTSV_{ht}$	number of regional transportation vehicle
Binary Variables	
IE_{net}	1, if the node is chosen as a feedstock supplier,0, otherwise
XD_{hnmt}	1, if there is hydrogen direct transportation, 0, otherwise
XF_{hnmt}	1, if there is feedstock transportation, 0, otherwise
$XNCP_{nmt}$	1, if a pipeline is newly built for CO_2 transportation,0, otherwise
$XNPP_{hnmt}$	1, if a pipeline is newly built for hub transportation,0, otherwise
$XNSP_{hnmt}$	1, if a pipeline is newly built for regional transportation,0, otherwise
XP_{hnmt}	1, if there is hydrogen hub transportation, 0, otherwise
XPP_{hnmt}	1, if a pipeline is built for hub transportation,0, otherwise
XS_{hnmt}	1, if there is hydrogen regional transportation, 0, otherwise
XSP_{hnmt}	1, if a pipeline is built for regional transportation,0, otherwise

4.2.1/ OBJECTIVE FUNCTION

The model takes into account two aspects: economical and impact on the environment. The objectives are minimizing the levelized cost of hydrogen (LCOH) and global warming potential intensity (GWP) in the whole time period. It can be represented by the following function:

$$Minimize \qquad LCOH, GWP \tag{4.1}$$

$$LCOH = \frac{FCC + TCC + FRC + TRC + FOC + TOC + EC}{THD} \tag{4.2}$$

$$GWP = \frac{EM_{CO_2} + 28EM_{CH_4} + 265EM_{N_2O}}{THD} \tag{4.3}$$

The variables in the equation are defined as follows: FCC, FRC, and FOC refer to the total capital cost, replacement cost, and operating cost of facilities, respectively. TCC, TRC, and TOC are the total capital cost, replacement cost, and operating cost of transportation, respectively. EC denotes the cost of feedstock purchases. THD denotes the total hydrogen demand over the entire time period. EM_{CO_2}, EM_{CH_4} and EM_{N_2O} represent the different types of green house gas emission.

4.2.1.1/ DEMAND

Total hydrogen demand is determined by the current demand for fuel cell energy vehicles, the population of different regions, and the predicted penetration rate over different time periods.

$$THD = \sum_{nt} DEM_{nt} * X \tag{4.4}$$

Where DEM_{nt} represents the daily hydrogen demand in the node n at the time period t. X represents the operating days in a period.

4.2.1.2/ CAPITAL COST

The capital cost consists of the facility and transportation capital cost. The facility capital cost includes production, storage, off-site fueling, on-site fueling, and CO_2 storage. It is calculated as follows:

$$\begin{aligned} FCC = \sum_{t} (PV * (\sum_{n,p,i,k} NP_{npikt} * pcc_{pikt} + \sum_{n,i,r} NS_{nirt} * scc_{irt} + \sum_{n,i,j} NF_{nijt} * fcc_{ijt} \\ + \sum_{n,o,j} NOF_{nojt} * fcc_{ojt} + \sum_{n} NR_{nt} * ccc_t)) \end{aligned} \tag{4.5}$$

Where NP_{npikt}, NS_{nirt}, NF_{nijt}, NOF_{nojt}, NR_{nt} represent the number of new facilities build in the time period t. pcc_{pikt}, scc_{irt}, fcc_{ijt}, fcc_{ojt}, ccc_t denote the unite capital cost of production plants, storage center, off-site refueling station, onsite refueling station and CO_2 storage site respectively. The present value (PV) is used to derive the current value of a capital cost on a future date. It can be described as follows:

$$PV = \frac{(1 + ir)^t}{(1 + d)^t} \tag{4.6}$$

Where ir represents the inflation rate. d denotes the discount rate. The transportation capital cost (TCC) consist of the capital cost of road vehicle transportation (TCCV) and the investment costs for pipeline (TCCP), which is defined as:

$$TCC = TCCV + TCCP \tag{4.7}$$

$$TCCV = \sum_{t}(PV * (\sum_{h} NPV_{ht} * tcc1_{ht} + \sum_{h} NSV_{ht} * tcc2_{ht} + \sum_{h} NDV_{ht} * tcc_{ht})) \tag{4.8}$$

$$\begin{aligned} TCCP = \sum_{t}(PV * (\sum_{h,n,m} cph_t * XNPP_{hnmt} * l_{nm} + \sum_{h,n,m} cph_t * XNSP_{hnmt} * (l_{nm} + l_n^p) \\ + \sum_{n,m} cpc_t * XNCP_{nmt} * (l_{nm} + l_n^p))) \end{aligned} \tag{4.9}$$

Where NPV_{ht}, NSV_{ht} and NDV_{ht} represent the number of new transport equipment from production plants to storage center, storage center to distribution station and production plants to refueling station respectively. tcc_{ht}, $tcc1_{ht}$ and $tcc2_{ht}$ are the cost of each corresponding transportation mode in the time period t. $XNPP_{nmt}$, $XNSP_{nmt}$ and $XNCP_{nmt}$ are binary variables. It equals 1 if the pipeline transportation is new built from node n to m in the time period t. l_{nm} is the shortest distance between the two nodes. cph_t and cpc_t indicate the unit capital cost of H_2 and CO_2 pipeline respectively in the time period t.

Assuming that refueling stations are evenly distributed within the city. Ar_n denotes the total area of each city, while l_n^p signifies the estimated average distance for hydrogen transportation at this specific node.

$$l_n^p = \sqrt{Ar_n * \sum_{i,j,t} NTF_{nijt}} \tag{4.10}$$

4.2.1.3/ REPLACEMENT COST

The facilities will be replaced after run out the lifetime. The replacement cost in the entire operating period is related to the facility cost and replacement factor. The Replacement factor is calculated by the equation 3.8. The facility replacement cost can be obtained by the following equation:

$$\begin{aligned} FRC = \sum_{t}(PV * (\sum_{n,p,i,k} NP_{npikt} * pcc_{pikt} * PVP_{pikt} + \sum_{n,i,r} NS_{nirt} * scc_{irt} * PVS_{irt} \\ + \sum_{s,i,j} NF_{nijt} * fcc_{ijt} * PVF_{ijt} + \sum_{n,o,j} NOF_{nojt} * fcc_{ojt} * PVOF_{ojt} \\ + NR_{nt} * ccc_t * PVR_t)) \end{aligned} \tag{4.11}$$

Where PVP_{pikt}, PVS_{irt}, PVF_{ijt}, $PVOF_{ojt}$, PVR_t represent the replacement factor for production, storage, off-site fueling station, on-site fueling station and CO_2 storage site respectively. The transportation replacement cost is determined through the following equation:

$$TRC = \sum_{t} PV * (\sum_{h} PVTV1_{ht} * NPV_{ht} * tcc1_{ht} + \sum_{h} PVTV2_{ht} * NSV_{ht} * tcc2_{ht} + \sum_{h} PVTV_{ht} * NDV_{ht} * tcc_{ht} + \sum_{i,n,m} PVPH_{t} * (cph_{t} * XPP_{nmt} * l_{nm} + cph_{t} * XSP_{nmt} * l_{nm}) + \sum_{n,m} PVPC_{t} * cpc_{t} * XCP_{nmt} * l_{nm}) \tag{4.12}$$

where $PVTV1$, $PVTV2$, $PVTV$, $PVPH$, and $PVPC$ denote the replacement factor of hub, regional and direct vehicle transportaion, hydrogen transportation pipeline and CO_2 transportation pipeline respectively.

4.2.1.4/ OPERATING COST

The operating cost is obtained by multiplying the unit cost of production (poc_{pikt}), storage (soc_{irt}), off-site fueling (foc_{ijt}), on-site fueling (foc_{ojt}) and CO_2 storage (coc_{t}) by the daily production rate (PR_{npikt}), storage rate (SR_{nirt}), off-site refueling rate (FR_{nijt}), on-site refueling rate (FOR_{nojt}) and CO_2 storage rate (CR_{t}) in each time period t. Each of the variables is related to the facilities' form, size, and technology. As shown in the following equation:

$$FOC = \sum_{t} (X * PV * (\sum_{n,p,i,k} PR_{npikt} * poc_{pikt} + \sum_{n,i,r} SR_{nirt} * soc_{irt} + \sum_{n,i,j} FR_{nijt} * foc_{ijt} + \sum_{n,o,j} FOR_{nojt} * foc_{ojt} + CR_{t} * coc_{t})) \tag{4.13}$$

Where X represents the operating days in each period.

Following the whole hydrogen transportation pathway (figure 4.1), the operating cost (TOC) includes hydrogen first hub vehicle transportation (HTP) and pipeline transportation (PTP), hydrogen secondary regional vehicle transportation (HTS) and pipeline transportation (PTS), direct hydrogen transportation from production plants to demand city (HTD), and feedstock road transportation (FTC).

$$TOC = HTP + HTS + HTD + PTP + PTS + FTC \tag{4.14}$$

Hydrogen hub vehicle transportation is composed of fuel cost (HFC), labour cost (HLC), maintenance cost (HMC) and general cost (HGC). As shown in the following equation:

$$HTP = HFC + HLC + HMC + HGC \tag{4.15}$$

$$HFC = \sum_{h,n,m,t} X * fp_{ht} * \frac{2 * l_{nm} * TRP_{hnmt}}{fe_{h} * tcap1_{h}} \tag{4.16}$$

$$HLC = \sum_{h,n,m,t} X * dw_{ht} * \frac{TRP_{hnmt}}{tcap1_{h}} * (\frac{2 * l_{nm}}{sp_{h}} + lut_{h}) \tag{4.17}$$

$$HMC = \sum_{h,n,m,t} X * me_{ht} * \frac{2 * l_{nm} * TRP_{hnmt}}{tcap1_{h}} \tag{4.18}$$

$$HGC = \sum_{h,n,m,t} X * ge_{ht} * \frac{TRP_{hnmt}}{tma_h * tcap1_h} * (\frac{2 * l_{nm}}{sp_h} + lut_h) \tag{4.19}$$

Where TRP_{hnmt} represents the transportation flux from production node n to storage center m in mode h. fp_h, dw_h, me_h, ge_h, and tcr_h represent the fuel price (per liter fuel), driver wage (per hour), maintenance expense (per km), general expense (per day), and vehicle rental cost (per vehicle) of hydrogen transportation mode h, respectively. fe_h, sp_h, $tcap1_h$, tma_h, and lut_h denote the fuel economy, speed, capacity, availability (hours per day), and load/unload time of hydrogen transportation mode h, respectively.HTS and HTD have the same form as the calculation of HTP. The feedstock transportation vehicles are rented, so the additional rental cost is added to the calculation of $FTRC$, as follows:

$$FTRC = \sum_{f,t} X * NV_{ft} * rc_{ft} \tag{4.20}$$

Where NV_{ft} is the number required feedstock transportation vehicle. rc_{ft} denotes the daily rental cost. PTP and PTS is determined by multiplying the total pipeline capital cost $TCCP$ and ratio of daily operation cost POR.

$$PTP = TCCP_t * POR_t \tag{4.21}$$

4.2.1.5/ FEEDSTOCK COST

We treat the price of raw materials as stable in the same period. The feedstock purchase cost is equal to multiplying the total feedstock consumption rate (ESR_{et}) by unit cost (euc_{et}):

$$EC = \sum_{et} ESR_{et} * euc_{et} \tag{4.22}$$

The full raw material consumption rate consist of the consumption rate of off-site production ($PESR_{net}$) and on-site production ($OESR_{net}$).

$$ESR_{et} = \sum_{n} X * (PESR_{net} + OESR_{net}) \tag{4.23}$$

4.2.1.6/ EMISSIONS

The total emissions are consist of the emission from production (EMP_g), storage (EMS_g), transportation (EMT_g), and fueling station (EMF_g).

$$EM_g = EMP_g + EMS_g + EMT_g + EMF_g \tag{4.24}$$

We assume that facility emission rates decline at the rate of TE as technology evolves. The emission parameters EP in each period can be calculated as:

$$EP = (1 - TE)^{t-1} \tag{4.25}$$

Emissions from each process are divided into two parts, upstream emission and onsite emission. The calculation functions are developed from the functions in section 3.4.1.2 by incoporates the time variable.

4.2.2/ CONSTRAINTS

4.2.2.1/ FEEDSTOCK CONSTRAINTS

The feedstock consumed by production plants ($PESR_{ne}$) and on-site fueling stations ($OESR_{ne}$) can be obtained as follows:

$$PESR_{net} = \sum_{i,k} PR_{npikt} * \delta_{t,(e,p)} \tag{4.26}$$

$$OESR_{net} = \sum_{j} FOR_{nojt} * \delta_{t,(e,o)} \tag{4.27}$$

The sum of local feedstock supply point n and import from all supply nodes m meets total feedstock consumption at each node n and in each time period t. The mass balance of feedstock as follows:

$$FSR_{net} + \sum_{m,f:(e,f)} TRF_{fmnt} = \sum_{m,f:(e,f)} TRF_{fnmt} + PESR_{net} + OESR_{net} \tag{4.28}$$

$$IE_{net} * ecap_{net}^{min} \leq FSR_{net} \leq IE_{net} * ecap_{net}^{max} \tag{4.29}$$

Where FSR_{net} represents the raw material supply rate at node n. IE_{met} is binary variables. It equal to 1 if there are feedstock supply sites in the time period t. $ecap_{met}^{min}$ and $ecap_{met}^{max}$ are minimal and maximal support rates for different feedstock e at the site n.

4.2.2.2/ PRODUCTION CONSTRAINTS

The maximum and minimum capacity limits of production plants constrain their production rate PR_{npik} from surpassing them.

$$NTP_{npikt} * pcap_{pikt}^{min} \leq PR_{npikt} \leq NTP_{npikt} * pcap_{pikt}^{max} \tag{4.30}$$

where NTP_{npikt} represents the number of production plants in the time period t in the node n. $pcap^{min}pik$ and $pcap^{max}pik$ denote the minimum and maximum achievable production rates for various production technologies p and plant sizes k, respectively.

The number of total hydrogen production plants in each period is equal to the number of plants that built in the period t plus the total number of plants that built in the previous period t-1, as follows:

$$NTP_{npikt} = NP_{npikt} + NTP_{npik(t-1)} \tag{4.31}$$

Where NP_{npikt} is the number of new production plant producing hydrogen in the form i, with technology p, and size k constructed at time period t in the node n. NTP_{npik0} represents the number of existing production plants before the first time period.

4.2.2.3/ STORAGE CONSTRAINTS

The number of total storage center NTS_{nirt} and newly built storage facilities NS_{nirt} with size r in the time period t have the same constraints with production plants. It is defined as:

$$NTS_{nirt} = NS_{nirt} + NTS_{nir(t-1)} \tag{4.32}$$

The quantity in storage centers at node n (SR_{nirt}) must not surpass the minimum and maximum storage capacity limits.

$$NTS_{nirt} * tercap_{irt}^{min} \leq SR_{nirt} \leq NTS_{nirt} * tercap_{irt}^{max} \tag{4.33}$$

To mitigate uncertainties in production and demand, it is valuable to integrate storage facilities containing reserve stocks capable of catering to emergency supply needs over several days. The total storage rates within the same timeframe need to require Y times of total demand. Y signifies the duration for which hydrogen is to be stored.

$$\sum_{nir} SR_{nirt} \geq Y * \sum_{n} DEM_{nt} \tag{4.34}$$

4.2.2.4/ TRANSPORTATION CONSTRAINTS

The hydrogen transportation flow is shown in Figure 4.2. At each city n, the storage rate at the previous period $SR_{nri(t-1)}$ plus the hydrogen production rate PR_{npikt}, import from other production node m through road transportation TRP_{hmnt} and pipeline transportation $TRPP_{hmnt}$, import from other storage node m through vehicle transportation TRS_{hmnt} and pipeline transportation $TRSP_{hmnt}$, and import from other production node directly TRD_{hmnt} need to equal the sum of the hydrogen hub transportation rate to other node m TRP_{hnmt} and $TRPP_{hnmt}$, the hydrogen regional transportation $TRSP_{inmt}$ and TRS_{hnmt}, the hydrogen direct export TRD_{hnmt}, the stander refueling station demand FR_{nsijt}, and the storage rate at the period t SR_{nrit}.

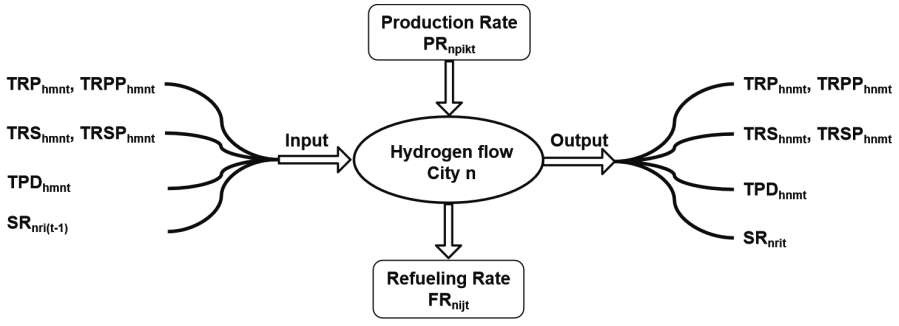

Figure 4.2: Hydrogen transportation flow

$$\begin{aligned}\sum_{r} SR_{nri(t-1)} + \sum_{p,k} PR_{npikt} + \sum_{h:(i,h),m} TRP_{hmnt} + \sum_{h:(i,h),m} TRPP_{hmnt} \\ + \sum_{h:(i,h),m} TRS_{hmnt} + \sum_{h:(i,h),m} TRSP_{hmnt} + \sum_{h:(i,h),m} TRD_{hmnt} \\ = \sum_{h:(i,h),m} TRP_{hnmt} + \sum_{h:(i,h),m} TRPP_{hnmt} + \sum_{h:(i,h),m} TRS_{hnmt} \\ + \sum_{h:(i,h),m} TRSP_{hnmt} + \sum_{h:(i,h),m} TRD_{hnmt} + \sum_{s,i,j} FR_{nijt} + \sum_{r} SR_{nrit}\end{aligned} \tag{4.35}$$

The transportation flow of feedstock (TRF_{fnmt}), hydrogen at the production center (TRP_{hnmt}), and hydrogen at the storage center (TRS_{hnmt}) cannot exceed their minimal and maximal limit of capacity. The hydrogen transportation flow from the production node to the refueling node directly (TRD_{hnmt}) cannot exceed the capacity of a trailer or truck.

$$XP_{hnmt} * tcap1_h^{min} \leq TRP_{hnmt} \leq XP_{hnmt} * tcap1_h^{max} \tag{4.36}$$

$$XS_{hnmt} * tcap2_h^{min} \leq TRS_{hnmt} \leq XS_{hnmt} * tcap2_h^{max} \tag{4.37}$$

$$XD_{hnmt} * tcap_h^{min} \leq TRD_{hnmt} \leq XD_{hnmt} * tcap_h^{max} \tag{4.38}$$

$$XF_{fnmt} * tcapf_f^{min} \leq TRF_{fnmt} \leq XF_{fnmt} * tcapf_f^{max} \tag{4.39}$$

Pipeline transportation cannot exceed its daily maximum and minimum flow limits.

$$XPP_{hnmt} * tcapp1_h^{min} \leq TRPP_{hnmt} \leq XPP_{hnmt} * tcapp1_h^{max} \tag{4.40}$$

$$XSP_{hnmt} * tcapp2_h^{min} \leq TRSP_{hnmt} \leq XSP_{hnmt} * tcapp2_h^{max} \tag{4.41}$$

The pipeline used in period t is equal to the sum of the newly built pipeline in period t and the pipeline invested in period t-1.

$$XPP_{hnmt} = XNPP_{hnmt} + XPP_{hnm(t-1)} \tag{4.42}$$

$$XSP_{hnmt} = XNSP_{hnmt} + XSP_{hnm(t-1)} \tag{4.43}$$

Only one direction occurred in the transportation between different nodes.

$$XPP_{hnmt} + XPP_{hmnt} \leq 1 \tag{4.44}$$

$$XSP_{hnmt} + XSP_{hmnt} \leq 1 \tag{4.45}$$

The number of transport equipments are defined as follows.

$$NTPV_{ht} \geq \sum_{n,m} \frac{TRP_{hnmt}}{tma_h * tcap1_h} * (\frac{2 * l^r_{nm}}{sp_h} + lut_h) \tag{4.46}$$

$$NTSV_{ht} \geq \sum_{n,m} \frac{TRS_{hnmt}}{tma_h * tcap2_h} * (\frac{2 * (l^r_{nm} + l^p_n)}{sp_h} + lut_h) \tag{4.47}$$

$$NTDV_{ht} \geq \sum_{n,m} \frac{TRD_{hnmt}}{tma_h * tcap1_h} * (\frac{2 * (l^r_{nm} + l^p_n)}{sp_h} + lut_h) \tag{4.48}$$

$$NTPV_{ht} = NPV_{ht} + NTPV_{h(t-1)} \tag{4.49}$$

$$NTSV_{ht} = NSV_{ht} + NTSV_{h(t-1)} \tag{4.50}$$

$$NTDV_{ht} = NDV_{ht} + NTDV_{h(t-1)} \tag{4.51}$$

Where $tcap1$ and $tcap2$ are the maximal capacity for the hub and regional transportation. The variable tma signifies the amount of time available for work each day. The running speed is denoted by sp, and lut refers to the time taken to load and unload the transportation mode h.

4.2.2.5/ Fueling station constraints

The fueling rate (FR_{nsijt}) and on-site fueling rate (FOR_{nojt}) must not exceed their respective minimum and maximum capacity limits.

$$NTF_{nijt} * fcap^{min}_{ij} \leq FR_{nijt} \leq NTF_{nijt} * fcap^{max}_{ij} \tag{4.52}$$

$$NTOF_{nojt} * Ocap^{min}_{oj} \leq FOR_{nojt} \leq NTOF_{nojt} * Ocap^{max}_{oj} \tag{4.53}$$

The number of the off-site fueling stations and on-site fueling stations is limited by:

$$NTF_{nijt} = NF_{nijt} + NTF_{nij(t-1)} \tag{4.54}$$

$$NTOF_{nojt} = NOF_{nojt} + NTOF_{noj(t-1)} \tag{4.55}$$

Where NTF_{nij0} and $NTOF_{noj0}$ are the existing number of fueling station and on-site fueling station before the first investment, respectively. NF_{nijt} and NOF_{nojt} represent the number of new constructed fueling station. NTF_{nijt} and $NTOF_{nojt}$ denote the total number of fueling station in the node n at time period t.

The total fueling rate in off-site fueling station and on-site fueling station must be greater than the total demand in each period and node.

$$\sum_{n,i,j} FR_{nijt} + \sum_{n,o,j} FOR_{nojt} \geq \sum_{n} DEM_{nt} \tag{4.56}$$

4.3/ CASE STUDY: FRANCE

France was selected as the case study region. On one hand, the country aspires to develop a fully integrated hydrogen energy system, covering production to end-use. On the other hand, it benefits from substantial policy support in this endeavor (France Hydrogène, 2021). Currently, it used about 1 million tonnes of hydrogen every year, including pure hydrogen, and partly mixed with other gases (RTE, 2020). To evaluate the benefits and constraints of a multi-period centralized storage model (CSM), we devised 36 distinct scenarios. Specifically, we first analyzed the performance of the model in 10 and 15 nodes, while examining six different demand scenarios. Subsequently, we compared the results of the 10-node configuration with two decentralized storage models. In decentralized model 1 (DSM1), storage facilities and production centers were co-located at the same node, which is in line with most hydrogen supply chain network design models. In decentralized model 2 (DSM2), storage centers were established near production sites and also demand sites.

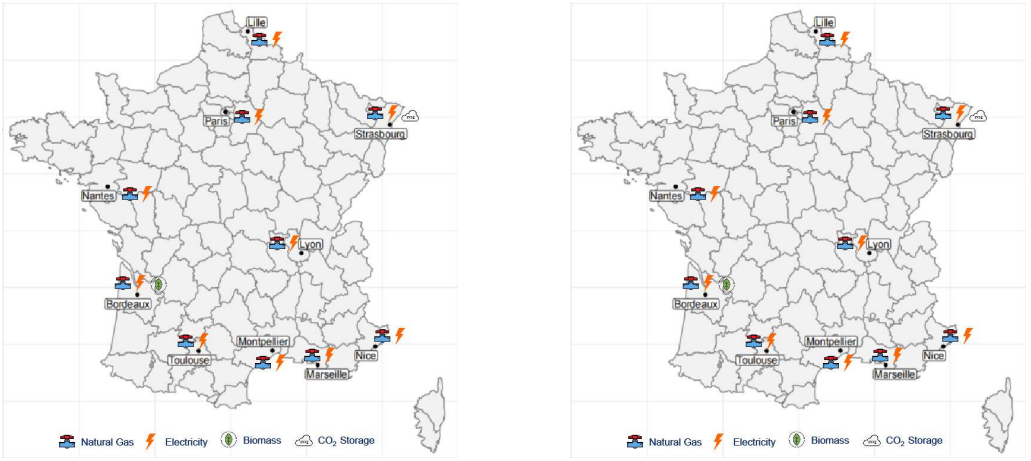

Figure 4.3: Map of cities and energy distribution

To forecast the demand for hydrogen, we divide regions based on administrative provinces, taking into account factors such as the current population of the region, the number of vehicles owned, annual income, and main economic indicators. Within this framework, the greater the population and the number of vehicles, the higher the demand for hydrogen, and the higher annual income contributes to the faster adoption of new energy vehicles. In the main economies, we categorize it into three types: the first category includes areas specialized in agriculture and tourism as well as residential areas; the second category encompasses large cities with highly concentrated urban functions, regions with diversified economies, and cities with a high number of employers; the third category refers to areas specialized in industry. Each category is assigned a value of 1, 2, or 3, respectively. The more the main economy leans towards industry, the more applications scenarios there are for hydrogen. The proportion of each factor was calculated and assigned a weight of 40%, 40%, 10%, and 10% to obtain a demand factor (as equation 4.57) for each region, calculated value shown in the appendix A.8. Based on the calculation, we have selected the top 10 and 15 areas with the most prominent factors. The selected cities are shown in figure 4.3.

$$DMR_n = R_{population} * 0.4 + R_{vehicles} * 0.4 + R_{income} * 0.1 + R_{economic} * 0.1 \tag{4.57}$$

We employ market penetration rates for different periods and demand rates for different regions to investigate various hydrogen demand scenarios. The demand rate for each region is calculated using the formula outlined in equation 4.58, where $DM_{adequaten}$ represents the total market demand for hydrogen under conditions where it fully replaces petroleum. According to (Department, 2022), the average annual driving distance per vehicle in France is approximately 13,117 km. Given that hydrogen has an efficiency of about 100 km per kilogram, and with 2,137,153 vehicles in operation across 10 cities and 2,557,805 vehicles across 15 cities (Transition & Ministry, 2021), the daily demand for hydrogen amounts to 768,028 kilograms in the first scenario and 919,198 kilograms in the second.

$$DEM_{nt} = DM_{adequaten} * DMR_n * MPR_t \tag{4.58}$$

The goal of substituting 80 percent of vehicle energy with alternative sources by 2050 is established. The timeline from 2023 to 2050 is segmented into four phases: 2023-2029 (period 1), 2030-2036 (period 2), 2037-2043 (period 3), and 2044-2050 (period 4). Drawing on past studies, the progression of energy technology is generally modeled using S-curve regression (Chen, Chen, & Lee, 2010). To assess the effectiveness of the centralized storage model under diverse scenarios and to understand the impact of fluctuating demand patterns on the supply chain, varying regression rates are applied across the four periods, with six scenarios selected for analysis (Figure 4.4). A minimum penetration rate of 5% is anticipated in the first period, with all scenarios projected to achieve 80% by the final period. Over a span of seven years, the hydrogen demand is expected to remain relatively stable, with specifics on different penetration rates detailed in the Appendix A.9.

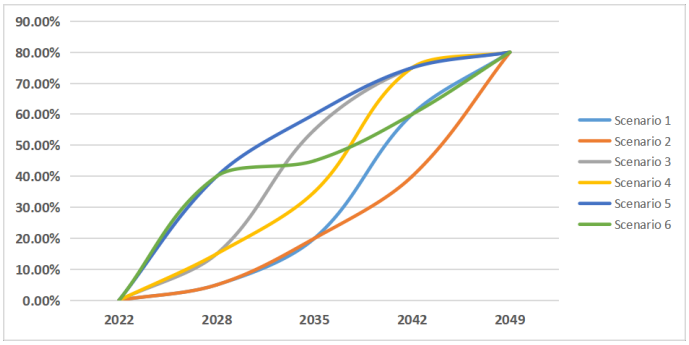

Figure 4.4: Hydrogen demand scenarios

In accordance with the climate law enacted in 2021, France is prohibited from promoting the use of coal as an energy source (Institute, 2021). Consequently, we have selected three widely employed production techniques: water electrolysis, steam methane reforming, and biomass gasification. The distribution of the raw materials required for the three production technology in France is shown in figure 4.3. The model's input data include the capital cost of production plants, storage, fueling station, operational costs and capacity, pipeline construction and vehicle costs, raw material prices, and other technical constraints mostly from Seo (Seo et al., 2020). The specific data is shown in the table

A.7. The economic parameters are estimated based on market experience. The inflation rate is assumed to be 0.06, and the discount rate is 0.08. Other assumption includes the following:

- Raw material prices are not subject to market fluctuations;
- The capital cost of facilities remains stable over all periods;
- There is no limit to the number of production plants, storage centers, and refueling stations that can be built at each node;
- In each period, for the production plants, there is the option to increase the production rate to the maximum productivity or decrease to the minimum productivity. For storage facilities, there is the option to increase or reduce equipment usage within the capacity limit or stop using the site (small scale).

4.4/ RESULTS

To address this multi-period mixed integer programming model, we employed a computer equipped with 16 GB of RAM and an Intel i7 CPU running at 1.80 GHz. The experiments were executed using the CPLEX 12.9 optimization solver. In the case study, the ten-nodes scenario has 68147 constraints and 39032 variables, 139532 constraints and 79212 variables included in the 15-nodes scenarios. The model faces the difficulty of a long time converging due to the size of the problem. Considering both solution quality and processing time, we established the convergence threshold to be less than 1%, with a maximum model runtime of up to 20 hours.

4.4.1/ ECONOMIC PERFORMANCE EVALUATION

Table 4.3 presents a comprehensive breakdown of the LCOH results for all the scenarios considered in this study over the entire time frame. The CSM consistently achieves a lower or equal LCOH compared to the two types of DSM in all scenarios, owing to the construction of large-scale production and storage centers. A close comparison of the LCOH results of DSM1 and CSM for each period reveals minimal differences between them. It's noteworthy that CSM and DSM1 even share the same configuration in certain scenarios. This underscores the effectiveness of co-locating production plants and storage centers within the same vicinity, particularly when the number of nodes is limited. However, a significant cost differential is observed in the first period when compared to DSM2. Figure 4.5 depicts the average LCOH of the three models across all six scenarios for each period, and it is evident that the cost of the hydrogen system does not follow a linear trend as demand increases over time. Following a substantial drop in the second period, the rate of cost decline becomes slower across all three models in the 10 cities case, which also exists in the 15 cities centralized case. The trends of CSM and DSM1 are always close, while the cost gap between the DSM and DSM2 gradually diminishes as time progresses. On the other hand, CSM does not always exhibit the lowest cost in each period, but it maintains the lowest average cost throughout the entire time horizon. This can be observed in the detailed results of each scenario, CSM results are higher than DSM1 in some periods. The reason behind this trend is the strategic construction of larger production plants or fewer quantities of storage facilities at optimal intervals to

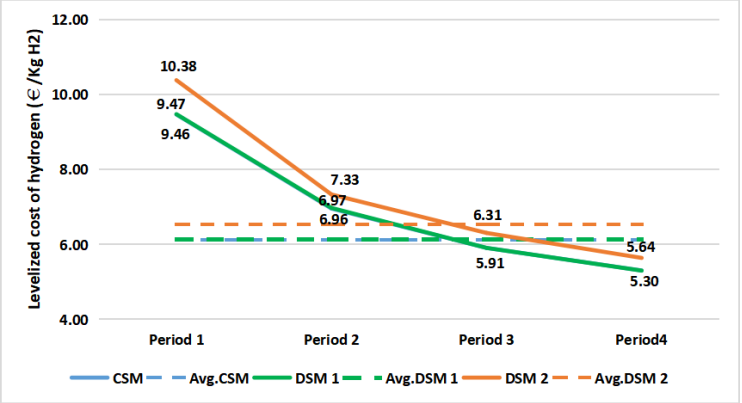

((a)) 10 nodes

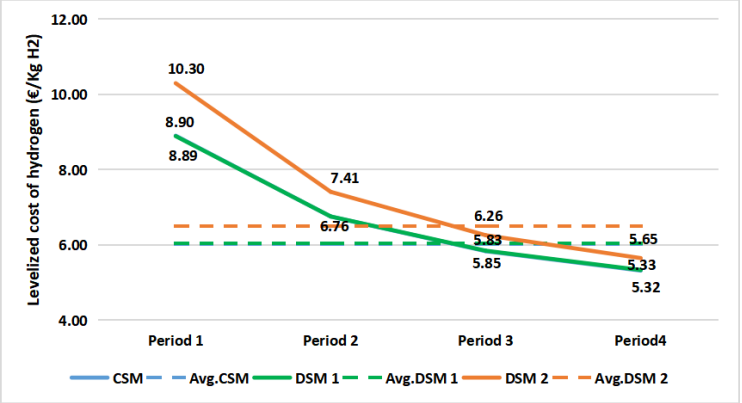

((b)) 15 nodes

Figure 4.5: Trend of average levelized cost of hydrogen

achieve optimal efficiency, which results in higher initial investment expenses for some periods. However, this approach ultimately facilitates the overall optimization of the hydrogen supply chain network.

Upon analyzing various scenarios, the most notable disparity between the CSM and DSM is evident in scenario 2 with 15 nodes. In this scenario, the cost savings achieved by CSM amount to 0.527 euros per kilogram of hydrogen, marking a reduction of approximately 8.6%, equating to a total investment saving of 1.795 billion euros over the entire period.

Figure 4.6 presents a cost breakdown for CSM and two types of DSM under demand scenario 1. It can be seen that the ten cities case (CSM-10) has a similar cost component to the 15 cities case (CSM-15) in the CSM. The process of production consistently accounts for the most significant proportion of the total cost and is generally followed by the cost of the refueling station. In contrast, transport costs represent a minor component of the entire supply chain cost. Comparing the total costs of the CSM with DSM1 and DSM2, the former achieves cost savings of 0.011€/ kg and 0.398€/ kg of hydrogen in the ten-node scenarios, respectively. The costs of raw materials and refueling processes are relatively similar in all cases. The cost savings resulting from the introduction of a centralized storage model are attributed to the combined cost optimization of production, storage, and transportation processes. As a result, the total system cost is reduced, and the findings are consistent with those of a previous study conducted in a single period.

Scenario	Time period				Average cost	GWP (CO_2 equiv)
	Period 1	Period 2	Period 3	Period 4		
Centralized Model (€/ kg H_2)						
10 Nodes S1	10.814	7.322	6.377	5.363	6.134	17.302
10 Nodes S2	10.866	7.346	6.301	5.768	6.308	17.237
10 Nodes S3	9.037	6.968	5.670	5.137	6.022	17.284
10 Nodes S4	9.021	7.804	5.892	5.150	6.158	17.297
10 Nodes S5	8.525	6.048	5.618	5.137	6.024	17.308
10 Nodes S6	8.525	6.249	5.576	5.267	6.125	17.328
15 Nodes S1	9.848	7.265	6.143	5.359	6.011	17.223
15 Nodes S2	9.839	7.198	6.184	5.618	6.138	17.256
15 Nodes S3	8.723	6.672	5.646	5.179	5.936	17.213
15 Nodes S4	8.634	7.350	5.850	5.218	6.063	17.291
15 Nodes S5	8.189	6.066	5.614	5.236	6.006	17.301
15 Nodes S6	8.189	5.981	5.570	5.305	6.023	17.284
Decentralized Model 1 (€/ kg H_2)						
10 Nodes S1	10.860	7.381	6.397	5.353	6.144	17.285
10 Nodes S2	10.866	7.389	6.292	5.763	6.309	17.275
10 Nodes S3	9.037	6.968	5.670	5.137	6.022	17.284
10 Nodes S4	9.021	7.804	5.892	5.150	6.158	17.297
10 Nodes S5	8.525	6.048	5.618	5.137	6.024	17.308
10 Nodes S6	8.525	6.249	5.576	5.267	6.125	17.328
15 Nodes S1	9.848	7.243	6.184	5.349	6.019	17.205
15 Nodes S2	9.768	7.209	6.216	5.622	6.148	17.258
15 Nodes S3	8.723	6.672	5.646	5.179	5.936	17.275
15 Nodes S4	8.634	7.377	5.856	5.216	6.069	17.271
15 Nodes S5	8.189	6.060	5.610	5.261	6.011	17.298
15 Nodes S6	8.189	5.981	5.567	5.378	6.049	17.309
Decentralized Model 2 (€/ kg H_2)						
10 Nodes S1	12.113	7.967	6.760	5.655	6.533	17.254
10 Nodes S2	12.113	7.980	6.687	6.028	6.689	17.228
10 Nodes S3	10.067	7.428	6.019	5.449	6.431	17.295
10 Nodes S4	9.832	7.379	6.497	5.684	6.574	17.218
10 Nodes S5	9.079	6.516	5.888	5.437	6.395	17.267
10 Nodes S6	9.069	6.714	5.978	5.585	6.535	17.329
15 Nodes S1	12.144	8.022	6.617	5.674	6.497	17.206
15 Nodes S2	12.135	8.076	6.692	5.956	6.664	17.250
15 Nodes S3	9.851	7.215	6.008	5.509	6.382	17.238
15 Nodes S4	9.827	8.025	6.235	5.530	6.528	17.234
15 Nodes S5	8.917	6.560	5.967	5.569	6.444	17.289
15 Nodes S6	8.917	6.571	6.027	5.662	6.520	17.286

Table 4.3: Levelized cost over entire time horizon

Figure 4.7, 4.8 and 4.9 show the system configuration for each period in the CSM and DSM at the demand scenario 1 with ten cities, respectively. Natural gas is chosen as the raw material in all cases. In the processes of transportation and storage, the majority of hydrogen operates in liquid form throughout the entire period. The choice of liquid storage indicates that it remains the most cost-effective method under the current technical conditions.

In the initial period of the CSM, a production plant utilizing Steam Methane Reforming (SMR) technology is established alongside a small storage center at the same site. Moving into the second period, expansion occurs with the addition of a medium-sized pro-

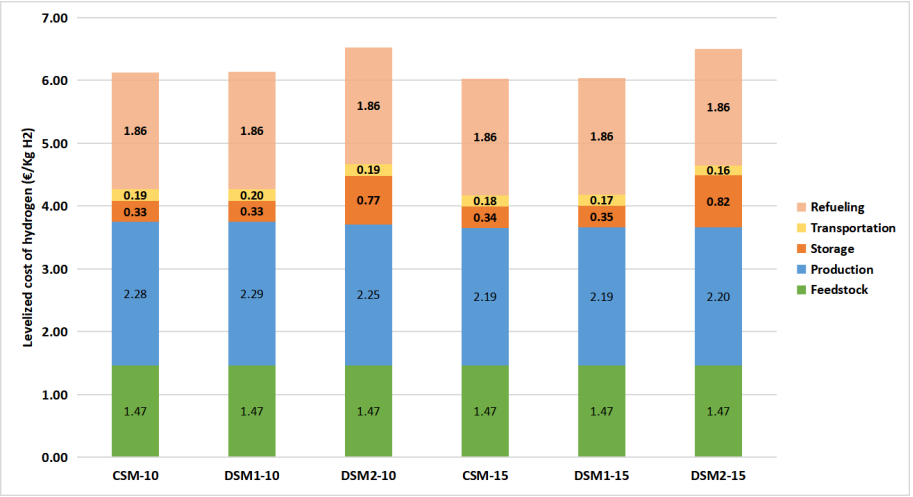

Figure 4.6: Composition of LCOH

duction plant at the same location. The small storage centers were abandoned and a large-scale liquid storage center and a large-scale compress gaseous storage center were built at two locations respectively. The third period witnesses the establishment of a large-scale production facility and storage center in Lyon. Presently, the system predominantly sources hydrogen from two production nodes, with excess hydrogen beyond storage capacity transported from Lyon to the Paris storage center for storage. In the final period, no new plants are introduced, with only adjustments made to facility capacities and storage rates to meet demand requirements. The majority of demands are met by the large-scale plant in Lyon. Over about 30 years, the system necessitates the construction of one large-scale liquid production plant, two medium-scale liquid production plants, one medium-scale gaseous production plant, three large-scale storage centers, and one small-scale storage center.

Both DSM1 and DSM2 entail a commensurate number and scale of production facilities compared to the CSM but are geographically dispersed across different nodes. Additionally, it becomes apparent from the graphical representations that neither DSM nor CSM opt for on-site production due to the prevalence of higher construction costs, elevated operating expenditures, and constrained capacity. It is worth noting that during period 3, the CSM opted to establish a new production and storage center in Lyon while transporting a portion of the hydrogen to stores in Paris. Conversely, in the DSM 1 model, the decision was made to construct two large storage centers during this period to accommodate the hydrogen flow generated by a single large production center. This choice stemmed from the node's productivity exceeding the maximum capacity of a single storage center. To maximize storage center utilization, minimize facility construction investments, and simultaneously leverage the cost advantages of large production centers, CSM carried out this choice and substantiated the advantages of the model.

4.4.2/ Environment performance evaluation

The results presented in Table 4.3 show that the average GWP of centralized storage systems is marginally lower than the first decentralized model , while higher than the second types of decentralized storage systems. This difference can be main attributed to

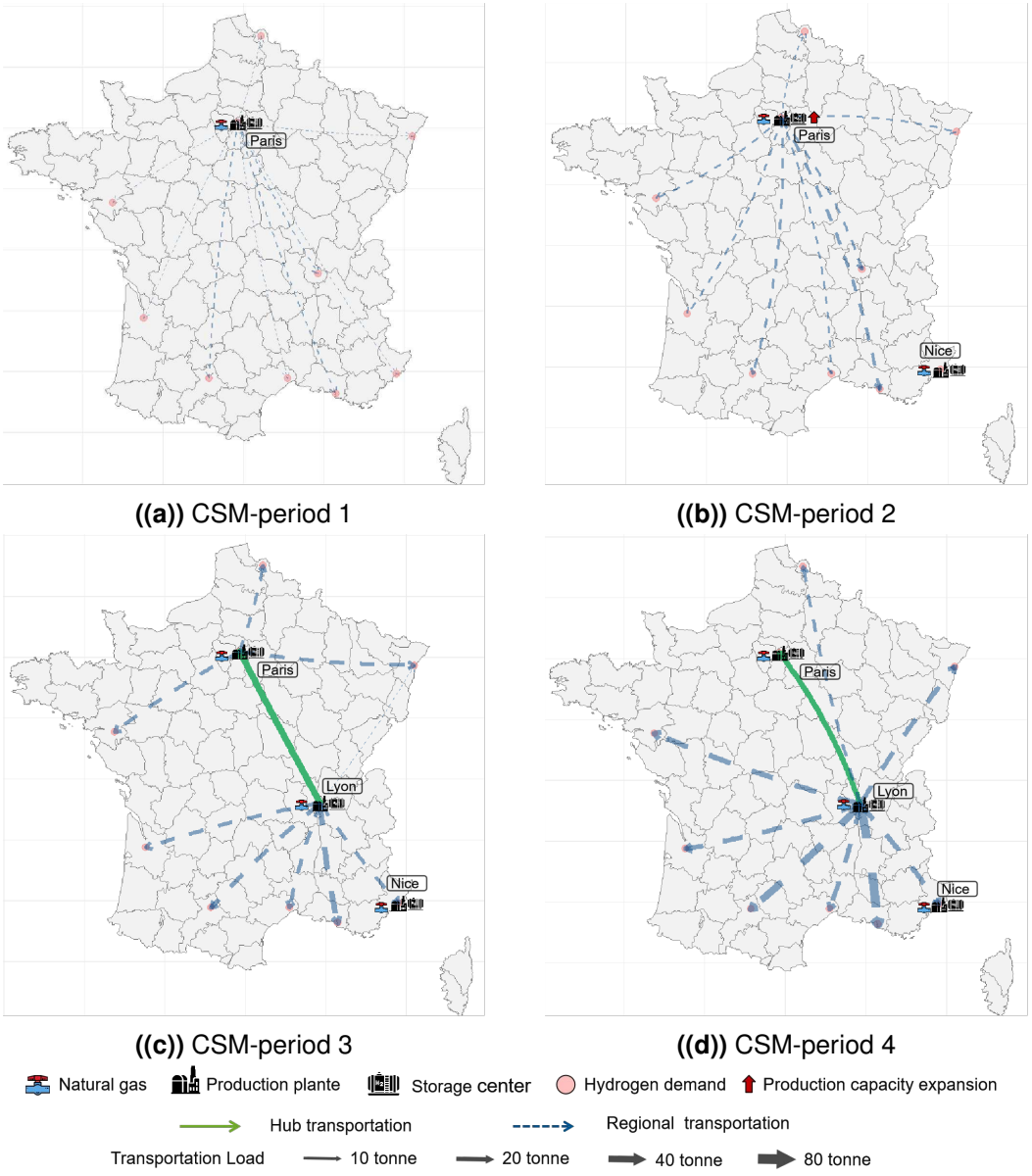

Figure 4.7: Configuration of Multi-period Centralized storage HSC for 10 cities

the preference of DSM 2 for more and more dispersed production and storage facilities, which reduces the need for hydrogen transportation, resulting in lower emissions from transport. In CSM model where cost is the primary goal, the centralized storage model prefers to build large-scale centralized storage centers to reduce total costs. While, the increase in emissions in the DSM 1 model is mostly due to the increase in transportation emissions caused by the location restrictions of production and storage nodes. The composition of emissions shown in Figure 4.10 indicates that hydrogen production consistently contributes to over 90% of emissions in all models, followed by storage emissions, transport emissions, and refueling emissions. When minimizing costs is used as the objective function without limiting emissions, DSM 2 generally outperforms CSM in terms of unit emissions across the entire hydrogen supply chain. However, we found that when emissions in the supply chain system are restricted, the CSM is superior in terms of investments. Figure 4.11 shows the experimental results. We constrained the emissions

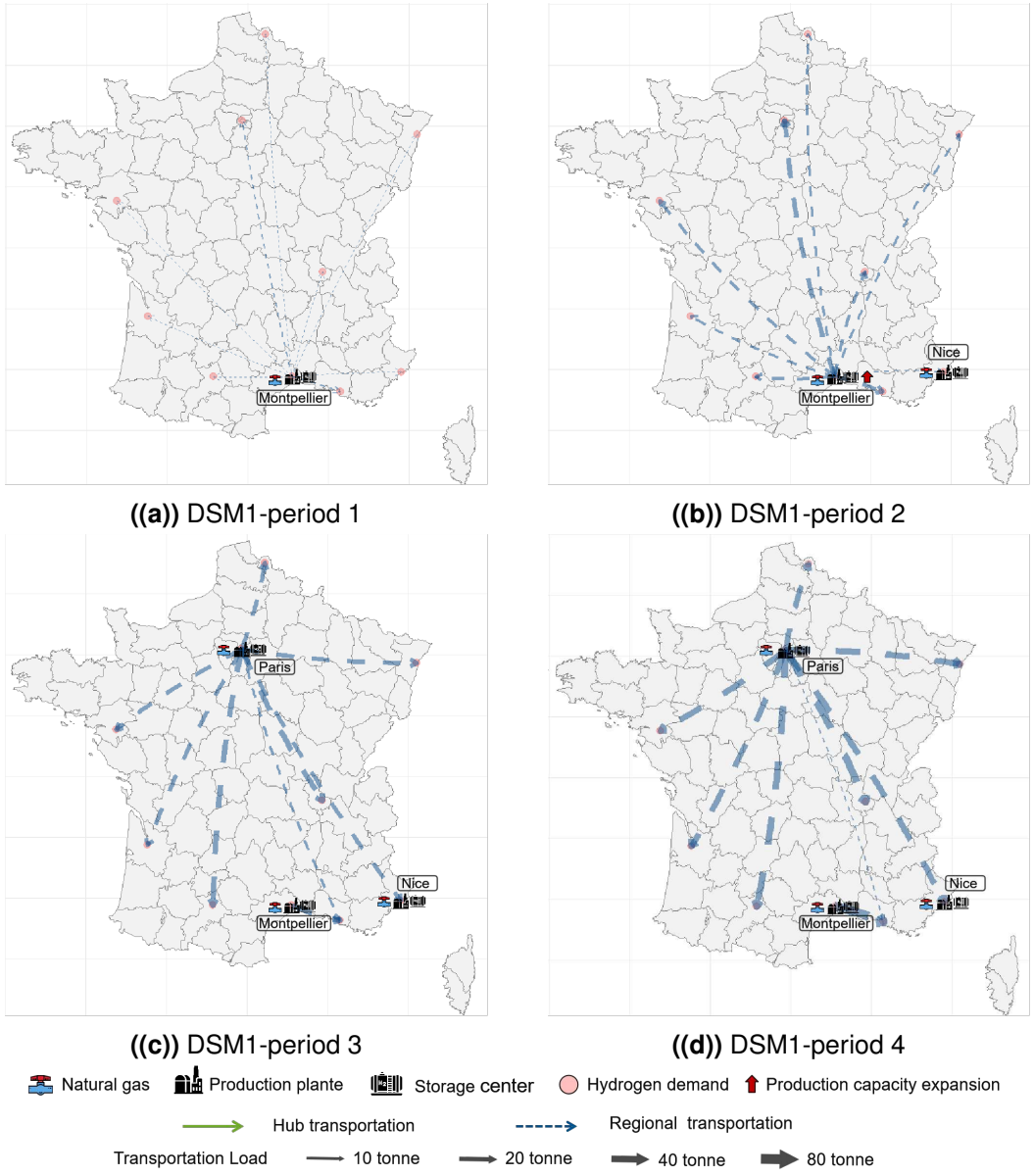

((a)) DSM1-period 1 **((b))** DSM1-period 2

((c)) DSM1-period 3 **((d))** DSM1-period 4

Figure 4.8: Configuration of Multi-period DSM1 for 10 cities

per kilogram of hydrogen to 3, 4, 6, 8, 12, and 16 kilograms CO2-equivalent and obtained the corresponding system cost. The results indicate that, at the same emission level, the CSM always has a lower cost than the DSM1 and DSM2. Furthermore, the model initially employs natural gas as the feedstock for hydrogen production and introduces biomass as a raw material when emissions are reduced to approximately 14 kilograms of CO2 equivalent. Subsequently, water electrolysis technology and CO2 capture systems are introduced when the reduction reaches approximately 10 kilograms CO2-equivalent. This implies that natural gas is still the optimal choice for the current parameters until transitioning to biomass and electricity.

In summary, the centralized storage model exhibits superior cost performance compared to the two decentralized storage models, whether considering unrestricted emissions or aiming for emission control targets. Within the current technical landscape, Steam

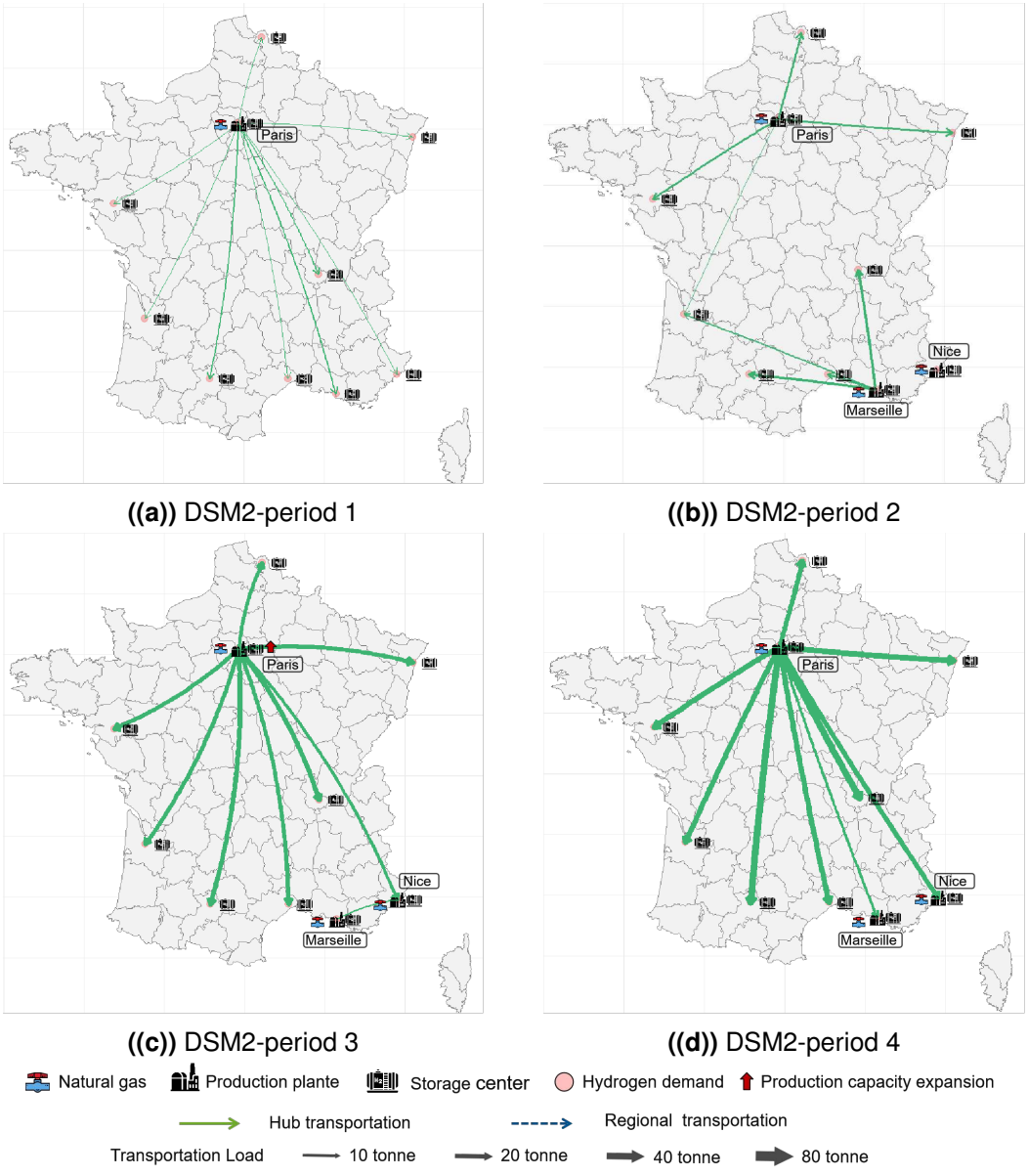

Figure 4.9: Configuration of Multi-period DSM2 for 10 cities

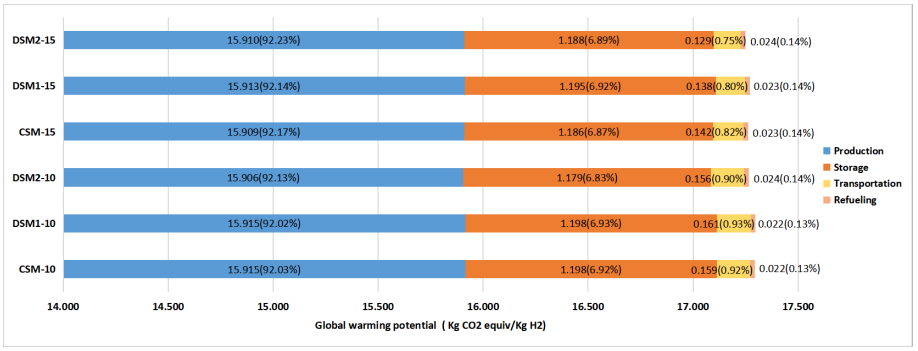

Figure 4.10: Composition of GWP

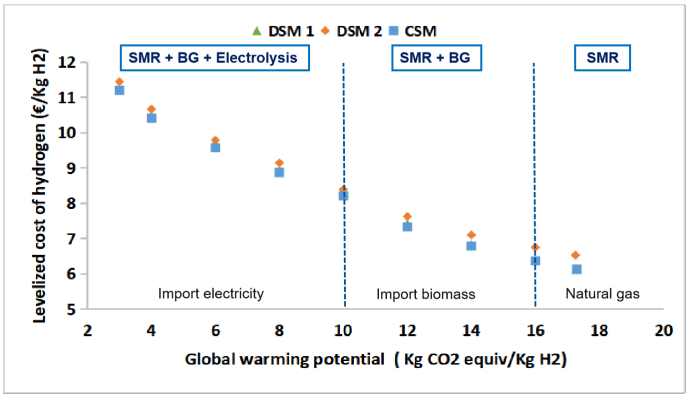

Figure 4.11: Results of three models with emission constraints in scenario 1

Methane Reforming coupled with liquid storage and transport emerges as the most cost-effective method. The case study conducted in France underscores a predilection for large-scale production and storage facilities, leading to the formation of a central circle supply node system structure.

4.5/ CONCLUSION

This chapter proposes a multi-period and bi-objective (cost and environmental impact) centralized storage optimization model for hydrogen supply chain systems. The model takes into account various types of production methods, transport combinations, storage methods, and demand requirements. It can help decision makers to identify the investment timing and design the optimal configuration of the supply chain, including the type of facilities, quantity, timing, and location of installation. We used the optimization solver to solve the mathematical problem and obtained a solution set.

The model was applied to a case study in France to propose optimal configurations in six different scenarios for 10 and 15 cities and compare with two types of decentralized models. The results demonstrate that the centralized storage model consistently has a lower cost than both of the decentralized models under the objective of investment optimization. This is especially true for scenarios with more demand nodes. Although the emissions are slightly higher than those from DSM 2 under unlimited emission conditions, the CSM model still performs better than the decentralized model in terms of cost when faced with emission constraints. Additionally, the study finds that SMR and liquid storage and transport are cost-effective methods in the current technical context. Overall, this study provides valuable insights into the optimal configuration of hydrogen supply chain systems and can be beneficial for decision-makers in the industry.

We examined four periods and a maximum of 15 cities in this case study and we could not get a solution with a gap less than 1% in 20 hours in 15 nodes case in the optimization solver. If there are more periods and nodes, the solver needs quite a long time to perform the operations, which makes the model less flexible. Besides, the availability of intermittent energy sources, including solar, tidal, and wind, is also a factor to be considered. In the following study, we will focus on building new computation methods that reduce the running time and increase the accuracy of the results.

5

METAHEURISTICS FOR LARGE-SCALE HSCND PROBLEM

In this chapter, the research focus transitions from model design to solution methods. Chapter 4 provides a detailed analysis of the design and optimization of a centralized storage system within the hydrogen supply chain (HSC), emphasizing the balance between economic efficiency and environmental sustainability across multiple periods under various demand scenarios. This approach underscores the significance of strategic planning and optimization techniques in addressing the complexities and dynamic nature of HSC. However, it was also found that the current solution has unreasonable computational time problems. To address the challenge of running time on a large-scale computation, the research focuses on proposing an algorithm combining a metaheuristic algorithm and mixed integer linear programming in this chapter. The algorithm is compared with the results obtained by the Cplex solver in an instance of France. This method provides the necessary tool to navigate the vast search spaces and complex constraints of large-scale HSC, offering innovative solutions that can accommodate the variability in such complex systems.

5.1/ INTRODUCTION

The HSCND problems studied above are all solved by building a mixed integer planning model and using an optimization solver. Unfortunately, the computational capacity and speed of this method are very limited. In complex cases, such as large networks spanning numerous periods, various raw materials, and multiple objectives, it require extensive computational resources. The commercial optimization solvers cannot find the global optimal solution in a reasonable computation time. Therefore, it is urgent to find an efficient algorithm to solve this problem.

The two-stage computational strategy is an approach proposed during the solution process of mixed integer programming. It decomposes the calculation into two levels, typically optimizing the location, scale, and type of production and storage in the first stage. In the second stage, the optimization of hydrogen flow is conducted. This method is more efficient than exact solution approaches (Cantú et al., 2021), however, in some instances, the interrelation between location and transportation is overlooked. Metaheuristic algorithms are adept at tackling intricate optimization challenges. These methods, unlike exact solutions, may not always deliver the optimal solution but are capable of identify-

ing high-quality solutions efficiently and with reduced computational demands. In recent years, metaheuristic algorithms have been employed to solve complex real-world problems arising in various domains such as economics, engineering, politics, management, and engineering (V. Kumar, Chhabra, & Kumar, 2014), as mentioned in the chapter of State of Art. Among metaheuristic algorithms, Genetic Algorithms (GAs) are renowned, inspired by the principles of natural selection and genetics (Michalewicz & Schoenauer, 1996). Originally proposed by John Holland in the nineteenth century (Lambora, Gupta, & Chopra, 2019), genetic algorithms are known for their exceptional global search capabilities, effectively avoiding local optima to find global solutions. These algorithms are not only robust and insensitive to initial parameters but are also particularly well-suited for parallel processing, significantly enhancing computational efficiency. They are also highly flexible, and easily integrated with other algorithms to form more powerful hybrid methods, and their implementation and parameter tuning processes are straightforward.

In Chapter 4, we have developed a mixed integer programming model that incorporates multiple production technologies, various storage and transportation methods, dual objectives, and multiple periods. This model is computed using the commercial optimization solver, Cplex. It is clear that the model described contains a very large number of variables, e.g. when the number of nodes reaches 50, it contains over 600,000 variables, which makes it take quite a long time in the solver (ILOG CPLEX) to find the optimal solution. Given the limitations of commercial solvers, a novel two-stage GA-based algorithm (HGA) was developed to provide a solution to this challenge. The following section provides a detailed description of the algorithmic framework, along with the processes and operators related to genetic algorithms. In Section 3, an application study conducted in France is discussed, where the effectiveness of the method is evaluated by comparing it with the precise approaches solved using the CPLEX solver. Section 4 summarizes the methodologies proposed and discusses the implications of the findings, offering insights into potential improvements and areas for further research in optimizing hydrogen supply chains using genetic algorithms.

5.2/ METHODOLOGY

5.2.1/ FRAMEWORKS OF ALGORITHM

The frameworks of the proposed hybrid algorithm demonstrated in Fig.5.1. In this algorithm, the problem-solving process is segmented into three distinct stages to enhance efficiency. The first stage determines the optimal number of production and storage facilities. This is achieved through the implementation of the previous mixed integer linear model without transportation costs. The primary objective of this initial stage is to effectively reduce the solution space. Moving on to the second stage, the methodology involves the main steps of the genetic algorithm. It starts by randomly creating chromosomes to map out where production and storage sites should be, based on the best numbers found in the first stage. This process enriches the diversity of solutions explored. Following their generation, these chromosomes are subjected to a series of evolutionary operations, including selection, crossover, and mutation. Each operation plays a crucial role in simulating natural evolutionary processes, driving the population towards increasingly viable solutions. The third stage of the algorithm uses the outcomes of the evolutionary process as foundational input parameters. With these parameters, the solver is

tasked with calculating the overall cost associated with the hydrogen supply chain, which serves as a representation of fitness. The subsequent section is devoted to an in-depth exploration of this algorithm, offering a comprehensive exposition of each stage.

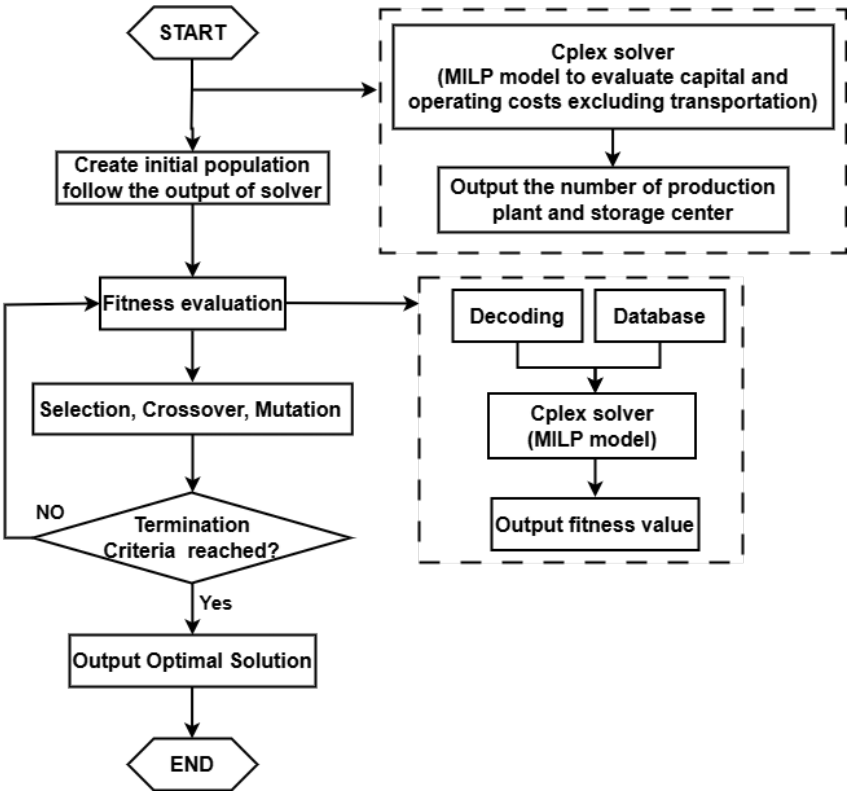

Figure 5.1: Flowchart of the proposed methodology

5.2.2/ GENETIC ALGORITHM

In the process of the genetic algorithm, initially, a random population is generated, along with the initialization of the best solution. The algorithm then enters a loop that continues until a predefined stopping criterion is met. Within this loop, the fitness of each individual is evaluated using an optimization solver. The current best solution is recorded, and the chromosomes with the worst performance are removed from the population. Subsequently, the algorithm employs genetic operations, including selection, crossover, and mutation, to further refine the population. Each undergoes adjustments to ensure its feasibility, paving the way for the formation of a new generation. This iterative process aims to continuously enhance the overall fitness of the population, culminating in the output of the final population. The pseudo-code presented in algorithm 1 outlines the proposed hybrid genetic algorithm.

The chromosomes belonging to a population are optimized simultaneously. The number of individuals optimized at the same time in each step depends on the given parameter settings. The number of individuals in the N+1 generation is equal to the number of individuals in the Nth generation. Below, all details of each sub-step in the evolutionary optimization process are explained. These steps are repeated for each generation during the optimization process until the results meet the stopping criteria.

Algorithm 1 The pseudo-code for proposed hybrid genetic algorithm

Created initial random population Pop;
Initialization the best solution I_{best};
while stopping criterion is not met **do**
    Evaluate each individual's fitness in the current population by optimization solver;
    Record the best solution I'_{best};
    if $I_{best} < I'_{best}$ **then**
        Replace the worst solution in Pop with I_{best};
    end if
    Randomly generate N_{del} individuals to replace the last N_{del} individuals ranked by fitness the current population;
    Deal with the population by selection, crossover, and mutation operator;
    Each individual is adjusted to feasible;
    Obtain the the new population Pop in the current generation;
end while
Output: Pop, I_{best}.

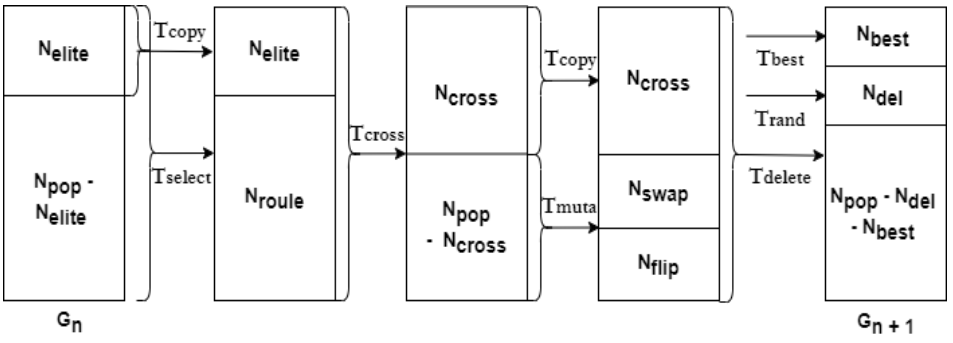

Figure 5.2: Schematic diagram of GA optimization process

1) The top N_{elite} individuals are chosen and directly carried over to the next generation through the T_{copy} operator. The remaining N_{pop} - N_{elite} individuals are then selected from the entire population using the selection operator, T_{select};

2) From the current generation, individuals are paired up into N_{pop}/2 couples. Each pair subsequently undergoes the crossover process facilitated by the T_{cross} operator;

3) A portion of the individuals is directly carried over to the next generation through the T_{copy} operator at this stage, while another segment of the population contributes to the formation of new offspring via two distinct mutation operators, T_{muta};

4) The newly formed offspring undergo simulation to calculate the fitness of the objective function. Following this, the existing population is sorted based on their fitness levels;

5) Individuals ranked last N_{del} in fitness are deleted by the deletion operator T_{del};

6) Individuals that are removed are substituted with new ones, randomly created by the T_{rand} operator, and with globally optimal individuals produced by the T_{best} operator.

Figure 5.2 is a schematic of the sub-steps executed from the G_n to the $G_n + 1$ generation. The following section provides a detailed description of the genetic operators.

5.2.3/ INITIALIZATION

The chromosome is structured as t one-dimensional arrays, with each array reflecting the establishment status of a production plant or storage facility during a specified time frame. Here, 't' matches the total count of periods under consideration. Within these arrays, individual genes represent the existence of a production plant or storage facility in a particular region, with the gene count aligning with the number of cities involved. The complete gene set includes segments for both production and storage elements. Fig.5.3 provides a chromosome illustration. For gene representation, binary encoding is utilized: '0' denotes the non-existence, and '1' illustrates the presence of a production plant or storage facility in a city.

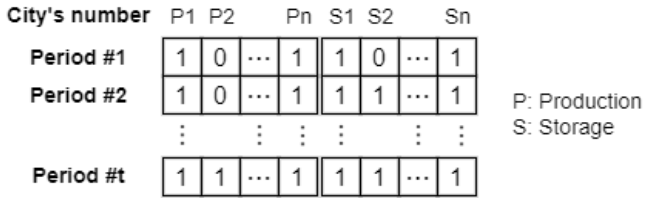

Figure 5.3: Example of chromosome

The initial feasible solution is generated through random selection and state transition. Initially, a population is created with all individual attributes set to 0. Then, for each individual in the population, a location is randomly chosen, and the element at that location is changed from 0 to 1. This process repeats until the sum of elements representing production plants and storage facilities reaches the maximum value for each period (stopping criterion). However, during the initialization process, random generation may lead to in-

Algorithm 2 The pseudo-code for generating the initial feasible solution

Input: Population size N_{pop}, Chromosome size $2n$, Period t, population Pop;
Create a population Pop initialized with 0;
for s = 0 to N_{pop} **do**
  while stopping criterion is not met **do**
    select an individual I from Pop, randomly select a position in I and set the element to 1;
  end while
  for p = 0 to t **do**
    for c = 0 to $2n$ **do**
      if individual $I[p, c]$ = 1 **then**
        $I[p + 1, c]$ = 1
      end if
    end for
  end for
end for
Output: Pop

feasible chromosomes. For instance, a situation might arise where a production plant is built at node n in period t, but does not exist in period t+1. Such a scenario is unreasonable and its frequent occurrence can reduce the efficiency of the algorithm during iteration. Therefore, after randomly generating the population, a correction is performed to ensure a feasible state. In the mentioned infeasible instance, the gens at that position in period t+1 is assigned to "1". The pseudo code is shown in Algorithm 2.

5.2.4/ SELECTION

This study employs two distinct chromosome selection methods within its genetic algorithm framework to optimize the generation of new individuals. These methods are pivotal for navigating the search space efficiently and avoiding premature convergence to suboptimal solutions. The first is the elite selection method, which is a deterministic process. It operates under the principle of "survival of the fittest," where the top n best-performing chromosomes, based on their fitness evaluations, are directly copied into the next generation without alteration. This method guarantees that the genetic material of the best solutions is not lost during the evolutionary process. The second is the roulette wheel method, which introduces a stochastic element to the selection process. Individuals are selected based on probabilities proportional to their fitness values, mimicking the roulette wheel's spin. This method calculates the cumulative probability for each individual, where the chance of being selected for the next generation correlates with the individual's fitness. Higher fitness values result in higher probabilities of selection, but unlike the elite method, even lower-fitness individuals have a chance of being selected. This probabilistic approach ensures genetic diversity within the population by allowing a broader spectrum of individuals to contribute their genetic material and preventing premature convergence. The pseudo-code of selection is presented in algorithm 3.

Algorithm 3 The pseudo-code of selection

Input: Elitism rate P_e, Pop;
Calculate the number of elites $N_e = N_{pop} * P_e$;
Sort the individual fitness and find the top N_e elite;
Calculating the number of individuals selected for roulette $N_r = N_{pop} - N_e$;
for i = 1 to N_r **do**
    Compute the probability for each individual I;
    Compute the cumulative probability M_n;
    Generate a random number $r \in]0, 1]$;
    if $r < M_1$ **then**
        Select individual 1;
    else
        if $M_{n-1} < r < M_n$ **then**
            Select individual n;
        end if
    end if
end for
Integrated all selected individuals and save them in Pop_1;
Output: Pop_1.

5.2.5/ CROSSOVER OPERATOR

The crossover operation is a fundamental genetic algorithm technique used to combine the genetic information of two parent chromosomes to generate new offspring. This process is inspired by biological reproduction, where genetic material from two parents is mixed to produce offspring with characteristics derived from both. Fig.5.4 provides a clear example of how genetic material is recombined to foster diversity and innovation within the population in our study. It depicts two chromosomes, each spanning two periods. In the crossover operation, the crossover point(s) is randomly determined and can be anywhere along the length of the chromosomes. It is indicated by a red dashed line in the example. At this point, by splitting and exchanging the genetic material to the right of the crossover point between the two parent chromosomes, we can obtain two distinct offspring chromosomes. This crossover process is repeated multiple times across the population to create a new generation of chromosomes. Algorithm 4 provides the pseudo-code for this process.

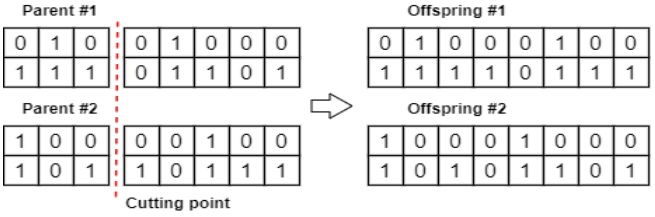

Figure 5.4: Example of crossover operator

Algorithm 4 The pseudo-code of crossover

Input: Crossover probability P_c, population Pop_1;
Randomly arrange individuals in Pop_1;
for j = 1 to $N_{pop}/2$ **do**
  Select individual pair I_a,I_b;
  Generate a random number $c \in]0, 1[$;
  if $P_c < c$ **then**
    Generate a random integer number representing cross-point $X \in (0, n)$;
    Set $Off_a \leftarrow crossover(I_a, I_b)$, $Off_b \leftarrow crossover(I_b, I_a)$
    Save Off_a and Off_b to Pop_2;
  end if
end for
Output: Pop_2.

5.2.6/ MUTATION OPERATOR

Mutation operators introduce variations by altering the genetic makeup of individuals, thus enabling the exploration of new areas in the solution space that might not be reachable through crossover operations alone. We have employed two most used mutation operators, swap mutation and bit flip mutation.The swap mutation operator generally introduces genetic variation by randomly selecting two positions within a chromosome and swapping their values. It can lead to significant changes in the chromosome, facilitating

the algorithm's jump to different parts of the solution space. The bit-flip mutation focuses on altering a single gene, making minor improvements based on the current solution. By integrating these two approaches, the algorithm can explore a wider range of genetic variations, increasing the opportunities to escape local optima and enhancing the algorithm's overall performance.

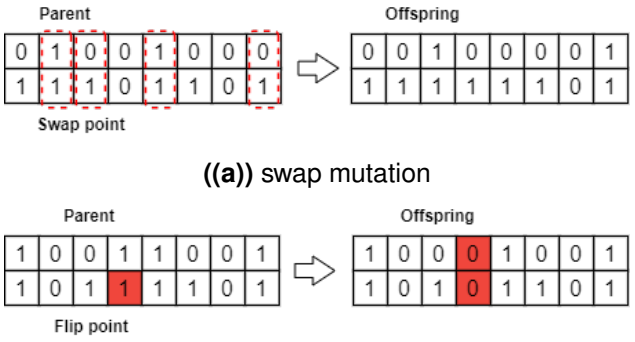

((a)) swap mutation

((b)) bits flip mutation

Figure 5.5: Example of mutation operator

Fig.5.5(a) illustrates an example of this study, where we randomly choose four columns within the chromosome. The first two columns form a group, from which selections are made from the gene columns representing the production plant's status. The last two columns form another group, with selections made from the gene columns representing the storage facility's status. Then, within each group, the values of these two columns are swapped. The bit flip mutation involves randomly selecting a gene (indicated by a red square in Fig.5.5(b) and changing its value from 0 to 1 or from 1 to 0.

Besides, to ensure the feasibility of the individual after the bit flip mutation, we applied corrective measures. If a gene is flipped from 1 to 0, any dependent gene in the preceding period is also set to 0 to maintain consistency. Conversely, flipping a gene from 0 to 1 necessitates adjusting all corresponding genes in subsequent periods within the same column to 1, ensuring that the mutation does not violate the problem's constraints. Algorithm 5 shows the detailed process. The mutation is useful for maintaining diversity within the population and can help prevent the algorithm from becoming stuck in local optima.

5.2.7/ FITNESS

The fitness function plays a crucial role in the genetic algorithm by quantitatively assessing each chromosome. In this study, the function is defined as the inverse of the levelized cost of hydrogen, as the equation 5.1 . It includes the total raw material cost, capital cost, and operational cost and is obtained by the exact solver CPLEX. As these costs increase, fitness decreases, enhancing the probability that less cost-efficient solutions are phased out in favor of more economical ones.

$$Fitness = 1/LCOH \tag{5.1}$$

Algorithm 5 The pseudo-code of mutation and feasibility correction

Input: Mutation probability P_m, Mutation rate R_m, Population Pop_2;
for l = 0 to N_{pop}/2 **do**
  Generate random number $s \in]0,1[$;
  if $P_m < s$ **then**
    Generate two random integer pairs, representing the mutation columns $x_1, x_2 \in]0,n[$, $y_1, y_2 \in]n,2n[$;
    Select an individual I_l, mutates the individuals and generates a new solution $I_l^{'}$;
  end if
end for
for k = N_{pop}/2 to N_{pop} **do**
  Generate random number $q \in]0,1[$;
  if $P_m < q$ **then**
    Generate two random integer number to locate mutant point $x \in]0,t[$ and $y \in]0,2n[$;
    Select an individual I_k, mutates the individuals and generates a new solution $I_k^{'}$;
  end if
  if $I_k^{'}$ [x,y] = 1 **then**
    Setting the value in column y after row x to 1;
  else
    Setting the value in column y before row x to 0;
  end if
end for
Save $I_k^{'}$ and $I_l^{'}$ to Pop_3, update $Pop = Pop_3$.
Output: Pop_3

5.3/ NUMERICAL EXPERIMENTS AND RESULTS

The experiments were conducted on a computer equipped with 16 GB of RAM and an Intel i7 CPU operating at 1.80 GHz. The solution for the mixed integer linear programming model was obtained using CPLEX solver version 12.10. The proposed hybrid heuristic algorithm was implemented using the Python programming language.

5.3.1/ INSTANCE

The case study selected France as the experimental region. The time frame from 2023 to 2050 was segmented into four periods, with hydrogen penetration rates of 5%, 20%, 60%, and 80% assumed for these respective periods. The shortest distances between cities were acquired from Google Maps. Other model parameters, including facility unit costs, operational costs, capacity constraints, and hydrogen demand were established in the chapter 4.

We conducted algorithm testing across six different nodes quantities: 5, 10, 15, 20, 30, and 50. Each node was considered a potential location for production, storage, and refueling facilities. Given the solver's inability to find an optimal solution for the MILP problem

within a reasonable time, we constrained its termination criteria to reach a specified GAP ($|bestbound - bestinteger|/(1e-10+|bestinteger|)$) of 0%, 1%, 2%, 3%, 4%, and 5%, with a maximum runtime limit of 100 hours in the Cplex. The best bound is the minimum of the optimal relaxed solution for all active nodes (nodes that have not yet been explored), which is obtained by relaxing the integer constraints into continuous constraints. The best integer refers to the optimal integer solution of the objective function value found so far using the branch-and-bound method.

The parameters for the GA algorithm were set as follows: a crossover probability of 0.8, a mutation probability of 0.2, and a population size of 20. We implemented two different mutation methods on 50% of the population. The stopping criterion was defined as the global optimal solution remaining unchanged for 5, 10, 20, 20, 20, 20 consecutive iterations. These parameters were established beforehand via thorough initial experiments. Additionally, each case was repeated for 10 tests.

5.3.2/ COMPUTATIONAL RESULTS

The results of the six instances are shown in Table. 5.1. The Optimal Solution column signifies the solution derived from the Cplex solver. Times indicate the total computational time required to solve each problem. For the proposed genetic algorithm, the table displays both the minimum cost solution and the average solution obtained across ten times operation, along with the average deviation (AD) between them (calculated as follow) and the average time taken to solve each running.

$$AD = (AverageSolution - OptimalSolution)/OptimalSolution \tag{5.2}$$

In all instances, the best solutions obtained closely approximate the optimal solutions calculated by Cplex, with differences ranging from 0 to 0.016 euros per kilogram of hydrogen. In smaller cases, such as the one involving five nodes in this experiment, the best solution matches the optimal solution precisely. Furthermore, the gap between the average and optimal solutions (MILP) across ten iterations is consistently minimal, varying within a narrow range of 0% to 0.59%.

The proposed algorithm is effective in reducing the computation time of the model. In the first five instances, the computation time of GA is significantly lower than that of the solver. Meanwhile, in the 50 nodes case, Cplex failed to identify a feasible solution within the specified time constraint with a GAP below 5%, whereas the proposed algorithm successfully achieved this. Moreover, the experimental results show that the convergence of the algorithm is very fast.

Fig.5.6 illustrates the convergence of operations for scenarios involving production, storage, and refueling, each with 30 potential nodes. Evidently, the algorithm begins to exhibit convergence characteristics after more than 40 iterations.

However, the computational time of the HGA increases significantly as the problem size increases. On the one hand, this is due to the fact that fitness calculations with the solver are necessitated in each iteration. On the other hand, the process of obtaining the optimal solution in the last step of the algorithm is also performed in the optimization solver through MILP. Thus, even when production site selection becomes a deterministic parameter, solving the large-scale model still demands a substantial computational effort.

No	Nodes' number	MILP		GA (run 10 times)			AD (%)
		Cost	Time(s)	Best-cost	Average-cost	Time (s)	
N1	5	6.252	952	6.252	6.252	574	0.00
N2	10	6.134	47064	6.136	6.144	3557	0.16
N3	15	6.006	101769	6.015	6.021	8522	0.25
N4	20	5.930	165205	5.946	5.955	12072	0.42
N5	30	5.928	211347	5.943	5.963	20643	0.59
N6	50	––	360000	5.872	5.909	28272	––

Table 5.1: Numerical results of tested instances

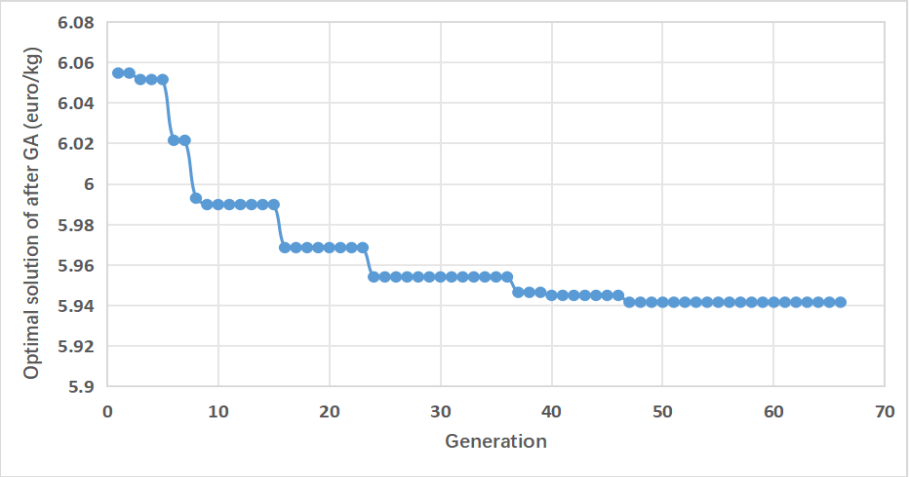

Figure 5.6: Convergence of HGA in the 30 nodes instance

5.3.3/ SENSITIVITY ANALYSIS

To develop management strategies for large-scale hydrogen supply chain network design, this study follows the experimental data from Chapter 4 and conducts a case study in France. The case involves production, storage, and refueling with 50 potential nodes each. Considering that the outcomes of the model are heavily dependent on demand quantity, and given the inherent uncertainties in demand estimation methods, alongside the feasibility and economic benefits of using existing natural gas pipelines for hydrogen transport, we have decided to conduct a sensitivity analysis on two critical parameters: demand level and pipeline construction costs. This analysis is intended to assess the sensitivity of the overall network costs and emissions to changes in these parameters.

Each parameter was set at six levels, including the standard level, 85%, 70%, 55%, 40%, and 25%. In the standard level, we selected the configuration of scenario one in the previous chapter. To illustrate how demand levels influence the costs associated with different processes, the overall cost has been segmented into costs for raw materials, production, storage, transportation, and refueling. For a clearer representation of transportation methods, costs related to transportation have been further categorized into costs for vehicle transportation and pipeline construction.

The LCOH and GWP for each parameter are illustrated in the following figures. It is evident from Figure 5.7 that as demand increases, the LCOH gradually decreases. This reflects the effect of economies of scale, where higher operational scales can reduce

the unit cost of the supply chain. However, this reduction is not strictly linear. There is a rapid decline in unit costs from 25% to 70% of the demand number, but the marginal contribution diminishes once the scale reaches 70%. This indicates that at this point, the impact of demand on cost is quite limited. Additionally, the GWP data show a relatively stable trend, with slight fluctuations as demand increases, but overall changes are minimal. This suggests that the environmental impact of the hydrogen supply chain remains stable across different operational scales.

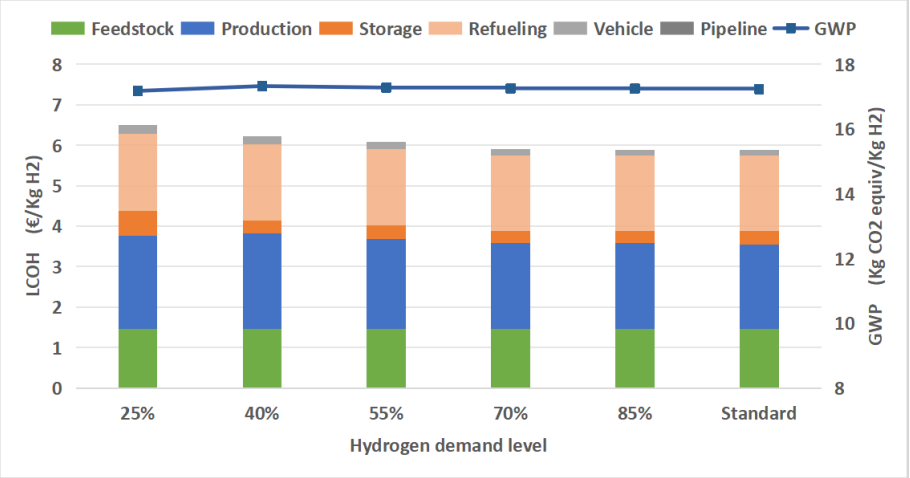

Figure 5.7: Sensitivity indices of demand level

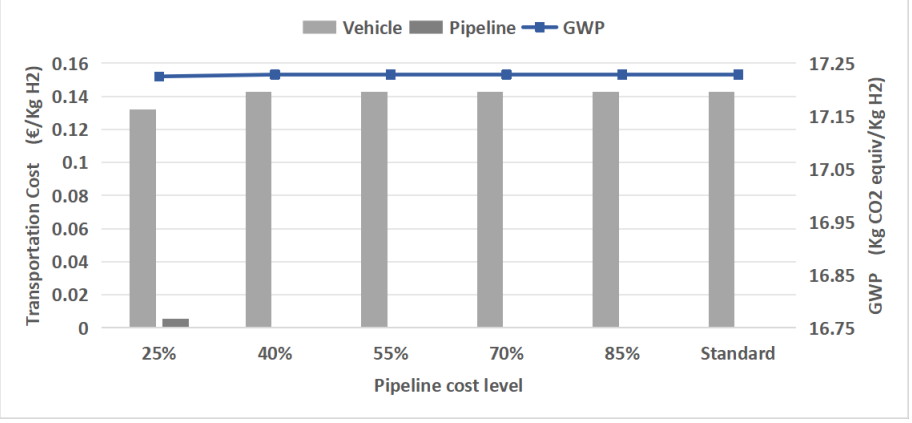

Figure 5.8: Sensitivity indices of pipeline cost level

Figure 5.8 illustrates the selection of two transportation modes in the supply chain under different pipeline cost level. It is observed that among the five parameters closer to the standard level, the configuration of the supply chain does not change with the reduction in pipeline costs. The reason is that the system aims to minimize costs and does not choose pipeline transportation after weighing the costs. However, when the pipeline costs are reduced to 25% of the standard level, there begins to be a small portion of hydrogen transported via pipelines. This suggests that the corresponding pipeline costs can serve as an indicator of whether to install pipelines at this level of demand.

5.3.4/ OPTIMAL CONFIGURATION

Figure 5.9 displays the optimal configuration for each period in a hydrogen supply chain network with 50 nodes under standard demand, including the types of raw materials, production, storage, and refueling station locations, transportation routes, and flow rates of each edge. The configuration reveals that large hydrogen production plants and storage centers are typically chosen, with storage centers built close to production plants. In the first period, two locations are selected, with one serving as the main supply node. The primary reason is that the cost savings from centralized large-scale production and storage offset the increased costs of total long-distance transportation. In the second period, hydrogen produced at a newly built large production plant in Paris is transported to another city for storage, as that city has surplus storage capacity. As demand increases, by the last period, a pattern with four production and storage centers is established, which

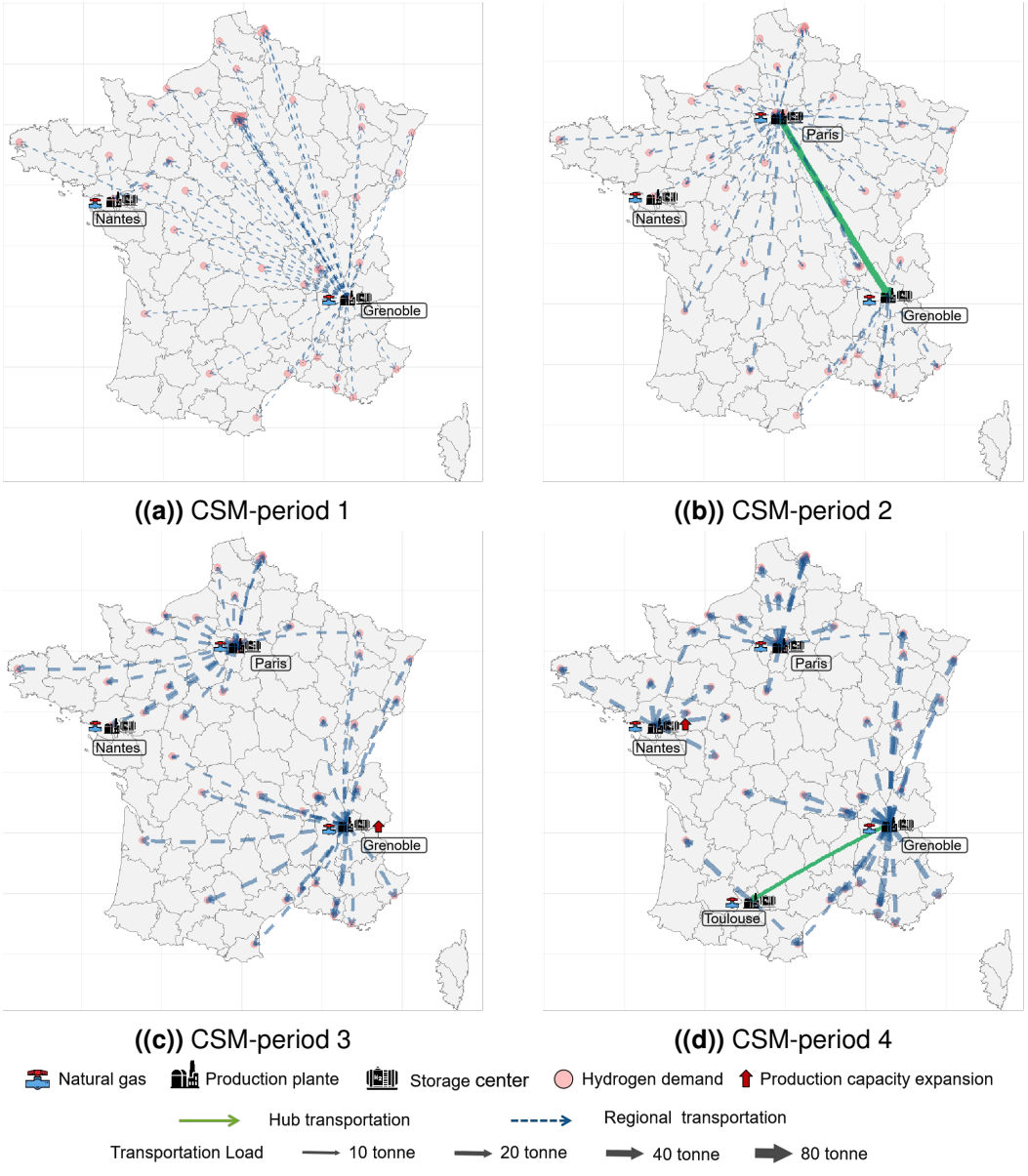

Figure 5.9: Configuration for 50 cities

covers as much demand as possible with the shortest transportation distances. Furthermore, pipelines were not selected as transportation tools in any period in this scenario, indicating that neither the demand level nor the pipeline cost level was sufficient to install pipelines in the scenario. Overall, these results demonstrate that in large-scale HSCN design, there is a tendency to gravitate towards large-scale production and storage, forming multiple centralized distributions to save costs.

5.4/ CONCLUSION

In this chapter, we developed an algorithm that combines genetic algorithms with mixed-integer linear programming to address the large-scale computational challenges encountered in the hydrogen supply chain network design. The model focuses on optimizing the location, size, and energy flow configurations while integrating various production, transportation, and storage technologies. To assess the performance of the proposed algorithm, we conducted a series of numerical experiments. The results indicate that, compared to traditional optimization solvers Cplex, genetic algorithms can more efficiently produce high-quality solutions. Moreover, we applied this method to the design of a large-scale hydrogen supply chain network in France, specifically considering different demand scenarios and variations in pipeline transportation costs, to devise the optimal network configuration. This case study not only demonstrates the practicality of our approach to managing complex problems but also provides robust strategies and insights for the future optimization of hydrogen supply chain networks.

III

CONCLUSION

6

CONCLUSIONS AND PERSPECTIVES

6.1/ CONCLUSIONS

Deploying hydrogen supply chains (HSCN) is fraught with challenges, particularly concerning the economic viability and environmental considerations of hydrogen production, storage, and distribution processes. Optimizing these supply chains necessitates a holistic approach to balance economic efficiency, environmental sustainability, and technological feasibility while accommodating the multifaceted dynamics of energy markets and regulatory frameworks.

The thesis provides an exhaustive review of the advancements in HSCNs, including hydrogen production, storage, transportation, and refueling station technologies. It highlights the technological progress made to date and identifies existing gaps, such as the need for better cost and emission assessments and more efficient hydrogen storage solutions, laying the groundwork for the contributions of the thesis. A novel method for optimizing HSCN is introduced by incorporating Life Cycle Costing (LCC) and Life Cycle Assessment (LCA) into the design process. This approach ensures the proposed supply chain models are not only economically viable but also minimize environmental impacts, aligning with sustainability goals. A bi-objective optimization model that addresses both economic and environmental performance is developed. Applied to a case study in the Franche-Comté region of France, this model demonstrates the potential for optimizing HSCN designs in real-world scenarios, offering insights into balancing cost and sustainability considerations. Another significant contribution is the exploration of a centralized hydrogen storage strategy, assessed through a multi-period and bi-objective optimization framework. Evaluated in a national context in France, this strategy reveals the benefits of centralized storage in reducing overall supply chain costs and environmental impacts, providing a promising direction for future HSCN development. Additionally, to address the computational challenges of optimizing HSCN, the thesis presents metaheuristic algorithms capable of efficiently solving large-scale design problems. This contribution is pivotal for enabling the practical application of optimization models to complex, real-world HSCN scenarios.

6.2/ PERSPECTIVES

As research and development continue to progress in this area, there are still many limitations in current studies. The following outlines several key points for the path forward in

the thesis.

- High integration of the supply chain with various renewable energy systems. The supply of renewable energy is highly uncertain, with the availability of different energy sources varying at the same time and in different regions. Capturing this supply situation within the supply chain and optimizing the synergy between production and renewable energy can ensure a stable and cost-effective supply of green hydrogen;
- Global supply chain and international cooperation network design. Most of the current research is conducted within national or regional scopes. However, adopting an international perspective can more accurately simulate supply chain dynamics. Establishing a global hydrogen supply chain is necessary to ensure hydrogen supply security and promote the development of the global market.
- Consideration of social factors. As the hydrogen economy develops, it is crucial to consider the cost and environmental impacts of the entire supply chain. Furthermore, seriously addressing the social impacts of transitioning to a hydrogen economy, including effects on employment and community engagement, cannot be overlooked.

References

Abdin, Z., Zafaranloo, A., Rafiee, A., Mérida, W., Lipiński, W., & Khalilpour, K. R. (2020). Hydrogen as an energy vector. Renewable and sustainable energy reviews, 120, 109620.

Agnolucci, P., Akgul, O., McDowall, W., & Papageorgiou, L. G. (2013). The importance of economies of scale, transport costs and demand patterns in optimising hydrogen fuelling infrastructure: An exploration with SHIPMod (Spatial hydrogen infrastructure planning model). International Journal of Hydrogen Energy, 38(26), 11189–11201. Retrieved from http://dx.doi.org/10.1016/j.ijhydene.2013.06.071 doi: 10.1016/j.ijhydene.2013.06.071

Alazemi, J., & Andrews, J. (2015). Automotive hydrogen fuelling stations: An international review. Renewable and sustainable energy reviews, 48, 483–499.

Almansoori, A., & Betancourt-Torcat, A. (2016). Design of optimization model for a hydrogen supply chain under emission constraints-a case study of germany. Energy, 111, 414–429.

Almansoori, A., & Shah, N. (2006). Design and operation of a future hydrogen supply chain: snapshot model. Chemical Engineering Research and Design, 84(6), 423–438.

Almansoori, A., & Shah, N. (2009). Design and operation of a future hydrogen supply chain: multi-period model. International journal of hydrogen energy, 34(19), 7883–7897.

Almansoori, A., & Shah, N. (2012). Design and operation of a stochastic hydrogen supply chain network under demand uncertainty. International journal of hydrogen energy, 37(5), 3965–3977.

Almaraz, S. D.-L., Azzaro-Pantel, C., Montastruc, L., & Boix, M. (2015). Deployment of a hydrogen supply chain by multi-objective/multi-period optimisation at regional and national scales. Chemical Engineering Research and Design, 104, 11–31.

Almaraz, S. D.-L., Azzaro-Pantel, C., Montastruc, L., & Domenech, S. (2014). Hydrogen supply chain optimization for deployment scenarios in the midi-pyrénées region, france. International journal of hydrogen energy, 39(23), 11831–11845.

Almaraz, S. D.-L., Azzaro-Pantel, C., Montastruc, L., Pibouleau, L., & Senties, O. B. (2013). Assessment of mono and multi-objective optimization to design a hydrogen supply chain. international journal of hydrogen energy, 38(33), 14121–14145.

Almaraz, S. D.-L., Rácz, V., Azzaro-Pantel, C., & Szántó, Z. O. (2022). Multiobjective and social cost-benefit optimisation for a sustainable hydrogen supply chain: Application to hungary. Applied Energy, 325, 119882.

André, J., Auray, S., Brac, J., De Wolf, D., Maisonnier, G., Ould-Sidi, M.-M., & Simonnet, A. (2013). Design and dimensioning of hydrogen transmission pipeline networks. European Journal of Operational Research, 229(1), 239–251.

André, J., Auray, S., De Wolf, D., Memmah, M.-M., & Simonnet, A. (2014). Time development of new hydrogen transmission pipeline networks for france. International journal of hydrogen energy, 39(20), 10323–10337.

Antonini, C., Treyer, K., Streb, A., van der Spek, M., Bauer, C., & Mazzotti, M. (2020). Hydrogen production from natural gas and biomethane with carbon capture and storage–a techno-environmental analysis. Sustainable Energy & Fuels, 4(6), 2967–2986.

Apostolou, D., & Xydis, G. (2019). A literature review on hydrogen refuelling stations and infrastructure. current status and future prospects. Renewable and Sustainable Energy Reviews, 113, 109292.

Argonne National Laboratory. (2012). GREET Life-cycle Model: User Guide (Tech. Rep.). Author.

Ashuri, T., Zaaijer, M., Martins, J., van Bussel, G., & van Kuik, G. (2014, 8). Multidisciplinary design optimization of offshore wind turbines for minimum levelized cost of energy. Renewable Energy, 68, 893–905. Retrieved from https://www.sciencedirect.com/science/article/pii/S0960148114001360 doi: 10.1016/J.RENENE.2014.02.045

Atilhan, S., Park, S., El-Halwagi, M. M., Atilhan, M., Moore, M., & Nielsen, R. B. (2021). Green hydrogen as an alternative fuel for the shipping industry. Current Opinion in Chemical Engineering, 31, 100668.

Azzaro-Pantel, C. (2018). Hydrogen supply chain: Design, deployment and operation. Academic Press.

Badescu, V. (2006, 9). Optimum size and structure for solar energy collection systems. Energy, 31(12), 1819–1835. Retrieved from https://www.sciencedirect.com/science/article/pii/S0360544205001829 doi: 10.1016/J.ENERGY.2005.09.008

Balat, M. (2008). Hydrogen-rich gas production from biomass via pyrolysis and gasification processes and effects of catalyst on hydrogen yield. Energy Sources, Part A, 30(6), 552–564.

Balcombe, P., Anderson, K., Speirs, J., Brandon, N., & Hawkes, A. (2017). The natural gas supply chain: the importance of methane and carbon dioxide emissions. ACS Sustainable Chemistry & Engineering, 5(1), 3–20.

Balta-Ozkan, N., & Baldwin, E. (2013). Spatial development of hydrogen economy in a low-carbon uk energy system. international journal of hydrogen energy, 38(3), 1209–1224.

Bauer, A., Mayer, T., Semmel, M., Morales, M. A. G., & Wind, J. (2019). Energetic evaluation of hydrogen refueling stations with liquid or gaseous stored hydrogen. International Journal of Hydrogen Energy, 44(13), 6795–6812.

Bernal-Agustín, J. L., & Dufo-López, R. (2009, 10). Simulation and optimization of stand-alone hybrid renewable energy systems. Renewable & Sustainable Energy Reviews, 13(8), 2111–2118. Retrieved from https://www.sciencedirect.com/science/article/pii/S1364032109000215 doi: 10.1016/J.RSER.2009.01.010

Biezma, M., & Cristóbal, J. S. (2006, 4). Investment criteria for the selection of cogeneration plants—a state of the art review. Applied Thermal Engineering, 26(5-6), 583–588. Retrieved from https://www.sciencedirect.com/science/article/pii/S1359431105002243 doi: 10.1016/J.APPLTHERMALENG.2005.07.006

Bique, A. O., Maia, L. K., Grossmann, I. E., & Zondervan, E. (2021). Design of hydrogen supply chains under demand uncertainty–a case study of passenger transport in germany. Physical Sciences Reviews.

Bique, A. O., Maia, L. K., La Mantia, F., Manca, D., & Zondervan, E. (2019). Balancing costs, safety and co2 emissions in the design of hydrogen supply chains. Computers & Chemical Engineering, 129, 106493.

Bique, A. O., & Zondervan, E. (2018). An outlook towards hydrogen supply chain networks in 2050—design of novel fuel infrastructures in germany. Chemical Engineering Research and Design, 134, 90–103.

Bockris, J. O. M. (2013). The hydrogen economy: Its history. International Journal of Hydrogen Energy, 38(6), 2579–2588.

Boretti, A., & Banik, B. K. (2021). Advances in hydrogen production from natural gas reforming. Advanced Energy and Sustainability Research, 2(11), 2100097.

Branker, K., Pathak, M., & Pearce, J. (2011, 12). A review of solar photovoltaic levelized cost of electricity. Renewable & Sustainable Energy Reviews, 15(9), 4470–4482. Retrieved from https://www.sciencedirect.com/science/article/pii/S1364032111003492?via%3Dihub doi: 10.1016/J.RSER.2011.07.104

Brey, J., Brey, R., Carazo, A., Contreras, I., Hernandez-Diaz, A., & Gallardo, V. (2006). Designing a gradual transition to a hydrogen economy in spain. Journal of power sources, 159(2), 1231–1240.

Budsberg, E., Crawford, J., Gustafson, R., Bura, R., & Puettmann, M. (2015). Ethanologens vs. acetogens: Environmental impacts of two ethanol fermentation pathways. Biomass and Bioenergy, 83, 23–31.

California Air Resources Board. (2020). 2020 Annual Evaluation of Fuel Cell Electric Vehicle Deployment and Hydrogen Fuel Station Network Development (Tech. Rep.). California Environmental Protection Agency.

Câmara, D., Pinto-Varela, T., & Barbósa-Povoa, A. P. (2019). Multi-objective optimization approach to design and planning hydrogen supply chain under uncertainty: A portugal study case. In Computer aided chemical engineering (Vol. 46, pp. 1309–1314). Elsevier.

Cantú, V. H., Azzaro-Pantel, C., & Ponsich, A. (2020). Multi-objective evolutionary algorithm based on decomposition (moea/d) for optimal design of hydrogen supply chains. In Computer aided chemical engineering (Vol. 48, pp. 883–888). Elsevier.

Cantú, V. H., Azzaro-Pantel, C., & Ponsich, A. (2021). A novel matheuristic based on bi-level optimization for the multi-objective design of hydrogen supply chains. Computers & Chemical Engineering, 152, 107370.

Cantú, V. H., Ponsich, A., Azzaro-Pantel, C., & Carrera, E. (2023). Capturing spatial, time-wise and technological detail in hydrogen supply chains: A bi-level multi-objective optimization approach. Applied Energy, 344, 121159.

Cany, C., Mansilla, C., da Costa, P., & Mathonnière, G. (2017). Adapting the french nuclear fleet to integrate variable renewable energies via the production of hydrogen: Towards massive production of low carbon hydrogen? International Journal of Hydrogen Energy, 42(19), 13339–13356.

Carrera, E., & Azzaro-Pantel, C. (2021). Bi-objective optimal design of hydrogen and methane supply chains based on power-to-gas systems. Chemical Engineering Science, 246, 116861.

Cell, F., et al. (2020). Road map to a us hydrogen energy: reducing emissions and driving growth across the nation.

Cerniauskas, S., Junco, A. J. C., Grube, T., Robinius, M., & Stolten, D. (2020). Options of natural gas pipeline reassignment for hydrogen: Cost assessment for a germany case study. International Journal of Hydrogen Energy, 45(21), 12095–12107.

Chen, Y.-H., Chen, C.-Y., & Lee, S.-C. (2010). Technology forecasting of new clean energy: The example of hydrogen energy and fuel cell. African Journal of Business Management, 4(7), 1372.

Chi, J., & Yu, H. (2018). Water electrolysis based on renewable energy for hydrogen

production. Chinese Journal of Catalysis, 39(3), 390–394.
Cho, S., & Kim, J. (2019). Multi-site and multi-period optimization model for strategic planning of a renewable hydrogen energy network from biomass waste and energy crops. Energy, 185, 527–540.
Cho, S., Woo, Y.-b., Kim, B. S., & Kim, J. (2016). Optimization-based planning of a biomass to hydrogen (b2h2) system using dedicated energy crops and waste biomass. Biomass and Bioenergy, 87, 144–155.
Chouhan, V. K., Khan, S. H., & Hajiaghaei-Keshteli, M. (2022). Sustainable planning and decision-making model for sugarcane mills considering environmental issues. Journal of environmental management, 303, 114252.
Collins, L. (2023). Hydrogen explosion in austria. Retrieved from https://www.hydrogeninsight.com/industrial/hydrogen-explosion-in-austria-i-live-more-than-3km-away-and-the-blast-made-my-windows-shake/2-1-1498784
Contaldi, M., Gracceva, F., & Mattucci, A. (2008). Hydrogen perspectives in italy: analysis of possible deployment scenarios. International Journal of Hydrogen Energy, 33(6), 1630–1642.
Cormos, C.-C., Petrescu, L., & Cormos, A.-M. (2014). Assessment of hydrogen production systems based on natural gas conversion with carbon capture and storage. In Computer aided chemical engineering (Vol. 33, pp. 1081–1086). Elsevier.
Cucchiella, F., & D'Adamo, I. (2013, 12). Issue on supply chain of renewable energy. Energy Conversion and Management, 76, 774–780. Retrieved from https://www.sciencedirect.com/science/article/pii/S0196890413004548 doi: 10.1016/J.ENCONMAN.2013.07.081
Dayhim, M., Jafari, M. A., & Mazurek, M. (2014). Planning sustainable hydrogen supply chain infrastructure with uncertain demand. International Journal of Hydrogen Energy, 39(13), 6789–6801.
del Pozo, C. A., Cloete, S., & Álvaro, Á. J. (2021). Carbon-negative hydrogen: Exploring the techno-economic potential of biomass co-gasification with co2 capture. Energy Conversion and Management, 247, 114712.
Demirbas, M. F., Mustafa, B., & Havva, B. (2009). Potential contribution of biomass to the sustainable energy development. Energy Conversion and Management, 50(7), 1746-1760.
Department, S. R. (2022). Average annual passenger car journeys in france from 2004 to 2018, by fuel type. Retrieved from https://www.statista.com/statistics/1105129/distance-traveled-in-average-by-passenger-car-france/
Department of Energy. (2006). H2A Delivery Components Model Version 1.1 : User's Guide (Tech. Rep.). Department of Energy. Retrieved from http://www.hydrogen.energy.gov/pdfs/h2a_delivery_doc.pdf
Department of Energy. (2012). H2A Central Hydrogen Production Model , Version 3: User Guide (Tech. Rep.). National Renewable Energy Laboratory. Retrieved from https://www.hydrogen.energy.gov/h2a_production.html
Department of Energy. (2015). H2A Delivery Scenario Analysis Model (Tech. Rep.). Author.
Edwards, P. P., Kuznetsov, V. L., & David, W. I. (2007). Hydrogen energy. Philosophical Transactions of the Royal Society A: Mathematical, Physical and Engineering Sciences, 365(1853), 1043–1056.
Ehrenstein, M., Galán-Martín, Á., Tulus, V., & Guillén-Gosálbez, G. (2020). Optimising fuel supply chains within planetary boundaries: A case study of hydrogen for road transport in the uk. Applied Energy, 276, 115486.

Ehrenstein, M., Wang, C.-H., & Guillén-Gosálbez, G. (2019). Strategic planning of supply chains considering extreme events: Novel heuristic and application to the petrochemical industry. Computers & Chemical Engineering, 125, 306–323.

El-Shafie, M. (2023). Hydrogen production by water electrolysis technologies: a review. Results in Engineering, 101426.

El-Taweel, N. A., Khani, H., & Farag, H. E. (2018). Hydrogen storage optimal scheduling for fuel supply and capacity-based demand response program under dynamic hydrogen pricing. IEEE transactions on smart grid, 10(4), 4531–4542.

Erbach, G., & Jensen, L. (2021). Eu hydrogen policy: Hydrogen as an energy carrier for a climate-neutral economy. Retrieved from https://www.europarl.europa.eu/RegData/etudes/BRIE/2021/689332/EPRS_BRI(2021)689332_EN.pdf

Erdoğan, A., Geçici, E., & Güler, M. G. (2023). Design of a future hydrogen supply chain: A multi-objective model for turkey. International Journal of Hydrogen Energy, 48(31), 11775–11789.

Erdoğan, A., & Güler, M. G. (2023). Optimization and analysis of a hydrogen supply chain in terms of cost, co2 emissions, and risk: the case of turkey. International Journal of Hydrogen Energy, 48(60), 22752–22765.

Farhana, K., Mahamude, A. S. F., & Kadirgama, K. (2024). Comparing hydrogen fuel cost of production from various sources-a competitive analysis. Energy Conversion and Management, 302, 118088.

Faria, R., Marques, P., Moura, P., Freire, F., Delgado, J., & de Almeida, A. T. (2013, 8). Impact of the electricity mix and use profile in the life-cycle assessment of electric vehicles. Renewable & Sustainable Energy Reviews, 24, 271–287. Retrieved from https://www.sciencedirect.com/science/article/pii/S1364032113002220 doi: 10.1016/J.RSER.2013.03.063

Faye, O., Szpunar, J., & Eduok, U. (2022). A critical review on the current technologies for the generation, storage, and transportation of hydrogen. International journal of hydrogen energy, 47(29), 13771–13802.

Fazli-Khalaf, M., Naderi, B., Mohammadi, M., & Pishvaee, M. S. (2020). Design of a sustainable and reliable hydrogen supply chain network under mixed uncertainties: A case study. International journal of hydrogen energy, 45(59), 34503–34531.

Forghani, K., Kia, R., & Nejatbakhsh, Y. (2023). A multi-period sustainable hydrogen supply chain model considering pipeline routing and carbon emissions: The case study of oman. Renewable and Sustainable Energy Reviews, 173, 113051.

France Hydrogène. (2021). L'hydrogène dans le monde. Retrieved from https://www.france-hydrogene.org/publication/lhydrogene-dans-le-monde/

Full, J., Merseburg, S., Miehe, R., & Sauer, A. (2021). A new perspective for climate change mitigation—introducing carbon-negative hydrogen production from biomass with carbon capture and storage (hybeccs). Sustainability, 13(7), 4026.

Gabrielli, P., Charbonnier, F., Guidolin, A., & Mazzotti, M. (2020). Enabling low-carbon hydrogen supply chains through use of biomass and carbon capture and storage: a swiss case study. Applied energy, 275, 115245.

Gao, J., & You, F. (2015, 7). Shale Gas Supply Chain Design and Operations toward Better Economic and Life Cycle Environmental Performance: MINLP Model and Global Optimization Algorithm. ACS Sustainable Chemistry & Engineering, 3(7), 1282–1291. Retrieved from http://pubs.acs.org/doi/10.1021/acssuschemeng.5b00122 doi: 10.1021/acssuschemeng.5b00122

Gao, J., & You, F. (2017). Modeling framework and computational algorithm for hedging against uncertainty in sustainable supply chain design using functional-unit-based

life cycle optimization. Computers & Chemical Engineering, 107, 221–236.
Gao, J., & You, F. (2018a). Dynamic material flow analysis-based life cycle optimization framework and application to sustainable design of shale gas energy systems. ACS Sustainable Chemistry & Engineering, 6(9), 11734–11752.
Gao, J., & You, F. (2018b). Integrated hybrid life cycle assessment and optimization of shale gas. ACS Sustainable Chemistry & Engineering, 6(2), 1803–1824.
Gebreslassie, B. H., Slivinsky, M., Wang, B., & You, F. (2013, 3). Life cycle optimization for sustainable design and operations of hydrocarbon biorefinery via fast pyrolysis, hydrotreating and hydrocracking. Computers & Chemical Engineering, 50, 71–91. Retrieved from https://www.sciencedirect.com/science/article/pii/S0098135412003250 doi: 10.1016/J.COMPCHEMENG.2012.10.013
Gebreslassie, B. H., Waymire, R., & You, F. (2013, 5). Sustainable design and synthesis of algae-based biorefinery for simultaneous hydrocarbon biofuel production and carbon sequestration. AIChE Journal, 59(5), 1599–1621. Retrieved from http://doi.wiley.com/10.1002/aic.14075 doi: 10.1002/aic.14075
Genovese, M., & Fragiacomo, P. (2023). Hydrogen refueling station: overview of the technological status and research enhancement. Journal of Energy Storage, 61, 106758.
Ghazvini, M., Sadeghzadeh, M., Ahmadi, M. H., Moosavi, S., & Pourfayaz, F. (2019). Geothermal energy use in hydrogen production: A review. International Journal of Energy Research, 43(14), 7823–7851.
Gielen, D., Taibi, E., & Miranda, R. (2019). Hydrogen: A reviewable energy perspective: Report prepared for the 2nd hydrogen energy ministerial meeting in tokyo, japan.
Gnanapragasam, N. V., & Rosen, M. (2017). A review of hydrogen production using coal, biomass and other solid fuels. Biofuels, 8(6), 725–745.
Gondal, I. A., & Sahir, M. H. (2013). Model for biomass-based renewable hydrogen supply chain. International journal of energy research, 37(10), 1151–1159.
Gong, J., & You, F. (2014, 9). Global optimization for sustainable design and synthesis of algae processing network for CO 2 mitigation and biofuel production using life cycle optimization. AIChE Journal, 60(9), 3195–3210. Retrieved from http://doi.wiley.com/10.1002/aic.14504 doi: 10.1002/aic.14504
Goodarzian, F., Kumar, V., & Abraham, A. (2021). Hybrid meta-heuristic algorithms for a supply chain network considering different carbon emission regulations using big data characteristics. Soft Computing, 25, 7527–7557.
Grigoratos, T., Fontaras, G., Giechaskiel, B., & Zacharof, N. (2019). Real world emissions performance of heavy-duty euro vi diesel vehicles. Atmospheric environment, 201, 348–359.
Guillén-Gosálbez, G., & Grossmann, I. E. (2009, 1). Optimal design and planning of sustainable chemical supply chains under uncertainty. AIChE Journal, 55(1), 99–121. Retrieved from http://doi.wiley.com/10.1002/aic.11662 doi: 10.1002/aic.11662
Guillén-Gosálbez, G., Mele, F. D., & Grossmann, I. E. (2010). A bi-criterion optimization approach for the design and planning of hydrogen supply chains for vehicle use. AIChE Journal, 56(3), 650–667.
Gül, T., Kypreos, S., Turton, H., & Barreto, L. (2009). An energy-economic scenario analysis of alternative fuels for personal transport using the global multi-regional markal model (gmm). Energy, 34(10), 1423–1437.
Güler, M. G., Geçici, E., & Erdoğan, A. (2021). Design of a future hydrogen supply chain: A multi period model for turkey. International Journal of Hydrogen Energy, 46(30),

16279–16298.

Gunawan, T. A., Williamson, I., Raine, D., & Monaghan, R. F. (2021). Decarbonising city bus networks in ireland with renewable hydrogen. International Journal of Hydrogen Energy, 46(57), 28870–28886.

Guo, J.-X., Tan, X., Zhu, K., & Gu, B. (2022). Integrated management of mixed biomass for hydrogen production from gasification. Chemical Engineering Research and Design, 179, 41–55.

Han, J.-H., Ryu, J.-H., & Lee, I.-B. (2012). Modeling the operation of hydrogen supply networks considering facility location. International journal of hydrogen energy, 37(6), 5328–5346.

Han, J.-H., Ryu, J.-H., & Lee, I.-B. (2013). Multi-objective optimization design of hydrogen infrastructures simultaneously considering economic cost, safety and co2 emission. Chemical Engineering Research and Design, 91(8), 1427–1439.

Han, S., & Kim, J. (2019). A multi-period milp model for the investment and design planning of a national-level complex renewable energy supply system. Renewable Energy, 141, 736–750.

Haron, R., Mat, R., Abdullah, T. A. T., & Rahman, R. A. (2018). Overview on utilization of biodiesel by-product for biohydrogen production. Journal of Cleaner Production, 172, 314–324.

He, C., Sun, H., Xu, Y., & Lv, S. (2017). Hydrogen refueling station siting of expressway based on the optimization of hydrogen life cycle cost. International Journal of Hydrogen Energy, 42(26), 16313–16324. Retrieved from http://dx.doi.org/10.1016/j.ijhydene.2017.05.073 doi: 10.1016/j.ijhydene.2017.05.073

He, G., Mallapragada, D. S., Bose, A., Heuberger, C. F., & Gençer, E. (2021). Hydrogen supply chain planning with flexible transmission and storage scheduling. IEEE Transactions on Sustainable Energy, 12(3), 1730–1740.

Hermesmann, M., Tsiklios, C., & Müller, T. (2023). The environmental impact of renewable hydrogen supply chains: Local vs. remote production and long-distance hydrogen transport. Applied Energy, 351, 121920.

Hong, X., Thaore, V. B., Karimi, I. A., Farooq, S., Wang, X., Usadi, A. K., ... Johnson, R. A. (2021). Techno-enviro-economic analyses of hydrogen supply chains with an asean case study. International Journal of Hydrogen Energy, 46(65), 32914–32928.

Huang, X. (2007, 4). Optimal project selection with random fuzzy parameters. International Journal of Production Economics, 106(2), 513–522. Retrieved from https://www.sciencedirect.com/science/article/pii/S092552730600168X doi: 10.1016/J.IJPE.2006.06.011

Hugo, A., Rutter, P., Pistikopoulos, S., Amorelli, A., & Zoia, G. (2005). Hydrogen infrastructure strategic planning using multi-objective optimization. International Journal of Hydrogen Energy, 30(15), 1523–1534.

Hwang, J.-J. (2013, 3). Sustainability study of hydrogen pathways for fuel cell vehicle applications. Renewable & Sustainable Energy Reviews, 19, 220–229. Retrieved from https://www.sciencedirect.com/science/article/pii/S1364032112006454 doi: 10.1016/J.RSER.2012.11.033

Hwangbo, S., Lee, I.-B., & Han, J. (2016). Multi-period stochastic mathematical model for the optimal design of integrated utility and hydrogen supply network under uncertainty in raw material prices. Energy, 114, 418–430.

Hwangbo, S., Lee, I.-B., & Han, J. (2017). Mathematical model to optimize design of integrated utility supply network and future global hydrogen supply network under

demand uncertainty. Applied energy, 195, 257–267.
Hwangbo, S., Nam, K., Han, J., Lee, I.-B., & Yoo, C. (2018). Integrated hydrogen supply networks for waste biogas upgrading and hybrid carbon-hydrogen pinch analysis under hydrogen demand uncertainty. Applied Thermal Engineering, 140, 386–397.
Hydrogen Council. (2021). Hydrogen insights 2021 (Tech. Rep.).
Ibrahim, Y., & Al-Mohannadi, D. M. (2023). Optimization of low-carbon hydrogen supply chain networks in industrial clusters. International Journal of Hydrogen Energy, 48(36), 13325–13342.
Ingason, H. T., Ingolfsson, H. P., & Jensson, P. (2008). Optimizing site selection for hydrogen production in iceland. International journal of hydrogen energy, 33(14), 3632–3643.
Institute, G. R. (2021). Law no 2021-1104 on the fight on climate change and resilience. Retrieved from https://climate-laws.org/geographies/france/laws/law-no-2021-1104-on-the-fight-on-climate-change-and-resilience
International Energy Agency. (2019). The future of hydrogen – seizing today's opportunities (Tech. Rep.).
International Energy Agency. (2021a). Deployment Status of Fuel Cells in Road Transport: 2021 Updat (Tech. Rep.).
International Energy Agency. (2021b). Global hydrogen review 2021 (Tech. Rep.).
International Energy Agency. (2021c). Technology roadmap - hydrogen and fuel cells (Tech. Rep.).
Ishaq, H., Dincer, I., & Crawford, C. (2022). A review on hydrogen production and utilization: Challenges and opportunities. International Journal of Hydrogen Energy, 47(62), 26238–26264.
ISO. (2006). ISO 14040: Environmental Management-Life Cycle Assessment-Principles and Frame Work. Geneva: International Organization for Standardization.
Iverson, Z., Achuthan, A., Marzocca, P., & Aidun, D. (2013, 4). Optimal design of hybrid renewable energy systems (HRES) using hydrogen storage technology for data center applications. Renewable Energy, 52, 79–87. Retrieved from https://www.sciencedirect.com/science/article/pii/S0960148112006830 doi: 10.1016/J.RENENE.2012.10.038
Jagannath, A., & Almansoori, A. (2014). Modeling of hydrogen networks in a refinery using a stochastic programming appraoch. Industrial & Engineering Chemistry Research, 53(51), 19715–19735.
Jeong, C., & Han, C. (2011). Byproduct hydrogen network design using pressure swing adsorption and recycling unit for the petrochemical complex. Industrial & engineering chemistry research, 50(6), 3304–3311.
Jiang, H., Qi, B., Du, E., Zhang, N., Yang, X., Yang, F., & Wu, Z. (2021). Modeling hydrogen supply chain in renewable electric energy system planning. IEEE Transactions on Industry Applications, 58(2), 2780–2791.
Joffe, D., Hart, D., & Bauen, A. (2004). Modelling of hydrogen infrastructure for vehicle refuelling in london. Journal of power sources, 131(1-2), 13–22.
Johnson, N., & Ogden, J. (2012, 3). A spatially-explicit optimization model for long-term hydrogen pipeline planning. International Journal of Hydrogen Energy, 37(6), 5421–5433. Retrieved from http://dx.doi.org/10.1016/j.ijhydene.2011.08.109http://linkinghub.elsevier.com/retrieve/pii/S0360319911020349 doi: 10.1016/j.ijhydene.2011.08.109
Kalinci, Y., Hepbasli, A., & Dincer, I. (2012). Life cycle assessment of hydrogen production from biomass gasification systems. International journal of hydrogen energy,

37(19), 14026–14039.

Kanoglu, M., Bolatturk, A., & Yilmaz, C. (2010). Thermodynamic analysis of models used in hydrogen production by geothermal energy. International journal of hydrogen energy, 35(16), 8783–8791.

Kazi, M.-K., Eljack, F., El-Halwagi, M. M., & Haouari, M. (2021). Green hydrogen for industrial sector decarbonization: Costs and impacts on hydrogen economy in qatar. Computers & Chemical Engineering, 145, 107144.

Khademi, M. H., Alipour-Dehkordi, A., & Nalchifard, F. (2023). Sustainable hydrogen and syngas production from waste valorization of biodiesel synthesis by-product: Green chemistry approach. Renewable and Sustainable Energy Reviews, 175, 113191.

Ki-Jong, W. (2012). Korea's green growth based on oecd green growth indicators. Retrieved from https://www.oecd.org/greengrowth/Korea's%20GG%20report%20with%20OECD%20indicators.pdf

Kim, A., Kim, H., Lee, H., Lee, B., & Lim, H. (2021). Comparative economic optimization for an overseas hydrogen supply chain using mixed-integer linear programming. ACS Sustainable Chemistry & Engineering, 9(42), 14249–14262.

Kim, J., Lee, Y., & Moon, I. (2008). Optimization of a hydrogen supply chain under demand uncertainty. International Journal of Hydrogen Energy, 33(18), 4715–4729.

Kim, J., Lee, Y., & Moon, I. (2011). An index-based risk assessment model for hydrogen infrastructure. International journal of hydrogen energy, 36(11), 6387–6398.

Kim, J., & Moon, I. (2008). Strategic design of hydrogen infrastructure considering cost and safety using multiobjective optimization. International Journal of Hydrogen Energy, 33(21), 5887–5896.

Kim, M., & Kim, J. (2016). Optimization model for the design and analysis of an integrated renewable hydrogen supply (irhs) system: application to korea's hydrogen economy. International Journal of Hydrogen Energy, 41(38), 16613–16626.

Kim, M., & Kim, J. (2017a). An integrated decision support model for design and operation of a wind-based hydrogen supply system. International journal of hydrogen energy, 42(7), 3899–3915.

Kim, M., & Kim, J. (2017b). An integrated decision support model for design and operation of a wind-based hydrogen supply system. International Journal of Hydrogen Energy, 42(7), 3899–3915. Retrieved from http://linkinghub.elsevier.com/retrieve/pii/S0360319916332001 doi: 10.1016/j.ijhydene.2016.10.129

Kırtay, E. (2011). Recent advances in production of hydrogen from biomass. Energy conversion and management, 52(4), 1778–1789.

Konda, N. M., Shah, N., & Brandon, N. P. (2011). Optimal transition towards a large-scale hydrogen infrastructure for the transport sector: The case for the netherlands. International Journal of Hydrogen Energy, 36(8), 4619–4635.

Kumar, S. S., & Himabindu, V. (2019). Hydrogen production by pem water electrolysis–a review. Materials Science for Energy Technologies, 2(3), 442–454.

Kumar, V., Chhabra, J. K., & Kumar, D. (2014). Parameter adaptive harmony search algorithm for unimodal and multimodal optimization problems. Journal of Computational Science, 5(2), 144–155.

Lahnaoui, A., Wulf, C., Heinrichs, H., & Dalmazzone, D. (2018, 8). Optimizing hydrogen transportation system for mobility by minimizing the cost of transportation via compressed gas truck in North Rhine-Westphalia. Applied Energy, 223, 317–328. Retrieved from https://www.sciencedirect.com/science/article/pii/S0306261918304380?via%3Dihubhttp://linkinghub.elsevier.com/retrieve/pii/S0306261918304380 doi: 10.1016/j.apenergy.2018.03.099

Lambora, A., Gupta, K., & Chopra, K. (2019). Genetic algorithm-a literature review. In 2019 international conference on machine learning, big data, cloud and parallel computing (comitcon) (pp. 380–384).

Lebrouhi, B., Djoupo, J., Lamrani, B., Benabdelaziz, K., & Kousksou, T. (2022). Global hydrogen development-a technological and geopolitical overview. International Journal of Hydrogen Energy, 47(11), 7016–7048.

Lee, D.-Y., Elgowainy, A., & Dai, Q. (2018). Life cycle greenhouse gas emissions of hydrogen fuel production from chlor-alkali processes in the united states. Applied Energy, 217, 467–479.

Lee, J.-S., Cherif, A., Yoon, H.-J., Seo, S.-K., Bae, J.-E., Shin, H.-J., ... Lee, C.-J. (2022). Large-scale overseas transportation of hydrogen: Comparative techno-economic and environmental investigation. Renewable and Sustainable Energy Reviews, 165, 112556.

Li, G., Cui, P., Wang, Y., Liu, Z., Zhu, Z., & Yang, S. (2020). Life cycle energy consumption and ghg emissions of biomass-to-hydrogen process in comparison with coal-to-hydrogen process. Energy, 191, 116588.

Li, J., Wei, Y.-M., Liu, L., Li, X., & Yan, R. (2022). The carbon footprint and cost of coal-based hydrogen production with and without carbon capture and storage technology in china. Journal of Cleaner Production, 362, 132514.

Li, L., Feng, L., Manier, H., & Manier, M.-A. (2022). Life cycle optimization for hydrogen supply chain network design. International Journal of Hydrogen Energy.

Li, L., Manier, H., & Manier, M.-A. (2020). Integrated optimization model for hydrogen supply chain network design and hydrogen fueling station planning. Computers & Chemical Engineering, 134, 106683.

Li, M., Ming, P., Huo, R., Mu, H., & Zhang, C. (2023). Optimizing design and performance assessment of a sustainability hydrogen supply chain network: A multi-period model for china. Sustainable Cities and Society, 92, 104444.

Lin, T., Rodríguez, L. F., Shastri, Y. N., Hansen, A. C., & Ting, K. (2013, 5). GIS-enabled biomass-ethanol supply chain optimization: model development and Miscanthus application. Biofuels, Bioproducts and Biorefining, 7(3), 314–333. Retrieved from `http://doi.wiley.com/10.1002/bbb.1394` doi: 10.1002/bbb.1394

Liu, H., & Liu, S. (2021). Life cycle energy consumption and ghg emissions of hydrogen production from underground coal gasification in comparison with surface coal gasification. International Journal of Hydrogen Energy, 46(14), 9630–9643.

Lotfi, R., Kargar, B., Hoseini, S. H., Nazari, S., Safavi, S., & Weber, G.-W. (2021). Resilience and sustainable supply chain network design by considering renewable energy. International Journal of Energy Research, 45(12), 17749–17766.

Maestre, V., Ortiz, A., & Ortiz, I. (2023). Decarbonizing the spanish transportation sector by 2050: Design and techno-economic assessment of the hydrogen generation and supply chain. International Journal of Hydrogen Energy, 48(99), 39514–39530.

Mah, A. X. Y., Ho, W. S., Hassim, M. H., Hashim, H., Muis, Z. A., Ling, G. H. T., & Ho, C. S. (2022). Spatial optimization of photovoltaic-based hydrogen-electricity supply chain through an integrated geographical information system and mathematical modeling approach. Clean Technologies and Environmental Policy, 1–20.

MahmoumGonbadi, A., Genovese, A., & Sgalambro, A. (2021). Closed-loop supply chain design for the transition towards a circular economy: A systematic literature review of methods, applications and current gaps. Journal of Cleaner Production, 323, 129101.

Mavrotas, G. (2009). Effective implementation of the ϵ-constraint method in Multi-

Objective Mathematical Programming problems. Applied Mathematics and Computation, 213(2), 455–465. doi: 10.1016/j.amc.2009.03.037

Melaina, M. W., Antonia, O., & Penev, M. (2013). Blending hydrogen into natural gas pipeline networks: a review of key issues.

Melo, M., Nickel, S., & Saldanha-da Gama, F. (2009, 7). Facility location and supply chain management – A review. European Journal of Operational Research, 196(2), 401–412. Retrieved from https://www.sciencedirect.com/science/article/pii/S0377221708004104?via%3Dihub doi: 10.1016/J.EJOR.2008.05.007

Meng, L., He, J., Hu, S., & Han, C. (2023). Strategic reliable supply chain network design: determining tradeoffs between cost and risk. International Journal of Production Research, 61(11), 3621–3633.

Michalewicz, Z., & Schoenauer, M. (1996). Evolutionary algorithms for constrained parameter optimization problems. Evolutionary computation, 4(1), 1–32.

Midilli, A., Kucuk, H., Topal, M. E., Akbulut, U., & Dincer, I. (2021). A comprehensive review on hydrogen production from coal gasification: Challenges and opportunities. International Journal of Hydrogen Energy, 46(50), 25385–25412.

Moreno-Benito, M., Agnolucci, P., & Papageorgiou, L. G. (2017). Towards a sustainable hydrogen economy: Optimisation-based framework for hydrogen infrastructure development. Computers & Chemical Engineering, 102, 110–127. Retrieved from http://dx.doi.org/10.1016/j.compchemeng.2016.08.005 doi: 10.1016/j.compchemeng.2016.08.005

Moreno-Camacho, C. A., Montoya-Torres, J. R., Jaegler, A., & Gondran, N. (2019). Sustainability metrics for real case applications of the supply chain network design problem: A systematic literature review. Journal of Cleaner Production, 231, 600–618.

Murthy Konda, N., Shah, N., & Brandon, N. P. (2012). Dutch hydrogen economy: evolution of optimal supply infrastructure and evaluation of key influencing elements. Asia-Pacific Journal of Chemical Engineering, 7(4), 534–546.

Myhre, G., Shindell, D., & Pongratz, J. (2014). Anthropogenic and natural radiative forcing. Cambridge University Press.

Navas-Anguita, Z., García-Gusano, D., Dufour, J., & Iribarren, D. (2021). Revisiting the role of steam methane reforming with co2 capture and storage for long-term hydrogen production. Science of the total Environment, 771, 145432.

Negri, V., Galán-Martín, Á., Pozo, C., Fajardy, M., Reiner, D. M., Mac Dowell, N., & Guillén-Gosálbez, G. (2021). Life cycle optimization of beccs supply chains in the european union. Applied Energy, 298, 117252.

Newell, P., & Ilgen, A. G. (2019). Overview of geological carbon storage (gcs). In Science of carbon storage in deep saline formations (pp. 1–13). Elsevier.

Nunes, P., Oliveira, F., Hamacher, S., & Almansoori, A. (2015). Design of a hydrogen supply chain with uncertainty. International Journal of Hydrogen Energy, 40(46), 16408–16418.

Ochoa Bique, A., Maia, L. K., Grossmann, I. E., & Zondervan, E. (2023). Design of hydrogen supply chains under demand uncertainty–a case study of passenger transport in germany. Physical Sciences Reviews, 8(6), 741–762.

Ochoa Robles, J., Giraud Billoud, M., Azzaro-Pantel, C., & Aguilar-Lasserre, A. A. (2019). Optimal design of a sustainable hydrogen supply chain network: application in an airport ecosystem. ACS sustainable chemistry & engineering, 7(21), 17587–17597.

Ocko, I. B., & Hamburg, S. P. (2022). Climate consequences of hydrogen emissions. Atmospheric Chemistry and Physics, 22(14), 9349–9368.

Ogumerem, G. S., Kim, C., Kesisoglou, I., Diangelakis, N. A., & Pistikopoulos, E. N.

(2018). A multi-objective optimization for the design and operation of a hydrogen network for transportation fuel. Chemical Engineering Research and Design, 131, 279–292.

Orsi, F., Muratori, M., Rocco, M., Colombo, E., & Rizzoni, G. (2016, 5). A multi-dimensional well-to-wheels analysis of passenger vehicles in different regions: Primary energy consumption, CO2 emissions, and economic cost. Applied Energy, 169, 197–209. Retrieved from https://www.sciencedirect.com/science/article/pii/S0306261916301623 doi: 10.1016/J.APENERGY.2016.02.039

Pareek, A., Dom, R., Gupta, J., Chandran, J., Adepu, V., & Borse, P. H. (2020). Insights into renewable hydrogen energy: Recent advances and prospects. Materials Science for Energy Technologies, 3, 319–327.

Parker, N., Fan, Y., & Ogden, J. (2010, 7). From waste to hydrogen: An optimal design of energy production and distribution network. Transportation Research Part E: Logistics and Transportation Review, 46(4), 534–545. Retrieved from http://linkinghub.elsevier.com/retrieve/pii/S1366554509000404http://dx.doi.org/10.1016/j.tre.2009.04.002 doi: 10.1016/j.tre.2009.04.002

Peng, W., Xin, B., & Xie, L. (2023). Optimal strategies for production plan and carbon emission reduction in a hydrogen supply chain under cap-and-trade policy. Renewable energy, 215, 118960.

Peschel, A. (2020). Industrial perspective on hydrogen purification, compression, storage, and distribution. Fuel Cells, 20(4), 385–393.

Pflugmann, F., & De Blasio, N. (2020). The geopolitics of renewable hydrogen in low-carbon energy markets. Geopolitics, History, and International Relations, 12(1), 9–44.

Pires, J., Martins, F., Alvim-Ferraz, M., & Simões, M. (2011). Recent developments on carbon capture and storage: An overview. Chemical engineering research and design, 89(9), 1446–1460.

Previsic, M. (2011). Economic methodology for the evaluation of emerging renewable technologies. Prepared for US DOE, Sacramento, CA: RE Vision Consulting, LLC.

PricewaterhouseCoopers. (2022). The green hydrogen economy predicting the decarbonisation agenda of tomorrow. Retrieved from https://www.pwc.com/gx/en/industries/energy-utilities-resources/future-energy/green-hydrogen-cost.html

Qadrdan, M., Saboohi, Y., & Shayegan, J. (2008). A model for investigation of optimal hydrogen pathway, and evaluation of environmental impacts of hydrogen supply system. International journal of hydrogen energy, 33(24), 7314–7325.

Qu, R., Zhang, W., Liu, N., Zhang, Q., Liu, Y., Li, X., ... Feng, L. (2018). Antioil ag3po4 nanoparticle/polydopamine/al2o3 sandwich structure for complex wastewater treatment: dynamic catalysis under natural light. ACS Sustainable Chemistry & Engineering, 6(6), 8019–8028.

Ransikarbum, K., Chanthakhot, W., Glimm, T., & Janmontree, J. (2023). Evaluation of sourcing decision for hydrogen supply chain using an integrated multi-criteria decision analysis (mcda) tool. Resources, 12(4), 48.

Rathi, T., Pinto, J. M., & Zhang, Q. (2023). Strategic low-carbon hydrogen supply chain planning under market price uncertainty. In Computer aided chemical engineering (Vol. 52, pp. 3357–3362). Elsevier.

Ren, J., Musyoka, N. M., Langmi, H. W., Mathe, M., & Liao, S. (2017). Current research trends and perspectives on materials-based hydrogen storage solutions: A critical

review. International journal of hydrogen energy, 42(1), 289–311.

Ren, L., Zhou, S., & Ou, X. (2020). Life-cycle energy consumption and greenhouse-gas emissions of hydrogen supply chains for fuel-cell vehicles in china. Energy, 209, 118482.

Reuß, M., Grube, T., Robinius, M., & Stolten, D. (2019). A hydrogen supply chain with spatial resolution: Comparative analysis of infrastructure technologies in germany. Applied Energy, 247, 438–453.

Reyes-Barquet, L. M., Rico-Contreras, J. O., Azzaro-Pantel, C., Moras-Sánchez, C. G., González-Huerta, M. A., Villanueva-Vásquez, D., & Aguilar-Lasserre, A. A. (2022). Multi-objective optimal design of a hydrogen supply chain powered with agro-industrial wastes from the sugarcane industry: a mexican case study. Mathematics, 10(3), 437.

Robles, J. O., Almaraz, S. D.-L., & Azzaro-Pantel, C. (2016). Optimization of a hydrogen supply chain network design by multi-objective genetic algorithms. In Computer aided chemical engineering (Vol. 38, pp. 805–810). Elsevier.

Robles, J. O., Azzaro-Pantel, C., & Aguilar-Lasserre, A. (2020). Optimization of a hydrogen supply chain network design under demand uncertainty by multi-objective genetic algorithms. Computers & Chemical Engineering, 140, 106853.

Robles, J. O., Azzaro-Pantel, C., Garcia, G. M., & Lasserre, A. A. (2020). Social cost-benefit assessment as a post-optimal analysis for hydrogen supply chain design and deployment: Application to occitania (france). Sustainable Production and Consumption, 24, 105–120.

RTE. (2020). The transition to low-carbon hydrogen in france: Opportunities and challenges for the power system by 2030-2035 (Tech. Rep.). Retrieved from `https://assets.rte-france.com/prod/public/2021-03/Hydrogen%20report_0.pdf`

Ruan, Y., Liu, Q., Li, Z., & Wu, J. (2016, 10). Optimization and analysis of Building Combined Cooling, Heating and Power (BCHP) plants with chilled ice thermal storage system. Applied Energy, 179, 738–754. Retrieved from `https://www.sciencedirect.com/science/article/pii/S0306261916309503` doi: 10.1016/J.APENERGY.2016.07.009

Sabio, N., Gadalla, M., Guillén-Gosálbez, G., & Jiménez, L. (2010). Strategic planning with risk control of hydrogen supply chains for vehicle use under uncertainty in operating costs: a case study of spain. International journal of hydrogen energy, 35(13), 6836–6852.

Sabio, N., Kostin, A., Guillén-Gosálbez, G., & Jiménez, L. (2012). Holistic minimization of the life cycle environmental impact of hydrogen infrastructures using multi-objective optimization and principal component analysis. International journal of hydrogen energy, 37(6), 5385–5405.

Sahay, N., & Ierapetritou, M. (2014). Hybrid simulation based optimization framework for centralized and decentralized supply chains. Industrial & Engineering Chemistry Research, 53(10), 3996–4007.

Salahi, F., Daneshvar, A., Homayounfar, M., & Shokouhifar, M. (2021). A comparative study of meta-heuristic algorithms in supply chain networks. Journal of Industrial Engineering International, 17(1), 52–62.

Salehi-Amiri, A., Zahedi, A., Akbapour, N., & Hajiaghaei-Keshteli, M. (2021). Designing a sustainable closed-loop supply chain network for walnut industry. Renewable and Sustainable Energy Reviews, 141, 110821.

Sánchez, A., Martín, M., & Zhang, Q. (2021). Optimal design of sustainable power-to-fuels supply chains for seasonal energy storage. Energy, 234, 121300.

Saracoglu, I., Topaloglu, S., & Keskinturk, T. (2014). A genetic algorithm approach for multi-product multi-period continuous review inventory models. Expert Systems with Applications, 41(18), 8189–8202.

Schneider, S., Bajohr, S., Graf, F., & Kolb, T. (2020). State of the art of hydrogen production via pyrolysis of natural gas. ChemBioEng Reviews, 7(5), 150–158.

Schoettle, B., Sivak, M., & Tunnell, M. (2016). A survey of fuel economy and fuel usage by heavy-duty truck fleets. No. SWT-2016-12, http://atri-online.org/wpcontent/uploads/2016/10/2016. ATRI-UMTRI. FuelEconomyReport. Final_-. pdf.

Sdanghi, G., Maranzana, G., Celzard, A., & Fierro, V. (2019). Review of the current technologies and performances of hydrogen compression for stationary and automotive applications. Renewable and Sustainable Energy Reviews, 102, 150–170.

Seo, S.-K., Yun, D.-Y., & Lee, C.-J. (2020). Design and optimization of a hydrogen supply chain using a centralized storage model. Applied energy, 262, 114452.

Sgobbi, A., Nijs, W., De Miglio, R., Chiodi, A., Gargiulo, M., & Thiel, C. (2016). How far away is hydrogen? its role in the medium and long-term decarbonisation of the european energy system. international journal of hydrogen energy, 41(1), 19–35.

Shamsi, H., Tran, M.-K., Akbarpour, S., Maroufmashat, A., & Fowler, M. (2021). Macro-level optimization of hydrogen infrastructure and supply chain for zero-emission vehicles on a canadian corridor. Journal of cleaner production, 289, 125163.

Short, W., Packey, D. J., & Holt, T. (1995). A Manual for the Economic Evaluation of Energy Efficiency and Renewable Energy Technologies (Tech. Rep.). National Renewable Energy Laboratory. Retrieved from `https://www.nrel.gov/docs/legosti/old/5173.pdf`

Siddiqui, O., & Dincer, I. (2018). Examination of a new solar-based integrated system for desalination, electricity generation and hydrogen production. Solar Energy, 163, 224–234.

Singh, S., Jain, S., Venkateswaran, P., Tiwari, A. K., Nouni, M. R., Pandey, J. K., & Goel, S. (2015). Hydrogen: A sustainable fuel for future of the transport sector. Renewable and sustainable energy reviews, 51, 623–633.

Slinn, M., Kendall, K., Mallon, C., & Andrews, J. (2008). Steam reforming of biodiesel by-product to make renewable hydrogen. Bioresource technology, 99(13), 5851–5858.

Solis, C. M. A., San Juan, J. L. G., Mayol, A. P., Sy, C. L., Ubando, A. T., & Culaba, A. B. (2021). A multi-objective life cycle optimization model of an integrated algal biorefinery toward a sustainable circular bioeconomy considering resource recirculation. Energies, 14(5), 1416.

Statista. (2021). Power sector carbon intensity outlook in france 2020-2050. Retrieved from `https://www.statista.com/statistics/1190067/carbon-intensity-outlook-of-france/#statisticContainer`

Statista Search Department. (2021). Estimated number of plug-in electric vehicles in use in selected countries as of 2020 (in 1,000 units) [infographic]. Retrieved from `https://www.statista.com/statistics/244292/number-of-electric-vehicles-by-country/`

Statistics, N. I. O., & Studies, E. (2022). Growth and structure of the population in 2019. Retrieved from `https://www.insee.fr/en/statistiques/zones/6455994?debut=0&q=Population+census`

Sun, H., He, C., Wang, H., Zhang, Y., Lv, S., & Xu, Y. (2017). Hydrogen station siting optimization based on multi-source hydrogen supply and life cycle cost. International

journal of hydrogen energy, 42(38), 23952–23965.
Sönnichsen, N. (2021). Hydrogen: Fuel of the future? a statista dossierplus on hydrogen and its relevance in the net zero economy of tomorrow (Tech. Rep.).
Thitakamol, B., Veawab, A., & Aroonwilas, A. (2007). Environmental impacts of absorption-based co2 capture unit for post-combustion treatment of flue gas from coal-fired power plant. International Journal of Greenhouse Gas Control, 1(3), 318–342.
Tian, X., Meyer, T., Lee, H., & You, F. (2020). Sustainable design of geothermal energy systems for electric power generation using life cycle optimization. AIChE Journal, 66(4), e16898.
Timmerberg, S., & Kaltschmitt, M. (2019). Hydrogen from renewables: Supply from north africa to central europe as blend in existing pipelines–potentials and costs. Applied energy, 237, 795–809.
Transition, E., & Ministry, T. C. (2021). Données sur le parc automobile français au 1er janvier 2021. Retrieved from https://www.statistiques.developpement-durable.gouv.fr/donnees-sur-le-parc-automobile-francais-au-1er-janvier-2021
United Nations. (2015). The 17 goals. Retrieved from https://sdgs.un.org/goals
United Nations Framework Convention on Climate Change. (2021). Glasgow climate pact. Retrieved from https://unfccc.int/sites/default/files/resource/cop26_auv_2f_cover_decision.pdf
United Nations Framework Convention on Climate Change. (2023). Cop28 agreement signals "beginning of the end" of the fossil fuel era. Retrieved from https://unfccc.int/news/cop28-agreement-signals-beginning-of-the-end-of-the-fossil-fuel-era
Uris, M., Linares, J. I., & Arenas, E. (2015, 8). Size optimization of a biomass-fired cogeneration plant CHP/CCHP (Combined heat and power/Combined heat, cooling and power) based on Organic Rankine Cycle for a district network in Spain. Energy, 88, 935–945. Retrieved from https://www.sciencedirect.com/science/article/pii/S0360544215009494 doi: 10.1016/J.ENERGY.2015.07.054
Usman, M. R. (2022). Hydrogen storage methods: Review and current status. Renewable and Sustainable Energy Reviews, 167, 112743.
van Renssen, S. (2020). The hydrogen solution? Nature Climate Change, 10(9), 799–801.
Vijayakumar, V., Jenn, A., & Ogden, J. (2023). Modeling future hydrogen supply chains in the western united states under uncertainties: an optimization-based approach focusing on california as a hydrogen hub. Sustainable Energy & Fuels, 7(5), 1223–1244.
Vom Scheidt, F., Qu, J., Staudt, P., Mallapragada, D. S., & Weinhardt, C. (2022). Integrating hydrogen in single-price electricity systems: The effects of spatial economic signals. Energy Policy, 161, 112727.
Waltho, C., Elhedhli, S., & Gzara, F. (2019). Green supply chain network design: A review focused on policy adoption and emission quantification. International Journal of Production Economics, 208, 305–318.
WHA International, I. (2023). Top industrial uses of hydrogen, and the need for industrial hydrogen safety. Retrieved from https://wha-international.com/hydrogen-in-industry/
Wickham, D., Hawkes, A., & Jalil-Vega, F. (2022). Hydrogen supply chain optimisation for the transport sector–focus on hydrogen purity and purification requirements. Ap-

plied Energy, 305, 117740.
Wikipedia contributors. (2020). Life-cycle assessment. Retrieved from https://en.wikipedia.org/w/index.php?title=Life-cycle_assessment&oldid=841261075
Wikipedia contributors. (2021). Internal rate of return — Wikipedia, The Free Encyclopedia. Retrieved from https://en.wikipedia.org/w/index.php?title=Internal_rate_of_return&oldid=841267870
Won, W., Kwon, H., Han, J.-H., & Kim, J. (2017). Design and operation of renewable energy sources based hydrogen supply system: Technology integration and optimization. Renewable Energy, 103, 226–238.
Woo, Y.-B., & Kim, B. S. (2019). A genetic algorithm-based matheuristic for hydrogen supply chain network problem with two transportation modes and replenishment cycles. Computers & Industrial Engineering, 127, 981–997.
Woo, Y.-b., Seolhee, C., Jiyong, K., & Kim, B. S. (2016). Optimization-based approach for strategic design and operation of a biomass-to-hydrogen supply chain. international journal of hydrogen energy, 41(12), 5405-5418.
Wu, W., Wang, P.-H., Lee, D.-J., & Chang, J.-S. (2017, 7). Global optimization of microalgae-to-biodiesel chains with integrated cogasification combined cycle systems based on greenhouse gas emissions reductions. Applied Energy, 197, 63–82. Retrieved from https://www.sciencedirect.com/science/article/pii/S0306261917303586 doi: 10.1016/J.APENERGY.2017.03.117
Wulf, C., & Kaltschmitt, M. (2018). Hydrogen supply chains for mobility—environmental and economic assessment. Sustainability, 10(6), 1699.
Yan, J. (2018). Negative-emissions hydrogen energy. Nature Climate Change, 8(7), 560–561.
Yan, X., & Crookes, R. J. (2009, 12). Life cycle analysis of energy use and greenhouse gas emissions for road transportation fuels in China. Renewable & Sustainable Energy Reviews, 13(9), 2505–2514. Retrieved from https://www.sciencedirect.com/science/article/pii/S1364032109001208 doi: 10.1016/J.RSER.2009.06.012
Yáñez, M., Ortiz, A., Brunaud, B., Grossmann, I. E., & Ortiz, I. (2018). Contribution of upcycling surplus hydrogen to design a sustainable supply chain: The case study of northern spain. Applied energy, 231, 777–787.
Yang, G., Jiang, Y., & You, S. (2020). Planning and operation of a hydrogen supply chain network based on the off-grid wind-hydrogen coupling system. International Journal of Hydrogen Energy, 45(41), 20721–20739.
Yilmaz, C., & Kanoglu, M. (2014). Thermodynamic evaluation of geothermal energy powered hydrogen production by pem water electrolysis. Energy, 69, 592–602.
Yoon, H.-J., Seo, S.-K., & Lee, C.-J. (2022). Multi-period optimization of hydrogen supply chain utilizing natural gas pipelines and byproduct hydrogen. Renewable and Sustainable Energy Reviews, 157, 112083.
You, F., & Wang, B. (2011, 9). Life Cycle Optimization of Biomass-to-Liquid Supply Chains with Distributed–Centralized Processing Networks. Industrial & Engineering Chemistry Research, 50(17), 10102–10127. Retrieved from http://pubs.acs.org/doi/abs/10.1021/ie200850t doi: 10.1021/ie200850t
Yue, D., Kim, M. A., & You, F. (2013, 8). Design of Sustainable Product Systems and Supply Chains with Life Cycle Optimization Based on Functional Unit: General Modeling Framework, Mixed-Integer Nonlinear Programming Algorithms and Case Study on Hydrocarbon Biofuels. ACS Sustainable Chemistry & Engineering, 1(8),

1003–1014. Retrieved from http://pubs.acs.org/doi/10.1021/sc400080x doi: 10.1021/sc400080x

Yue, D., Slivinsky, M., Sumpter, J., & You, F. (2014, 3). Sustainable Design and Operation of Cellulosic Bioelectricity Supply Chain Networks with Life Cycle Economic, Environmental, and Social Optimization. Industrial & Engineering Chemistry Research, 53(10), 4008–4029. Retrieved from http://pubs.acs.org/doi/10.1021/ie403882v doi: 10.1021/ie403882v

Zhao, H., Kamp, L. M., & Lukszo, Z. (2021). Exploring supply chain design and expansion planning of china's green ammonia production with an optimization-based simulation approach. International Journal of Hydrogen Energy, 46(64), 32331–32349.

Zhao, N., Lehmann, J., & You, F. (2020). Poultry waste valorization via pyrolysis technologies: economic and environmental life cycle optimization for sustainable bioenergy systems. ACS Sustainable Chemistry & Engineering, 8(11), 4633–4646.

Zhao, X., & You, F. (2021). Consequential life cycle assessment and optimization of high-density polyethylene plastic waste chemical recycling. ACS Sustainable Chemistry & Engineering, 9(36), 12167–12184.

Zore, U. K., Yedire, S. G., Pandi, N., Manickam, S., & Sonawane, S. H. (2021). A review on recent advances in hydrogen energy, fuel cell, biofuel and fuel refining via ultrasound process intensification. Ultrasonics sonochemistry, 73, 105536.

Züttel, A. (2004). Hydrogen storage methods. Naturwissenschaften, 91, 157–172.

List of Figures

List of Tables

IV

APPENDIX

A

CASE STUDY INPUTS

INPUTS IN CHAPTER 3

Table A.1: Parameters of hydrogen production plants

	Depreciation length (years)	Lifetime (years)	Capital cost (K€)	Operating cost (€/kg)	Max capacity (kg/day)	Min capacity (kg/day)
Steam methane reforming (GH_2)						
Small	20	40	1,050	0.34	2,000	1,000
Medium	20	40	1,698	0.31	3,500	2,500
Large	20	40	2,276	0.30	5,000	4,000
Biomass gasification (GH_2)						
Small	20	40	4,091	4.01	2,000	1,000
Medium	20	40	7,026	2.48	3,500	2,500
Large	20	40	9,640	1.90	5,000	4,000

Data source: The depreciation length and lifetime are obtained from Hydrogen Analysis (H2A) project (Department of Energy, 2015). The capital cost, operating cost, max capacity and min capacity are obtained from L. Li et al. (2020).

Table A.2: Parameters of the CCS system

	Depreciation length (years)	Lifetime (years)	Capital cost (K€)	Operating cost (€/kg)	Max capacity (kg)	Min capacity (kg)
CCS system	20	40	2,030	0.09	200,000	0

Data source:The depreciation length and lifetime are obtained from Hydrogen Analysis (H2A) project (Department of Energy, 2015). The capital cost, operating cost, max capacity and min capacity are obtained from L. Li et al. (2020).

Table A.3: Parameters of hydrogen storage sites

	Depreciation length (years)	Lifetime (years)	Capital cost (K€)	Operating cost (€/kg)	Max capacity (kg)	Min capacity (kg)
Gaseous storage	15	20	6,397	0.31	7,080	0

Data source: The Hydrogen Analysis (H2A) project (Department of Energy, 2015).

Table A.4: Parameters of transportation

	Depreciation length (years)	Lifetime (years)	Capital cost	Max capacity (kg)	Min capacity (kg)
Truck (biomass)	5	15	402K€/unit	69,400	8000
Tube trailer	5	15	643K€/unit	5,000	50
CO_2 pipeline	20	20	80K€/km	500,000	0

Data source: The depreciation length and lifetime are obtained from Hydrogen Analysis (H2A) project (Department of Energy, 2015). The capital cost, operating cost, max capacity and min capacity are obtained from L. Li et al. (2020).

Note: The maximum capacity of the pipeline is base on the assumption that individual nodes cannot transportation more than it total produced emission.

Table A.5: General parameters of feedstock and hydrogen transportation

	Truck (For biomass)	Tube trailer (For hydrogen)
Wage	20.47€/h	20.47€/h
Fuel economy	2.76 km/L	2.76 km/L
Fuel price	1.46€/kg	1.46€/kg
General expenses	7.32€/d	7.32€/d
Load/unload time	2.00 h	2.00 h
Maintenance expenses	0.09€/km	0.09€/km
Average speed	55km/h	55km/h
Availability	18h/d	18h/d
Capacity	8000 kg	380Kg
Maximum transportation capacity	69,400kg/d	5,000kg/d

Data source: The data are obtained from L. Li et al. (2020).

Table A.6: Parameters of fueling stations

Facility Type	Depreciation length (years)	Lifetime (years)	Capital cost (K€/unit)	Operating cost (€/kg)	Max capacity (kg)
Gaseous station					
Small	5	20	1,083	3.28	150
Medium	5	20	1,865	2.20	300
Large	5	20	2,104	1.28	600
Extralarge	5	20	4,208	1.28	1,200

Data source: The depreciation length and lifetime are obtained from Hydrogen Analysis (H2A) project (Department of Energy, 2015). The capital cost, operating cost, max capacity and min capacity are obtained from L. Li et al. (2020).

Table A.7: Feedstock price and conversion rates input

Parameter	Unit	Value
Nature gas price	€/Nm^3	0.36
Biomass price	€/kg	0.05
Electricity price	€/kWh	0.085
Conversion rate (SMR)	Nm^3 Natural gas/ kg H_2	4.07
Conversion rate (Biomass Gasification)	kg Biomass/ kg H_2	19.39
Conversion rate (Electrolysis)	kWh Electricity/ kg H_2	54.60

INPUTS IN CHAPTER 4 & 5

Table A.8: Population, vehicle number, income and main economic of chosen cities

No	City	Population	Vehicle	Income	Main Economic
C1	Paris	2165423	594635	28570	2
C2	Marseille	870731	367514	19370	2
C3	Lyon	522969	207469	24150	2
C4	Toulouse	493465	219680	21440	2
C5	Nice	342669	158923	20530	2
C6	Nantes	318808	137270	22960	2
C7	Montpellier	295542	127517	18870	2
C8	Strasbourg	287228	116207	19220	2
C9	Bordeaux	260958	113362	23360	2
C10	Lille	234475	94576	19580	2
C11	Rennes	220488	97168	21760	2
C12	Reims	181194	83874	19280	2
C13	Toulon	178745	84775	19950	2
C14	Saint-Étienne	173821	79305	18410	3
C15	Le Havre	168290	75530	19380	2
C16	Grenoble	158198	63890	21170	2
C17	Dijon	158002	77060	21830	2
C18	Angers	155850	70285	20420	2
C19	Villeurbanne	152212	62651	20610	2
C20	Nîmes	148561	79545	18020	2
C21	Clermont-Ferrand	147865	73954	19720	2
C22	Aix-en-Provence	145133	82064	24590	2
C23	Le Mans	143847	74290	20480	2
C24	Brest	139926	70042	20520	2
C25	Tours	137087	63439	20560	2
C26	Amiens	134706	77294	18820	2
C27	Limoges	130876	75147	19720	2
C28	Annecy	130721	76793	21370	2
C29	Boulogne-Billancourt	121583	56932	16910	2
C30	Perpignan	119344	64719	16730	1
C31	Metz	118489	63092	20010	2
C32	Besançon	117912	59631	19890	2
C33	Orléans	116269	56522	20420	2
C34	Seine-Saint-Denis	112852	40423	17270	2
C35	Rouen	112321	67542	20620	2
C36	Montreuil	111240	33479	20000	2
C37	Argenteuil	111038	44564	18430	2
C38	Mulhouse	108312	49875	16100	2
C39	Caen	106230	51404	20770	2
C40	Nancy	105058	45715	20500	2
C41	Roubaix	98828	34979	16680	2
C42	Tourcoing	98656	43034	16680	2
C43	Nanterre	96277	53965	20730	2

C44	Vitry-sur-Seine	95510	32216	18880	2
C45	Créteil	93246	35783	20250	2
C46	Avignon	91143	51313	16910	2
C47	Poitiers	89212	47129	19300	2
C48	Aubervilliers	88948	21800	15800	2
C49	Asnières-sur-Seine	87143	30355	26460	2
C50	Aulnay-sous-Bois	86969	33443	17330	2

Main economic includes 1: Areas specialized in agriculture and tourism, or Residential areas; 2: Large cities with a high concentration of metropolitan functions, Areas with diversified economies and other cities with large employers; 3: Specialized areas in industry.
Data source: The population are obtained from Institut national de la statistique et des ètudes économiques (Statistics & Studies, 2022). The number of vehicle are obtained from Ministère de la transition écologique et de la cohésion des territoires (Transition & Ministry, 2021).

Table A.9: Hydrogen demand of each penetration rate

Rate	**5%**	**15%**	**20%**	**35%**	**40%**	**45%**	**55%**	**60%**	**75%**	**80%**
C1	10913	32740	43654	76394	87307	98220	120047	130961	163701	174614
C2	5603	16809	22412	39220	44823	50426	61632	67235	84043	89646
C3	3570	10709	14279	24989	28558	32128	39268	42838	53547	57117
C4	3537	10612	14150	24762	28300	31837	38912	42450	53062	56600
C5	2675	8024	10699	18723	21398	24073	29422	32097	40121	42796
C6	2489	7467	9956	17423	19912	22401	27379	29868	37335	39825
C7	2296	6888	9184	16071	18367	20663	25255	27551	34439	36734
C8	2197	6591	8788	15379	17575	19772	24166	26363	32954	35151
C9	2165	6494	8658	15152	17317	19482	23811	25975	32469	34634
C10	1902	5707	7609	13316	15218	17120	20925	22827	28534	30436
C11	1914	5743	7657	13399	15314	17228	21056	22971	28713	30627
C12	1675	5025	6700	11726	13401	15076	18426	20101	25127	26802
C13	1685	5054	6738	11792	13477	15161	18531	20215	25269	26954
C14	1758	5273	7031	12304	14062	15819	19335	21093	26366	28124
C15	1581	4744	6325	11069	12650	14231	17394	18975	23719	25300

Table A.10: Parameters of hydrogen transportation

Transport Mode	Lifetime (years)	Capital cost (€)	Min capacity (kg/day)	Max capacity (kg/day)
Tube trailer	5	220000	0	400
Tank truck	5	440000	0	4000
pipeline	30	250782	10000	500000

Table A.11: Parameters of refueling station - Large scale

Refueling Mode	Lifetime (years)	Capital cost (€)	Operating cost (€/kg)	Min capacity (kg/day)	Max capacity (kg/day)
Gaseous station	20	4207508	1.28	0	1200
Liquid Station	20	3143310	1.45	0	1200

Table A.12: Geographic distance between each city

	C1	C2	C3	C4	C5	C6	C7	C8	C9	C10	C11	C12	C13	C14	C15	C16	C17	C18	C19	C20	C21	C22	C23	C24	C25	C26	C27	C28	C29	C30	C31	C32	C33	C34	C35	C36	C37	C38	C39	C40	C41	C42	C43	C44	C45	C46	C47	C48	C49	C50
C1	0	775	466	678	932	385	748	491	584	225	354	144	839	552	197	578	315	296	471	713	424	759	209	592	234	159	393	560	11	849	331	415	127	20	136	12	30	477	239	348	238	239	14	10	14	690	341	8	10	18
C2	775	0	314	404	207	994	170	801	645	1000	1052	798	67	333	965	308	506	906	318	122	476	32	898	1282	799	930	596	378	777	319	768	539	759	786	906	780	800	694	1009	715	1004	1007	796	772	774	101	779	783	786	787
C3	466	314	0	471	435	686	304	493	557	691	743	489	378	63	657	114	197	597	8	253	166	298	588	971	463	620	411	145	466	452	457	227	423	476	594	470	490	376	698	405	694	697	486	461	464	228	442	473	476	478
C4	678	404	471	0	561	588	243	942	245	895	705	813	468	408	848	532	647	635	542	291	375	387	623	882	524	825	290	647	673	205	932	734	555	693	798	683	692	859	777	879	907	910	688	674	676	330	414	686	683	690
C5	932	207	435	561	0	1152	328	786	804	1158	1210	956	150	491	1123	466	664	1164	476	280	572	178	1054	1437	955	1086	752	486	932	475	923	695	915	942	1062	936	956	696	1164	871	1160	1163	952	927	930	262	876	939	942	944
C6	385	994	686	588	1152	0	828	866	349	600	114	519	1052	664	385	796	640	91	691	875	538	970	185	296	209	505	327	782	378	788	711	739	317	399	386	395	398	864	292	772	632	632	385	380	382	911	184	395	388	397
C7	748	170	304	243	328	828	0	791	487	964	918	788	233	322	918	298	495	772	307	56	336	153	757	1125	658	881	424	413	742	157	756	527	624	758	867	752	761	683	926	703	976	978	757	743	745	96	548	754	752	760
C8	491	801	493	942	786	866	791	0	943	525	835	350	866	551	699	529	332	777	483	741	628	786	660	1042	658	520	731	431	476	940	163	244	551	466	636	462	514	114	728	149	533	527	506	464	462	716	759	474	506	492
C9	584	645	557	245	804	349	487	943	0	806	473	724	710	535	692	666	646	403	561	533	375	630	424	644	330	730	222	698	578	448	907	734	443	599	626	595	579	858	583	879	817	818	585	580	582	572	229	594	588	597
C10	225	1000	691	895	1158	600	964	525	806	0	571	207	1065	750	316	804	502	553	697	940	639	974	424	758	455	120	608	769	233	1064	364	586	348	207	235	215	237	596	372	399	15	15	247	226	225	905	556	213	244	205
C11	354	1052	743	705	1210	114	918	835	473	571	0	483	1110	721	279	849	617	129	744	967	573	1025	153	240	251	430	450	844	342	911	675	723	299	363	310	360	362	789	185	675	581	582	350	344	346	955	272	358	352	367
C12	144	798	489	813	956	519	788	350	724	207	483	0	863	547	351	601	299	430	495	737	548	782	342	725	373	169	526	551	151	936	191	342	266	137	281	138	169	394	383	196	210	211	161	140	138	713	474	150	156	140
C13	839	67	378	468	150	1052	233	866	710	1065	1110	863	0	397	1030	372	570	970	382	186	475	84	905	1344	836	993	659	487	839	382	830	602	822	849	968	843	863	757	1071	778	1067	1070	849	834	837	161	815	846	849	851
C14	552	333	63	408	491	664	322	551	535	750	721	547	397	0	721	155	255	575	67	271	144	316	566	950	450	697	337	186	478	463	514	292	400	488	658	482	502	441	729	461	771	772	488	473	476	231	430	485	488	536
C15	197	965	657	848	1123	385	918	699	692	316	279	351	1030	721	0	768	505	298	661	904	571	949	211	466	310	181	540	733	191	1017	539	605	280	210	90	208	191	671	98	557	313	314	188	208	214	879	410	201	194	211
C16	578	308	114	532	466	796	298	529	666	804	849	601	372	155	768	0	306	705	104	245	273	264	695	1079	597	718	493	106	575	444	566	312	557	585	704	579	592	422	807	513	803	806	585	570	572	220	563	581	584	590
C17	315	506	197	647	664	640	495	332	646	502	617	299	570	255	505	306	0	551	202	444	322	488	457	860	415	468	415	265	314	642	267	95	296	324	443	318	332	219	546	215	513	516	324	309	312	419	494	321	324	329
C18	296	906	597	635	1164	91	772	777	403	553	129	430	970	575	298	705	551	0	602	826	450	866	96	365	127	417	260	711	290	754	616	650	228	306	298	300	309	730	233	634	524	527	297	291	294	767	141	302	300	311
C19	471	318	8	542	476	691	307	483	561	697	744	495	382	67	661	104	202	602	0	256	171	301	593	977	494	625	391	138	471	455	462	221	428	481	600	475	489	373	703	410	699	702	481	466	469	232	447	478	481	486
C20	713	122	253	291	280	875	56	741	533	940	967	737	186	271	904	245	444	826	256	0	325	106	808	1170	710	866	482	361	713	205	704	475	678	723	842	717	736	628	945	651	941	944	723	708	710	44	606	719	722	728
C21	424	476	166	375	572	538	336	628	375	639	573	548	475	144	571	273	322	450	171	325	0	396	424	812	325	558	194	307	417	434	582	384	300	434	530	428	437	509	594	529	650	651	433	419	421	388	306	430	427	439
C22	759	32	298	387	178	970	153	786	630	974	1025	782	84	316	949	264	488	866	301	106	396	0	859	1268	760	917	583	347	763	306	755	526	720	773	893	768	787	678	995	702	989	990	773	758	761	84	739	770	773	778
C23	209	898	588	623	1054	185	757	660	424	424	153	342	905	566	211	695	457	96	593	808	424	859	0	397	98	330	316	693	203	820	529	577	162	219	211	213	214	643	160	579	435	436	211	204	207	779	202	216	213	224
C24	592	1282	971	882	1437	296	1125	1042	644	758	240	725	1344	950	466	1079	860	365	977	1170	812	1268	397	0	491	623	616	1086	585	1084	912	960	545	602	499	596	600	1026	374	888	770	771	596	587	589	1198	478	598	595	607
C25	234	799	463	524	955	209	658	658	330	455	251	373	836	450	310	597	415	127	494	710	325	760	98	491	0	374	219	595	234	722	560	521	117	250	309	244	253	619	260	505	466	467	249	235	237	682	105	246	243	255
C26	159	930	620	825	1086	505	881	520	730	120	430	169	993	697	181	718	468	417	625	866	558	917	330	623	374	0	533	710	142	989	362	554	273	140	120	147	128	565	250	379	147	152	137	153	157	840	481	135	132	134
C27	393	596	411	290	752	327	424	731	222	608	450	526	659	337	540	493	415	260	391	482	194	583	316	616	219	533	0	499	387	493	693	496	269	403	480	389	407	620	494	641	619	620	403	389	391	518	123	400	396	408
C28	560	378	145	647	486	782	413	431	698	769	844	551	487	186	733	106	265	711	138	361	307	347	693	1086	595	710	499	0	561	561	463	194	561	571	690	565	585	322	793	406	779	780	571	556	558	339	579	567	570	576
C29	11	777	466	673	932	378	742	476	578	233	342	151	839	478	191	575	314	290	471	713	417	763	203	585	234	142	387	561	0	842	338	415	123	30	128	19	15	481	233	392	237	238	9	15	21	690	334	17	12	28
C30	849	319	452	205	475	788	157	940	448	1064	911	936	382	463	1017	444	642	754	455	205	434	306	820	1084	722	989	493	561	842	0	904	676	724	859	967	853	862	825	990	851	1075	1075	858	844	846	244	619	855	852	863
C31	331	768	457	932	923	711	756	163	907	364	675	191	830	514	539	566	267	616	462	704	582	755	529	912	560	362	693	463	338	904	0	267	450	324	474	323	347	243	577	60	373	368	354	329	325	684	664	334	345	326
C32	415	539	227	734	695	739	527	244	734	586	723	342	602	292	605	312	95	650	221	475	384	526	577	960	521	554	496	194	415	676	267	0	411	421	539	415	434	134	643	207	590	591	420	406	408	453	550	417	420	425
C33	127	759	423	555	915	317	624	551	443	348	299	266	822	400	280	557	296	228	428	678	300	720	162	545	117	273	269	561	123	724	450	411	0	129	219	130	143	512	307	398	358	359	134	114	117	646	218	133	136	141
C34	20	786	476	693	942	399	758	466	599	207	363	137	849	488	210	585	324	306	481	723	434	773	219	602	250	140	403	571	30	859	324	421	129	0	133	9	21	477	250	346	218	219	27	20	19	699	350	11	19	4
C35	136	906	594	798	1062	386	867	636	626	235	310	281	968	658	90	704	443	298	600	842	530	893	211	499	309	120	480	690	128	967	474	539	219	133	0	132	109	609	131	495	267	268	126	153	156	818	410	119	116	142
C36	12	780	470	683	936	395	752	462	595	215	360	138	843	482	208	579	318	300	475	717	428	768	213	596	244	147	389	565	19	853	323	415	130	9	132	0	23	466	255	305	225	226	23	14	14	693	395	9	18	12
C37	30	800	490	692	956	398	761	514	579	237	362	169	863	502	191	592	332	309	489	736	437	787	214	600	253	128	407	585	15	862	347	434	143	21	109	23	0	503	232	373	234	235	9	29	38	712	353	14	5	25
C38	477	694	376	859	696	864	683	114	858	596	789	394	757	441	671	422	219	730	373	628	509	678	643	1026	619	565	620	322	481	825	243	134	512	477	609	466	503	0	708	176	607	616	486	458	454	602	676	481	486	478
C39	239	1009	698	777	1164	292	926	728	583	372	185	383	1071	729	98	807	546	233	703	945	594	995	160	374	260	250	494	793	233	990	577	643	307	250	131	255	232	708	0	596	399	400	225	253	255	917	359	239	235	251
C40	348	715	405	879	871	772	703	149	879	399	675	196	778	461	557	513	215	634	410	651	529	702	579	888	505	379	641	406	392	851	60	207	398	346	495	305	373	176	596	0	419	420	334	310	308	627	605	320	325	316
C41	238	1004	694	907	1160	632	976	533	817	15	581	210	1067	771	313	803	513	524	699	941	650	989	435	770	466	147	619	779	237	1075	373	590	358	218	267	225	234	607	399	419	0	5	239	237	236	917	567	223	230	217
C42	239	1007	697	910	1163	632	978	527	818	15	582	211	1070	772	314	806	516	527	702	944	651	990	436	771	467	152	620	780	238	1075	368	591	359	219	268	226	235	616	400	420	5	0	240	239	238	919	569	225	232	219
C43	14	796	486	688	952	385	757	506	585	247	350	161	849	488	188	585	324	297	481	723	433	773	211	596	249	137	403	571	9	858	354	420	134	27	126	23	9	486	225	334	239	240	0	25	31	705	347	17	9	29
C44	10	772	461	674	927	380	743	464	580	226	344	140	834	473	208	570	309	291	466	708	419	758	204	587	235	153	389	556	15	844	329	406	114	20	153	14	29	458	253	310	237	239	25	0	7	685	336	17	25	23
C45	14	774	464	676	930	382	745	462	582	225	346	138	837	476	214	572	312	294	469	710	421	761	207	589	237	157	391	558	21	846	325	408	117	19	156	14	38	454	255	308	236	238	31	7	0	688	338	19	27	21
C46	690	101	228	330	262	911	96	716	572	905	955	713	161	231	879	220	419	767	232	44	388	84	779	1198	682	840	518	339	690	244	684	453	646	699	818	693	712	602	917	627	917	919	705	685	688	0	667	698	701	706
C47	341	779	442	414	876	184	548	759	229	556	272	474	815	430	410	563	494	141	447	606	306	739	202	478	105	481	123	579	334	619	664	550	218	350	410	395	353	676	359	605	567	569	347	336	338	667	0	349	344	352
C48	8	783	473	686	939	395	754	474	594	213	358	150	846	485	201	581	321	302	478	719	430	770	216	598	246	135	400	567	17	855	334	417	133	11	119	9	14	481	239	320	223	225	17	17	19	698	349	0	10	13
C49	10	786	476	683	942	388	752	506	588	244	352	156	849	488	194	584	324	300	481	722	427	773	213	595	243	132	396	570	12	852	345	420	136	19	116	18	5	486	235	325	230	232	9	25	27	701	344	10	0	21
C50	18	787	478	690	944	397	760	492	597	205	367	140	851	536	211	590	329	311	486	728	439	778	224	607	255	134	408	576	28	863	326	425	141	4	142	12	25	478	251	316	217	219	29	23	21	706	352	13	21	0

Note: C1-C50 correspond to the cities in Table A.8.
Data source: Driving distance measured by Google Maps.

Table A.13: Parameters of hydrogen production plant - Large scale

Production Mode	Lifetime (years)	Capital cost (€)	Operating cost (€/kg)	Min capacity (kg/day)	Max capacity (kg/day)
SMR(GH_2)					
Small	40	61551808	0.457	10000	20000
Medium	40	184655425	0.307	25000	75000
Large	40	958754202	0.161	160000	480000
SMR(LH_2)					
Small	40	67626992	1.141	10000	20000
Medium	40	199260603	0.484	25000	75000
Large	40	953512560	0.216	160000	480000
BG(GH_2)					
Small	40	287647656	3.17	10000	20000
Medium	40	862942970	1.897	25000	75000
Large	40	3307321817	0.887	160000	480000
BG(LH_2)					
Small	40	293722840	3.854	10000	20000
Medium	40	833670741	2.074	25000	75000
Large	40	3352265046	0.942	160000	480000
WE(GH_2)					
Small	40	128730348	1.1	10000	20000
Medium	40	386191045	0.786	25000	75000
Large	40	772382090	0.691	75000	150000
WE(LH_2)					
Small	40	134805532	2.058	10000	20000
Medium	40	272065875	1.397	25000	75000
Large	40	801592446	0.825	75000	150000

Note: SMR: steam methane reforming technology; BG: biomass gasification technology. WE: water electrolysis.

Table A.14: Parameters of hydrogen storage plant - Large scale

Storage Mode	Lifetime (years)	Capital cost (€)	Operating cost (€/kg)	Min capacity (kg/day)	Max capacity (kg/day)
S1					
Small	40	7699111	12.581	0	5000
Medium	40	13101476	6.525	5000	10000
Large	40	26945482	1.009	12500	480000
S2					
Small	40	21999308	0.478	0	75000
Medium	40	52492548	0.186	135000	270000
Large	40	97370598	0.131	240000	480000
S3					
Small	40	29698419	0.478	0	75000
Medium	40	65594024	0.186	135000	270000
Large	40	124316080	0.131	240000	480000
S4					
Small	40	15924124	0.478	0	75000
Medium	40	37887370	0.186	135000	270000
Large	40	52427369	0.131	240000	480000
S5					
Small	40	23623235	0.478	0	75000
Medium	40	50988846	0.186	135000	270000
Large	40	79372851	0.131	240000	480000

B

MODEL CONSTRAINTS

MODEL CONSTRAINTS

Except for the storage constraints, the remains reported in this section are taken from the model of L. Li et al. (2020), including feedstock constraints, production constraints, transportation constraints, etc.

FEEDSTOCK CONSTRAINTS

The sum of the feedstock supply rate and the input rate from points m Q_{fmn} equal to the production utilization rate of raw material and output rate Q_{fnm}.

$$PESR_{ne} + \sum_{m,f:(e,f)\in EF} Q_{fmn} = \sum_{m,f:(e,f)\in EF} Q_{fnm} + \sum_{i,k} PR_{npik} * \delta_{(e,p)} \tag{B.1}$$

The feedstock supply rate for the on-site fueling station can be obtained as follow:

$$OESR_{ne} = \sum_{j} O_{nfj} * \delta_{(e,f)} \tag{B.2}$$

where $\delta_{(e,p)}$ is the conversion rate of feedstock to hydrogen. And $\delta_{(e,f)}$ is the conversion rate at on-site fueling station. It cannot exceed their minimal and maximal limitation in each node.

$$IE_{ne} * ecap_{ne}^{min} \leq PESR_{ne} \leq IE_{ne} * ecap_{ne}^{max} \tag{B.3}$$

$$IF_{no} * ecap_{ne}^{min} \leq OESR_{ne} \leq IF_{no} * ecap_{ne}^{max} \tag{B.4}$$

$$PESR_{ne} + OESR_{ne} \leq ecap_{ne}^{max}, \tag{B.5}$$

where IE_{ne} and IF_{no} are binary variables. It's equal to 1 if there are feedstock supply sites. $ecap_{ne}^{min}$ and $ecap_{ne}^{max}$ are minimal and maximal support rates for different feedstock e at the site n. IF_{no} equals 1 if there is an on-site fueling station of technology o at node n, and is defined by

$$IF_{no} = \sum_{j} IF_{noj} \tag{B.6}$$

The number of feedstock supply sites that supply feedstock of type e to hydrogen production plants (NE_e) is defined as

$$NE_e = \sum_{n} IE_{ne} \tag{B.7}$$

PRODUCTION CONSTRAINTS

The production rate of production plants (PR_{npik}) cannot exceed their minimal and maximal limit of capacity.

$$IP_{npik} * pcap_{pik}^{min} \leq PR_{npik} \leq IP_{npik} * pcap_{pik}^{max} \tag{B.8}$$

where IP_{npik} equal to 1 if there is a production center. $pcap_{pik}^{min}$ and $pcap_{pik}^{max}$ are minimal and maximal production rates for different production technology p and plant size k at the site n. The number of production plants NP_{pik} and total production rate (PR_{pik}) are given by:

$$NP_{pik} = \sum_{n} IP_{npik} \tag{B.9}$$

$$PR_{pik} = \sum_{n} PR_{npik} \tag{B.10}$$

Moreover, only one plant could be installed at each node.

$$IP_n = \sum_{p,i,k} IP_{npik}, \tag{B.11}$$

STORAGE CONSTRAINTS

The production of hydrogen corresponds to the demand of the given period. But considering the production speed of hydrogen, storage is necessary between the production step and the transportation step. We suppose that the storage sites are located at the same site as the associated production plants.

The storage rate in storage site (SR_{ni}) is equal to the production rate in the same node n and cannot exceed their minimal and maximal limit of capacity.

$$SR_{ni} = \sum_{pk} PR_{nipk} \tag{B.12}$$

$$IT_{ni} * tercap_{i}^{min} \leq SR_{ni} \leq IT_{ni} * tercap_{i}^{max} \tag{B.13}$$

where IT_{ni} equal to 1 if there is a storage site. $tercap_i^{min}$ and $tercap_i^{max}$ are minimal and maximal storage rate. The number of storage sites is defined as:

$$NT_i = \sum_n IT_{ni} \tag{B.14}$$

TRANSPORTATION CONSTRAINTS

The transportation flow of hydrogen (TR_{hnm}), feedstock (Q_{fnm}) and CO_2 (Q_{nm}) cannot exceed their minimal and maximal limit of transportation capacity.

$$X_{hnm} * tcap_h^{min} \leq TR_{hnm} \leq X_{hnm} * tcap_h^{max} \tag{B.15}$$

$$X_{fnm} * tcap_f^{min} \leq Q_{fnm} \leq X_{fnm} * tcap_f^{max}, \tag{B.16}$$

$$X_{nm} * tcap^{min} \leq Q_{nm} \leq X_{nm} * tcap^{max}, \tag{B.17}$$

where X_{hnm}, X_{fnm} and X_{nm} equal to 1 if there is transportation from node n to m. $tcap$ represents the capacity limit of transportation equipment.

Only one direction occurred in the transportation between different nodes.

$$X_{hnm} + X_{hmn} \leq 1 \tag{B.18}$$

$$X_{fnm} + X_{fmn} \leq 1 \tag{B.19}$$

$$X_{nm} + X_{mn} \leq 1 \tag{B.20}$$

The production node can only export hydrogen.

$$IP_n \geq X_{hnm} \tag{B.21}$$

Hydrogen is imported into the nodes that have standard fueling stations or fixed-location demand of Type A, or both:

$$SIF_n + id_n^{h,A} \geq X_{hmn} \tag{B.22}$$

where SIF_n equals 1 if there is a standard fueling station (of any technology, any hydrogen form, and any size) at this node. $id_n^{h,A}$ indicates whether node n has fixed-location demand of Type A.

A node cannot export feedstock when there is no feedstock supplier at this node (implies IE_n equals to 0):

$$IE_n \geq X_{fnm} \tag{B.23}$$

where IE_n is defined as

$$IE_n = \sum_{e \in E} IE_{ne} \tag{B.24}$$

where IE_{ne} equals 1 if node n is chosen as a feedstock supplier that supplies feedstock of type e to production plants.

The end of the feedstock transportation link can only be the production plants:

$$IP_n \geq X_{fmn} \tag{B.25}$$

where IP_n equals 1 if there is a production plant at node n.

A node can only export CO_2 when the emission of the production plant at this node is processed (means IM_n equals 1):

$$IM_n \geq X_{nm} \tag{B.26}$$

The CO_2 transportation link ends only at the nodes where CO_2 storage sites are located (means IR_n equals 1):

$$IR_n \geq X_{mn} \tag{B.27}$$

The number of transportation equipment are defined as follows:

$$NV_h \geq \sum_{n,m} \frac{TR_{hnm}}{tma_h * tcap_h} * (\frac{2 * l_{nm}}{sp_h} + lut_h) \tag{B.28}$$

where tma_h and $tcap_h$ denote the maximal capacity and available work time per day of transportation equipment. sp_h represents the running speed. lut_h is the load/unload time of hydrogen transportation mode h.

FUELING STATION CONSTRAINTS

The fueling rate (FR_{nsij}) and on-site fueling rate (FR_{noj}) cannot exceed their minimal and maximal limit of capacity.

$$IF_{nsij} * fcap_{sij}^{min} \leq FR_{nsij} \leq IF_{nsij} * fcap_{sij}^{max} \tag{B.29}$$

$$IF_{noj} * Ocap_{oj}^{min} \leq FR_{noj} \leq IF_{noj} * Ocap_{oj}^{max} \tag{B.30}$$

The total fueling rates (FR_{sij}, FR_{oj}) are defined as:

$$FR_{sij} = \sum_{n} FR_{nsij} \tag{B.31}$$

$$FR_{oj} = \sum_{n \in N} FR_{noj} \tag{B.32}$$

The number of fueling station NF_{sij} and on-site fueling station NF_{fj} are obtained as follows:

$$NF_{sij} = \sum_{n} IF_{nsij} \tag{B.33}$$

$$NF_{oj} = \sum_{n} IF_{noj} \tag{B.34}$$

If fixed-location hydrogen demand of Type B exists at node n (means $id_n^{h,B}$ equals 1), a standard fueling station should also be built at this node:

$$SIF_n \geq id_n^{h,B} \tag{B.35}$$

Demand constraints

The percentage of hydrogen fueling demand flow that can be captured ($DEM^{h,cap}$) should be equal to the number given as input ($dem^{h,exp}$):

$$DEM^{h,cap} = dem^{h,exp} \tag{B.36}$$

Because hydrogen fueling demand flow of OD (Origin–Destination) flow pairs are discrete values, the following constraints to replace the Eq. (B.36) are introduced:

$$dem^{h,exp} \leq DEM^{h,cap} \leq dem^{h,exp} + c \tag{B.37}$$

where c is a small positive number, which is set to 0.01 in this study, and $DEM^{h,cap}$ is defined by

$$DEM^{h,cap} = \frac{\sum_q f_q^{pair} * IC_q}{\sum_q f_q^{pair}} * 100 \tag{B.38}$$

where f_q^{pair} is the amount of hydrogen fueling demand flow of OD flow pair q, and IC_q equals 1 if flow pair q is captured. The total hydrogen production (THP) should exceed the total hydrogen demand THD.

$$THD = DEM^{h,exp} \tag{B.39}$$

$$THP = \sum_{npik} IP_{npik} * PR_{npik} + \sum_{noj} IO_{noj} * O_{noj} \tag{B.40}$$

$$THP \geq THD \tag{B.41}$$

A hydrogen fueling demand flow is captured if there is at least one fueling station (of any technology and any size) on one of the nodes that lie on the shortest path of this flow pair:

$$\sum_{n} IF_n \geq IC_q \tag{B.42}$$

where IF_n equals 1 if there is a fueling station (standard or on-site) at this node. The following equations ensure that only one fueling station could be installed at each node.

$$IF_n = SIF_n + OIF_n, \tag{B.43}$$

$$SIF_n = \sum_{s,i,j} IF_{nsij}, \tag{B.44}$$

$$OIF_n = \sum_{o,j} IF_{noj} \tag{B.45}$$

where SIF_n equals 1 if there is a standard fueling station at node n, and OIF_n equals 1 if there is an on-site fueling station at this node. IF_{nsij} equals 1 if there is a standard fueling station at node n, of technology s, hydrogen form i, and size j. IF_{noj} equals 1 if there is an on-site fueling station at node n, of technology o and size j.

The fueling rate at node n (FR_{nsij}, FR_{noj}) should be able to cover the amount of hydrogen fueling demand flow captured by the fueling station established at that node:

$$\sum_{s,i,j} FR_{nsij} \geq SIF_n * f_n^{node} \tag{B.46}$$

$$\sum_{o,j} FR_{noj} \geq OIF_n * f_n^{node} \tag{B.47}$$

where f_n^{node} is the hydrogen fueling demand flow of node n.

The amount of hydrogen produced by the production plant PR_{npik} plus the amount input from other nodes TR_{hmn} should equal to the sum of the amount of fueling FR_{nsij} plus the amount of hydrogen output to other nodes TR_{hnm} at node n for hydrogen form i and fixed location demand $dem_{ni}^{h,A}$ and $dem_{ni}^{h,B}$.

$$\sum_{p,k} PR_{npik} + \sum_{m,h} TR_{hmn} = \sum_{m,h} TR_{hnm} + \sum_{s,j} FR_{nsij} + dem_{ni}^{h,A} + dem_{ni}^{h,B} \tag{B.48}$$

EMISSION CONSTRAINTS

The CO_2 processing rate (CR_n) cannot exceed certain limits:

$$IR_n * ccap_n^{min} \leq CR_n \leq IR_n * ccap_n^{max} \tag{B.49}$$

where IR_n equals 1 if there is a CO_2 storage site at node n. The bounds of CO_2 processing capacity are represented by $ccap$.

The total processing rate of CO_2 (CR) is given by:

$$CR = \sum_{n} CR_n \tag{B.50}$$

The emission mass balance should be satisfied at each node n to quantify the infrastructure needs for a CCS system.

$$PER_n^c + \sum_{m} Q_{mn} = \sum_{m} Q_{nm} + CR_n \tag{B.51}$$

In the equation, PER_n^c represents the emission rate of a production plant at node n, where emissions are processed. Q_{mn} is the CO_2 transportation flux from node m to n, whereas Q_{nm} is the flux from node n to m.

The production rate of a production plant where emissions are processed (PR_{npik}^c) can be obtained by the following equation:

$$PR_{npik}^c = IM_n * PR_{npik}, \quad \forall n \in N, p \in P, i \in I, k \in K \tag{B.52}$$

where PR_{npik} represents the production rate of a production plant at node n, and IM_n denotes whether the emission of this plant is processed.

The Eq. (B.52) is nonlinear and can be linearized by the following constraints:

$$PR_{npik}^c \leq IM_n * pcap_{pik}^{max} \tag{B.53}$$

$$PR_{npik}^c \leq PR_{npik} \tag{B.54}$$

$$PR_{npik}^c \geq PR_{npik} - (1 - IM_n) * pcap_{pik}^{max}, \tag{B.55}$$

where $pcap_{pik}^{max}$ is the upper limit of production capacity.